CORA Cork Open Research Archive
Cartlann Taighde Oscailte Chorcaí

Title	FLT3-driven redox signalling in acute myeloid leukaemia
Authors	Corcoran, Aoife
Publication date	2013-01
Original Citation	Cororan, A., 2013. FLT3-driven redox signalling in acute myeloid leukaemia. PhD Thesis, University College Cork.
Type of publication	Doctoral thesis
Link to publisher's version	http://dx.doi.org/10.1158/1538-7445.AM2012-2545, http://dx.doi.org/10.3109/10715762.2012.733385, http://online.liebertpub.com/doi/abs/10.1089/ars.2012.5028
Rights	© 2013, Aoife Corcoran - http://creativecommons.org/licenses/by-nc-nd/3.0/
Download date	2026-11-04 11:18:45
Item downloaded from	https://hdl.handle.net/10468/962



UCC
University College Cork, Ireland
Coláiste na hOllscoile Corcaigh

FLT3-Driven Redox Signalling in Acute Myeloid Leukaemia

A thesis submitted to the National University of Ireland, Cork, in fulfilment of the requirements for the degree of

Doctor of Philosophy

by

Aoife Corcoran, BSc.



Department of Biochemistry,

University College Cork

January 2013

Supervisor: Professor Thomas G. Cotter

Head of Department: Professor Thomas G. Cotter

Acknowledgements

I must first thank my supervisor Professor Tom Cotter, who provided the impetus and ideas for this work, and who supported and believed in me throughout - I am grateful to have had the opportunity to learn from the best. I must also give a huge thank you to Kate Cotter, who made me feel at home from day one, and who has continued to be a tireless source of energy and assistance.

I was fortunate to interact with a vibrant, dynamic group in the Cotter Lab and I owe a huge thanks to every single member, past- Claire, Ruth, Carolyn, Chris, Ashley, Dani, Maryanne, Sara, Dave, Brendan, Steve, Sorcha; present- Gillian, Will, John, Joanna, Fran; as well as the new recruits Eileen and Niamh. I wish you all the very best and I value the time that I have spent as part of this warm and wonderful group.

The brilliant initiative that is the PhD Scholars Programme in Cancer Biology, supported by the Health Research Board, gave me the chance to grow as a researcher, but it would not have been possible without the one and only Dr. Kellie Dean. Your positivity, kindness, un-ending support and encouragement made a difficult journey that much easier. Similarly, I am grateful to my thesis committee Professor Rosemary O'Connor, Professor Tommie MacCarthy and Dr.Karen Keeshan for the time, effort and dedication which was so willingly given throughout the four years.

The learning curve which I have been on has been very steep at times, and I have navigated it with the assistance and instruction of people who showed me the 'tricks of the trade'. For this reason I thank Professor Dave Sheehan and his group- Wentao and Louis-Charles, for an education in 2D gels; Miriam, Suzanne and Don in the S.E.M. facility; and Olive in the Biochemistry Dept. for endless favours.

To all the friends that I have made in U.C.C. and beyond during this process, as well as those friends lucky enough not to be involved but who still got to listen to all that whingeing- thank you!

Lastly, I am most indebted to those closest to me. My mam – who is always ready to listen, comfort and reassure, and as a result probably knows more than she ever

wanted to about cells and reactive oxygen species! My dad, a real scientist, who never stops teaching and never stops learning, and is still the person I turn to with my ‘homework’ questions! I am so grateful to you both for your wisdom, encouragement and patience; truly I could not have achieved this without you. To Sinead and Dara, for all the much needed distractions and laughs, and for even being interested! And to John, for being there throughout, for the joy and the inspiration.

To everyone still waiting for good news or the right medicine

‘Happy is he who gets to know the reasons for things.’

-Virgil

Table of Contents

Declaration i

Abstract ii

Abbreviations iv

Chapter 1

General Introduction 1

1. Leukaemia

1.1 Classification of Leukaemia 2

1.2 Acute Myeloid Leukaemia 2

Phases of disease 3

Molecular mechanisms of disease 4

FLT3 mutations 8

1.3 Mechanisms of FLT3-ITD pathogenesis 10

1.4 Treatment of Acute Myeloid Leukaemia 12

2. Reactive Oxygen Species Signalling 14

2.1 Reactive Oxygen species 14

Antioxidants 18

Peroxiredoxins 20

2.2 NADPH oxidase 23

2.3 Redox signalling 27

3. Objectives 30

Chapter 2

Materials and Methods 32

Chapter 3

Regulation of tyrosine phosphorylation by Nox-derived reactive oxygen species in a FLT3-ITD cell line 46

Chapter 4

FLT3 regulation of p22phox drives redox-modulation of Src and Ezrin and influences leukaemic cell migration 93

Chapter 5

Regulation of phosphatase expression and activity by FLT3-ITD in the MOLM-13 cell line 152

Chapter 6

General Discussion 227

Bibliography 236

Appendix 1

FLT3-driven redox-modulation of Ezrin regulates leukemic cell migration. Corcoran A, Cotter TG.(2013) *Free Radic Res*; Jan;47(1):20-34. doi: 10.3109/10715762.2012.733385.

Appendix 2

Redox Regulated Growth Factor Survival Signalling. Woolley, J., Corcoran, A., Groeger, G., Landry, W., Cotter, T.G. (2013) *Antioxid Redox Signal*; Dec 2; Epub ahead of print, doi:10.1089/ars.2012.5028.

Appendix 3

Redox Regulation of Kinases. Corcoran, A., Cotter, T.G. (2013) *FEBS J;* under review.

Declaration

This thesis has not been submitted in whole or in part to this or any other university for any degree and is, unless otherwise stated, the original work of the author.

Signed: _____

Aoife Corcoran

Abstract

Acute myeloid leukaemia refers to cancer of the blood and bone marrow characterised by the rapid expansion of immature blasts of the myeloid lineage. The aberrant proliferation of these blasts interferes with normal haematopoiesis, resulting in symptoms such as anaemia, poor coagulation and infections. The molecular mechanisms underpinning acute myeloid leukaemia are multi-faceted and complex, with a range of diverse genetic and cytogenetic abnormalities giving rise to the acute myeloid leukaemia phenotype. Amongst the most common causative factors are mutations of the *FLT3* gene, which codes for a growth factor receptor tyrosine kinase required by developing haematopoietic cells. Disruptions to this gene can result in constitutively active FLT3, driving the de-regulated proliferation of undifferentiated precursor blasts. FLT3-targeted drugs provide the opportunity to inhibit this oncogenic receptor, but over time can give rise to resistance within the blast population. The identification of targetable components of the FLT3 signalling pathway may allow for combination therapies to be used to impede the emergence of resistance. However, the intracellular signal transduction pathway of FLT3 is relatively obscure. The objective of this study is to further elucidate this pathway, with particular focus on the redox signalling element which is thought to be involved. Signalling *via* reactive oxygen species is becoming increasingly recognised as a crucial aspect of physiological and pathological processes within the cell. The first part of this study examined the effects of NADPH oxidase-derived reactive oxygen species on the tyrosine phosphorylation levels of acute myeloid leukaemia cell lines. Using two-dimensional phosphotyrosine immunoblotting, a range of proteins were identified as undergoing tyrosine phosphorylation in response to

NADPH oxidase activity. Ezrin, a cytoskeletal regulatory protein and substrate of Src kinase, was selected for further study.

The next part of this study established that NADPH oxidase is subject to regulation by FLT3. Both wild type and oncogenic FLT3 signalling were shown to affect the expression of a key NADPH oxidase subunit, p22phox, and FLT3 was also demonstrated to drive intracellular reactive oxygen species production. The NADPH oxidase target protein, Ezrin, undergoes phosphorylation on two tyrosine residues downstream of FLT3 signalling, an effect which was shown to be p22phox-dependent and which was attributed to the redox regulation of Src. The cytoskeletal associations of Ezrin and its established role in metastasis prompted the investigation of the effects of FLT3 and NADPH oxidase activity on the migration of acute myeloid leukaemia cell lines. It was found that inhibition of either FLT3 or NADPH oxidase negatively impacted on the motility of acute myeloid leukaemia cells. The final part of this study focused on the relationship between FLT3 signalling and phosphatase activity. It was determined, using phosphatase expression profiling and real-time PCR, that several phosphatases are subject to regulation at the levels of transcription and post-translational modification downstream of oncogenic FLT3 activity.

In summary, this study demonstrates that FLT3 signal transduction utilises a NADPH oxidase-dependent redox element, which affects Src kinase, and modulates leukaemic cell migration through Ezrin. Furthermore, the expression and activity of several phosphatases is tightly linked to FLT3 signalling. This work reveals novel components of the FLT3 signalling cascade and indicates a range of potential therapeutic targets.

Abbreviations

AC-220	Quizartinib
Abl	Abelson murine leukaemia viral oncogene
Ala	Alanine
ALL	Acute lymphocytic leukaemia
AML	Acute myeloid leukaemia
AML1	Acute myeloid leukaemia-1 transcription factor
ANGPTL4	Angiopoietin-related protein 4
AP-1	Activator protein 1
APL	Acute promyelocytic leukaemia
ASK-1	Apoptosis signal-regulating kinase 1
ATM	Ataxia telangiectasia mutated
ATP	Adenosine triphosphate
BAF3	Murine bone marrow-derived pro-B-cell line
B-ALL	B-cell acute lymphocytic leukaemia
Bapta-AM	1,2- bis(o-aminophenoxy)ethane-N,N,N,N-tetraacetic acid
Bcr	Breakpoint cluster region protein
BIAM	N-(biotinoyl)-N′-(iodoacetyl)ethylenediamine
Bim-1	BES1-interacting Myc-like protein 1
BMM	Bone marrow-derived macrophages
BRCA1	Breast cancer type 1 susceptibility protein
BSA	Bovine serum albumin
C57/BL6	C57 black 6 mouse
Ca^{2+}	Calcium ion
cAMP	Cyclic adenosine monophosphate
CBFB	Core-binding factor beta
CD	Cluster of differentiation
Cdc	Cell division cycle

CDH1	Cadherin-1 gene
CDK	Cyclin-dependent kinase
CDS	Coding DNA sequence
C/EBPα	CCAAT/enhancer binding protein alpha
CEP-701	Lestaurtinib
CHAPS	3-[(3-cholamidopropyl)dimethylammonio]-1-propanesulfonate
CLL	Chronic lymphocytic leukaemia
CML	Chronic myeloid leukaemia
CN-AML	Karyotypically normal AML
CO_2	Carbon dioxide
Cox	Cyclooxygenase
CPM	Counts per minute
CREB	cAMP response element-binding protein
Csk	c-Src tyrosine kinase
Cys	Cysteine
DAB	Diaminobenzidine
DCF	2,7-dichlorodihydrofluorescein diacetate
ddH_2O	Double distilled water
DEP-1	Density induced phosphatase-1
DMSO	Dimethylsulfoxide
DNA	Deoxyribonucleic acid
DPI	Diphenyleneiodonium chloride
DSS	Disuccinimidyl suberate
DSP	Dual specificity phosphatases
dT	Deoxy-thymine
DTT	Dithiothreitol
dNTP	Deoxyribonucleotide triphosphate
Duox	Dual oxidase
EBP-50	ERM binding protein 50

ECL	Enhanced chemiluminescence
ECM	Extracellular matrix
EGF	Epidermal growth factor
EGFR	Epidermal growth factor receptor
EOL1	Human eosinophilic cell line
ER	Endoplasmic reticulum
ERBB2	Erythroblastic leukaemia viral oncogene homolog 2
Erk	Extracellular regulated kinase
ERM	Ezrin Radixin Moesin
ETO	Eight-twenty-one corepressor
EVI1	Ecotropic viral integration site 1
FAB	French American British
FACS	Fluorescence assisted flow cytometry
F-Actin	Filamentous actin
FAD	Flavin adenine dinucleotide
FBS	Foetal bovine serum
FGF	Fibroblast growth factor
FGFR	Fibroblast growth factor receptor
FL	FLT3 ligand
FL-1	Follicular lymphoma-1
FLK2	Foetal liver kinase 2
FLT3	Fms-like tyrosine kinase 3
FMS	Human colony-stimulating factor 1 receptor
FOXO	Forkhead transcription factor
Fps	Feline sarcoma oncogene
GAPDH	Glyceraldehyde 3-phosphate dehydrogenase
GDI	GDP-dissociation inhibitor
GDP	Guanidine diphosphate
GEF	Guanine exchange factors

GFP	Green fluorescent protein
GKT137831	Genkyotex nox 1/4 inhibitor
Grb2	Growth factor receptor-bound protein 2
Grx	Glutaredoxin
GSH	Reduced glutathione
GSK3ß	Glycogen synthase kinase 3 beta
GSSG	Oxidized glutathione
GTP	Guanidine triphosphate
H_2O_2	Hydrogen peroxide
H_2DCFDA	2,7-dichlorodihydrofluorescein diacetate
HAEC	Human aortic endothelial cells
HCl	Hydrochloric acid
HDAC	Histone deacetylase
HeLa	Henrietta Lacks-derived cell line
HER	Human epidermal growth factor receptor
HETE	Hydroxyeicosatetraenoic acid
HGF	Hepatocyte growth factor
Hic1	Hypermethylated in cancer 1 protein
HIF-1α	Hypoxia inducible factor 1alpha
HIR	Human insulin receptor
HL60	Human promyelocytic leukaemia cells
HMGB	High mobility group box protein
hnRNP	Heterogeneous nuclear ribonucleoproteins
HOCl	Hypochlorous acid
HPV	Human papilloma virus
HPETE	Hydroperoxyeicosatetraenoic acid
HRP	Horseradish peroxidase
HSP	Heat shock protein
HUVEC	Human umbilical vein endothelial cells

IAA	Iodoacetamide
ICAM	Intercellular adhesion molecule
IDH	Isocitrate dehydrogenase
IGF	Insulin-like growth factor
IgG	Immunoglobulin G
IL-3	Interleukin-3
IP	Immunoprecipitation
IPG	Immobilised pH gradient
IR	Insulin receptor
ITD	Internal tandem duplication
JAK	Janus kinase
JMML	Juvenile myelomonocytic leukaemia
JNK	c-Jun N-terminal kinase
KAP	Kinase associated phosphatase
kDa	Kilodalton
KIT	Hardy-Zuckerman 4 feline sarcoma viral oncogene
KPPS	Kinexus^{TM} Phosphatase Screen
LAR	Leukocyte common antigen-related phosphatase
LC	Liquid chromatography
Lox	Lipoxygenase
LPS	Lipopolysaccharide
MAB	Monoclonal antibody
MAPK	Mitogen-activated protein kinase
M-CSF	Macrophage colony-stimulating factor
MDS	Myelodysplastic syndrome
MEK	MAPK/ERK kinase
MKP2	MAP kinase phosphatase 2
MLL	Mixed lineage leukaemia
MLN518	Tandutinib

M-MLV	Moloney Murine Leukaemia Virus
MnSOD	Mitochondrial superoxide dismutase
MPO	Myeloperoxidase
MPS	Myeloproliferative syndrome
mRNA	Messenger RNA
Msr	Methionine sulphoxide reducatase
Myb	Myeloblastosis oncogene
Myc	Myelocytomatosis viral oncogene
NAD	Nicotinamide adenine dinucleotide
NADP	Nicotinamide adenine dinucleotide phosphate
NADPH	Reduced nicotinamide adenine dinucleotide phosphate
NCBI	National Center for Biotechnology Information
NEM	N-ethylmaleimide
NIH	National Institute of Health
NO	Nitric oxide
Nox	NADPH oxidase
NoxA1	Nox1 activator subunit
NoxO1	Nox1 organiser subunit
NP-40	Nonyl phenoxypolyethoxylethanol-40
NPM1	Nucleophosmin 1
nr	Non-redundant
NRAS	Neuroblastoma ras viral oncogene
NRT	Non-reverse transcriptase control
NSC23766	N6-[2-[[4-(diethylamino)-1-methylbutyl]amino]-6-methyl-4-pyrimidinyl]-2-methyl-4,6-quinolinediamine
O_2	Molecular oxygen
$O_2^{\cdot-}$	Superoxide
$^1O_2$	Singlet oxygen
O_3	Ozone

$OH^{\cdot -}$	Hydroxyl radical
$P15^{ink4B}$	Cyclin-dependent kinase 4 inhibitor B
PAC1	Phosphatase of activated cells 1
PAGE	Polyacrylamide gel electrophoresis
PBS	Phosphate buffered saline
PCR	Polymerase chain reaction
PDB	Protein Data Bank
PDGF	Platelet-derived growth factor
PDGFR	Platelet-derived growth factor receptor
PEST	Proline, glutamic acid, serine, and threonine motif
PFF	Peptide fragment fingerprinting
Ph	Philadelphia chromosome
phox	Phagocytic NADPH oxidase
PI3K	Phosphatidylinositol 3-kinase
Pim-1	Proviral integration site 1oncogene
PIR	Protein Information Resource
PKC412	Midostaurin
PKC	Protein kinase C
PKB	Protein kinase B/Akt
PKG	cGMP-dependent protein kinase
PLCγ1	Phospholipase Cgamma 1
PP1	Protein phosphatase 1
PP1/Cα	Protein phosphatase 1, catalytic subunit alpha
PP2	4-Amino-3-(4-chlorophenyl)-1-(t-butyl)-1H-pyrazolo[3,4-d]pyrimidine, 4-Amino-5-(4-chlorophenyl)-7-(t-butyl)pyrazolo[3,4-d]pyrimidine
PP2A	Protein phosphatase 2A
PP2Cα	Protein phosphatase 2C alpha
PP5C	Protein phosphatase 5C

PP6C	Protein phosphatase 6C
PRF	Protein Research Foundation
PRL-3	Phosphatase of regenerating liver-3
Prx	Peroxiredoxin
P-Ser	Phosphoserine
PSTP	Protein serine threonine phosphatase
PSTYP	Dual specificity phosphatase
PtdIns	Phosphatidylinositol
PTEN	Phosphatase and tensin homolog
P-Thr	Phosphothreonine
PTP	Protein tyrosine phosphatase
PTP1B	Protein tyrosine phosphatase 1B
PTPH1	Protein tyrosine phosphatase H1
PTPMEG	Metabolic, endocrine and gastrointestinal PTP
PTPN1	PTP1B gene
PTPN6	SHP2 gene
P-Tyr	Phosphotyrosine
PU-1	Purine-rich box-binding transcription factor
PYP	Protein tyrosine phosphatase
Rac1/2	Ras-related C3 botulinum toxin substrate 1/2
RAR	Retinoic acid receptor
Ras	Rat sarcoma protein kinase
RasGAP	Ras GTPase activating protein
Rcf	Relative centrifugal force
RIPA	Radio immunoprecipitation assay
RNA	Ribonucleic acid
RNS	Reactive nitrogen species
$RO_2^{\bullet}$	Peroxyl radical
$RO^{\cdot}$	Alkoxyl radical

ROS	Reactive oxygen species
Ros	Avian UR2 sarcoma virus oncogene homolog 1
RPMI	Roswell Park Memorial Institute
rRNA	Ribosomal RNA
RT-PCR	Reverse transcriptase polymerase chain reaction
RTK	Receptor tyrosine kinase
RUNX	Runt-related transcription factor
SA	Streptavidin
Scr	Scrambled siRNA
SDS	Sodium dodecyl sulphate
SDS-PAGE	Sodium dodecyl sulfate polyacrylamide gel electrophoresis
SEM	Scanning electron microscopy
SFK	Src family kinase
SH2	Src homology 2 domain
Shc	Src homology 2 domain-containing-transforming protein
SHP-1	Src homology region 2 domain-containing phosphatase-1
SHP-2	Src homology region 2 domain-containing phosphatase-2
shRNA	Short hairpin RNA
siRNA	Short interfering RNA
SMMHC	Smooth muscle myosin heavy chain
SNP	Single nucleotide polymorphism
SOCS	Suppressors of cytokine signalling
SOH	Sulfenic acid
SO_2H	Sulfinic acid
SO_3H	Sulfonic acid
SOD	Superoxide dismutase
Src	Sarcoma kinase
STAT	Signal transducer and activator of transcription
STK1	Stem cell kinase 1

SU11248	Sunitinib
T-ALL	T-cell acute lymphocytic leukaemia
TCA	Trichloroacetic acid
TC-PTP	T-cell protein tyrosine phosphatase
TET2	Tet methylcytosine dioxygenase 2
TGF-ß	Transforming growth factor beta
TK	Tyrosine kinase
TKD	Tyrosine kinase domain
Tks	Tyrosine kinase substrate
TNF-α	Tumour necrosis factor alpha
TP53	P53 gene
Trx	Thioredoxin
TrxR	Thioredoxin reductase
Ub	Ubiquitin
UCSC	University of California, Santa Cruz
UniProt	Universal Protein Resource
UV	Ultraviolet radiation
VAS2870	1,3-Benzoxazol-2-yl-3-benzyl-3H-[1,2,3]triazolo[4,5-d]pyrimidin-7-yl sulfide, 7-(1,3-Benzoxazol-2-ylsulfanyl)-3-benzyl-3H-[1,2,3]triazolo[4,5-d]pyrimidine, 7-(2-Benzoxazolylthio)-3-(phenylmethyl)-3H-1,2,3-triazolo[4,5-d]pyrimidine
VEGF	Vascular endothelial growth factor
VEGFR	Vascular endothelial growth factor receptor
VHR	Vaccinia H1-related phosphatase
WHO	World health organisation
WT	Wild type
WT-1	Wilms tumor protein-1
ZO-1	Zonula occludens protein -1

Chapter 1

General Introduction

1. Leukaemia

1.1 Classification of Leukaemia

The term leukaemia is derived from the Greek *leukos* (white) and *aima* (blood), and refers to a spectrum of haematological neoplasms of the blood and bone marrow characterised by the de-regulated expansion of white blood cells. With an incidence rate of 12.3 per 100,000 in adults, leukaemia accounts for approximately 3% of cancers diagnosed each year and accounts for a third of all cancer-deaths in children under 15 years (LLS, 2011a). Leukaemia is classified according to the lineage of white blood cells affected, myeloid or lymphoid, as well as whether the rate of progression is chronic or acute. Acute leukaemia, which is the most common form in children, refers to the rapid accumulation of immature blasts, while chronic leukaemia describes the excessive build up of more mature abnormal cells over a period of months or years (LLS, 2011b).

1.2 Acute Myeloid Leukaemia

Acute Myeloid Leukaemia (AML) accounts for about 25% of all leukaemias and is the second most frequent form after Chronic Lymphocytic Leukaemia (CLL) (Jemal *et al.*, 2002). AML is characterised by the rapid expansion of immature precursor myeloid blasts, which do not differentiate into mature and functional monocytes or granulocytes, but accumulate in the bone marrow and interfere with normal haematopoiesis (Bonnet and Dick, 1997). It is thought that a small sub-population of leukaemic stem cells are responsible for the generation and maintenance of leukaemia as the leukaemic blasts themselves are limited in their proliferative capacity (Bonnet and Dick, 1997). The leukaemic stem cells originate

from haematopoietic stem cells of the myeloid lineage which have undergone a disruption in their development due to transforming mutations. This disruption leads to a block in the differentiation of the progenitor cell which then gives rise to the pool of leukaemic blasts which are similarly halted at that level of differentiation. The transformation event can occur at various stages of stem cell development, which is why there is an extensive degree of heterogeneity amongst patients with AML at the genetic, phenotypic and clinical levels (Fialkow *et al.,* 1981; Griffin and Lowenberg, 1986). There are two classification systems for AML; the French-American-British (FAB) classification system which divides AML into 8 subtypes, M0-M7, according the type of cell affected and the stage of differentiation using light microscopy and cytogenetics (Bennett *et al.*, 1976), and the World Health Organisation (WHO) classification which uses morphology, immunophenotype, genetics, and clinical features to describe the sub-types (Vardiman *et al.*, 2002).

Phases of the disease

AML can arise very rapidly and if untreated can prove fatal in a matter of months. Some AML sub-types are preceded by a pre-leukaemic blood disorder such as myelodysplastic syndrome (MDS) or myeloproliferative syndrome (MPS), periods of anaemia and poor blood cell production which can then develop into leukaemia. These disorders are more common in the elderly and are viewed as a phase in a multi-step pathogenesis with approximately 30% of patients with MDS going on to develop AML (Nolte and Hofmann, 2011). It is thought that the accumulation of genetic and molecular abnormalities in the early stages of MDS trigger the progression from dysplasia to neoplasia (Nolte and Hofmann, 2011). The progression to AML is diagnosed by the percentage of defective bone marrow blasts

with cut-off points of 30% for FAB classification and 20% in the WHO system (Vardiman *et al.*, 2002). AML can also occur in patients who have undergone chemotherapy for another malignancy (Thirman *et al.*, 1993), been exposed to benzene or other carcinogenic aromatic compounds (Austin *et al.*, 1988) or high doses of ionising radiation (Bizzozero *et al.*, 1966). In these cases the exposure to the mutagen causes genetic mutations or chromosomal abnormalities which lead to AML. Familial AML, caused by the transmission of inherited mutations accounts for the increased likelihood of members of the same family developing the disease (Gunz and Veale, 1969). AML can also arise as the result of other genetic disorders such as Down's syndrome (Evans and Steward, 1972), Li-Fraumeni (Anensen *et al.*, 2006), Fanconi's anaemia (Butturini *et al.*, 1994), neurofibromatosis type 1 (Balgobind *et al.*, 2008), or Noonan syndrome (Chantrain *et al.*, 2007).

Molecular mechanisms of disease

AML refers a heterogeneous group of diseases, the molecular basis of which can be complex and multi-factorial. A range of genetic as well as cytogenetic abnormalities have been identified which lead to the molecular alterations giving rise to the AML phenotype. Chromosomal aberrations including balanced translocations, inversions, deletions, monosomies and trisomies are detected in 51% of AML cases (Dohner and Dohner, 2008), and were widely used in the past as both diagnostic and prognostic factors in AML. The advancement of molecular genetics techniques in recent years, such as microarray technology, has allowed high density genomic-wide analysis and has resulted in the identification of specific gene mutations and de-regulations which contribute to the initiation and progression of AML.

Chromosomal abnormalities

The most common chromosomal aberrations which occur in AML are; 1% inversion(3)/translocation(3;3), 1% translocation(6;9), 2% translocation(11q23), 2% translocation (9;11), 6% inversion(16)/translocation(16;16), 5% translocation(8;21), 23% are defined as having a various karyotypes including trisomy 8, 11, 13, 21 and 22, loss of 5q, chX , Y or 7, and 11% as being a complex karyotype of multiple losses, gains and rearrangements (Dohner and Dohner, 2008; Nolte and Hofmann, 2011).

Gene mutations

The cytogenetic abnormalities mentioned above can give rise to gene mutations, but in the 49% of AML cases which are defined as karyotypically normal (CN-AML), these mutations can occur independently of any chromosomal changes. The most common gene mutations associated with AML fall into two classes, signal transduction genes which do confer a proliferative or survival advantage but do not affect differentiation (Class I), and transcription factor genes which affect differentiation and apoptosis (Class II). The Class I genes are *nucleophosmin 1* (*NPM1)*, *Fms-related tyrosine kinase II (FLT3*), *NRAS*, and *KIT* whereas Class II genes include *CBFB/SMMHC*, *AML1/ETO*, *RUNX*, *PML/RARα*, *EVI1* and *WT1* (Nolte and Hofmann, 2011; Gilliland and Griffin, 2002). It is proposed in the 'two-hit' hypothesis of leukaemic progression, that expression of both classes of genes together contributes to the AML phenotype of impaired differentiation and enhanced survival (Gilliland and Griffin, 2002).

Additionally, in AML sub-types classified as being of a complex aberrant karyotype, mutations in the *TP53* gene are more common than in CN-AML (Haferlach *et al.*, 2008). As a tumour suppressor which triggers apoptosis in DNA-damaged and potentially tumourigenic cells, disruption or loss of one or both alleles of *TP53* is common in a wide range of tumour types and is associated with genomic instability and aneuploidy (Schmitt *et al.*, 2002).

Mutations in the cytosolic isocitrate dehydrogenase I (*IDH1)* gene and its mitochondrial homolog *IDH2* have been linked to the activation of HIF-1α, which promotes tumour growth in low oxygen conditions (Ward *et al.*, 2010; Zhao *et al.*, 2009), as well as disruptions of the epigenetic regulation (Prensner and Chinnaiyan, 2011). *IDH* mutations have been identified in breast, colon cancers (Yen *et al.*, 2010) and glioblastomas (Dang *et al.*, 2010; Prensner and Chinnaiyan, 2011), and when *IDH* mutations occur in AML they are viewed as poor prognostic indicators and are thought to drive disease progression (Prensner and Chinnaiyan, 2011).

Epigenetic modifications

While not strictly a gene mutation, epigenetic alterations can prove as disruptive to gene expression and function as conventional sequence mutations. Hypermethylation of DNA and acetylation of histones are the mechanisms by which genes are rendered silent while the gene sequence itself remains unchanged. The addition of methyl groups to CpG islands in gene promoters prevents the binding of transcription factors and other proteins that affect transcription (Watt and Molloy, 1988). Hypermethylation is detected in the promoter region of $P15^{INK4B}$, an inhibitor of the complex cyclin D/cyclin dependent kinase 4, in gliomas, acute lymphoblastic leukaemia (ALL) and AML (Herman *et al.*, 1997; Jaenisch and Bird, 2003). Other

targets for hypermethylation in AML are the oestrogen receptor gene (Issa *et al.*, 1996), E-Cadherin gene *(CDH1)*(Corn *et al.*, 2000) and the zinc finger transcription factor gene *HIC-1* (Aggerholm *et al.*, 1999; Issa *et al.*, 1997).

Histone acetylation is the process whereby acetyl groups are added to lysines in the N-terminal tail of histone proteins, resulting in a neutralisation of the overall positive charge on the histones leading to a looser association between the histone proteins and the negatively charged DNA (Clayton *et al.*, 2006). This process is carried out by histone acetylases and facilitates increased access to the DNA by transcription factors and RNA polymerases, allowing increased transcription. Acetylation is a reversible process and the acetyl groups can be removed by histone de-acetylases (HDAC), the recruitment of which is altered in a range of tumour types including AML, leading to repression of genes. Crucially in AML this results in the silencing of transcription factor determinant *C/EBPα* which regulates granulocytic maturation (Pabst *et al.*, 2001).

Single nucleotide polymorphisms

In addition to these mutations and modifications, in which the genes affected can be functionally linked to AML progression, single nucleotide polymorphisms (SNPs) in the *TET2* oncogene have been detected in ~15% of MDS and AML (Kosmider *et al.*, 2009).While the function of this gene in leukemogenesis and normal haematopoiesis is not yet known, the *TET2* mutation is detectable in the early stages of MDS and so is classified as a favourable prognostic marker in contrast to mutations in *NRAS* (Paquette *et al.*, 1993) and *TP53* (Christiansen *et al.*, 2001) or hypermethylation of $p15^{INK4B}$ (Christiansen *et al.*, 2003) which are viewed as late-stage mutations and offer poor prognosis.

FLT3 mutations

The FMS-like tyrosine kinase 3 (FLT3), also known as foetal liver kinase 2 (FLK2) and human stem cell kinase 1 (STK1) (Small *et al.*, 1994), is a membrane-bound receptor tyrosine kinase (RTK) and member of the RTK subclass III which also includes macrophage-colony stimulating factor (M-CSF) receptor (FMS), KIT and platelet-derived growth factor (PDGF) (Nolte and Hofmann, 2011, Stirewalt and Radich, 2003). This subclass regulates the survival, apoptosis, differentiation and proliferation of haematopoietic cells, and FLT3 is mostly expressed on early progenitor cells of the myeloid and lymphoid lineages which are $CD34^+$ (Nolte and Hofmann, 2011, Stirewalt and Radich, 2003). RTK III members contain five immunoglobin-like extracellular domains, a transmembrane domain, a juxtamembrane domain and two intracellular tyrosine kinase domains (TKD) linked by a kinase insert domain (Stirewalt and Radich, 2003). There are two forms of the FLT3 receptor, a 160 kDa mature glycosylated form which is membrane-bound and a 130 kDa non-glycosylated form which is cytoplasmic (Carow *et al.*, 1996; Lyman *et al.*, 1993). Glycosylation signals the maturation of the receptor and its translocation to the membrane. The inactive receptor exists in monomeric form at the membrane until it is bound by the FLT3 ligand (FL), a cell surface transmembrane protein type I which undergoes proteolytic processing or alternative splicing to become a secreted polypeptide (Wodnar-Filipowicz, 2003). FL is produced by marrow stromal fibroblasts and T lymphocytes and displays synergy with other growth factors and interleukins to stimulate proliferation of early progenitor or stem cells (Lyman, 1995). When FL binds FLT3 it induces dimerisation of the receptor and autophosphorylation of its TKDs, this stimulates phosphorylation of downstream

effectors, following which the dimerised receptors become internalised and degraded within the cell (Stirewalt and Radich, 2003).

Dosil *et al*. (1993) first investigated the signalling pathways stimulated by FLT3 by generating a chimeric receptor composed of the extracellular domain of FMS and the transmembrane and cytoplasmic domains of murine FLK2/FLT3. They demonstrated that FLT3 signalling in interleukin 3 (IL-3)-dependent Ba/F3 lymphoid cells removed the requirement for IL-3, promoted and maintained cell proliferation. They also showed that PLCγ1, Ras GTPase-activating protein (RasGAP), the p85 subunit of phosphatidylinositol 3'-kinase (PI3K), the adaptor proteins Shc and the growth factor receptor-bound protein 2 (Grb2), the guanine nucleotide exchange factor Vav, and the proto-oncogenic tyrosine-protein kinases Fyn and Src are components of theFLK2/FLT3 signal transduction pathway. Of those components, PLCγ1, p85, Shc, Grb2, and Src family TKs, physically associate with the FLK2/FLT3 cytoplasmic domain. More recently, FLT3 signalling was also shown to result in the activation of Akt and MAPK further downstream (Hayakawa *et al.*, 2000; Takahashi, 2006).

FLT3 is also one of the most commonly mutated genes in haematological malignancies and can be detected in 1-3% of patients with ALL, 5-10% of MDS patients and in 15-35% of AML patients (Nakao *et al.*, 1996; Stirewalt and Radich, 2003) and confers a poor prognosis (Pratz and Levis, 2008). The two most common types of FLT3 mutations are internal tandem duplications of exons 14 and 15 of the juxtamembrane domain (FLT3-ITD), which are detectable in about 15% of AML patients, commonly in patients with translocations t(15;17) but also in AML-CN patients with *NPM1* mutations (Takahashi, 2011), and missense point mutations in

exon 20 of the TK domain (FLT3-TKD) which are found in 5-10% of AML cases (Stirewalt and Radich, 2003). In both instances the mutations result in the constitutive activation and autophosphorylation of the receptor in the absence of the FL, though reports indicate that stimulation with FL can result in increased abnormal blast proliferation in patients who have the FLT3-ITD mutation as well as those who have wild type FLT3 (FLT3-WT) (Bruserud *et al.*, 2003), suggesting that the mutant receptor may still be responsive to the ligand and stimulation with the ligand can further increase signalling from the already constitutively active receptor if it positioned correctly at the membrane. However, when the receptor is mutated it can become retained in biosynthetic compartments such as the endoplasmic reticulum (ER) instead of being trafficked to the membrane (Schmidt-Arras *et al.*, 2009). Choudhary *et al.* (2009) showed that this mis-localisation results in altered signalling from the constitutively active receptor with aberrant activation of STAT5 and its transcriptional targets Pim-1/2 but no activation of PI3K or MAPK pathways which are usually triggered by constitutive signalling from the mutant receptor at the membrane.

1.3 Mechanisms of FLT3-ITD pathogenesis

Oncogenic FLT3-ITD signalling is thought to contribute to AML progression in two ways. Firstly *via* direct activation of the pro-survival Ras/MEK/Erk and PI3K/Akt pathways (Gilliland and Griffin, 2002), which are also stimulated by wild type FLT3 but only in response to appropriate growth factor stimulation by FL binding. In addition to this and in contrast to FLT3-WT signalling, FLT3-ITD activates STAT5, especially when the receptor is localised to the ER as mentioned above. This results in up-regulation of STAT5 target gene SOCS which alters

cytokine signalling (Choudhary *et al.*, 2007), proto-oncogenes Pim-1/2 serine/threonine kinases which promote cell cycle progression, apoptosis and transcriptional activation (Bachmann and Moroy, 2005; Choudhary *et al.*, 2009), cyclin D1, c-myc and the anti-apoptotic gene p21 (Calo *et al.*, 2003; Takahashi *et al.*, 2004). As well as STAT5, FLT3-ITD influences several myeloid transcription factors such as PU.1 (Rosenbauer *et al.*, 2004)and C/EBPα (Radomska *et al.*, 2006) both of which are inhibited by FLT3-ITD activity causing a block in differentiation of myeloid precursor cells and an accumulation of immature blasts (Zheng and Small, 2005). Through activating the PI3K/Akt pathway FLT3-ITD indirectly negatively regulates the FOXO family of forkhead transcription factors, specifically FOXO3a and its target genes pro-apoptotic *Bim1* and cyclin-dependent kinase inhibitor *P27KIP1* (Takahashi, 2011).

FLT3 signalling has also been associated with the increased production of reactive oxygen species (ROS) which can cause double-stranded breaks in DNA, contributing to the genomic instability so frequently observed in AML (Sallmyr *et al.*, 2008b). As well causing DNA damage, increased ROS levels can have a transforming effect on the cell by functioning as signalling molecules and stimulating abnormal proliferation and survival (Naughton *et al.*, 2009). The recognition of ROS as signalling molecules in their own right has been prompted by the emergence of evidence for ROS playing a role in a diverse range of cellular processes including cell survival (Naughton *et al.*, 2009), regulation of transcription factors (Tothova *et al.*, 2007), and migration (Diaz *et al.*, 2009; Ferraro *et al.*, 2006). Increased levels of ROS production, driven by the activity of oncogenes and growth factors, have been detected in a number of tumour types (Hole *et al.*, 2012,

Mitsushita *et al.*, 2004; Weinberg and Chandel, 2009; Wu, 2006) leading to aberrant oxidant signalling and contributing to a tumourigenic phenotype. Specifically with regard to haematopoietic tumours, oxidative stress triggered by excessive production of ROS can be found in myeloid leukaemias including chronic myeloid leukaemia (CML) and AML as well as acute lymphoblastic leukaemia (ALL) and MDS (Battisti *et al.*, 2008; Farquhar and Bowen, 2003; Hole *et al.*, 2012). It is thought that FLT3 signalling triggers ROS generation by activating the NADPH oxidase (Nox) family of ROS producers, *via* STAT5a and Rac1 in AML cells (Reddy *et al.*, 2011; Sallmyr *et al.*, 2008a).

1.4 Treatment of AML

AML treatment is divided into two phases, chemotherapeutic induction of remission and post-remission consolidation therapy which consists of additional chemotherapy and/or allogenic or autologous stem cell transplantation. The average complete response rate, when the cancer disappears after treatment, with this mode of treatment is between 60% to 70% with long-term survival rates from 25% to 35% (Kantarjian *et al.*, 2008). The induction of remission phase aims to reduce the amount of abnormal cells to an undetectable level, however despite this intervention, some leukaemic cells can remain in number too low to be detected and if the initial induction phase is not followed by a consolidation phase then the patient is likely to relapse (Abeloff, 2004). The consolidation treatment options are considered based on the genetic basis for the disease and can therefore vary from patient to patient depending on the karyotype and mutation profile of the affected cells (Estey, 2001). Patients with karyotypes that are considered favourable, such as those with inv(16), t(8;21), and t(15;17), are given a further dose of intensive chemotherapy

(Appelbaum *et al.*, 2000; Mayer *et al.*, 1994). Whereas patients with high-risk cytogenetics, underlying MDS, or therapy-related AML are classified as being at high risk of relapse and for these patients allogenic stem cell transplantation from a suitable donor is usually attempted (Appelbaum *et al.*, 2000).

FLT3 mutations are one of the more common molecular abnormalities found in AML, and so FLT3 has become the focus of worldwide research in an attempt to develop a targeted therapy. In general AML patients with FLT3-ITD mutations have pronounced leukocytosis, a hypercellular bone marrow and intermediate risk cytogenetics. The complete remission rate after induction is similar to that of patients with wild type FLT3 but there is a much greater risk of relapse (Levis and Small, 2003). It is thought that targeting FLT3-ITD alone will not significantly improve the outcome for patients with the mutation, but that in combination with chemotherapy may generate synergistic effects which will improve upon results seen with chemotherapy alone (Pratz and Levis, 2008). To date, more than 20 compounds have been reported in the literature to function as FLT3-ITD inhibitors (Pratz and Levis, 2008, Wiernik, 2010), and several of these have been taken to clinical trials (DeAngelo *et al.*, 2006; Fischer *et al.*, 2010; Giles *et al.*, 2003; Kindler *et al.*, 2010, O'Farrell *et al.*, 2003; Smith *et al.*, 2004; Stone *et al.*, 2005; Weisberg *et al.*, 2002). The compounds are heterocyclic and either function as ATP competitors or are structurally analogous to the intermediary complex of a tyrosine covalently bound to ATP, so that they fit into the ATP-binding compartment of FLT3-ITD, as well as that of other RTKs. This prevents ATP binding, which is necessary to initiate the FLT3-ITD auto-phosphorylation signalling cascade (Pratz and Levis, 2008). Clinical trials have shown that the FLT3-ITD inhibitors Lestaurtinib (CEP-701), Midostaurin

(PKC412), Sunitinib (SU11248) and Tandutinib (MLN518) inhibit FLT3-ITD autophosphorylation *in vivo*, resulting in the clearance of peripheral blood leukaemia cells, yet only very rarely affecting the bone marrow population (Weisberg *et al.*, 2009).This means that the effects were short-lived, as the leukaemic stem cells in the bone marrow re-populated the peripheral blood with resistant blasts, highlighting the limits of the FLT3-ITD inhibitors as a monotherapy. However, several FLT3-ITD inhibitors have been tested in combination with conventional chemotherapeutics (Stone *et al.*, 2012) and are hoped to provide a viable treatment opportunity, especially to patients for whom transplantation is not an option. Similar approaches in ALL patients who carry Bcr-Abl, the chimeric oncogenic TK, have yielded very positive results in clinical trials which combined the TK inhibitor Imatinib with chemotherapeutic agents (Thomas *et al.*, 2004).

2. ROS Signalling

2.1 ROS

ROS refers to the highly reactive derivatives of oxygen including radicals such the oxygen ions superoxide ($O_2^{\bullet-}$), hydroxyl ($^{\bullet}OH$), peroxyl ($RO_2^{\bullet}$), and alkoxyl ($RO\cdot$), possessing unpaired valence shell electrons, as well as the non-radical peroxides hypochlorous acid (HOCl), ozone (O_3), singlet oxygen ($^1O_2$), and hydrogen peroxide (H_2O_2) (Bedard and Krause, 2007) which, because of their un-stable O-O linkage, are volatile sources of further radicals (Nic *et al.*, 2006). In cell biology, ROS have been long regarded as by-products of a cascade of reactions, stemming from cellular oxygen metabolism. Aerobic respiration results in the production of ROS as a side effect of the activity of the electron transport chain (Figure 1). In this situation, $O_2^{\bullet-}$ is formed when oxygen is prematurely reduced by a

single electron, but the free radical is quickly neutralised by the mitochondrion's own antioxidant defence system of mitochondrial superoxide dismutase (SOD) and peroxidases. Conditions of hypoxia, damage to the mitochondria itself, or reduced levels of these free radical scavenging enzymes result in increased 'leakage' of ROS from the mitochondria, leading to an intracellular environment of oxidative stress which triggers apoptosis (Simon *et al.*, 2000).

These ROS, if permitted to accumulate to toxic levels, can have detrimental effects on cellular biomolecules, such as proteins and lipids, leading to apoptosis. In addition to this, exposure of DNA to ROS results in the formation of double stranded breaks and oxidatively modified bases. These lesions can interfere with the coding sequences, as in the case of cytosine deamination events causing G-C to T-A transition mutations, as well as disrupting DNA structure or RNA polymerase activity. These lesions, if not repaired, can also trigger apoptosis or may even prove oncogenic (Cooke *et al.*, 2003). It has been shown that many different tumour types produce ROS at levels higher than in their normal counterparts (Hole *et al.*, 2012; Mitsushita *et al.*, 2004; Weinberg and Chandel, 2009; Wu, 2006), stimulating pro-mutagenic lesions which contribute to the tumourigenic phenotype.

Other molecules prone to oxidative damage include lipids. Lipid peroxidation, particularly of the polyunsaturated fatty acids which compose the plasma membrane and internal cellular compartmental membranes, results in the formation of fatty acid radical and lipid peroxides, leading to deterioration and eventual rupturing of the cell membrane (Mylonas and Kouretas, 1999).

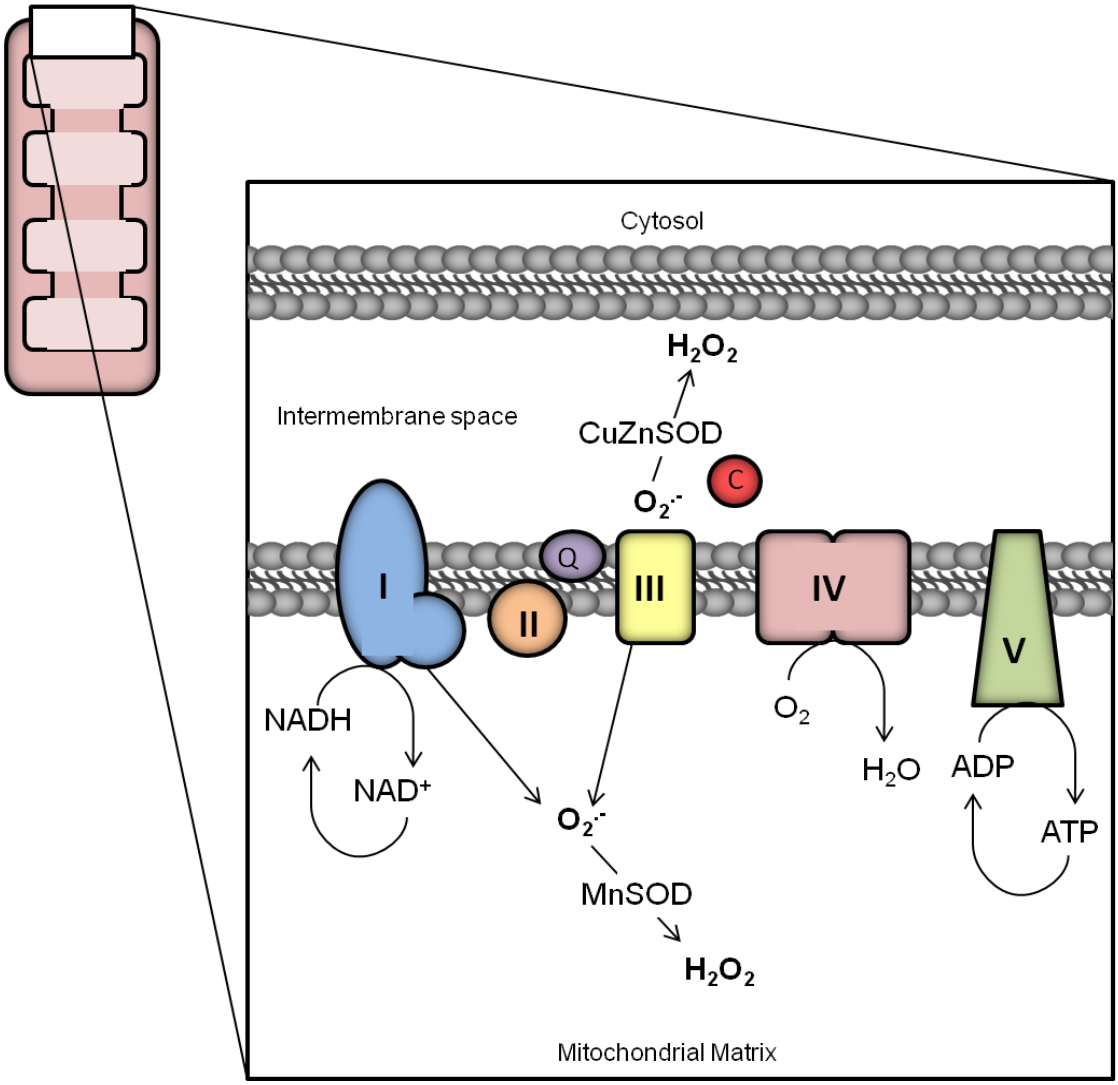


Figure 1. ROS production by the mitochondrial respiratory chain

The inner mitochondrial membrane bound-respiratory chain consists of Complex I- NADH dehydrogenase complex, II- succinate-dehydrogenase coenzyme Q reductase, III- cytochrome b-c1 complex, IV- cytochrome oxidase complex and V- ATP synthase. During the transfer of electrons from NADH to oxygen (O_2) and the concurrent production of ATP, the relationship between the pool of available NADH electron donors, local O_2 concentration and the efficiency of ATP synthase determines the amount of superoxide ($O_2^{\bullet-}$) which is produced. Mitochondrial antioxidants manganese superoxide dismutase (MnSOD) in the matrix, and copper/zinc SOD (CuZnSOD), localised to the intermembrane space, convert the $O_2^{\bullet-}$ into the membrane permeable hydrogen peroxide (H_2O_2).

Proteins are the main targets of ROS within the cell, accounting for approximately 69% of oxidation events, due to their abundance and high rate constants for oxidation-reactions compared to lipids (18%) and nucleic acids (15%) (Davies, 2005; Sheehan, 2006). Thus, it is possible that proteins evolved to act as a form of buffer, by absorbing oxidants and preventing oxidation-induced DNA mutation, or oxidation and rupture of lipid membranes. This trade-off would have resulted in oxidative-modifications to proteins. The consequences of protein-oxidation depend on the concentration and species of ROS involved, but also vary hugely from protein to protein depending on their individual biochemical and structural characteristics. Oxidation-induced changes in the charge, size, hydrophobicity or polarity of the amino acids in a polypeptide can affect its secondary and tertiary structure, dictating the stability and activity of the whole protein. Oxidation of amino acid side chains causes inter- and intra-molecular cross-linkages while the polypeptide backbone is prone to $^{\bullet}OH$ attack resulting in protein fragmentation and degradation (Berlett and Stadtman, 1997). Sulfur-containing amino acids such as cysteine and methionine are the most easily oxidized (Janssen-Heininger *et al*., 2008), and also the most relevant, from a physiological perspective, as these oxidation events can be reversible (Hoshi and Heinemann, 2001).

Also warranting a mention at this point is the analogous process of s-nitrosylation. This system of the covalent attachment of a nitrogen monoxide group to a cysteine residue, has been extensively reviewed (Hess *et al*., 2005), and occurs as a result of exposure to reactive nitrogen species (RNS). An ‘acid-base’ motif is thought to signify s-nitrosylation-susceptible sites on proteins, which is based on the

relative placement of charged amino acids in order to facilitate a low pKa (Stamler *et al.*, 1997).

Hess *et al.*, (2005) comment on the potential cross-talk between oxidation and s-nitrosylation, as dual systems of cysteine modification, and propose a redox-signalling model whereby s-nitrosylation functions as the 'primary effector', and oxidation as a form of allosteric moderator, affecting the ability of a target to respond to s-nitrosylation. As outlined by Hess *et al*. (2005), this model applies readily to the ryanodine receptor/Ca2+ channel and erythrocytic haemoglobin.

Antioxidants

Cells have evolved a variety of methods of coping with and reducing oxidative stress because of the potentially devastating effects which intracellular oxidants can inflict. Oxidation of methionine within proteins is thought to represent a form of antioxidant system, by readily scavenging oxidant species and thereby limiting the exposure of other residues (Luo and Levine, 2009). The oxidation of methionine results in the generation of methionine-sulfoxide and can be reversed by the activity of methionine sulfoxide reductase (MsrA/B) utilising a thioredoxin (Trx) co-factor (Lee and Gladyshev, 2011). This suggests that the cycling of methionine between oxidized and reduced states is an enzymatically-regulated mechanism which has evolved to buffer against the presence of ROS. Methionine oxidation can also proceed past the formation of methionine sulfoxide, to the hyperoxidized form methionine sulfone, which cannot be reversed (Stadtman *et al*. 2003).

Endogenous cellular antioxidant enzymes are also expressed in virtually every cell type and efficiently scavenge and neutralise free radicals to prevent toxic

accumulation. Amongst the most active and widespread antioxidants is the glutathione (GSH) system. GSH can reduce disulfide bonds formed as a result of cysteine oxidation, crucial for the regeneration of other anti-oxidants such as glutaredoxins (Grx) which rely on GSH as a co-factor. This reaction requires the oxidation of GSH to oxidized-GSH (GSSG), before it is reduced back to GSH by GSH reductases. GSH has such a prominent role in ROS defence that its own redox state is an important indicator of the redox state of the cell, so much so that the oxidised form is frequently used as a biomarker for oxidative stress (Pastore *et al.*, 2001).

The process of s-glutathionylation, the reversible formation of a mixed disulfide between an oxidized cysteine residue and GSH, occurs as a result of both oxidative and nitrosative stress and is thought to protect proteins from further oxidation as well as modulating their function to facilitate the relaying of signals (Dalle-Donne *et al.*, 2009; Giustarini *et al.*, 2005). Cysteines which are s-glutathionylated, in order to prevent hyperoxidation, are likely to be crucial to the stability or activity of the protein, though their modification may temporarily inactivate the enzyme, or alter its signalling capacity. This modification is reversed under reducing conditions by the actions of Grx or Trx (Shelton *et al*., 2005).

Another important antioxidant is Trx, part of a group of interacting molecules in the Trx system, The system refers to Trx, which catalyses the reduction of proteins through cysteine thiol-disulfide exchange, as well as Trx-reductase (TrxR) which regenerates Trx, and its co-factor and electron donor NADPH (Nordberg and Arner, 2001). Other ubiquitous antioxidants include SOD, which catalyses the conversion of $O_2^{\bullet -}$ to H_2O_2 (McCord and Fridovich, 1988), GSH

peroxidases, which convert lipid hydroperoxides to alcohols and H_2O_2 to H_2O (Arthur, 2000), and catalase which also neutralises H_2O_2 (Chelikani *et al.*, 2004).

Peroxiredoxins

More recently another class of cellular redox scavengers have emerged, the peroxiredoxins (Prx). These enzymes are defined by their ability to reduce hydroperoxides and peroxynitrite (Rhee *et al.*, 2012) . Similarly to GSH, the redox reaction catalysed by Prx involves the oxidation of Prx molecules themselves, and a thiol-dependent cycling back to the reduced state. Prx appear to be unique amongst cysteine-containing proteins, in that they are able to recover from hyper-oxidation of their cysteine residues to sulfinic acids. A slow reduction of sulfinic acid-containing Prx requires ATP-dependent activity of sulfiredoxins (Srx) and is thought to be an adaptation unique to eukaryotic cells to facilitate the temporary, localised accumulation of high levels of H_2O_2 for signalling purposes (Cordray *et al.*, 2007). This so called 'Floodgate' hypothesis with regard to Prx oxidation describes a dual role for Prx as general antioxidant defence enzymes, the 'ancestral role', as well as regulators of spatially defined redox signalling (Poole *et al.*, 2004; Wood *et al.*, 2003; Choi *et al.*, 2005; Rhee *et al.*, 2005).

The tight control of ROS levels within the cell highlights the potentially devastating effects that de-regulation of these molecules can have on the cellular integrity, genetic material and other crucial molecular components. However, more recently the recognition of ROS as mediators of cellular communications has prompted their classification as signalling mediators in their own right. Even prior to this role being identified, it was known that production of ROS was not always a side effect of cellular respiration. Aside from the incidental generation of ROS as by-

products of metabolism, the professional production of ROS is becomingly increasingly recognised as an important source of intercellular oxidants. The lipoxygenase (Lox) and cyclooxygenase (Cox) families of enzymes are responsible for ROS production for the purposes of fatty acid metabolism and the biosynthesis of hormones and inflammatory mediators (Figure 2). Lipid peroxide intermediates, such as hydroperoxyeicosatetraenoic acids (HPETEs), are formed initially which are highly reactive oxidising molecules themselves and have been shown to inactivate PTPs (Conrad *et al.*, 2010). In addition to this, 12-Hydroxyeicosatetraenoic acid (12(S)-HETE), and 15-S-Hydroxyeicosatetraenoic acid (15(S)-HETE), the end products of the Lox pathway, can stimulate ROS production by the Noxs (Serezani *et al.*, 2005).

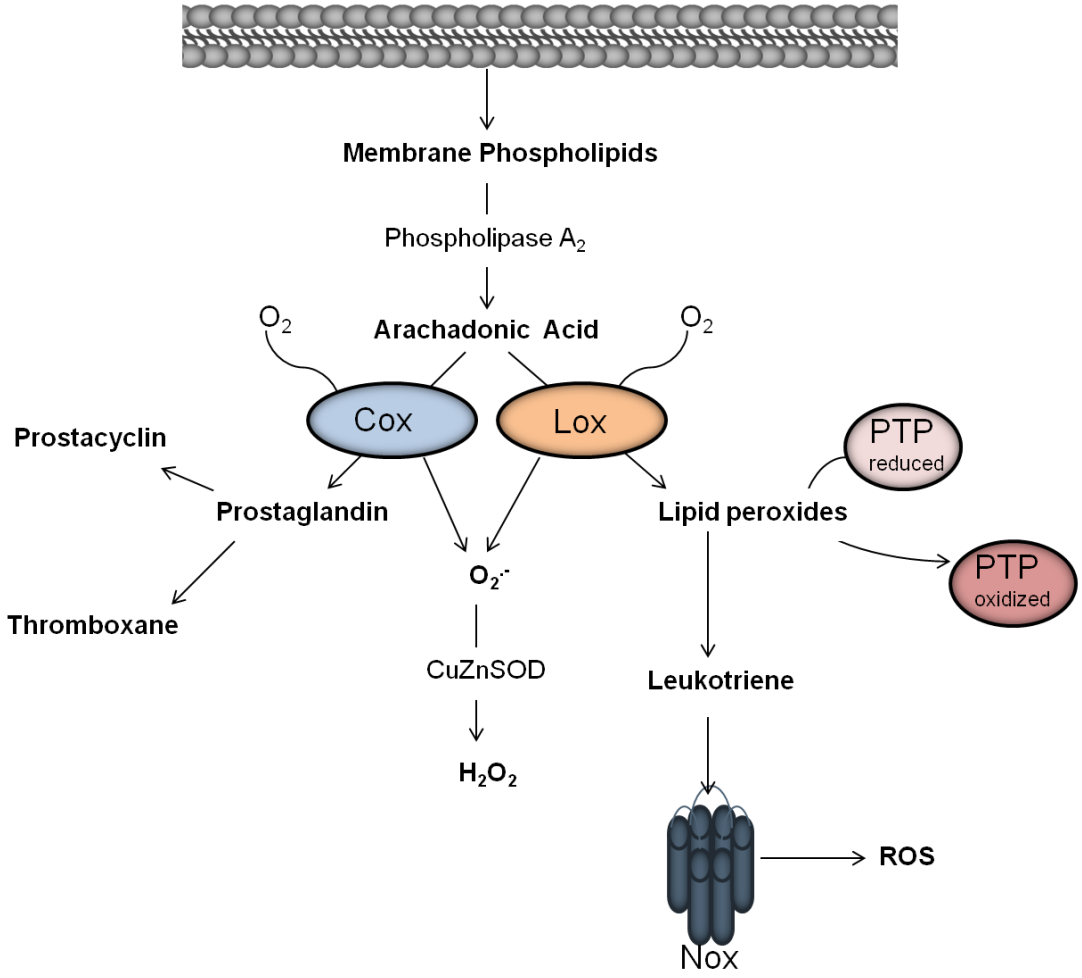


Figure 2. The production of ROS by the Lox and Cox

Eicosanoid biosynthesis proceeds *via* the oxidation of fatty acids, such as arachadonic acid, catalysed by the Lox enzymes, resulting in the formation of leukotrienes, or the Cox enzymes which produce prostaglandins. Both pathways require the addition of molecular oxygen (O_2) to arachadonic acid and involve the production of ROS as a by-product of this oxidative step.

2.2 Nox

The generation of ROS is known to be the primary function of the Nox family of enzymes (Figure 3). The ROS generated by the Nox in the phagosomes of professional phagocytic cells such as the neutrophils, monocytes, macrophages, dendritic cells, and mast cells were initially shown to be responsible for the killing of endocytosed bacterial pathogens (Robinson and Badwey, 1995). The subsequent discoveries of Nox enzymes in cells other than phagocytes, such as vascular smooth muscle cells (Griendling *et al.*, 1994), fibroblasts (Meier *et al.*, 1991), thyroid cells (De Deken *et al.*, 2000), neurons (Serrano *et al.*, 2003), hepatocytes (Reinehr *et al.*, 2005) and endothelial cells (Gorlach *et al.*, 2000) amongst others, prompted the question of what functions are being fulfilled by Nox enzymes in non-phagocytic cells.

The Nox family of professional ROS producers consists of 7 isoforms of the catalytic subunit of the Nox holoenzyme complex; Nox 1-5, as well as the Dual oxidases (Duox) 1 and 2. Nox 2, or gp91phox as it was originally called, is the prototypic Nox first identified in phagocytes as being required for oxidant-dependent microbial killing (Lambeth, 2004).The Nox isoforms share several conserved structural features. The catalytic subunit is a transmembrane protein containing electron-transferring FAD and heme groups capable of removing an electron from the preferential donor substrate, cytosolic NADPH, and using this electron to reduce molecular oxygen in the extracellular or phagosomal space, resulting in the generation of (Bedard and Krause, 2007). The generated can be transported across the plasma membrane through ion channels, but more frequently is rapidly converted into H_2O_2,, which may then diffuse back across the membrane with the aid of

aquaporin channel proteins (Bienert *et al.*, 2007). The Nox isoforms differ in terms of additional domains of the catalytic subunit. Nox 1, 2, 3 and 4 share the most homology (Bedard and Krause, 2007) and have very similar catalytic core domain structure, whereas Nox 5 contains an additional intracellular amino-terminal calcium binding domain (Banfi *et al.*, 2001). The Duox 1 and 2 possess this domain as well as a further transmembrane amino-terminal peroxidase-like domain, which faces into the extracellular space (Edens *et al.*, 2001).

The isoforms also vary in their requirements for the several Nox activator and regulatory subunits. These subunits were originally identified as being necessary for the formation of the active Nox2 enzyme complex but as further Nox isoforms were investigated, it appeared that these subunits were not always required for catalytic activity of individual Nox. Possibly the most crucial regulatory subunit is the small transmembrane protein p22phox, which functions as both a stabilising presence for the catalytic subunit, as well as an anchor for the other regulatory subunits which are not membrane bound. Originally isolated in complex with Nox 2, a complex titled flavocytochrome *b*558 (Parkos *et al.*, 1987), p22phox is necessary for the stability of Nox 1-4 (DeLeo *et al.*, 2000), whereas Nox 5 and Duox 1 and 2 appear to not require p22phox (Kawahara *et al.*, 2005).

Three cytosolic subunits are required for Nox 2 activation and must be recruited to the membrane in order to fulfil their functions. p47phox is termed the organiser subunit of Nox 2, as its binding to p22phox facilitates the assembly of the other subunits. In the cytosol, p47phox is bound to p67phox, the Nox 2 activator, so upon p47phox translocation to the membrane, p67phox is also brought into contact with the Nox 2 subunit. Another small subunit, p40phox, is bound to p47phox and

p67phox in the cytosol and is recruited to the membrane with p47phox, however it is unclear as to the precise function of p40phox, though studies seem to suggest that its presence enhances Nox 2 activity (Cross, 2000; Kuribayashi *et al.*, 2002; Tsunawaki *et al.*, 1996). Phosphorylation of cytosolic p47phox has been reported to occur *via* a range of kinase, including PKCα, βII, ζ(Fontayne *et al.*, 2002) δ (Bey *et al.*, 2004) Src (Chowdhury *et al.*, 2005), MAPK (Dang *et al.*, 2006) and Akt (Hoyal *et al.*, 2003) and appears to be one of the signals which triggers the translocation of p47phox to the membrane, but another requirement is phosphorylation of membrane phospholipids, by PI3K and phospholipase D, to which p47phox binds (Kanai *et al.*, 2001) .

Nox 1 differs from Nox 2 in that it uses its own unique organiser and regulatory subunits, NoxO1 (a p47phox homolog) and NoxA1(a p67phox homolog) respectively (Bedard and Krause, 2007). These subunits also appear to be employed preferentially by Nox 3, though there is evidence to suggest that Nox 3 can also be activated by p67phox (Banfi *et al.*, 2004a; Ueno *et al.*, 2005). In contrast, Nox 4 (Martyn *et al.*, 2006), Nox 5 (Banfi *et al.*, 2001) and Duox 1, 2 (Bedard and Krause, 2007) have no requirements for activator or organiser subunits, with Nox 5 (Banfi *et al.*, 2004b), and Duox1 and 2 activity being subject solely to Ca^{2+} levels (Ameziane-El-Hassani *et al.*, 2005). In addition to the phox subunits, another cytosolic factor required for Nox 1, 2, and possibly 3 (Ueyama *et al.*, 2006) and 4 (Gorin *et al.*, 2003) activity is the small GTPase Rac1, which when in its active GTP-bound state binds p67phox (Lapouge *et al.*, 2000) The exchange of GDP for GTP in Rac1, as catalysed by guanine exchange factors (GEFs) causes the release of Rac1 from its inhibitory RhoGDI partner and allows it to bind the Nox holoenzyme, forming an

active complex (Knaus *et al.*, 1991). In summary there are three separate events which trigger activation of Nox 1, 2 and 3; the phosphorylation of its cytosolic organiser subunits preceding their translocation to the membrane; the phosphorylation of membrane inositides to facilitate binding of the subunits, and the release of Rac1GTP from its inhibitory partner.

Nox 4 was long thought to be the only constitutively active member of the Nox family, under regulation by transcription factors at the level of mRNA rather than relying on cytosolic organiser and activator subunits (Von Löhneysen *et al.*, 2012; Serrander *et al.*, 2007). However, it has recently been proposed that Nox 4 requires the stabilising presence of p22phox with which it forms a heterodimer at the plasma membrane (Ambasta *et al*., 2004), and that this association is dependent on the polymerase delta-interacting protein (Poldip2) (Lyle *et al*., 2009).

The Nox are responsible for the generation of ROS in response to a variety of stimuli. These stimuli range from LPS and inflammatory mediators, a reminder of the original microbiocidal role of Nox, to B and T cell receptors (Richards and Clark, 2009; Jackson *et al.*, 2004) and growth factors such as PDGF, Thrombin, TNF- α, TGF-β, Angiotensin II (Brown and Griendling, 2009) and Bcr-Abl (Naughton *et al.*, 2009). The ability of Nox to produce ROS in the context of growth factor binding and receptor activation, and not exclusively as a host defence mechanism, suggests that the role of Nox enzymes has expanded to include the generation of oxidants for the purposes of signalling.

2.3 Redox signalling

There has been a recent emergence of evidence for ROS playing a role in a diverse range of cellular processes including cell survival (Naughton *et al.*, 2009), regulation of transcription factors and gene expression (Li *et al.*, 2009), cell senescence (Colavitti and Finkel, 2005), angiogenesis (Ushio-Fukai, 2006b), differentiation (Xiao *et al.*, 2009), cell death (Kim *et al.*, 2007), migration (Meng *et al.*, 2008) , cytoskeletal remodelling (Lyle *et al.*, 2009), proliferation (Jay *et al.*, 2008; Arnold *et al.*, 2001), transformation (Laurent *et al.*, 2008), insulin signalling (Mahadev *et al.*, 2004), oxygen sensing (Lee *et al.*, 2006), hormone synthesis (Pfarr *et al.*, 2006), invasion (Deem and Cook-Mills, 2004), regulation of cellular redox potential (Bedard and Krause, 2007), and protein folding and cross-linking (Santos *et al.*, 2009) .

The ability of Nox derived-ROS to regulate discrete signalling pathways and influence specific molecules and processes, lies in the compartmentalisation of the oxidant production. Individual Nox isoforms are localised to different sub-cellular compartments, allowing for co-localisation with specific ROS targets, thus reducing the likelihood of off-target redox signalling and insulating the local accumulation of ROS to prevent toxic side-effects (Terada, 2006). An example of this sequesterisation of Nox ROS production is the localisation of Nox 4 to the ER. Proteins regularly undergo redox processing as part of their maturation within the ER, resulting in modifications essential to their tertiary structure and function such as disulfide bond formation and protein folding (Appenzeller-Herzog *et al.*, 2010; Zito *et al.*, 2010). It has been recently demonstrated by Chen *et al.* (2008a) that ER-resident protein PTP1B, is subject to redox modification by Nox 4 focally activated

in the ER, but in this situation the oxidation transiently inhibits PTP1B to facilitate endocytosed EGFR signalling . The specificity of the redox signal was highlighted by the failure of Nox 4 to oxidise a cytosolic, mutant form of the phosphatase. Similarly, Nox localisation to endosomes, lipid rafts and caveolae confers the same type of sequesterisation of oxidants for precise signalling purposes (Ushio-Fukai, 2006a).

The availability of regulatory subunits, or co-factors such as Ca^{2+} in the case of Nox 5 and the Duox, also ensures that the production of ROS is spatially and temporally regulated. The recent identification and characterisation of two novel adaptor proteins for Nox1 and 3, Tks4 and Tks5 (Gianni *et al.*, 2009), highlights the role of Nox regulatory molecules in dictating the specificity of the redox signalling and tailoring it to the physiological needs of the cell. The Tks proteins function in a similar manner to p47 phox, i.e.as organiser subunits controlling the recruitment of other subunits to the membrane, but appear to operate only within the invadopodia and podosomes of migrating cells, ensuring that Nox activation occurs within the confines of these actin-rich invading structures, which seem to require ROS for their stabilisation. This mode of spatial regulation of Nox activity is also evident also in the case of PTP-PEST susceptibility to p47phox-dependent production of ROS at sites of focal adhesions (Wu *et al.*, 2005).

The compartmentalisation of the redox signal is also regulated in part by the ROS-scavenging systems discussed earlier. The specificity of these enzymes for particular ROS, their proximity to individual Nox as well as their ability to become variably oxidised all contribute to the formation of discrete redox circuits within the cell, ensuring the temporal and spatial production and activity of ROS is tightly

controlled. Despite this, de-regulated and aberrant production of ROS by Nox does occur and can have detrimental phenotypic effects on the cell. Nox have been implicated in a range of pathologies including neurodegenerative disorders (Gao *et al.*, 2012), asthma (Henricks and Nijkamp, 2001), cardiovascular disease (Heymes *et al.*, 2003), hypertension (Rey *et al.*, 2002) , photo-ageing (Valencia *et al.*, 2006), male infertility (Aitken and Baker, 2004) , pre-eclampsia (Brodsky *et al.*, 2004), cerebral and myocardial infarction (Hong *et al.*, 2006; Meischl *et al.*, 2006), septic shock and multi-organ failure (Abdelrahman *et al.*, 2005) , diabetes (Etoh *et al.*, 2003), acute renal failure (Nath and Norby, 2000) and retinal degeneration (Usui *et al.*, 2009).

In addition to this, the role of Nox as effectors of growth factors signalling means that their activity is subject to de-regulation in situations of oncogenic RTK signalling, constitutively active receptors or aberrant production of growth factors or ligands. Indeed a number of tumour types have been shown to produce higher levels of ROS than is physiologically normal (Hole *et al.*, 2012; Mitsushita *et al.*, 2004; Weinberg and Chandel, 2009; Wu, 2006), due to oncogenic RTK signalling, over-expression of the Nox enzymes themselves (Bedard and Krause, 2007; Cheng *et al.*, 2001), down-regulation of antioxidant scavenging enzymes (Yuzhalin and Kutikhin, 2012), or co-occurrence of all three of these situations. Increased ROS production proves tumourigenic through direct oxidation and damage of DNA, as discussed earlier, as well as through aberrant oxidant signalling, both contributing to a tumourigenic phenotype.

3. Objectives

As this project is concerned with AML, it is important to note that in haematopoietic tumours excessive production of ROS can be found in myeloid leukaemias including CML and AML as well as ALL and MDS (Battisti *et al.*, 2008; Farquhar and Bowen, 2003). It was recently shown that, in CML, the oncogenic RTK Bcr-Abl stimulates tumourigenic redox survival signalling *via* Nox (Naughton *et al.*, 2009). Given the established role for FLT3-ITD in driving AML progression, as well as recent evidence for both ROS production downstream of FLT3-ITD signalling (Sallmyr *et al.*, 2008b), and a link between FLT3-ITD and Nox (Reddy *et al.*, 2011; Sallmyr *et al.*, 2008a), we are confident that there is similar mechanism of oncogenic RTK-driven Nox activity operating in AML. Our hypothesis is that FLT3-ITD signals to one or more Nox isoforms, and that the ROS produced by Nox contributes to the phenotype of AML through aberrant redox signalling. The objectives of this project are three-fold. 1) To investigate signalling from FLT3 to Nox, 2) to identify the target pathways and proteins downstream of Nox-derived ROS in AML and the mechanisms whereby they are redox regulated and 3) to evaluate the contribution that this FLT3-driven redox signalling makes to the AML phenotype.

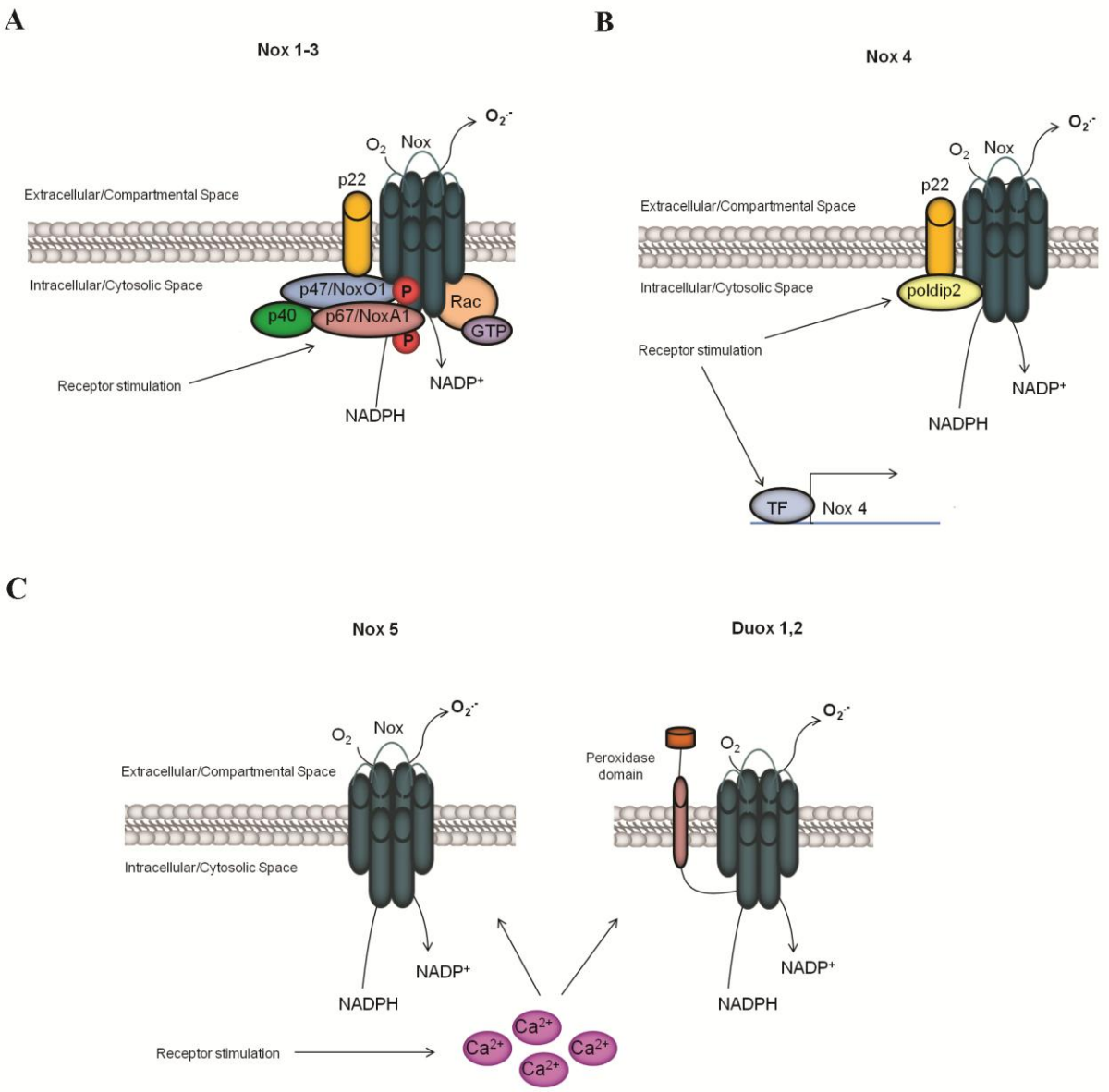


Figure 3. Nox production of ROS

The Nox family consists of 7 isoforms, Nox1-5 and Duox 1 and 2. Upon stimulation, the catalytic subunit removes an electron from cytosolic NADPH, and uses this electron to reduce O_2 generating $O_2^{\cdot-}$. **A)** p22phox is required by Nox1-3, and possibly 4, and functions as both a stabilising presence as well as an anchor for the other regulatory subunits. Nox 1-3 activation also requires recruitment of cytosolic subunits and Rac1-GTP. **B)** Nox 4 is thought to require Poldip2 to facilitate its binding to p22phox.**C)** Nox 5 and the Duox appear to require only Ca^{2+} for which they contain an additional binding domain. Duox also possess a further transmembrane peroxidase-like domain, although this is thought to be non-functional.

Chapter 2

Materials and Methods

Unless otherwise stated all reagents were purchased from Sigma Aldrich (Dublin, Ireland).

Antibodies

Primary antibodies used for immunoblotting were Ubiquitin (MAB1510) from EMD Millipore Corporation (MA, USA), Rac1 (Arc03) from Cytoskeleton Inc., PP6C (07-1224), Nox 2 (07-024) and PTP1B (07-088) from Upstate Biotechnology (Milton Keynes, UK). Nox 4 (ab61248), Rac2 (ab2244), Duox 2 (ab65813) and p-Ser PSR-45 (ab6639) from Abcam (Cambridge, UK). p-Tyr (610000) from BD Transduction Laboratories (Oxford, UK), β-Actin (A5441) from Sigma-Aldrich (Dublin, Ireland). PP2Cα (3549), p-FLT3 Tyr591 (3461), FLT3 8F2 (3462), Src (L4A1) (2110), p-Src Y416 (2101), Ezrin (3145), p-Ezrin Y353 (3144), p-Thr 42H4 (9386) all from Cell Signalling Technology (Boston, USA). Nox 1 (sc-25545), Nox 5 (sc-67006), Duox 1 (sc-48858), p47phox (sc-14015), p-Ezrin Y146 (sc-12941), Nox3 (sc-34699), p67phox (sc-15342), SHP-1 (sc-287), and p22phox (sc-20781) all from Santa Cruz Biotechnology Inc. (CA, USA). The Nox 4 antibody was a gift from Dr JD Lambeth (Emory University School of Medicine, Atlanta, GA). Horseradish peroxidise-conjugated secondary antibodies (Dako, Stockport, UK) were used for detection with enhanced chemiluminescence and Li-Cor IRDye secondary antibodies (Li-Cor Biosciences, Nebraska, USA) were used for detection with the Odyssey System.

Cell Culture

The human AML cell lines, MOLM-13, which is heterozygous for the FLT3-ITD mutation (Quentmeier *et al.*, 2003) and MV4-11 which is homozygous for the FLT3-ITD mutation (Quentmeier *et al.*, 2003), as well as the acute promyelocytic

leukaemia (APL) cell line HL-60 which is homozygous for FLT3-WT (Levis *et al.*, 2004), were all maintained in RPMI-1640 supplemented with 10% FBS, 1% penicillin/streptomycin and 2 mM l-glutamine in a humidified incubator at 37°C with 5% CO_2. For Nox inhibition, cells were treated with Apocynin, Rac1inhibitor NSC23766, Bapta-AM and the flavoprotein inhibitor diphenyleneiodonium chloride (DPI) at the indicated concentrations and times. Cells were also treated with Src family inhibitor PP2 (Calbiochem, Nottingham, UK), the FLT3-ITD inhibitor PKC412 (Tocris, Bristol, UK), FLT3 ligand (FL) (PeproTech EC Ltd., London, UK) and H_2O_2 at the indicated concentrations for the indicated times. Dimethylsulfoxide (DMSO) was used as a vehicle.

Flow Cytometric Analysis / Measurement of Intracellular ROS levels

Flow cytometry was carried out as previously described (Naughton *et al.*, 2009). Following treatments, ROS levels were determined by incubating the cells with 50 µM of the cell-permeable fluorescent probe 2,7-dichlorodihydrofluorescein diacetate (H_2DCFDA) (Invitrogen, Biosciences Ltd., Ireland) for 15 minutes in the dark. Cells were then analysed for mean fluorescent intensity of 10 000 events counted in the FL-1 channel on a FACSCalibur (BD Biosciences, Europe) using Cellquest Pro software (Becton Dickinson).

Western Blot analysis

Western Blotting was carried out as previously described (Naughton *et al.*, 2009). Briefly, whole cell lysates were prepared by harvesting cells from culture, washing in PBS and solubilising in RIPA lysis buffer (50 mM Tris-HCl pH7.4, 1% NP-40, 0.25% sodium deoxycholate, 150 mM sodium chloride, 1 mM EGTA, 1 mM sodium

orthovanadate, 1 mM sodium fluoride, 200 µM 4-(2-Aminoethyl) benzenesulfonyl fluoride hydrochloride and cocktail protease inhibitors (Roche, Welwyn, Hertforshire, UK) for 30 minutes at 4°C, followed by centrifugation at 14 000 *g* for 15 minutes at 4°C to remove cell debris. Protein concentrations were determined by Bio-Rad Protein Assay (Hemel, Hempstead, UK) and equal amounts (50 µg per lane) were separated by SDS-polyacrylamide gel electrophoresis (SDS-PAGE) and transferred to nitrocellulose membranes (Schleicher & Schuell, Dassel, Germany) before incubating with the appropriate antibodies. Membranes were developed using enhanced chemiluminescence (GE Healthcare, Buckinghamshire, UK) or the Odyssey Infrared Imager system and Odyssey software (version 2.1.12, Li-Cor Biosciences, USA). Densitometric analysis was carried out using ImageJ software (version 1.44, NIH, USA).

Myeloperoxidase stain

Cytospins were prepared using a Shandon Cytospin 2 Cytocentrifuge. MOLM-13 cell suspensions containing 1 x 10^5 cells were spun onto glass slides for 2 minutes at an Rcf of 17 x *g*. Cytospins were allowed to air dry for 1 hour and then fixed using ice cold 100% methanol for 2 minutes. Diaminobenzidine (DAB) solution consisting of 0.05% 3,3- DAB, 0.015% H_2O_2, and 0.01 M PBS was prepared and incubated with the cytospins for 20 minutes in the dark. Excess DAB solution was washed off with PBS and a counter stain of 1 µg/ml Hoescht (Thermo Fisher Scientific, Dublin, Ireland) was added for 1 hour and then cytospins were washed again with PBS. Slides were mounted with coverslips using Mowiol and dried at 37ºC for 1 hour before visualisation under 40X using a Leica DM LB2 microscope (Leica, Milton Keynes, UK). Light mode was used to visualise the DAB stain and fluorescent mode

was used to visualise the nuclear stain Hoescht. Whole blood sample, containing neutrophils, taken from a C57BL/6 mouse of age P8 was used as a positive control for myeloperoxidase.

Two-Dimensional SDS-PAGE

Samples containing 250 µg of total protein in RIPA lysis buffer were resuspended in 10% TCA and acetone to remove residual salts. The samples were incubated overnight at -20°C and then centrifuged at an Rcf of 15 000 x *g* for 30 minutes (4°C). The resulting pellet was resuspended in 125 µl rehydration buffer [5 M urea, 2 M thiourea, 2% 3-[(3-cholamidopropyl)dimethylammonio]-1-propanesulfonate (CHAPS) (Anachem), 4% carrier ampholytes (GE Healthcare), 1.5% 2-hydrooxyethyl disulfide (DeStreak, Sigma), and trace bromophenol blue] and loaded onto 7 cm pH 3-10 non linear immobilised pH gradient (IPG) strips (Immobiline™ DryStrip, GE Healthcare). The strip was allowed to passively rehydrate at room temperature for 16 hours. Isoelectric focusing was carried out on a Protean isoelectric focusing cell (Bio-Rad) using a rapid voltage increase procedure: 250 V for 15 min then increased to a maximum of 4000 V within 2 hours and kept at 4000 V for 20000 min. After isoelectric focusing, the strips were subjected to two-step equilibration in equilibration buffers (6 M Urea, 0.375M Tris-HCl pH 8.8, 2% SDS and 10% Glycerol) with 2% dithiothreitol (DTT) for the first step, and 2.5% iodoacetamide for the second step. The strips were then transferred on to the second-dimensional SDS-PAGE that was run on 12% polyacrylamide gels. Proteins were transferred and immunoblotted as for Western Blotting analysis. Gels used for spot-picking were stained with Instant Blue (Expedeon, Cambridgeshire, UK) for 1 hour followed by incubation in Brilliant Blue Colloidal Coomassie (0.02%

Colloidal Coomassie, 5% aluminium sulphate-14-18-hydrate, 10% ethanol and 2% orthophosphoric acid) overnight and de-stained in 10% ethanol and 2% orthophosphoric acid prior to excision. Protein spots of interest were excised using OMX-S device (OMX GmbH, Wessling, Germany).

Identification of Proteins by Peptide Fragment Fingerprinting (PFF)

PFF was performed at Aberdeen Proteomics Facility, University of Aberdeen, Scotland.

In gel digestion

Proteins in the gel pieces were digested with trypsin (sequencing grade, modified; Promega UK, Southampton, UK) using an Investigator ProGest robotic workstation (Genomic Solutions Ltd., Huntingdon, UK). Briefly, proteins were reduced with DTT (60°C, 20 minutes), s-alkylated with iodoacetamide (25°C, 10 minutes) then digested with trypsin (37°C, 8 hours). The resulting tryptic peptide extract was dried by rotary evaporation (SC110 SpeedVac; Savant Instruments, Holbrook, NY, USA) and dissolved in 0.1% formic acid for LC-MS/MS analysis.

Liquid Chromatography – Tandem Mass Spectrometry (LC-MS/MS)

Peptide solutions were analysed using an HCTultra PTM Discovery System (Bruker Daltonics Ltd., Coventry, UK) coupled to an UltiMate 3000 LC System (Dionex (UK) Ltd., Camberley, Surrey, UK). Peptides were separated on a Monolithic Capillary Column (200 μm i.d. x 5 cm; Dionex) at a flow rate of 2.5 μL/minute using a gradient of acetonitrile (6 – 38% over 12 minutes) in 0.04% (aq.) formic acid. Peptide fragment mass spectra were acquired in data-dependent AutoMS (2) mode with a scan range of 300 – 1500 m/z, 3 averages, and up to 3 precursor ions selected

from the MS scan (100 – 2200 m/z). Precursors were actively excluded within a 1.0 minute window, and all singly-charged ions were excluded. Peptide peaks were detected and deconvoluted automatically using DataAnalysis software (Bruker). Mass lists in the form of Mascot Generic Files were created automatically and used as the input for Mascot MS/MS Ions searches of the NCBInr database using the Matrix Science web server. The default search parameters used were: Enzyme = Trypsin;Max. missed cleavages = 1; Fixed modifications = Carbamidomethyl (C); Variable modifications = Oxidation (M); Peptide tolerance ± 1.5 Da; MS/MS tolerance ± 0.5 Da; Peptide charge = 2+and 3+; Instrument = ESI-TRAP.

Immunofluorescence

Glass coverslips were coated with 0.01% 70-150 kDa poly-l-lysine solution (Sigma Aldrich, Dublin Ireland) and UV sterilised. Cells were seeded onto coated coverslips at a density of 0.8 x 10^6 cells per ml and allowed to adhere overnight. Following 24 hour treatment, cells were fixed with 3% paraformaldehyde and permeabilised in PBS containing 0.2% BSA and 0.05% Saponin. Coverslips were then incubated with anti-Ezrin antibody (#3145, Cell Signalling Technologies, Boston, USA) at a dilution of 1:125 in 5% FBS/PBS for 2 hours at room temperature, washed in PBS three times and incubated with a secondary antibody goat anti-rabbit conjugated to Alexa fluor488 and nuclear stain Hoescht 1 µg/ml (Thermo Fisher Scientific, Dublin, Ireland) for 1 hour at room temperature. Following washes with PBS, the coverslips were mounted onto glass slides using Mowiol and dried overnight before imaging. Cells were visualised using a Leica DM LB2 microscope (Leica, Milton Keynes, UK). Images of the cells were acquired by Nikon Digital Sight DS-Fi1C camera (Nikon, Japan) using NIS-Elements software (version 3.0, Nikon, Japan).

Scanning Electron Microscopy

Cells were seeded as for immunofluorescence and, following 24 hour treatment, were fixed in 2% glutaraldehyde in a 0.165 M PO_4 buffer followed by a secondary fixation in osmium tetroxide (2% osmium tetroxide in 0.165 M PO_4). Samples were dehydrated in ethanol and air-dried from tetramethylsilane. Samples were mounted on stubs using double-sided carbon tape, and sputter coated with ~28 nm layer of gold, using a Polaron E5150 Sputter Coating Unit, to prevent surface charging by the electron beam. Samples were then examined using a Jeol Scanning Electron Microscope (JSM-5510, Jeol Ltd., Tokyo, Japan).

N-(biotinoyl)-N′-(iodoacetyl)ethylenediamine (BIAM)-labelling of reduced protein

N-(biotinoyl)-N′-(iodoacetyl)ethylenediamine (BIAM) labelling of reduced protein was carried out as previously described (Giannoni *et al.*, 2005). Briefly, whole cell lysates were prepared by harvesting cells from culture, washing in PBS and rapid freezing of cell pellet in liquid nitrogen. RIPA lysis buffer containing 100 µM BIAM(Invitrogen, Biosciences Ltd., Ireland) was also exposed to liquid nitrogen for 20 minutes to remove oxygen. The frozen cell pellet was then solubilised in the BIAM-containing RIPA buffer, sonicated in a bath sonicator for three periods of 1 minute each separated by 30 second intervals and incubated for 15 minutes at room temperature. Lysates were then centrifuged at an Rcf of 20 817 x *g* for 15 minutes at 4°C to remove cell debris and the clarified lysate was then separated by SDS-PAGE and transferred to nitrocellulose membranes, to detect the reduced portion of the total lysate, or subjected to immunoprecipitation with Src specific antibody prior to SDS-PAGE to detect reduced Src. In both cases the BIAM-labelled protein was detected with HRP-conjugated to streptavidin (HRP-SA) and ECL.

Immunoprecipitation

Immunoprecipitation was carried out using the Crosslink IP Kit (Thermo Fisher Scientific, Dublin, Ireland) according to the manufacturers' instructions. Briefly, 1mg of lysate was immunoprecipitated overnight with 10 µg of the appropriate antibody crosslinked to Protein A/G agarose using disuccinmidyl suberate (DSS). The immunocomplexes were separated by SDS-PAGE, transferred to nitrocellulose membrane and probed with the appropriate antibodies.

siRNA

For p22phox knockdown experiments, 2.5 x 10^6 cells were transfected with 50 ng scrambled siRNA or 50 ng siRNA targeting p22phox (Ambion Silencer Select, Applied Biosystems, Warrington, U.K.). The transfection of siRNA used the Amaxa Nucleofactor technology with the Amaxa cell optimisation kit V (Amaxa, Cologne, Germany) and followed the Amaxa guidelines using program D-023 for MOLM-13 and T-019 for HL60. Cells were lysed 24 hours post-transfection. HL60 cells were treated with 50 ng/ml FL for 30 minutes prior to lysis.

Chemotaxis assay

The chemotaxis assay was carried out as previously described by Zhou *et al*. (2010b), in 24-transwell chambers (Corning Costar, Cambridge, MA, USA). Briefly, cells (100 µl, 1 x 10^6 cells ml^{-1}) were treated as indicated in RPMI 1640 with FBS for 20 hours, serum starved in the same treatments for the final 4 hours of the 24 hour incubation and then added to the upper chamber which was separated from the lower well by a 5 µm pore-size polycarbonate membrane. RPMI 1640 containing 10% FBS was placed in the lower wells (600 µl) as a chemoattractant. Cells were allowed to

migrate for 4 hours at 37°C and 5% CO_2 atmosphere. The transwell was then fixed with methanol and stained for 5 minutes with 0.1% crystal violet. Cells were counted in five randomly selected fields per well under 20 X magnification on a Nikon Eclipse TS100 (Nikon, Japan).

Statistical analysis

Statistical analysis was performed using Student's *t*-test to evaluate the difference between experimental and control groups. Significance was defined at the level of $P<0.05$.

Kinexus^{TM} Phosphatase Expression Screen

20 x 10^6 cells were centrifuged at an Rcf of 500 x *g* for 2 minutes at 4°C in swinging bucket benchtop centrifuge. Media was removed and cell pellet was resuspended gently in ice-cold PBS followed by centrifugation as above. This was repeated to ensure complete removal of serum. Pellet was then homogenised in 200 µl of ice-cold lysis buffer (20 mM 3-(N-morpholino)propanesulfonic acid, 2 mM ethylene glycol tetraacetic acid, 5 mM ethylenediaminetetraacetic acid, 30 mM sodium fluoride, 60 mM β-glycerophosphate pH 7.2, 20 mM sodium pyrophosphate, 1 mM sodium orthovanadate, 1% Triton X-100, 1 mM phenylmethylsulfonyl fluoride, 5 µM pepstatin A, cocktail protease inhibitors [Roche, Welwyn, Hertforshire, UK], 1 mM DTT, distilled water). Sample was sonicated using a water bath sonicator four times for 10 seconds each time with 10-15 second intervals on ice to rupture the cells and to shear nuclear DNA. The homogenate was then centrifuged at an Rcf of 90 000 x *g* for 30 minutes at 4°C in a Beckman Table Top TL-100 ultracentrifuge. The supernatant fraction was removed and the protein concentration was determined

using the Bradford Protein Assay (Bio-Rad, Hemel, Hempstead, UK) with bovine serum albumin used as a protein standard. The Kinexus™ Protein Phosphatase Screening Service (KPPS 1.2) to determine the expression level of 30 phosphatases requires 500 µg of protein and this was diluted to 1 mg/ml in 4X SDS-PAGE sample buffer (50% glycerol, 125 mM Tris-HCl pH 6.8, 4% SDS, 0.08% Bromophenol blue, 5% β-mercaptoethanol, distilled water). The samples were then boiled for 4 minutes at 95°C and shipped in a 1.5 ml Eppendorf screw-cap vial to Kinetworks Screening Services, Kinexus™ Bioinformatics Corporation, Vancouver, CA. KPPS 1.2 then utilised multi-immunoblotting, which generated a unique identification pattern for each sample analysed and provided information about the quantitative expression level for each phosphatase detected. The identification and detection of each target protein was based on its immunoreactivity and apparent molecular mass.

BIAM-labelling and depletion prior to Kinexus™ Phosphatase Expression Screen

To determine the effect of PKC412 on phosphatase oxidation, BIAM-labelling was carried out as previously described in section titled 'N-(biotinoyl)-N′-(iodoacetyl)ethylenediamine (BIAM)-labelling of reduced protein', samples were then sonicated and ultracentrifuged as described in section titled 'Kinexus™ Phosphatase Expression Screen'. The supernatant fraction was removed and the protein concentration was determined using the Bradford Protein Assay (Bio-Rad, Hemel, Hempstead, UK) with bovine serum albumin used as a protein standard. 30 µg of total lysate was reserved at this point for comparison. 2 mg of lysate was incubated overnight in spin columns (Thermo Fisher Scientific, Dublin, Ireland) containing streptavidin-sepharose bead conjugate to bind the biotin-labelled portion of lysate. Flow-through was collected and designated biotin-depleted, and the biotin-

labelled portion was eluted. Biotin-labelled total lysate, biotin-labelled flow-through and biotin-depleted samples were separated using 12% SDS-PAGE, and Coomassie-stained to confirm changes in protein quantity. Replicate gels were transferred to nitrocellulose membranes and probed for biotin using HRP-conjugated streptavidin (HRP-SA) and ECL, with Ponceau used to confirm loading. When depletion was confirmed, depleted samples were diluted in 4X SDS-PAGE sample buffer as previously described, boiled for 4 minutes at 95°C and shipped in a 1.5 ml Eppendorf screw-cap vial to Kinetworks Screening Services, Kinexus^{TM} Bioinformatics Corporation, Vancouver, CA.

Quantitative Reverse Transcriptase Polymerase Chain Reaction (qRT-PCR)

Following a 24 hour treatment 5x 10^6 cells were harvested from each sample. Media was removed and total cellular RNA was isolated using the Isolate RNA mini kit (Bioline Ltd, UK), according to the manufacturer's protocol for eukaryotic cells.

The concentration of RNA in each sample was determined in triplicate by spectrophotometric analysis using a Biophotometer (Amersham Biosciences). 500 ng of RNA was then run on a 1% agarose gel to check integrity. RNA was treated to remove any contaminating DNA using DNase 1 amplification grade kit (Sigma-Aldrich) according to manufacturers' instructions.

cDNA was then synthesised from 2 µg RNA using 1x Moloney Murine Leukaemia Virus Reverse Transcriptase (M-MLV RT) buffer, 25 mM $MgCl_2$, 40 U/µl RNAse inhibitor, 200 U/µl M-MLV Reverse Transcriptase, 50 mM oligo dTs and 10 mM dNTPs (all from Promega, UK) or the equivalent volume of RNAse-free water for the non-reverse transcriptase control (NRT). The final volume of each replicate was

made up to 20 µl with RNAse free water and the reaction was run at 42ºC for 1 hour, 99ºC for 10 minutes, followed by overnight storage at 4ºC.

The real-time reverse transcriptase PCR reaction was used to amplify cDNA from 4 genes of interest; *PTPN1/SHP-1, PP2Cα, PP6C* and *PTPN6/PTP1B*, with *GAPDH* as a housekeeping gene for normalisation. Three technical replicates and one NRT control were used per sample for each gene. The qRT-PCR reaction was carried out on a DNA Engine Opticon 2.0 (MJ Research Inc., Waltham, USA), using Quantittect SYBR Green Sensimix kit and Quantitect Primer Assays (Qiagen, West Sussex, UK). Qiagen pre-designed primers were used for human PTPN1/SHP-1 (Hs_PTPN1_2_SG QT01006978), PP2Cα (Hs_PPP2CA_1_SG QT00085603), PP6C (Hs_PPP6C_1_SG QT00083433), PTPN6/PTP1B (Hs_PTPN6_1_SG QT00011725) and GAPDH (Hs_GAPDH_2_SG QT01192646). Briefly, 50 ng cDNA template was combined with 10 µl of 20X SYBR Green Sensimix and 2 µl 10X primer in 20 µl total reaction volume in a 96 well plate (Bio-Rad) and the PCR reaction was carried out as follows: 95ºC for 15 minutes followed by 44 cycles of 94ºC for 15 seconds, 56ºC for 30 minutes and 72ºC for 30 minutes. Relative mRNA levels for each gene were calculated from relative C(t) values and normalised against GAPDH.

Ubiquitination assay

10 x10^6MOLM-13 cells were treated with 5 µM proteasome inhibitor Lactacystin for 24 hours prior to lysis to prevent the degradation of ubiquitinated proteins. Cells were lysed in 1% SDS lysis buffer containing 10 mM N-Ethylmaleimide (NEM), a de-ubiquitinating enzyme inhibitor and vortexed, boiled for 10 minutes and sonicated for 3-4 seconds. Lysates were clarified by centrifugation at an Rcf of 20 817 *g* at 4°C for 10 minutes. The supernatants were transferred to a cold eppendorf

tube and protein concentration was determined using the Bradford reagent. 1 mg of lysate was immunoprecipitated overnight using Crosslink IP Kit (Thermo Fisher Scientific, Dublin, Ireland) according to the manufacturers' instructions, with 10 µg of SHP-1 antibody crosslinked to Protein A/G agarose using DSS. 10 mM NEM was included at all washing steps. The immunocomplexes were separated by 10% SDS-PAGE, transferred to nitrocellulose membrane, which was pre-soaked in transfer buffer containing 20% methanol and transferred in the same buffer. Membranes were autoclaved for 15 minutes prior to blocking to expose further ubiquitin moieties for detection, blocked in 5% BSA and probed with anti-ubiquitin and anti-SHP-1 antibodies.

Chapter 3

Regulation of tyrosine phosphorylation by Nox-derived reactive oxygen species in a FLT3-ITD cell line

Abstract

The emergence of evidence implicating reactive oxygen species as signalling mediators in their own right has been accompanied by the use of inhibitors of the NADPH oxidase enzymes in order to determine the functional significance of redox-signalling. The purpose of this chapter was to identify downstream targets of NADPH oxidase-derived reactive oxygen species signalling in AML cells which contain the constitutively active form of the receptor tyrosine kinase FLT3. This was achieved by performing a proteomic analysis utilising two-dimensional phosphotyrosine immunoblotting. The majority of the targets identified were cytoskeletal-associated proteins including Ezrin, a known regulator of the cytoskeleton, which was selected for further examination. The study demonstrated that inhibition of NADPH oxidase enzymes, using diphenyleneiodonium chloride in the AML cell line MOLM-13, resulted in a decrease in Ezrin tyrosine phosphorylation.

Introduction

The role played by tyrosine phosphorylation cascades in intracellular signal transduction, cannot be overstated. This ancient form of relaying information is thought to have evolved just before the appearance of multicellular organisms, about 600 million years ago (Pincus *et al.*, 2008) , and proved so beneficial and efficient in evolutionary terms that it formed the basis for a multitude of complex diverging and converging signalling networks underlying every aspect of cellular function (Mayer, 2008). From gene expression, differentiation, apoptosis, proliferation and bio-synthesis, there is barely a pathway or area of cellular activity which does not utilise this mechanism to some extent.

Although crucial to cellular functions, the amount of tyrosine phosphorylation occurring in the cell is actually relatively small compared to the frequency of threonine and serine phosphorylation. Chou *et al.* (2010) estimates that approximately one third of all cellular proteins become phosphorylated at a serine or threonine residue, compared with just 0.05-0.1% becoming tyrosine phosphorylated. Serine and threonine phosphorylation are important post-translational modifications necessary for the functioning of many proteins and, as Lim and Pawson (2010) point out, the emergence of serine/threonine kinases in very primitive eukaryotic single-celled organisms preceded that of TKs. However, the evolution of PTPs from a dual-specificity phosphatase ancestor (Alonso *et al.*, 2004) also preceded the appearance of TKs, highlighting the necessity of maintaining tight control over the phosphorylation of functionally important tyrosine residues which were occasionally phosphorylated by some serine/threonine kinases (Lim and Pawson, 2010).

The requirement for close regulation of tyrosine phosphorylation becomes apparent when one considers the degree to which this post-translational modification is utilised as a signalling mechanism within the cell. Many cell activities require tyrosine phosphorylation, including but not limited to proliferation, host immune defence, survival, apoptosis, cell cycle, senescence, gene expression, differentiation, metabolism, motility, adhesion and hormone response (Hunter, 2009). De-regulation of these core cellular processes can disrupt the correct functioning of the cell, with especially detrimental, oncogenic consequences in the case of aberrant cellular p-Tyr-mediated survival signalling within multi-celled organisms.

Tyrosine phosphorylation is a dynamic circuit subject to the activity of TKs, which phosphorylate substrates at tyrosine residues, and PTPs which negatively regulate the phosphorylation signal by removing the phosphate group. The regulation of these two families of enzymes is crucial to maintain their synergy, which in turn affects the integrity, duration and effectiveness of the signal. Regulation at the level of gene expression is crucial, as can be inferred from the many tumour types which display gene amplification or de-regulated transcription of proto-oncogenic TKs and receptor TKs (RTKs) (Little *et al.*, 2012; Mimae *et al.*, 2012), as well as tumours in which crucial tumour suppressive PTP genes have been deleted, silenced or otherwise transcriptionally repressed (Julien *et al.*, 2011;Tonks, 2006).

In addition to the regulation of gene expression, post-translational modifications of both TKs and PTPs allow for rapid, efficient responses at the level of protein activity and turnover. Modifications such as ubiquitination (Hicke, 2001) and sumolyation (Yang and Sharrocks, 2006), as well as proteolytic cleavage (Hunter, 2009) and dimerisation (Julien *et al.*, 2011) affect both RTKs and PTPs.

However, one of the most common mechanisms for TK and PTP regulation is phosphorylation. TKs and PTPs are positively and negatively regulated by phosphorylation themselves, the nature of the phosphorylated residue (serine, threonine or tyrosine) and its effect (i.e. inhibitory or stimulatory) is specific to the individual enzyme. An example of the complex nature of phosphorylation as a regulatory mechanism can be observed in the activation of Src kinase which requires both the removal of an inhibitory C-terminal tyrosine phosphorylation at Y527 by a phosphatase as well as autophosphorylation at Y416 before it can become active (Roskoski, 2005). As well as these phosphorylation events, recent evidence suggests that Src also requires oxidative activation, as will be discussed in more detail in Chapter 4.

In addition to phosphorylation, oxidation of PTPs is a very common mode of regulating these enzymes, the dual processes of phosphorylation and oxidation are often co-ordinated for fine-tuning of PTP activity during p-Tyr signalling which involves the production of ROS (Chiarugi and Buricchi, 2007). It can be said that the PTP family are the prototypic intermediary target in redox signalling. At physiological pH, the low pKa of a crucial cysteine residue in the highly conserved active site motif, C(X)5R, of these proteins ensures that they are extremely vulnerable to oxidation, which disrupts the nucleophilic potential of the active site and renders the enzyme inactive (Denu and Tanner, 1998; Leslie *et al.*, 2004).

Oxidation results in the formation of sulfenic acid (SOH) which, on the occasion of close proximity of another cysteine, can form a disulfide bond (S-S). The oxidation of cysteine to sulfenic acid is reversible and sulfenic-acid or disulfide-containing PTPs can be reduced by Trx, Grx, or GSH (Denu and Tanner, 1998),

allowing for a dynamic switch in PTP activity to facilitate the propagation of a signal accompanied by oxidant production. The duration or intensity of the signal can also be fine-tuned by the degree of PTP oxidation. At higher ROS concentrations, further oxidation of the sulfenic acid intermediate results in the formation of the more stable sulfinic (SO_2H) or sulfonic (SO_3H) acids. These hyper-oxidised PTPs are permanently inactivated, thus allowing for an increased period of signalling uninterrupted by phosphatase activity (Ray *et al.*, 2012).

Under normal physiological situations, PTPs are regenerated by endogenous antioxidants and the ROS level is carefully regulated to ensure that hyper-oxidation of PTPs is kept to minimum so that PTP inhibition by ROS serves to facilitate the necessary and temporary passage of a signal (Leslie *et al.*, 2004).

In conditions of de-regulated and constitutively active TK and RTK signalling involving ROS production, the phenomenon of redox regulation of PTPs can compound any pro-survival signalling effects of the constitutive phosphorylation and contribute to the development of an oncogenic phenotype. By inhibiting, either transiently or permanently, the negative regulators of the pathway, oxidants as signalling mediators shift the balance further in favour of the proliferative and anti-apoptotic message which is being propagated continuously by the phosphorylation cascade. The down regulation of antioxidant enzymes in tumourigenesis, as discussed earlier, can exacerbate this situation by removing the means of transiently-inhibited PTP regeneration and leading to the formation of an oxidative environment within the cell, not conducive to PTP activity. The subject of PTP regulation both at the level of gene transcription and post-translational modification will be discussed further in Chapter 5.

As an oncogenic RTK, FLT3-ITD can be expected to drive de-regulated tyrosine phosphorylation within the AML cell, through a variety of pathways which it stimulates. It has also been shown that the FLT3-ITD signalling pathway invokes the production of ROS (Sallmyr *et al.*, 2008a). Though the source of these ROS is not yet confirmed, it is suspected to be Nox-derived. In a situation analogous to that of Bcr-Abl-positive CML (Naughton *et al.*, 2009), it is likely that these ROS contribute in some way to the oncogenic phenotype of the AML cell, *via* oxidation of target proteins. Thus, the focus of this study is on the targets of redox regulation by Nox in an AML cell driven by the FLT3-ITD mutated receptor. It was decided to focus initially on changes in tyrosine phosphorylation in response to Nox signalling because of the prominent role of tyrosine phosphorylation in the FLT3-ITD context and the vulnerability of this signalling device to redox regulation. Also taken into consideration at this point was the relative scarcity of p-Tyr modifications in comparison to phosphothreonine (p-Thr) and phosphoserine (p-Ser), which was seen to be advantageous in a proposed search for meaningful protein targets against a background of phosphorylation "noise".

To identify p-Tyr changes downstream of Nox, an effective inhibitor of Nox activity is required, as is a means of detecting p-Tyr residues. The latter requirement is easily met by using a pan p-Tyr antibody to probe for proteins with phosphorylated tyrosine residues within a whole cell lysate. Antibodies such as this are broad in terms of specificity and will bind p-Tyr regardless of the surrounding amino acid sequence, ensuring an even coverage of the proteome.

The choice of an effective method of inhibiting Nox, however, poses more problems. With regard to the available Nox inhibitors, there is much difference in

opinion with regard to the most specific and efficient, and the choice is also limited by suitability to a particular cell type as well as the nature of the downstream effect of interest. Some compounds branded as Nox inhibitors, appear to function more preferentially as an anti-oxidant or free-radical scavenger (Heumuller *et al.*, 2008), rather than interacting with the Nox enzymes themselves, while for others the inhibition of Nox seems to be almost a by-product of the more general mode of action of the compound as a calcium chelator, in the case of Bapta-AM, or as a Rac-1 inhibitor. At the time of writing, several new compounds marketed as Nox inhibitors are emerging and becoming more visible in the literature (Cifuentes-Pagano *et al.*, 2012; Kim *et al.*, 2012) such as VAS 2870 (Ten Freyhaus *et al.*, 2006), GKT136901 (Page P *et al.*, 2008), ML171 (Gianni *et al.*, 2010), ebselen and its analogs (Smith *et al.*, 2012). It is possible that one or several of these, will be shown to demonstrate definitive, specific Nox inhibition. However, with regard to this study, it can be concluded that, after much analysis, the most suitable Nox inhibitor was selected for this cell type from the limited range available at the time. The importance of this selection and the consideration it entailed cannot be overlooked, as this initial exploratory step into tyrosine phosphorylation influenced by Nox activity would come to form the basis for the entire study.

Results

Expression of Nox isoforms, regulatory and organiser subunits in MOLM-13 cells

To investigate Nox-derived ROS targets in FLT3-ITD driven AML, we used an AML cell line which is heterozygous for the FLT3-ITD mutation, MOLM-13 (Quentmeier *et al.*, 2003). This cell line is classified as AML-M5a and was established at a period of relapse from the peripheral blood of a 20 year old male patient suffering from acute monocytic leukaemia which had originally developed from MDS (Matsuo *et al.*, 1997). The selection of a cell line heterozygous for the FLT3-ITD mutation rather than a cell line which carries two FLT3-ITD alleles, such as MV4-11 (Quentmeier *et al.*, 2003), was made based on the requirement for a cell line which would respond to stimulation with the FLT3 ligand (FL), i.e. one which contains a copy of the wild type FLT3 receptor and in which the FLT3 signalling pathways are not saturated by constitutive FLT3-ITD signalling driven by bi-allelic expression of the mutant.

MOLM-13 cells were examined, using western blotting, for expression of the individual Nox isoforms as well as Nox regulatory and organiser subunits. This was carried out to inform future decisions regarding choices of Nox inhibitors and siRNA targeting. The western blotting data revealed that MOLM-13 cells express Nox1, 2, 4, 5, p22phox, p47 phox and p67phox (Figure 4). There was no signal detected for Nox 3, which is known have a very limited expression pattern, primarily in the spleen, foetal kidney, liver, lung and inner ear (Cheng *et al.*, 2001). Additionally, there was no expression of Duox 1 or Duox 2 detected, but these proteins are thought

to be expressed pre-dominantly in the thyroid, salivary gland and gastrointestinal tract (De Deken *et al.*, 2000).

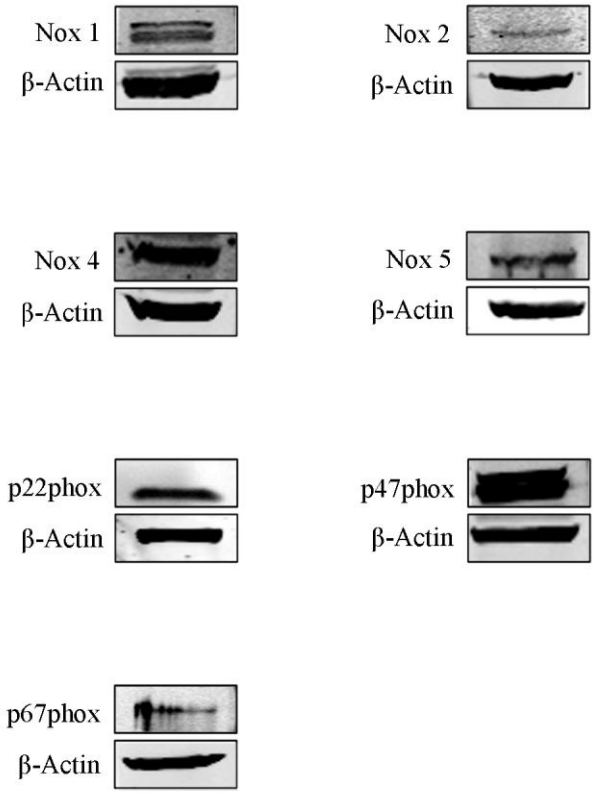


Figure 4. Nox expression in MOLM-13 cells

Western blot analysis of Nox isoforms 1, 2, 4 and 5, as well as transmembrane protein p22phox, organiser subunit p47phox and activator subunit p67phox, as expressed in the FLT3-ITD cell line MOLM-13. Nox 3 and Duox 1 and 2 were not detected. β-Actin is shown as a loading control.

Incubation of MOLM-13 cells with Nox inhibitor Apocynin does not reduce ROS and p-Tyr levels

Ideally, in order to determine the effects of Nox activity, the individual Nox subunits would be knocked down using short interfering RNA (siRNA) and the effects on the p-Tyr levels of the cell observed, allowing attribution of specific downstream targets to specific Nox. However, myeloid leukaemia cells have been widely classified as 'difficult to transfect' (Esendagli *et al.*, 2009; Marit *et al.*, 2000; Roddie *et al.*, 2000; Schakowski *et al.*, 2004; Uchida *et al.*, 2002), meaning that they are not amenable to the conventional lipid or amine-based reagents used as a vehicles for transfection. Instead, electroporation is often employed to deliver the nucleic acid into the cell (Schakowski *et al.*, 2004). This relatively harsh procedure is accompanied by a decrease in cell viability which creates problems for subsequent assays using the transfected cells (Crawley *et al.*, 1997). In addition to this drawback, the nature of the nucleic acid itself also causes difficulties for efficient transfection. The introduction of double stranded nucleic acids into macrophage-derived leukaemic cells, whose normal physiological role involves the phagocytosis of viral nucleic acids, prompts the haematopoietic interferon-inducible nuclear protein (Hin) 200 family of proteins to instigate a pro-apoptotic caspase cascade (Roberts *et al.*, 2009), again reducing the amount of viable transfected cells available for subsequent functional experiments.

Therefore, it was decided that the best course of action for the initial exploratory experiments into Nox activity, because of the hurdles presented by transfection of leukaemic cells, would be to use a chemical rather than genetic method of Nox inhibition.

The first Nox inhibitor which was investigated for its suitability was Apocynin. Named after the plant from which it was first isolated, *Apocynum cannabinum*, the methoxy-substituted catechol also known as acetovanillon, has been widely used to treat inflammatory conditions such as asthma, fever and rheumatism (Palmen *et al.*, 1995). Subsequent to its pharmacological isolation, the mode of action of Apocynin was discovered to be *via* inhibition of production by Nox (Hart *et al.*, 1990). This prompted the use of Apocynin in a wide range of studies into Nox activity (Gill and Wilcox, 2006; Stolk *et al.*, 1994; Williams and Griendling, 2007), as well as some controversy over the precise molecular mechanism by which Apocynin inhibits the burst by Nox. Some literature points to a role for Apocynin as a scavenger of free radicals and attribute its ROS-reducing effects to its antioxidant properties rather than any direct interaction with Nox enzymes (Heumuller *et al.*, 2008). Other studies suggest that it functions as an intracellular inhibitor of Nox holoenzyme assembly (Stolk *et al.*, 1994), while additional studies question the ability of Apocynin to inhibit Nox in systems other than phagocytic cells (Vejrazka *et al.*, 2005).

As MOLM-13 cells are monocyte-derived, it was assumed that Apocynin would inhibit Nox activity but fluorescence assisted cytometry (FACS), using the H_2DCFDA probe to detect oxidants, demonstrated no decrease in ROS levels in these cells upon treatment with increasing concentrations of Apocynin (Figure 5A). In addition to this, western blot analysis of whole MOLM-13 cell lysates, probed with a pan p-Tyr antibody showed no change in p-Tyr levels in MOLM-13 cells upon treatment with Apocynin at increasing concentrations (Figure 5B).

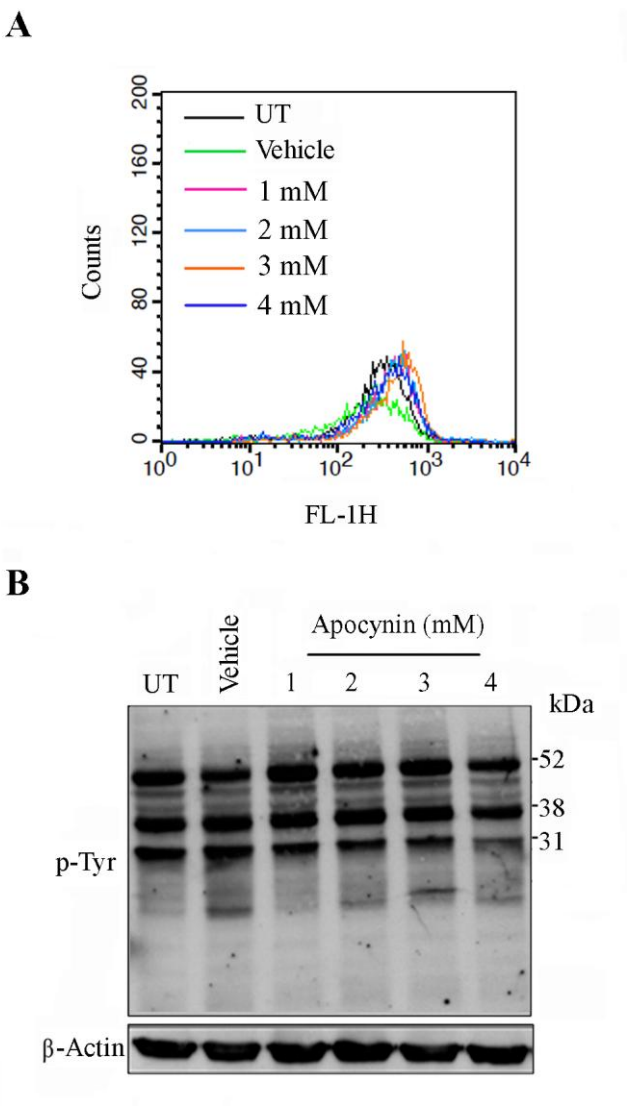


Figure 5. Effects of Nox inhibitor Apocynin on the ROS and p-Tyr levels of MOLM-13 cells. A) Intracellular ROS levels measured by relative DCF fluorescence (FL1-H) in untreated MOLM-13 cells overlaid with cells treated with the DMSO vehicle only or 1, 2, 3 or 4 mM Nox inhibitor Apocynin, for 24 hours. **B)** Western blot analysis of the p-Tyr profile of untreated MOLM-13 cells, cells treated with the DMSO vehicle only or with 1, 2, 3 or 4 mM Apocynin for 24 hours. β-Actin is shown as a loading control.

MOLM-13 cells do not express the Myeloperoxidase enzyme necessary for activation of Apocynin

It has been previously demonstrated that the monomeric form of Apocynin requires oxidative activation by myeloperoxidase (MPO) before it can form active Apocynin dimers (Ximenes *et al.*, 2007). MPO is a haemo-peroxidase found abundantly in the cytoplasmic granules of neutrophils, which when activated use the enzyme to produce microbiocidal hypochlorous acid. Circulating monocytes and macrophages have been shown to produce MPO (Loria *et al.*, 2008), however MPO-deficient monocytes and macrophages have also been observed in patients who suffer from hereditary MPO deficiency or acquired MPO deficiency (Locksley *et al.*, 1983), the latter frequently occurring as a result of AML, CML and MDS (Lanza, 1998). In addition to this, MOLM-13 cells, although of the myelomonocytic lineage, have clearly deviated from normal development pathway of this lineage and so cannot be assumed to express the same profile of enzymes as would be produced by normal monocytes. It was hypothesised at this point that the failure of Apocynin to decrease the ROS levels of MOLM-13 cells was due to an absence of the MPO enzyme. This was confirmed by a MPO histochemical stain (Figure 6), which used diaminobenzidine (DAB) as a target for H_2O_2 in the presence of MPO. The oxidation of DAB resulted in a brown chromogenic product visible in the control whole blood sample (Figure 6A), but the addition of DAB failed to elicit any colour change in the MOLM-13 cell sample (Figure 6B). This effectively eliminated Apocynin from the category of Nox inhibitors suitable for use our system.

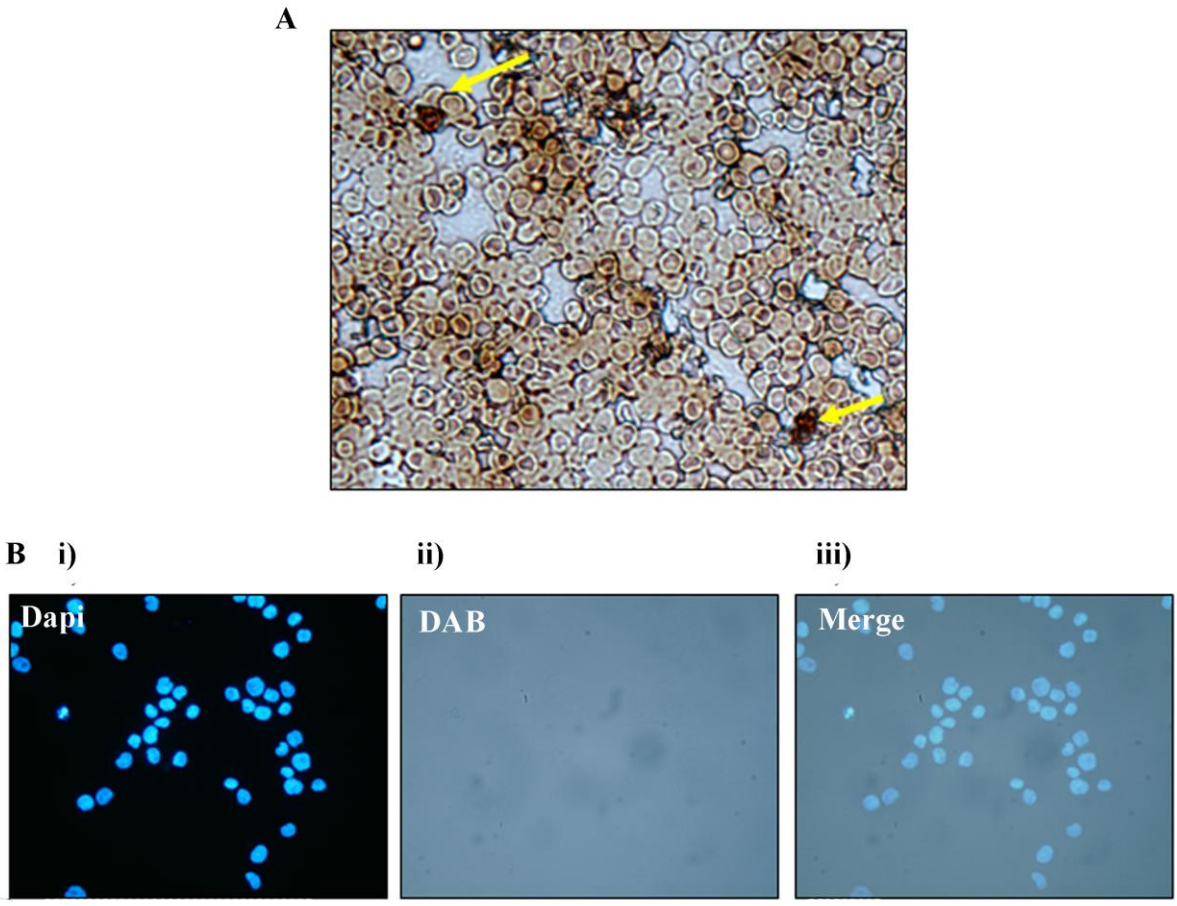


Figure 6. Myeloperoxidase stain performed on MOLM-13 cells

3,3'-Diaminobenzidine (DAB)-oxidation reaction for the detection of myeloperoxidase in cytospin preparations of **A)** whole blood sample, containing neutrophils indicated with arrows, taken from a C57BL/6 mouse of age P8 and imaged using a light microscope, **B)** MOLM-13 cells, counterstained with fluorescent nuclear probe Dapi and imaged under a fluorescent microscope i) and light microscope ii), with a merged image iii) to confirm presence of cells.

Incubation of MOLM-13 cells with calcium chelator Bapta-AM causes a slight decrease in ROS but does not affect p-Tyr levels

Another compound which has been used as a Nox inhibitor, is the calcium chelator 1,2- bis(o-aminophenoxy)ethane-N,N,N,N-tetraacetic acid (Bapta-AM) (Reistad and Mariussen, 2005; Yu *et al.*, 2005). The mode of action of this compound dictates its role as an inhibitor of Ca^{2+} -dependent Nox only, that is Nox 5 and the Duox. By determining the effect of Bapta-AM on p-Tyr levels, it would be possible to either narrow down the focus of this study to Nox 5 or rule it out as being involved in p-Tyr signalling in this system. Indeed the treatment of MOLM-13 cells with Bapta-AM resulted in a decrease in ROS levels (Figure 7A), but did not have a negative effect on the p-Tyr profile (Figure 7B). The decrease in ROS seemed to plateau after 1 µM and did not further decrease with increasing concentrations of Bapta-AM, suggesting that the Ca^{2+} -dependent Nox was fully inhibited at 1 µM. Western blot analysis showed that Bapta-AM slightly increased the level of p-Tyr in the cells, an effect attributable to the broad spectrum activity of the compound and its possible inhibitory effect on Ca^{2+} -dependent phosphatases (Maloney *et al.*, 1999). At this point it was concluded that Bapta-AM inhibits Nox 5 in MOLM-13 cells, and either this isoform is not involved in p-Tyr signalling or the broad targeting of Bapta-AM is masking any p-Tyr decrease which is occurring due to Nox 5 inhibition. Both possible explanations prompted us to cease using Bapta-AM as a Nox inhibitor for the purposes of this study.

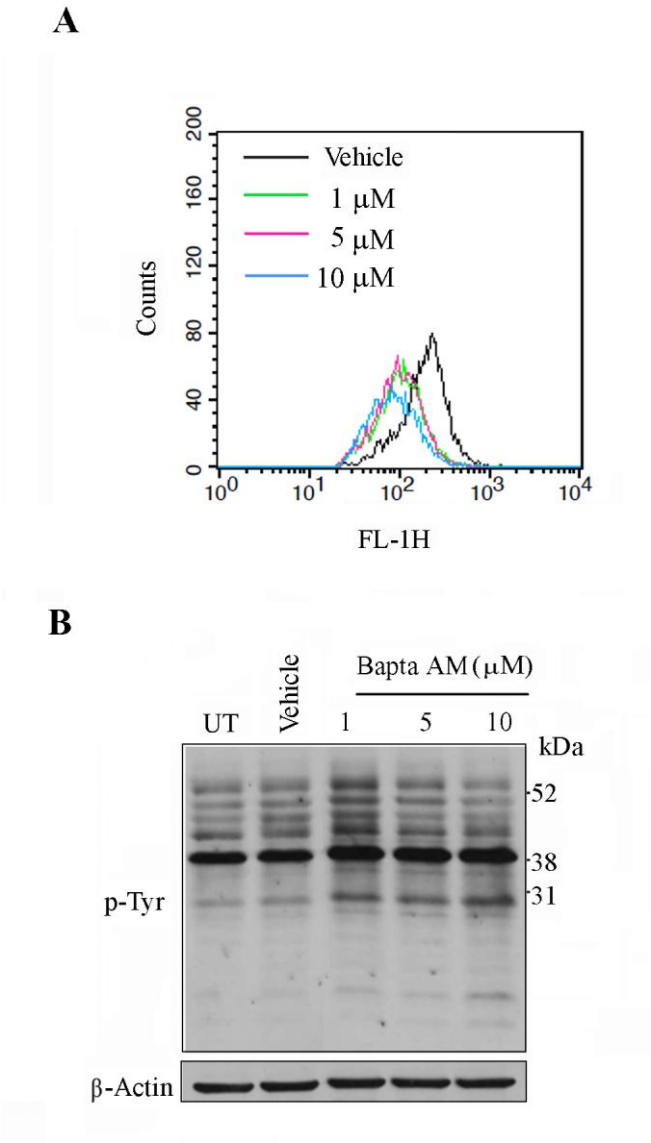


Figure 7. Effects of calcium chelator Bapta-AM on the ROS and p-Tyr levels of MOLM-13 cells. **A)** Intracellular ROS levels measured by relative DCF fluorescence (FL1-H) in untreated MOLM-13 cells overlaid with cells treated with the DMSO vehicle only or 1, 5 or 10 μM Bapta-AM, for 24 hours. **B)** Western blot analysis of the p-Tyr profile of untreated MOLM-13 cells, cells treated with the DMSO vehicle only or with 1, 5, 10 μM Bapta-AM for 24 hours. β-Actin is shown as a loading control.

Incubation of MOLM-13 cells with an inhibitor of Rac 1 GTPase does not result in a decrease in p-Tyr or ROS levels

The requirement of Rac 1-GTP for activation of Nox 1, 2 and possibly 3 and 4, provides an opportunity for effective inhibition of the activity of these Nox through inhibition of Rac 1. N6-[2-[[4-(diethylamino)-1-methylbutyl]amino]-6-methyl-4-pyrimidinyl]-2-methyl-4,6-quinolinediamine,trihydrochloride (NSC23766) inhibits Rac 1 by impairing its interaction with Rac-specific guanine nucleotide exchange factors (GEFs) TrioN and Tiam1 (Gao *et al.*, 2004). GEFs regulate the availability of Rac 1-GTP by substituting GTP for the GDP which is bound to Rac 1 (Ugolev *et al.*, 2008). The obvious pleiotrophic effects of inhibiting a molecule such as Rac 1, with its role as central node in a variety of signalling pathways (Pai *et al.*, 2010) have not prevented Rac 1 inhibitors such as NSC23766 from being widely used to implicate Nox activity in a range of systems (Gao *et al.*, 2004; Godfrey *et al.*, 2012). However, incubation of MOLM-13 cells with increasing concentrations of NSC23766 failed to reduce the levels of ROS being produced (Figure 8A), similarly there was no decrease in p-Tyr levels but instead a slight increase, likely due a stress response within the cell upon inhibition of such a crucial molecule (Figure 8B). The lack of any changes in cellular ROS suggests that the inhibitor is not effectively inhibiting Nox activity. There is some ambiguity in the literature with regard to the Rac isoform capable of activating Nox in haematopoietic systems. While some studies propose that the ubiquitous Rac 1 is the pre-dominant isoform associated with Nox in monocytic cells (Zhao *et al.*, 2003) others maintain that Rac 2 is solely responsible for Nox activation in haematopoietic cells (Hordijk, 2006). Further evidence points to the importance of the Rac effector domain, which is 100%

homologous between Rac 1 and Rac 2, in the Rac-p67phox interaction and cites this to suggests a redundancy between the two isoforms (Lapouge *et al.*, 2000; Kwong *et al.*, 1995) .This would explain the failure of a Rac 1 inhibitor to block Nox activity in cells which also express Rac 2.

MOLM-13 cells express Rac 1 and Rac 2

Indeed, western blot analysis of MOLM-13 cells, as well as another FLT3-ITD AML cell line MV4-11 showed that both Rac 1 and Rac 2 isoforms are highly expressed in these cells (Figure 9), providing evidence that some element of redundancy may account for the lack of effectiveness of the Rac 1 inhibitor. HeLa cells were used as both a positive control for Rac 1 expression (Burnham *et al.*, 2007) and a negative control for Rac 2 expression (Hordijk, 2006).

Nox inhibitor DPI causes a decrease in ROS and p-Tyr levels in MOLM-13 cells

Perhaps the most commonly used Nox inhibitor is diphenyleneiodonium chloride (DPI) (Cifuentes-Pagano *et al.*, 2012). DPI operates as a non-competitive inhibitor of flavin-containing enzymes, such as Nox, by abstracting an electron from the nucleophilic FAD group and generating a phenylated adduct which prevents electron transfer to the flavin site (O'Donnell *et al.*, 1993). While Bapta-AM or a Rac 1 inhibitor are thought to selectively inhibit specific Nox isoforms, the mode of action of DPI means that it is effective against all Nox and Duox family members, providing a broad basis from which to begin examining general Nox activity. Treatment of MOLM-13 cells with increasing concentrations of DPI for 24 hours resulted in a dose-dependent decrease in ROS (Figure 10A).

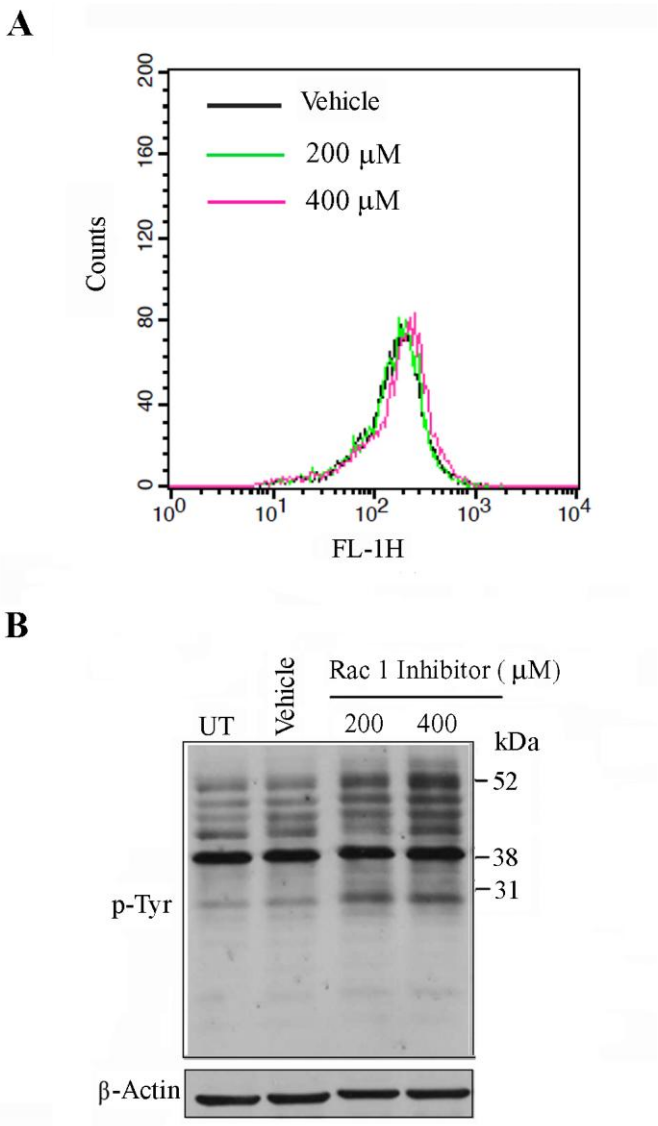


Figure 8. Effects of the Rac1 inhibitor NSC23766 on the ROS and p-Tyr levels of MOLM-13 cells. **A)** Intracellular ROS levels measured by relative DCF fluorescence (FL1-H) in MOLM-13 cells treated with the DMSO vehicle only and overlaid with cells treated with 200 or 400 µM NSC23766, for 24 hours. **B)** Western blot analysis of the p-Tyr profile of untreated MOLM-13 cells, cells treated with the DMSO vehicle only or with 200 or 400 µM NSC23766 for 24 hours. β-Actin is shown as a loading control.

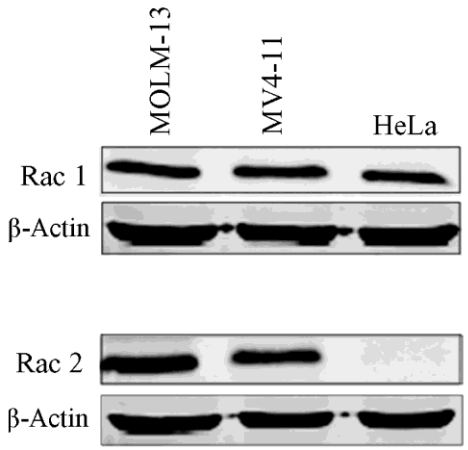


Figure 9. Rac 1 and Rac 2 expression in AML cell lines MOLM-13 and MV4-11
Western blot analysis of Rac 1 GTPase and Rac 2 GTPase in the AML cell lines MOLM-13 and MV4-11. The HeLa cell line is shown as positive control for the expression of Rac 1 GTPase and as a negative control for Rac 2 GTPase. β-Actin is shown as a loading control.

Although the greatest decrease was observed with 50 µM DPI, it was decided not to continue with this dose after Trypan Blue staining revealed a significant decrease in viability with this concentration of the compound, which was not observed for doses of 20 µM DPI and lower (Figure 10C). A concurrent decrease in p-Tyr occurred with increasing concentrations of DPI (Figure 10B) which was quantified by densitometry (Figure 10D).

To ensure that these effects on tyrosine phosphorylation were not unique to the MOLM-13 cells, the MV4-11 cell line was treated with 20 µM DPI for 24 hours, which resulted in a similar decrease in ROS (Figure 11A) and in p-Tyr (Figure 11B).

A dose of 20 µM was selected to progress with at this point, because of the decrease in p-Tyr and ROS observed without the viability of the cells becoming significantly compromised. A timecourse confirmed that 20 µM DPI gradually reduced both the ROS and p-Tyr levels from 1 to 24 hours (Figure 12A, 12B). To further confirm that DPI was indeed affecting the redox state of the cell, BIAM-labelling of MOLM-13 whole cell lysate was used to show that treatment of the cells with DPI was altering the amount of reduced proteins within the cell (Figure 12C).

Figure 10. The effects of the Nox inhibitor DPI on the ROS, viability and p-Tyr levels of MOLM-13 cells. **A)** Intracellular ROS levels measured by DCF fluorescence (FL1-H) in untreated MOLM-13 cells overlaid with cells treated with the DMSO vehicle only or 5, 20 or 50 μM Nox inhibitor DPI, for 24 hours. **B)** Western blot analysis of the p-Tyr profile of MOLM-13 cells treated with 5, 10 or 20 μM DPI for 24 hours. β-Actin is shown as a loading control. **C)** Histogram represents the viability of MOLM-13 cells after 24 hour incubation with 5, 10, 20 or 50 μM DPI as determined by Trypan Blue staining. Statistical analysis was performed using Student's *t*-test to evaluate the difference between untreated and treated samples. Significance was defined at the level of $P<0.05$. **D)** Histogram represents the densitometric analysis carried out the p-Tyr western blot profiles of three individual biological replicates of MOLM-13 cells treated with 5, 10 or 20 μM DPI or with the DMSO vehicle only for 24 hours. Statistical analysis was performed using Student's *t*-test to evaluate the difference between untreated and treated samples for each of three p-Tyr bands of 52, 38 and 31 kDa in size.

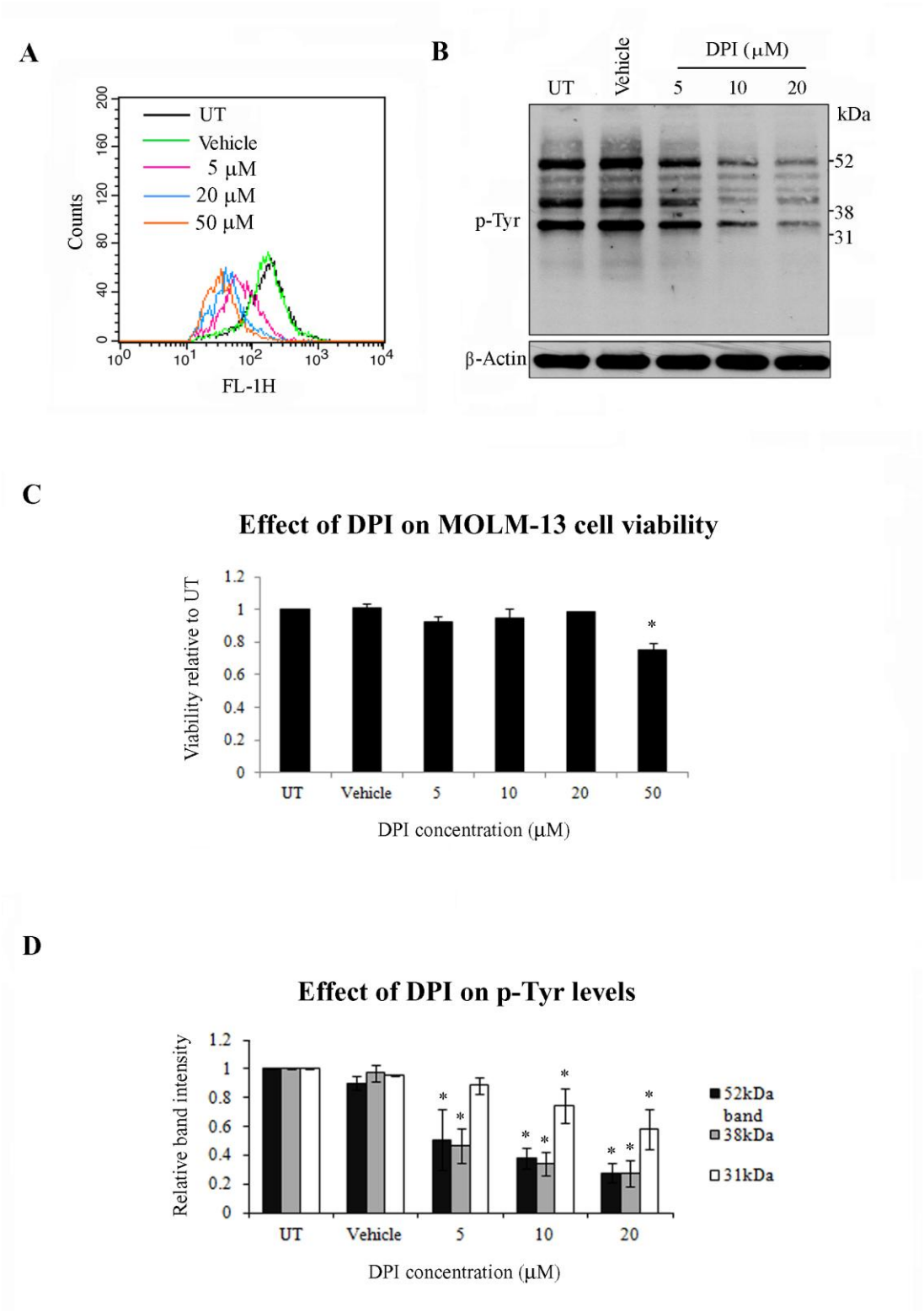


Figure 10. The effects of the Nox inhibitor DPI on the ROS, viability and p-Tyr levels of MOLM-13 cells (legend on facing page).

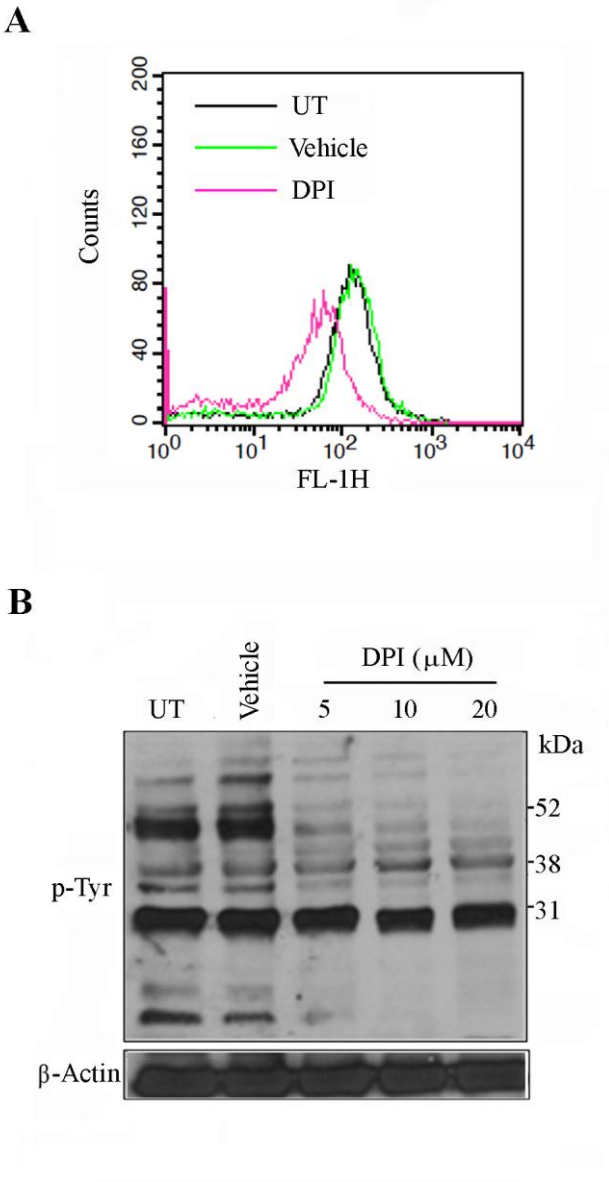


Figure 11. Effects of the Nox inhibitor DPI on the ROS and p-Tyr levels of MV4-11 cells. **A)** Intracellular ROS levels measured by relative DCF fluorescence (FL1-H) in MV4-11 cells treated with the DMSO vehicle only and overlaid with cells treated with 20 μM DPI, for 24 hours. **B)** Western blot analysis of the p-Tyr profile of untreated MV4-11 cells, cells treated with the DMSO vehicle only or with 20 μM DPI for 24 hours. β-Actin is shown as a loading control.

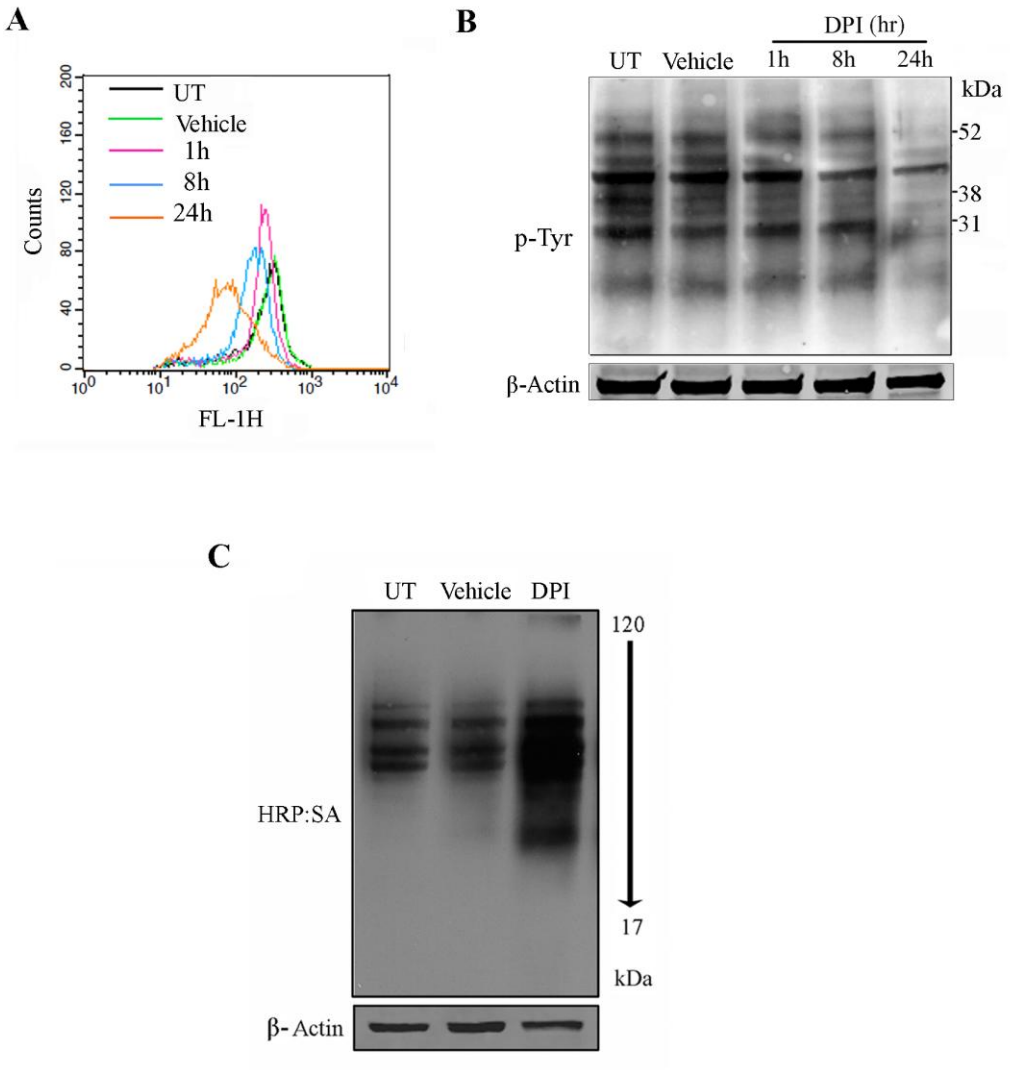


Figure 12. Optimisation of DPI incubation in MOLM-13 cells.

A) Intracellular ROS levels measured by relative DCF fluorescence (FL1-H) in MOLM-13 cells treated with the DMSO vehicle only and overlaid with cells treated with 20 µM DPI, for 1, 8, or 24 hours. **B)** Western blot analysis of the p-Tyr profile of untreated MOLM-13 cells, cells treated with the DMSO vehicle only or with 20 µM DPI for 1, 8 or 24 hours. **C)** HRP-SA detection of BIAM- labelled (reduced) protein content of MOLM-13 cells treated with 20 µM DPI for 24 hours. β-Actin is shown as a loading control.

The effect of the Nox inhibitor DPI on the p-Ser and p-Thr levels in MOLM-13 cells

The results generated thus far using DPI prompted exploration of whether this was an effect specific to phosphorylation at tyrosine residues or if the Nox inhibitor also affected serine and threonine phosphorylation. As phosphorylation of these residues is a far more common occurrence within the cell that tyrosine phosphorylation, should DPI also show an effect on p-Ser or p-Thr it would broaden the spectrum of Nox influence. However 20 μM DPI did not reduce levels of p-Ser within the MOLM-13 cells when used over a period of 1-24 hours (Figure 13A). In contrast, there appears to be an increase in p-Thr with DPI treatment at 1 hour and 8 hours before a dramatic decrease at 24 hours (Figure 13B). This pattern is different to p-Ser and does not align with the stepwise decrease seen in p-Tyr. Although there is no doubt that this result may be of interest, it fell beyond the scope of this study, which is focused on p-Tyr signalling, to investigate this angle any further.

Two-dimensional (2D) p-Tyr immunoblotting

The discrete p-Tyr bands observed in one-dimensional (1D) western blotting of a whole cell lysate with the pan p-Tyr antibody represented groups of proteins of similar molecular weights whose tyrosine phosphorylation was affected by DPI. In order to identify the specific proteins affected, the lysate would need to be further separated, providing a degree of resolution that would enable the visualisation of individual proteins. Two-dimensional SDS-PAGE is a process which was developed to fulfil this requirement.

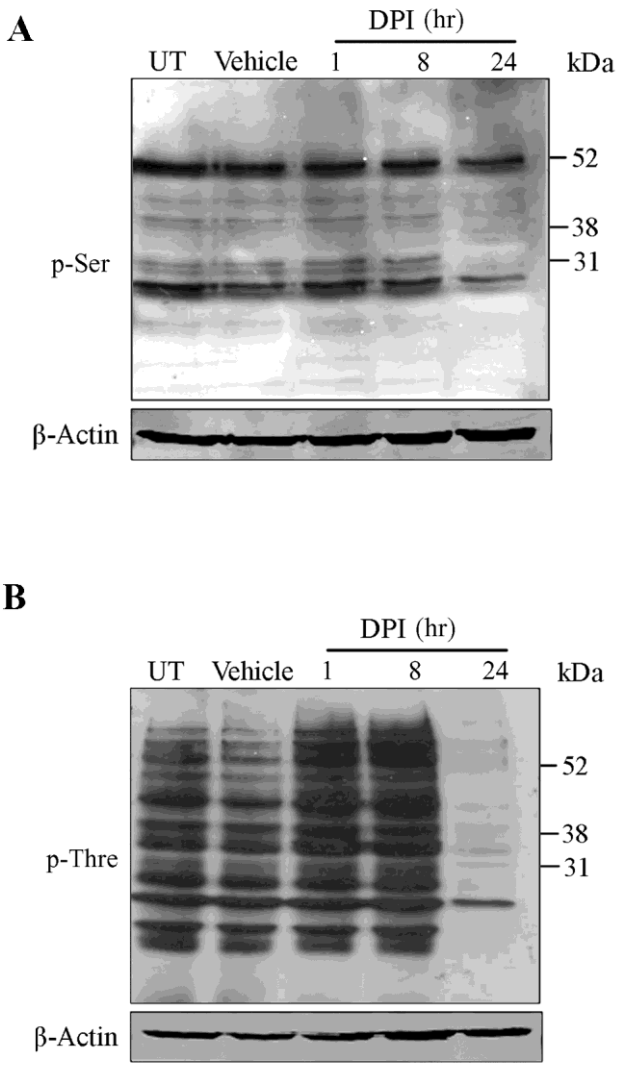


Figure 13. Effects of DPI on p-Ser and p-Thr levels of MOLM-13 cells

Western blot analysis of the **A)** phosphoserine (p-Ser) and **B)** phosphothreonine (p-Thr) profiles of MOLM-13 cells treated with 20 μM DPI for 1, 8 and 24 hours. β-Actin is shown as a loading control

This technique involves the separation of proteins firstly on the basis of their pH-dependent charge, through isoelectric focusing, and subsequently according to their size, on an SDS polyacrylamide gel. While many proteins may have a similar isoelectric point (pI) or molecular weight (mW) to another protein, it is less likely that they will share both distinct physiochemical characteristics, thus enabling the separation of up to 10 000 individual protein spots (O'Farrell, 1975). In combination with p-Tyr immunoblotting, 2D-SDS-PAGE allows the visualisation of discrete protein spots corresponding to individual proteins with phosphorylated tyrosine residues. Differences observed in samples treated with DPI can be used to identify the specific proteins affected.

Optimisation of two-dimensional gel p-Tyr immunoblotting

Appropriate sample preparation is crucial to the success of a 2D electrophoresis experiment. The method of preparation of protein samples for separation by 2D gel electrophoresis varies according to the nature of the material from which the protein is being extracted and often requires some optimisation to determine the correct protocol for the sample in question. Generally speaking, cell culture yields a cleaner sample than, for example, proteins extracted from animal tissue or other biological material which may contain albumin, IgG, lipids and other contaminating agents which may interfere with protein solubilisation and/or isoelectric focusing. It is advisable to keep the sample preparation as simple as possible as additional washing, precipitation and lyophilisation steps may not be necessary for the sample in question and may result in loss of protein.

Therefore, when considering how to prepare the protein samples extracted from MOLM-13 cells in culture it was decided to use the minimum amount of steps

necessary in order to maximise protein yield. The initial procedure involved simply washing the pellet in a wash buffer (250 mM sucrose, 10 mM Tris-HCl), resuspending the pelleted cells in a 2D lysis buffer (8 M urea, 4% 3-[(3-cholamidopropyl)dimethylammonio]-1-propanesulfonate, 2% IPG buffer (GE Healthcare, UK), 40 mM dithiothreitol, 200 μM 4-(2-Aminoethyl) benzenesulfonyl fluoride hydrochloride and cocktail protease inhibitors (Roche, Welwyn, Hertforshire, UK) and once the protein concentration has been determined using the Bradford Bio-Rad Assay (see Materials and Methods), the protein sample was added to the rehydration buffer and vortexed for 2 minutes to mix, then loaded onto the IPG strips as described in the Materials and Methods section.

The 2D lysis buffer was shown to be almost as effective as conventional RIPA lysis buffer in terms of protein yield (Figure 14A) and, as it did not contain any charged detergents, it was more suitable for the subsequent focusing steps.

The selection of IPG strips with a pH range of 3-10 came after comparison of both the 3-10 (Figure 14B) and 7-10 (Figure 14C) strips. It appeared that 7-10 was too narrow a range for broad examination of the total protein content of these cells and would be better suited to an investigation where a specific protein with an isoelectric point from 7-10 was of interest. Separation of MOLM-13 cell lysate with these strips resulted in a band of proteins forming at the pH 7 end of the gel, representing proteins with pIs of less than 7 which could not be separated and aggregated at this terminal of the IPG strip.

However, overall this method was yielding variable results with ‘Erratic Resistance’ frequently being recorded by the focuser and often resulting in an almost

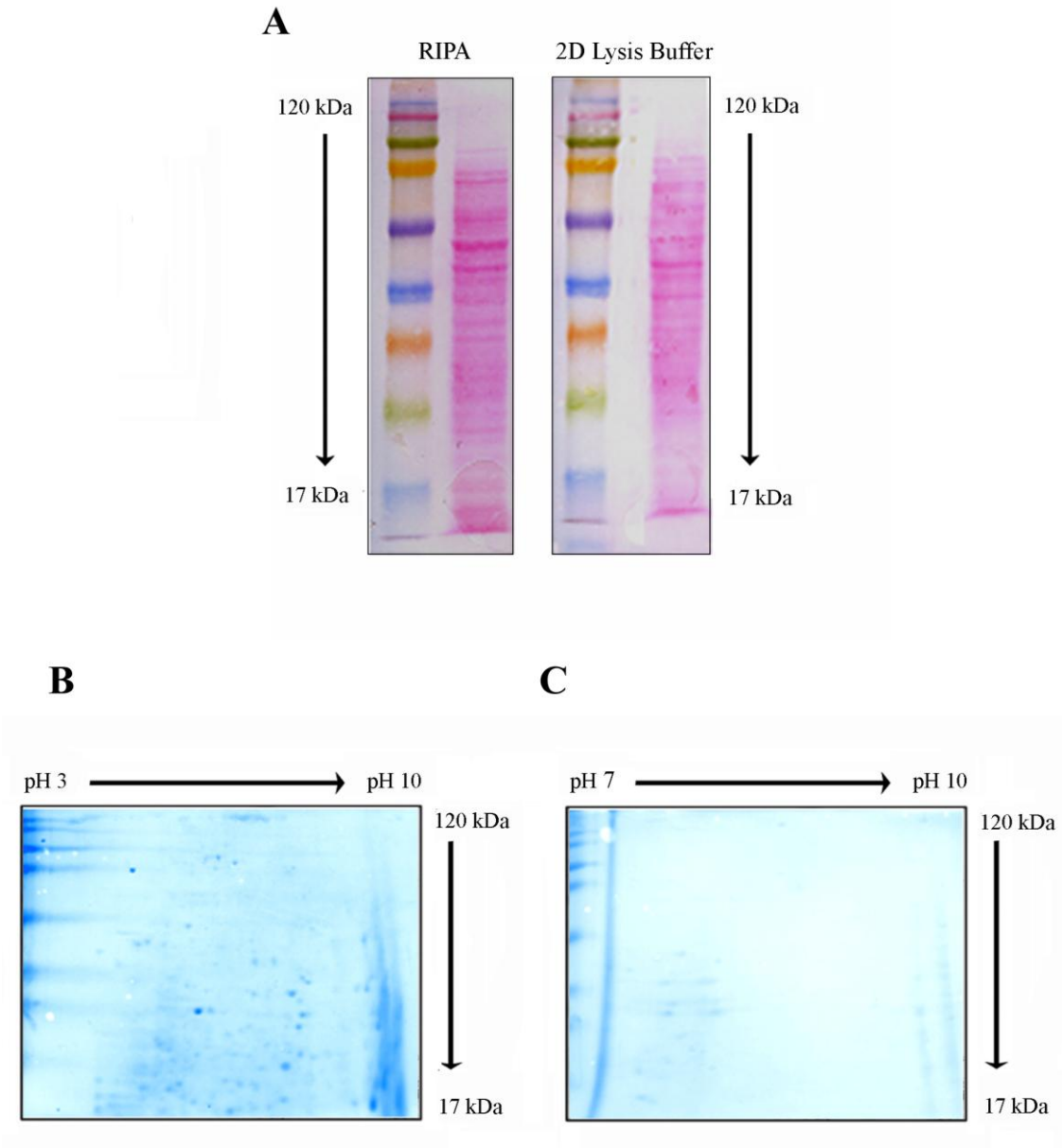


Figure 14. Optimisation of experimental conditions for 2D SDS-PAGE I.

A) Ponceau-stained nitrocellulose membranes showing result of SDS-PAGE carried out using MOLM-13 cells lysates prepared using RIPA lysis buffer or 2D lysis buffer. **B)** Coomassie-stained 2D gels, separated using IPG strips of pH range 3-10 or **C)** 7-10.

complete lack of protein in the second dimension SDS gels and p-Tyr blots except for a vertical smearing of aggregated, un-focused protein sample (Figure 15A).

This suggested that contaminants such as salts or other small ionic molecules, nucleic acids, polysaccharides, lipids or phenolic compounds, may have been present in the sample, interfering with the solubilisation and focusing of the proteins within the sample and preventing adequate first-dimension separation. The sucrose wash buffer was suspected as being a possible source of contaminating polysaccharides but removal of this washing step still resulted in poor focusing (15B). Washing of the cell pellet with PBS post harvesting was another possible source of contaminants, specifically salts, but again substitution of this wash with a sterilised water wash did not prevent the problem of inadequate focusing (15C). Accumulation of contaminants or precipitation of components of the lysis, wash or rehydration buffers over time while in storage was ruled out as being an issue when fresh buffers failed to improve the protein yield in the second dimension (15D).

Finally, in order to remove these contaminants the sample was precipitated with trichloroacetic acid (TCA) and ice-cold acetone, and then re-solubilised in the rehydration solution. TCA limits proteolysis, removes impurities and precipitates the protein, and acetone then removes the excess TCA as well as salts, lipids, nucleic acids and detergents (Jiang *et al.*, 2004; Méchin *et al.*, 2007). As TCA and acetone remove charged detergents, this precipitation step allowed us to use RIPA lysis buffer instead of 2D lysis buffer. RIPA lysis is known to result in a better protein yield of membrane proteins, lower background and minimal interference with proteins immunoreactivity (Gilbert *et al.*, 2002) but, because it contains charged

detergents (sodium deoxycholate) and salts (Tris-HCl, NaCl) which can also interfere with isoelectric focusing, removal of these is required prior to the first-dimension of separation. The combination of RIPA lysis buffer and TCA acetone precipitation results in protein spots becoming visible in the second- dimension SDS-PAGE upon staining with Colloidal Coomassie (Figure 16A). Addition of 2-Hydroxyethyl disulfide (De-Streak reagent) prior to focusing (Olsson *et al.*, 2002) also greatly improved the appearance of the SD- PAGE gel by preventing horizontal streaking of oxidised proteins (Figure 16B).

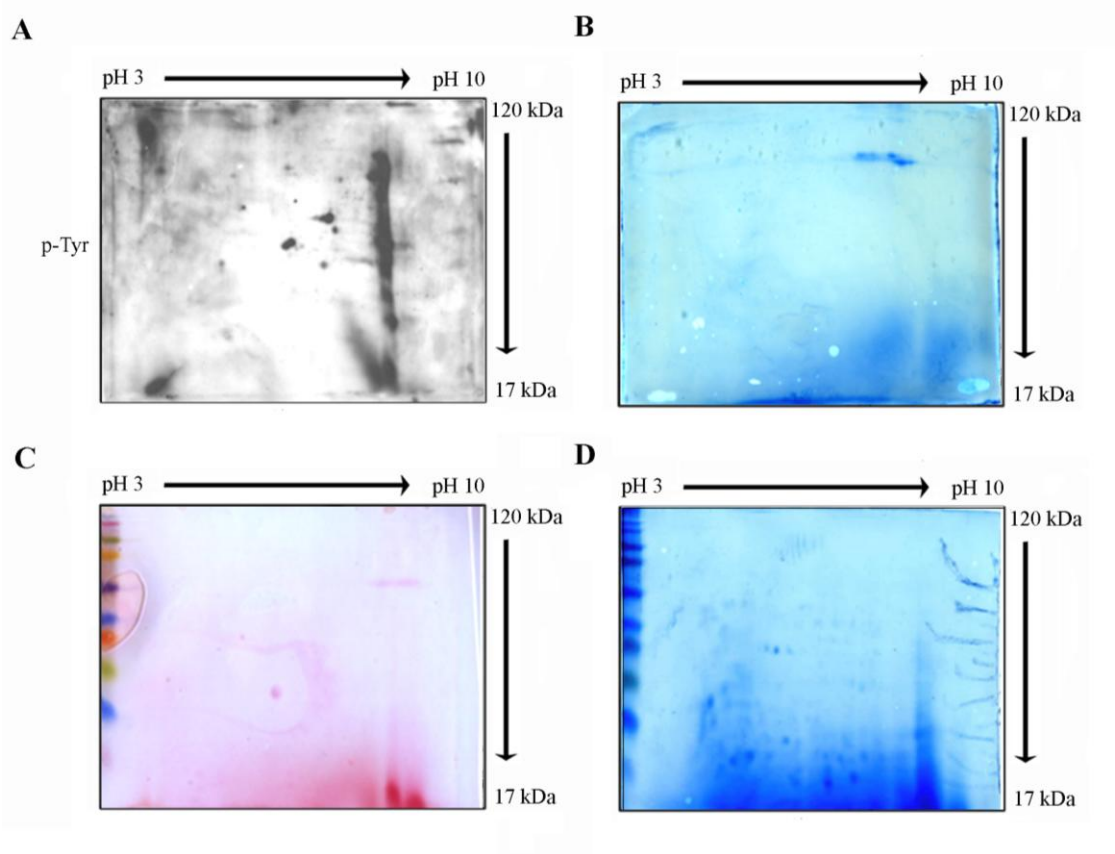


Figure 15. Optimisation of experimental conditions for 2D SDS-PAGE II.
A) 2D p-Tyr immunoblot result of 'Erratic Resistance' during the isoelectric focusing step. **B)** Coomassie-stained 2D gel after removal of sucrose wash step prior to focusing. **C)** Ponceau-stained nitrocellulose membrane of 2D SDS-PAGE after substitution of PBS wash with ddH_2O wash. **D)** Coomassie-stained 2D gel carried out using fresh rehydration and equilibration buffer stocks.

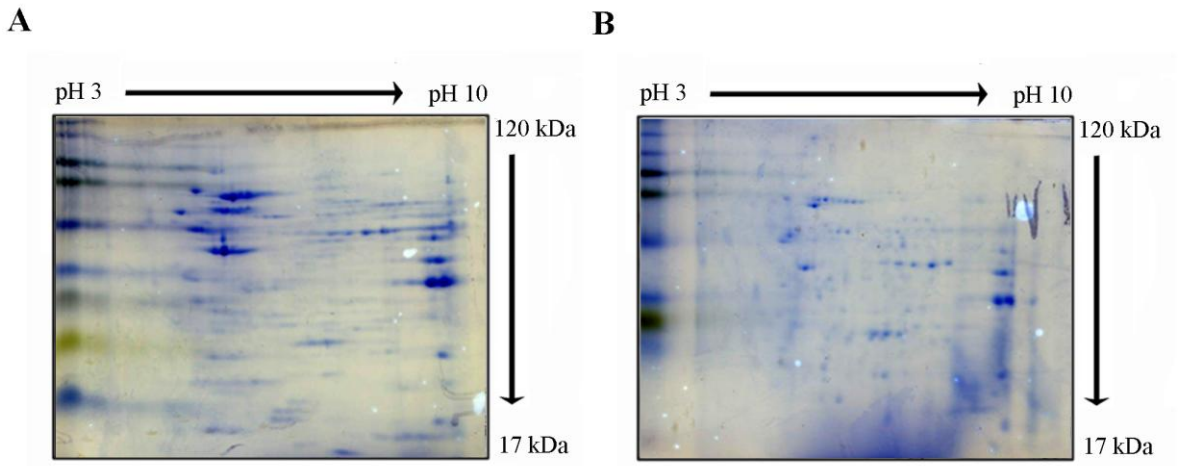


Figure 16. Effect of TCA/acetone precipitation on the isoelectric focusing of MOLM-13 cell lysates. A) Coomassie stained 2D gels prepared using trichloroacetic acid (TCA) acetone precipitation to remove contaminants prior to rehydration and **B)** the effects of addition of 2-hydroxyethyl disulfide (De-Streak reagent) to the rehydration buffer prior to focusing.

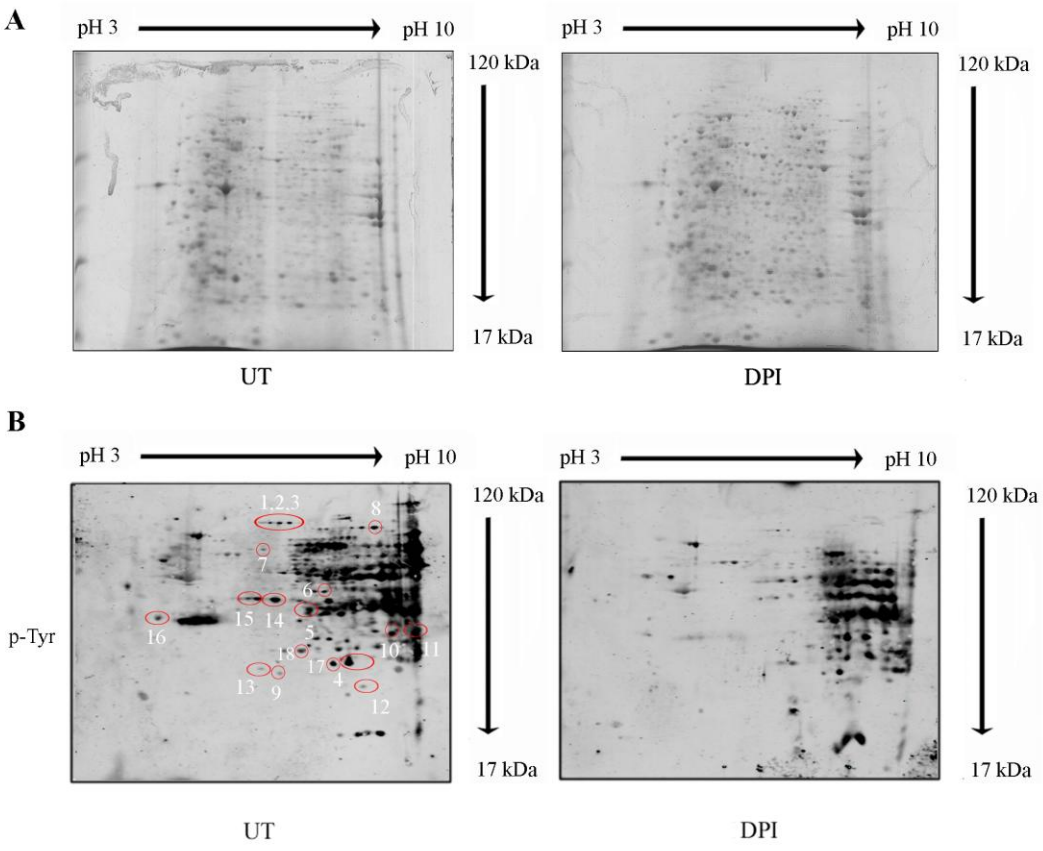
Identification of individual proteins whose tyrosine phosphorylation is affected by Nox activity

By comparing the 2D p-Tyr immunoblots of untreated MOLM-13 cells to those treated with 20 µM DPI for 24 hours, it was possible to select specific p-Tyr protein spots which were present in the untreated but absent in the DPI-treated samples, corresponding to proteins whose tyrosine phosphorylation state is dependent on Nox activity. Use of Fast Stain as a form of loading control to compare the whole protein profiles present on the membranes prior to incubation with the p-Tyr antibody, allowed the selection of proteins, from the corresponding Coomassie-stained 2D gel, which were differentially phosphorylated due to DPI and not differentially expressed or simply differentially loaded. 20 Protein spots were cut from the 2D Coomassie-stained gel replicates of the 2D p-Tyr immunoblots, which were run in parallel, and sent to Aberdeen Proteomics Facility for sequencing by tandem liquid chromatography mass spectrometry, and annotation using the National Centre for Biotechnology Information nr (NCBInr) database with the Matrix Science web server (Figure 17). The NCBInr is a protein database for Blast searches which contains frequently updated non-redundant sequences from GenBank coding sequence (CDS) translations, Protein Data Bank (PDB), Swiss-Prot, Protein Information Resource (PIR), and Protein Research Foundation (PRF). Of the 20 spots which were analysed, two did not return any significant hits. Spot no. 3 was identified as an un-named protein product (gi89054178). Table 1 represents the annotated spots which returned significant hits. In the case of more than one significant hit being returned for a single spot, the most significant as determined by Mascot and % coverage, is shown.

The protein products annotated from the screen were grouped according to their published functionality, as defined by the Universal Protein Resource (UniProt), in order to determine what category of proteins was most affected by Nox activity. The category of cytoskeletal or cytoskeletal-associated proteins was the largest (Figure 18), reflecting the emerging role for Nox in cell migration dynamics (Kim *et al.*, 2010; Schroder *et al.*, 2007). Ezrin, a member of the Ezrin/Radixin/Moesin family of cytoskeletal regulatory proteins was selected for further study, as a protein representative of the largest category of functionally annotated targets of Nox. Also contributing to this decision was the established role of Ezrin in tumourigenesis (Brambilla and Fais, 2009; Fais, 2004; Lugini *et al.*, 2003; Zhou *et al.*, 2010a) and the commercial availability of antibodies to two tyrosine phosphorylation sites on Ezrin Y146 and Y353, making Ezrin both a relevant and practical candidate for further investigation.

Ezrin tyrosine phosphorylation is affected by Nox inhibitor DPI

In order to confirm the results obtained through 2D p-Tyr immunoblotting, the phosphorylation of two tyrosine residues on Ezrin was examined by western blotting. Upon incubation of MOLM-13 cells with 20 μM DPI for 24 hours, a decrease in phosphorylation was observed at both Y146 and Y353 in Ezrin (Figure 19A), reflecting the pan p-Tyr western blot data, corresponding to a decrease in ROS and confirming the identification of Ezrin by 2D p-Tyr immunoblotting. A similar result was observed for the MV4-11 cell line (Figure 19B) suggesting that this effect may be more generally applicable to FLT3 mutated leukaemia cell lines, not just the unique cell line, MOLM-13.



C

1: Moesin
2: RDX protein (Radixin)
3: Cytovillin 2 (Ezrin)
4: gi89054178
5: Carbonic Anhydrase II
6: Fructose Bisphosphate Aldolase A
7: Heterogenous Nuclear Ribonucleoprotein H1
8: Heterogenous Nuclear Ribonucleoprotein K4
9: Fatty acid binding protein
10: High Mobility Group Protein B2
11: High Mobility Group Protein B1
12: Peptidylprolyl isomerase A (cyclophilin A)
13: Stathmin A
14: Heat Shock Protein B1/HSP 27
15: Heterogenous Nuclear Ribonucleoprotein C
16: Alpha Enolase
17: Alpha-Actin
18: Elongation factor 1B

Figure 17. Annotation of tyrosine phosphorylated proteins affected by Nox activity. Protein spots taken from **A)** Coomassie stained gel replicates of **B)** 2D p-Tyr immunoblots of untreated MOLM-13 cells and cells treated with 20 µM DPI for 24 hours. Spots indicated, numbered and annotated **C)** represent tyrosine phosphorylated proteins which are present in the untreated sample and absent in the DPI-treated sample.

Spot no.	Most significant hit	NCBI Accession no.	% Coverage	Mascot Score**
1	Moesin	gi4505257	17	95
2	RDX protein (Radixin)	gi33990951	15	130
3	Cytovillin 2 (Ezrin)	gi6457378	35	77
4	Unknown protein product	gi89054178	20	232
5	Carbonic Anhydrase II	gi4557395	44	214
6	Fructose Bisphosphate Aldolase A	gi4557305	45	525
7	Heterogenous Nuclear Ribonucleoprotein H1	gi48145673	17	104
8	Heterogenous Nuclear Ribonucleoprotein K4	gi73946435	28	194
9	Fatty acid binding protein	gi4557581	82	334
10	High Mobility Group Protein B2	gi11321591	39	133
11	High Mobility Group Protein B1	gi4504425	17	198
12	Peptidylprolyl isomerase A (cyclophilin A)	gi13937981	72	335
13	Stathmin A	gi5031851	45	132
14	Heat Shock Protein B1/HSP 27	gi4504517	62	313
15	Heterogenous Nuclear Ribonucleoprotein C	gi306875	14	99
16	Alpha Enolase	gi4503571	58	686
17	Alpha-Actin	gi4501881	49	706
18	Elongation factor 1B	gi4503477	45	279

*Defined as unambiguous if ≥ 15%

**Defined as significantly identical/extensively homologous if >44, P<0.05

Table 1. 2D p-Tyr sample submission protein identification report.

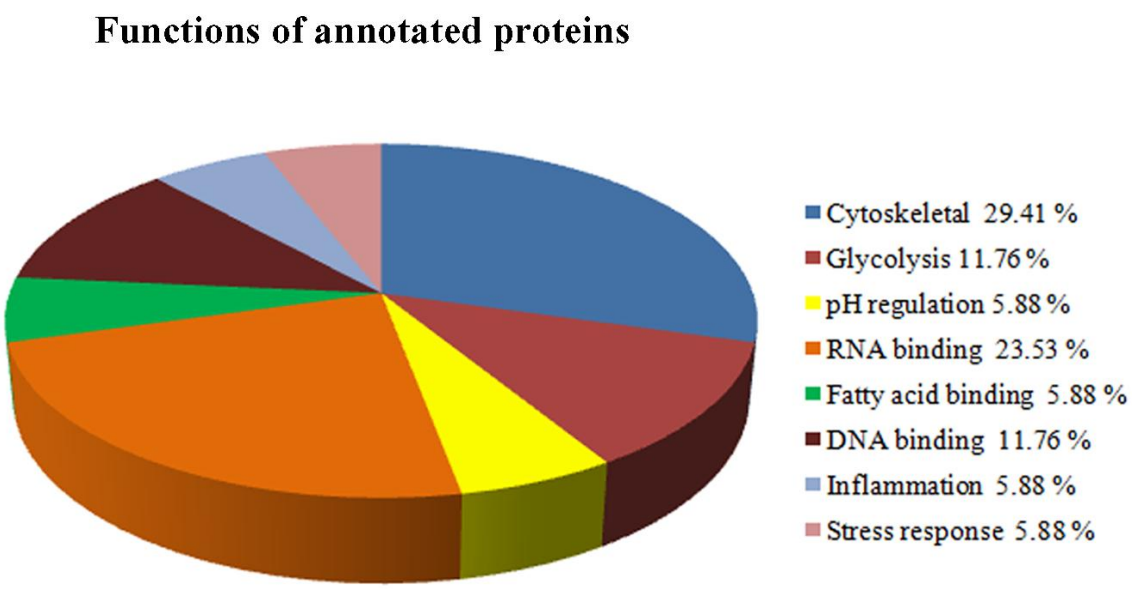


Figure 18. Categories of proteins affected by Nox activity.

Pie chart illustrating the proteins annotated from the 2D p-Tyr immunoblot samples submitted to Aberdeen Proteomic Facility, grouped according to function as defined by Universal Protein Resource (UniProt).

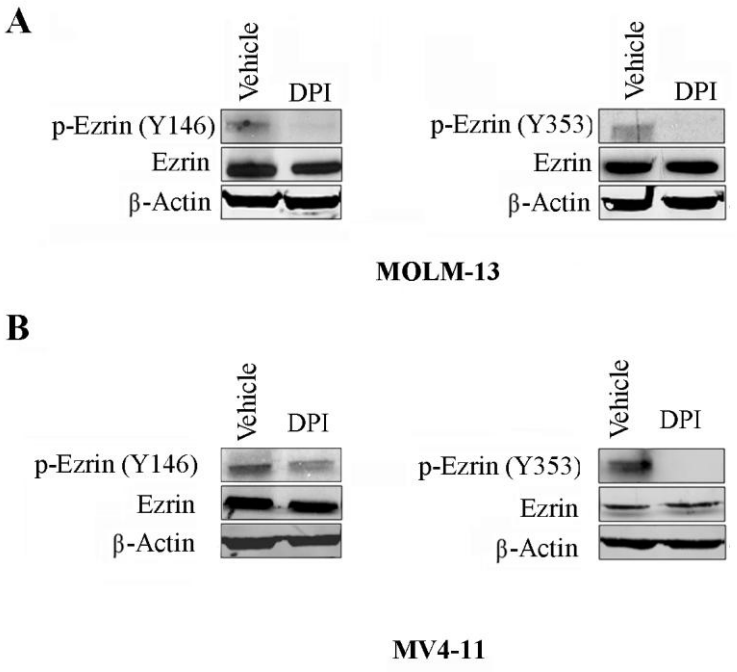


Figure 19. Ezrin tyrosine phosphorylation decreases upon Nox inhibition in MOLM-13 and MV4-11 cells. Western blot analysis of p-Ezrin Y146 and Y353 in **A)** MOLM-13 cells and **B)** MV4-11 cells treated with the DMSO vehicle only or with 20 μM DPI for 24 hours.

Discussion

The initial results detailed in this chapter relied upon the trial of a panel of Nox inhibitors in order to determine which provided the most efficient inhibition in our cell system. However, rather than finding ourselves in the position of having to choose between several highly suitable candidate compounds, the selection process, though lengthy, was easy. This was due to the failure of Apocynin and Rac1 inhibitor NSC23766 to affect the ROS levels of the MOLM-13 cells, which can be attributed to the lack of activating myeloperoxidase enzyme in the case of Apocynin and the presence of a compensating Rac isoform to overcome Rac1 inhibition.

The importance of exploring the reasons behind the failure of these inhibitors to elicit an ROS response is crucial to the interpretation of the result. It is important to distinguish between the possibility of simply an inefficient or inactive compound and the more profound situation of undetectable Nox involvement in the generation of ROS in these cells. The ROS reduction resulting from incubation with the calcium chelator Bapta-AM has implications for Ca^{2+}-dependent Nox only, Nox 5 and the Duox. The reduction in ROS plateaued at 1 μM suggesting that the Nox in question was fully inhibited, yet was not accompanied by a reduction in p-Tyr levels, the parameter chosen to represent a contribution to growth factor signalling. This can be interpreted to signify that the inhibited Nox does not influence p-Tyr within the cell, but of course this simply eliminates a single member of the Nox family and in no way informs us about the contribution of the Ca^{2+}-independent Nox. Thus, as useful as Bapta-AM may be in reducing ROS levels and facilitating research into Nox 5 and Duox 1 and 2 activities, it is limited in terms of attributing effects to broad Nox inhibition which is of more interest to this study. In fact the slight

increase in p-Tyr levels observed upon incubation with Bapta-AM, suggests that by chelating Ca^{2+} the compound is also causing some degree of stress to the cell, and providing further reason to avoid using such an inhibitor.

Western blotting using a pan antibody allowed visualisation of the p-Tyr signalling profile of the MOLM-13 cells, and observation of any global changes to the p-Tyr trend in order to judge the merit of using this readout as an indicator of the role of Nox. This broad-scale approach demonstrated that Nox activity positively influences the level of tyrosine phosphorylation within this cell line, phosphorylation which is strongly stimulated by the constitutively active RTK FLT3-ITD. As Nox enzymes do not have any kinase activity themselves, it can be concluded that they exert their effects on p-Tyr by regulation of redox-sensitive kinases or phosphatases.

The global profile of tyrosine phosphorylated proteins was translated into observable changes at an individual protein level through separation of lysates by 2D SDS-PAGE followed by p-Tyr immunoblotting. This technique requires a great deal of optimisation in order to meet the requirements of the specific experiment, with both the starting material and subsequent staining, blotting or sequencing steps affecting the way in which the samples are prepared. In general, lysates produced from cultured mammalian cells do not require precipitation or purification as would be required for samples of bodily fluids or homogenised animal or plant tissue. The relative lack of contaminants and non-protein impurities such as inorganic salts or minerals, connective tissue, extracellular matrix polysaccharides, bacteria, fungal or viral particles within the rigorously controlled cell culture environment means that, in theory, the cells can simply be lysed and used. However, in this instance we began to encounter erratic resistance readings on the isoelectric focuser during the focusing

step, accompanied by poor resolution of protein spots on the resulting polyacrylamide gel (Figure 15). The gels contained very few protein spots detectable by Coomassie staining and when transferred to the nitrocellulose membrane and stained with Fast-Stain similarly poor spot representation was observed. Probing with the p-Tyr antibody resulted in almost no detectable p-Tyr signal. A vertical smear was often observed towards the bottom of the stained gel and membrane and seemed to represent a condensed area of unfocused proteins which had migrated from the IPG strip into the polyacrylamide gel. This, in addition to the erratic resistance readings on the focuser, led us to conclude that the problem lay in the focusing step rather than the second dimension of separation.

Poor solubilisation of the protein sample in the rehydration buffer could result in loss of proteins either prior to the focusing, by simply remaining unsolubilised and not transferring to the IPG strip, or during the focusing step as some proteins have been shown to precipitate out of solution as they approach their isoelectric point (Rabilloud, 2009).This would result in under-representation of these proteins in the final polyacrylamide gel but does not account for the erratic resistance recorded on the focuser which indicates a high current flowing within the IPG strip. This can be explained by a high ampholyte concentration, low resistance water being used to dampen the electrode wicks or the presence of charged detergents in the rehydration buffer. As the rehydration buffer that was used did not contain any charged detergents this latter explanation was ruled out, similarly the water that was used to moisten the electrode wicks was double distilled and de-ionised resulting in an electrical conductivity of not more than 10 µS/cm (according to the Mili-Q water purification system specifications) enough to facilitate conductivity between the

electrode and the IPG strip but unlikely to be a rich source of charge-carrying molecules to contaminate the IPG strip. As carrier ampholytes are charged molecules themselves, their inclusion in the rehydration solution is necessary, to create equilibrium between the IPG strip and the buffer thus preventing the ampholytes within the IPG strip from leaching out into the buffer as well as to prevent isoelectric precipitation. However, carrier ampholytes are also potentially problematic as an excess of zwitterions could allow too much current to flow resulting in the erratic resistance reading. The rehydration solution which was used contained 4% (v/v) carrier ampholytes, and as 2-4% is generally recommended (Garfin, 2003) and this particular rehydration buffer composition had been previously used successfully by members of our laboratory (Tedesco *et al.*, 2010) we were satisfied that it was not the source of the erratic resistance. However, charged contaminants such as conductive salt ions within the sample itself would result in an effect similar to excessive carrier ampholytes, i.e. causing the target current (in this case 50 µA) to be reached prematurely during the initial low voltage steps and preventing further focusing (Rabilloud and Chevallet, 2000). In addition to this, uncharged contaminants within the sample, such as polysaccharides, can physically block the pores of the IPG strip, preventing the sample from entering and indirectly preventing focusing (Berkelman *et al.*, 2000).

A common problem in 2D SDS-PAGE, charged contaminants can be removed to some extent by the presence of electrode wicks which collect salts from the sample, preventing their accumulation at the anode and cathode which can create high conductivity and interfere with the pH gradient. But the wicks used here did not

seem to be efficiently removing the contaminants so the next option was to eliminate the contaminants from the lysate prior to solubilisation in the rehydration buffer.

Trichloroacetic acid (TCA) acetone precipitation is a method of removing substances such as salts, lipids and nucleic acids from protein lysates and is widely used in the preparation of samples for 2D SDS-PAGE (Link and LaBaer, 2011). Unfortunately this procedure can also reduce the protein content of the lysate as some proteins are insoluble in TCA or acetone, so a trade-off is required between improving the purity of the sample and the concomitant loss of proteins from it. In our situation, the presence of impurities was becoming such a problem that it was completely preventing successful 2D SDS-PAGE, so the TCA acetone precipitation was considered to be a worthwhile option. Including this step resulted in faultless isoelectric focusing and vastly improved the quality and quantity of the spot profile, allowing experiments to be carried out which resulted in annotation of individual protein targets. So the somewhat time-consuming optimisation of the 2D SDS-PAGE protocol was crucial to the quality of the final product and the quantity of data which could be extracted from it.

The grouping of the proteins identified by 2D SDS-PAGE was carried out based on functionality in order to identify cellular processes which are regulated by Nox in the FLT3-ITD cell line. Cytoskeletal regulation was the most highly represented function which tied in with the emerging role for both Nox and ROS in cellular motility and cytoskeletal dynamics.

However, the other categories of affected functions also proved interesting. Proteins which bind RNA such as hnRNPs featured strongly, and are known to play an important role in mRNA and pre-mRNA transport, processing and splicing.

Although there is a scarcity of data linking these proteins to Nox enzymes, there is evidence to suggest that they are subject to redox regulation (Stone and Collins, 2002; Stone *et al.*, 2003).

Glycolytic-related proteins have repeatedly been shown to be redox-sensitive due to the extensive cross-talk between components of glycolysis and of the antioxidant defence system, which promotes redox homeostasis (Hamanaka and Chandel, 2011). It appears that one of the most immediate intracellular responses to oxidative stress, is a shift to the pentose phosphate pathway of carbon metabolism, which ensures increased production of NADPH reducing equivalents in order to cope with the perceived change in redox state (Kruger *et al*., 2011). Glycolysis is a process which is inherently valuable to cancer cells and recent data from Lu *et al*. (2012) implicates Nox enzymes as supporting the increased glycolysis observed in tumours.

The DNA-binding high mobility group box (HMGB) proteins are known be redox sensitive proteins which operate at sites of oxidative DNA damage (Tang *et al.*, 2011), while proteins involved in stress responses such as heat shock protein 1 (HSP1) can act as chaperones to prevent oxidative damage to proteins, and regulate the cellular redox homeostasis by influencing the levels of cellular antioxidants such as GSH (Papp *et al.*, 2003). There is clearly a wide range of redox-influence within the cell and a rich variety of Nox targets which future studies can explore.

Ezrin, a member of the Ezrin/Radixin/Moesin (ERM) family, was selected in this case as representative of the category of cytoskeletal regulatory proteins because it also represented a link between Nox-derived ROS and cellular motility, two themes which have been repeatedly connected but the molecular basis of their connection is yet to be clearly defined. Ezrin is also of interest from a cancer

perspective, with an established role in metastasis (Brambilla and Fais, 2009; Fais, 2004; Federici *et al.*, 2009; Zhou *et al.*, 2010a) and an emerging role in proliferative signalling (Gautreau *et al.*, 1999; Heiska *et al.*, 2011; Kishore *et al.*, 2005; Srivastava *et al.*, 2005). Ezrin has been previously shown to be increased in leukaemic cells (Monni *et al.*, 2008) and has been identified as a target of oncogenic signalling from extracellular signalling mediators PDGF, EGF and HGF as well as intracellular oncogenic kinases Src, Lck and Rho (Crepaldi *et al.*, 1997; Fazioli *et al.*, 1993; Monni *et al.*, 2008).

Phosphorylation of Ezrin has been shown to regulate its activation and cytoskeletal associations (Chen *et al.*, 1994; Kondo *et al.*, 1997; Simons *et al.*, 1998), but much of the data favour a role for threonine phosphorylation in the structural organisation and localisation of Ezrin (Hayashi *et al.*, 1999; Matsui, 1998) and propose a signalling role for the phosphorylation of its tyrosine residues at Y146 and Y353 (Berryman *et al.*, 1995; Gautreau *et al.*, 1999; Heiska *et al.*, 2011). Krieg and Hunter (1992) showed that Ezrin is phosphorylated at these sites in response to epidermal growth factor (EGF) signalling and Berryman *et al*. (1995) went on to link this tyrosine phosphorylation to Ezrin oligomerisation and the subsequent appearance of microvilli. In our FLT3-ITD cell line, Ezrin tyrosine phosphorylation at residues Y146 and Y353 is reduced upon 24 hours of Nox inhibition. This implicates tyrosine phosphorylated Ezrin as a possible propagator of the oncogenic signals originating from FLT3 in MOLM-13 cells.

Chapter 4

FLT3 regulation of p22phox drives redox-modulation of Src and Ezrin and influences leukaemic cell migration

Abstract

The concept of reactive oxygen species being produced *via* the activation of specific oncogenes provides a basis for generating genomic instability and pro-survival signalling in tumour cells. This section demonstrates that oncogenic FLT3 signalling affects the activity of the NADPH oxidase enzymes through regulation of p22phox protein expression. FLT3 activity also affects the tyrosine phosphorylation of Ezrin, the downstream target of NADPH oxidase-derived ROS, in a p22phox-dependent manner. Inhibition of FLT3-ITD, using the staurosporine derivate PKC412, or of Nox, using diphenyleneiodonium chloride, also triggered a shift in Ezrin sub-cellular localisation as detected by immunofluorescence. The change in Ezrin localisation coincided with altered cell morphology, observed using scanning electron microscopy and a decreased ability to migrate through a polycarbonate transwell membrane. The results indicate that FLT3 drives production of ROS by Nox, which stimulates changes in Ezrin tyrosine phosphorylation and localisation *via* redox regulation of Src kinase. Furthermore, inhibition of FLT3-ITD signalling leads to alterations in MOLM-13 cell morphology and has a significant influence on cell motility.

Introduction

As an oncogenic RTK, FLT3-ITD is responsible for driving the molecular signalling events which ultimately contribute to the AML phenotype. The exact nature of these signal transduction events remains somewhat undefined apart from the established involvement of the Akt and MAPK (Hayakawa *et al.*, 2000; Takahashi, 2006) pathways which drive proliferation of the FLT3-ITD immature blasts. An area which has received attention of late is the possibility of a redox element functioning within the FLT3-ITD signalling pathway.

This possibility was heralded by the elucidation of an analogous signalling pathway in CML by Naughton *et al*. (2009), whereby the oncogenic RTK Bcr-Abl stimulates proliferative ROS production *via* Nox 4. It had been previously shown that Bcr-Abl-transformed cells generate increased levels of ROS compared to their untransformed counterparts (Sattler *et al.*, 2000), an observation echoed in FLT3-ITD-transformed cells, as well as FLT3-ITD containing AML cell lines and primary cells taken from AML patients with the FLT3-ITD mutation (Sallmyr *et al.*, 2008a). The increased ROS levels were thought to cause genomic instability, driving further oncogenic mutations (Sallmyr *et al.*, 2008b). When contemplating the source of this ROS, it is tempting to attribute it to the upregulated mitochondrial activity needed to support the chronic proliferation of the tumour cells. However, as demonstrated by Piccoli *et al*. (2005), haematopoietic stem cells have a low mitochondrial O_2 consumption rate corresponding to a low number of mitochondrial respiratory chain complexes. Further examination showed that 50% of the total O_2 consumption by these cells was due to Nox activity, making the Nox family very relevant to the redox profile of haematopoietic cells.

Sallmyr *et al*. (2008a) went on to link FLT3-ITD and downstream ROS production *via* Nox by focusing on the established status of STAT5 as a FLT3-ITD substrate (Piloto *et al.*, 2007). pSTAT5 has also been shown to interact with Rac 1-GTP, which is a crucial component of the Nox holoenzyme complex for at least 3 of the Nox isoforms (Kawashima *et al.*, 2006), and as a substrate for Bcr-Abl, has also been implicated as important factor in the initial transformation and maintenance of CML (Chatain *et al.*, 2012) . Sallmyr *et al*. (2008a) demonstrated that the amount of pSTAT5 binding to active Rac 1-GTP was increased in 32D cells with the FLT3-ITD mutation. They also used knockdown of STAT5 to reduce the ROS levels of 32D cells transformed with FLT3-ITD and showed that inhibition of FLT3-ITD using CEP-701 prevented Rac 1-GTP binding to Nox. Altogether this indicated that an interaction between pSTAT5 and Rac 1-GTP resulted in Nox activation downstream of FLT3-ITD.

Recently, Reddy *et al*. (2011) expanded this model by showing that in a range of haematopoietic cell lines containing oncogenic RTKs, including the FLT3-ITD cell line MOLM-13, the processes of growth and migration were heavily influenced by Nox isoforms 2 and 4 as well as p22phox. This again suggested a role for Nox in cellular functions driven by FLT3-ITD. However, in this situation the mode of FLT3-ITD driven regulation of Nox was concluded to be *via* control of the availability of the Nox substrate NADPH.

In contrast to this mechanism, it was demonstrated by Woolley *et al*. (2012) that in the FLT3-ITD cell line MV4-11, inhibition of FLT3-ITD signalling, using either PKC412 or CEP-701, resulted in a decrease in the protein levels of p22phox, suggesting a further scenario whereby FLT3 may regulate Nox activity. Woolley *et*

al. went on to clarify that the decrease in p22phox at a protein level did not correspond to a decrease in p22phox mRNA, but did correspond to post-translational regulation of p22phox through ubiquitination and proteasomal degradation.

The reported multi-layered regulation of Nox by FLT3-ITD, suggests at least that there is a connection between the two worth investigating. It also implies that Nox-derived ROS, produced in response to FLT3-ITD, function in a signalling capacity, mediating the FLT3-ITD-driven processes of growth and migration, as suggested by Reddy *et al*. (2011), and possibly proliferation, if the CML model proposed by Naughton *et al*. (2009) is representative of the situation in other haematopoietic tumours driven by oncogenic RTKs.

In the previous chapter the regulatory role played by Nox in p-Tyr signalling was demonstrated using 1- and 2-D p-Tyr immunoblotting. The targets identified represent proteins which undergo a decrease in tyrosine phosphorylation upon Nox inhibition, prompting the question of what intermediary effector detects changes in ROS levels and translates these into changes at the level of p-Tyr of specific proteins, and to what end.

Effectors of redox signalling can be identified by their common structural characteristics which render them susceptible to oxidation by ROS. One such group of affected molecules and probably the most widely studied in terms of redox-regulated protein targets, is the PTPs (Figure 20). These enzymes contain a crucial cysteine residue in their highly conserved active site motif which, at physiological pH, has a very low pKa, resulting in a propensity to become easily oxidised. Oxidation of this cysteine leads to a sulfenic acid-containing active site which is non-functional, creating a window of

phosphorylation signalling un-interrupted by phosphatase activity, until the enzyme is reduced and regenerated by Trx, Grx or GSH (Ostman *et al.*, 2011).

Locally higher levels of ROS can cause further oxidation to sulfinic acid or even the hyper-oxidised sulfonic acid form which, being more stable than the sulfenic intermediate, are not as amenable to reduction by cellular antioxidants. In fact, sulfinic and sulfonic-state PTPs are permanently inactivated, providing the opportunity for sustained phosphorylation signalling, until the inactive PTPs are degraded and replaced (Ostman *et al.*, 2011). Thus the duration of the phosphorylation signal can be modified by the levels of the accompanying oxidants. Many redox-sensitive PTPs are also regulated by phosphorylation, and it is becomingly increasingly obvious that these dual processes of PTP regulation do not occur in isolation but are tightly co-ordinated to temper the phosphorylation signal (Chiarugi and Buricchi, 2007).

The discrete targeting that can be achieved through the utilisation of oxidants as a signalling device has been demonstrated repeatedly by the PTP model (Choi *et al.*, 2011; Juarez *et al.*, 2008). The differential sensitivity of PTPs to both the nature of the oxidant species and the levels of ROS being produced, in addition the proximity of only the intended target PTP to the ROS source, confers a degree of specificity comparable to the enzyme-substrate 'lock and key' paradigm, and prevents the kind of 'collateral damage' which might compromise the integrity of the propagated signal.

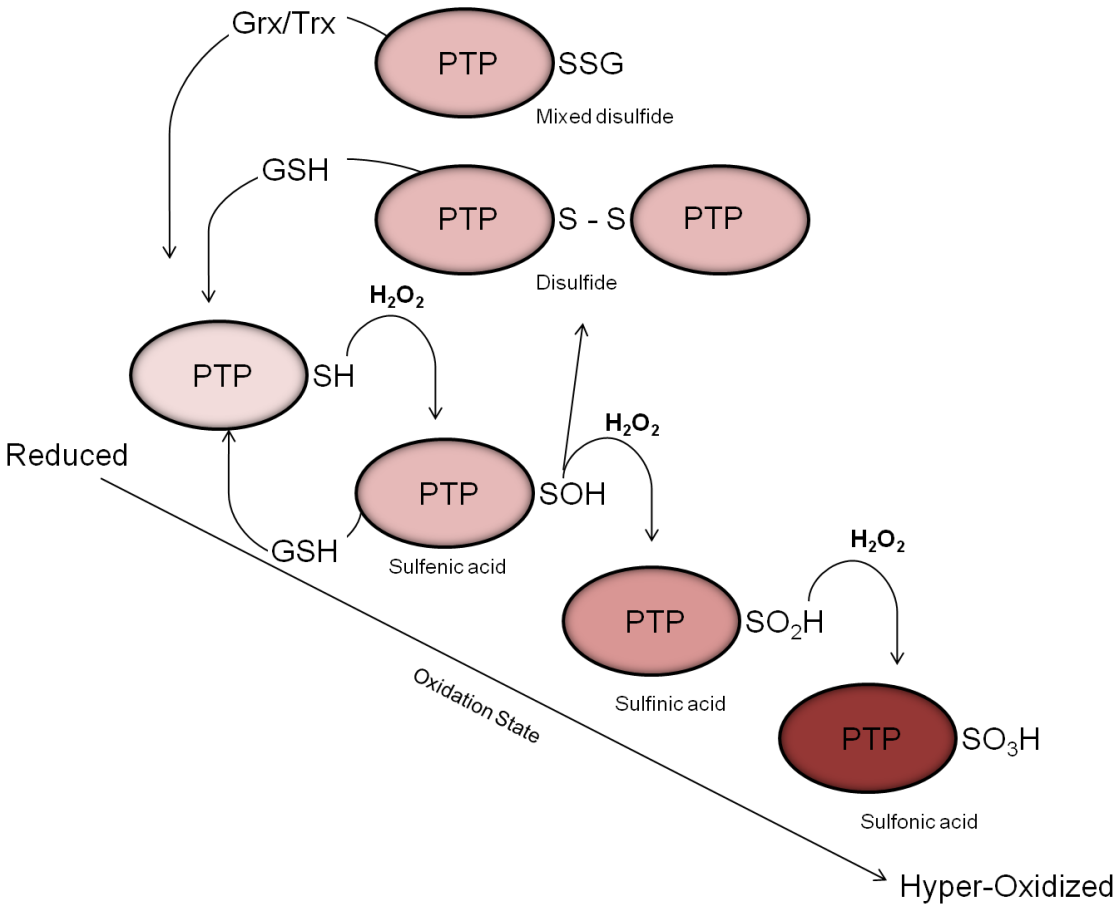


Figure 20. Oxidation states of PTPs

PTPs are highly susceptible to oxidation at physiological pH due to the low pKa of the catalytic cysteine residue located in the highly conserved PTP active site motif. Exposure of reduced PTPs (SH) to oxidants such as hydrogen peroxide (H_2O_2) results in the reversible formation of a sulfenic acid intermediate (SOH), which renders the enzyme inactive. Proximity to another cysteine at this stage favours the formation of a disulfide bond (S-S), or the formation of a mixed disulfide with GSH (PTP-SSG). Reduction of a disulfide or sulfenic acid-containing PTP by glutathione (GSH) returns the enzyme to its active state (SH), whereas further oxidation of the sulfenic acid intermediate results in the formation of the more stable sulfinic (SO_2H) or sulfonic (SO_3H) acids, hyper-oxidised and permanently inactivated.

While the redox-regulation of PTPs is an area which has been widely contributed to and acutely developed, it is reasonable to assume that PTPs are not the only molecules susceptible to oxidation for signalling purposes. Oxidation has been implicated as a signalling device in the regulation of GTPases (Heo, 2011), transcription factors (Li *et al.*, 2010), proteases (Guttmann and Ghoshal, 2011) and protein disulfide isomerases (Chen *et al.*, 2008b), amongst others.

The involvement of redox regulation of PTPs in p-Tyr signal transduction, prompts the question of whether the PTP counterpoint, the TKs, are similarly regulated by ROS. With a precedent set by the dual roles of phosphorylation as both a kinase-activating and phosphatase-inactivating mechanism, is there enough evidence to support the hypothesis that oxidation fulfils a similar function in the p-Tyr signalling machine?

PTKs are the other half of the p-Tyr signalling dynamic, described as the 'writer' to the PTPs 'eraser' in the p-Tyr toolkit model proposed by Lim and Pawson (2010). Such an interdependent system of signal transduction requires precise and co-ordinated regulation at every step, lest the powerful p-Tyr signal which features so prominently in almost every cellular function, become derailed.

The non-redox regulation of kinases through post-translational modifications such as phosphorylation as well as activator and inhibitor binding, has been extensively reviewed and can be summarised as a highly complex process with individual kinases and kinase families displaying idiosyncratic profiles of positive and negative regulatory modes. Similarly, the indirect redox regulation of kinases through the oxidative inactivation of inhibitory PTPs, has been widely documented

(Chiarugi and Cirri, 2003) and represents an important mechanism of redox-mediated p-Tyr signalling.

Early evidence for the direct modification of kinases by ROS centred on the *in vitro* oxidation of Src kinase by nitric oxide (NO)-releasing agents resulting in enhanced catalytic activity (Akhand *et al.*, 1999; Minetti *et al.*, 2002). Subsequent studies by Senga *et al*. (2000) identified a number of cysteine residues in Src necessary for the enzymes stability and transformative ability. Giannoni *et al*. (2005) focused on Cys245 and Cys487 which were demonstrated to undergo intramolecular disulfide bridge linkage upon exposure to ROS, leading to a level of Src activation not observed in the redox-insensitive Cys-Ala mutants. This collection of work was crucial in formulating the concept of phases of kinase activation through phosphorylation and de-phosphorylation steps, with a final super-activation state being achieved through oxidation. This concept and the supporting literature which has emerged since, demonstrating direct redox regulation of Src kinase in a variety of systems was recently and comprehensively reviewed by Giannoni *et al*. (2010).

Even in the two years since this review, further studies have emerged attesting to the direct redox regulation of Src kinase in different cell systems and with diverse signalling outcomes. Most recently, Xi *et al*. (2011) showed that, under conditions of hyperglycemia, IGF-1 signalling leads to enhanced Src activation through direct oxidation by Nox 4 in vascular smooth muscle cells. Lee *et al*. (2011) similarly demonstrates that vascular c-Src forms a signalling axis with VEGF-derived ROS through the direct oxidation of cysteine residues on both c-Src and VEGFR, resulting in activation of the c-Src-PI3K-Akt pathway downstream of VEGFR but not the PLCγ1-Erk1/2 pathway, which is also downstream of the

receptor. The redox-specific activation of VEGFR appears to lead exclusively to redox activation of c-Src allowing the cell to sense the redox status of the endothelium and respond with specific pathway activation.

The vulnerability of cells to de-regulated kinase activity and the subsequent risks of tumourigenesis have been widely documented, with an emphasis on the activation of kinases such as Src, through constitutive phosphorylation or overexpression. However the ability of redox-regulated kinases such as Src to become activated through oxidation represents another potential avenue for pro-tumourigenic activity, especially within the oxidising environment of many cancer cells which display higher levels of ROS than their non-cancer counterparts (Hole *et al.*, 2012; Mitsushita *et al.*, 2004; Weinberg and Chandel, 2009; Wu, 2006).

One of Hanahan and Weinberg's (2000) hallmark tumourigenic characteristics is the focus of a recent paper by Zhu *et al*. (2011), in which the authors demonstrate a role for redox-regulation of Src in conferring anoikis-resistance to tumours. Oxidative activation of Src is triggered by a high ratio of $O_2^{-\cdot}$:H_2O_2, caused by Nox activation downstream of integrin stimulation, echoing the findings of Giannoni *et al*.(2005). However in the situation described by Zhu and colleagues, cell attachment to the ECM *via* integrins is mimicked by angiopoietin-like 4 protein (ANGPTL4) engagement of integrins of cells in suspension, stimulating the ROS production, activation of Src and subsequent pro-survival signalling normally associated with cell adhesion and eliminating the dependence of tumour cells on ECM or cell-cell contact.

Although these studies support a model whereby Src is activated in response to ROS, data consistent with an inhibitory role for ROS in Src activity has also been

proffered by Kemble *et al.* (2009). In contrast to the majority of published studies, yet echoing the earlier results of Cunnick *et al*. (1998), Kemble proposes that, upon oxidation, intermolecular disulfide bridges form between Cys277 residues on two Src molecules, resulting in inactive Src dimers. According to the authors this scenario is also applicable to FGFR1 because of its corresponding cysteine residue.

The contrast and seeming disparity between this work and other studies can be explained in part by the different conditions used by different groups. Kemble highlights two advantages of a cell-free assay over cellular techniques when examining redox-regulation of proteins. Firstly, in a cell-free system the absence of any Src-regulatory proteins, which may be the legitimate targets of oxidants, ensures that any effects on Src observed can be attributed to direct oxidation of the kinase itself and not to indirect effects *via* oxidation of mediators. Secondly, great care must be taken during the processes of lysis and immunoprecipitation, used to isolate Src from cells, in order to preserve the intracellular redox state of the kinase, by minimising both exposure to environmental oxygen as well as the release of cellular oxidants during lysis. However, cell-free assays alone cannot faithfully replicate the physiological scenario of localised ROS production in proximity to relevant protein targets, nor do they address the issue of oxidant concentration carefully tempered by the presence of cellular antioxidants and Prxs. In addition to this, it is likely that the physiological redox regulation of Src is complex enough to involve both the redox-activation and inactivation of Src depending on the ROS concentration as well as the sensitivity and accessibility of individual cysteine residues. As argued by Giannoni *et al*. (2010), oxidation of Cys277 might well be an artefact of the process of

isolating Src, and may not occur within intact cells due to the native conformation of the enzyme.

It is interesting at this point to note that Tang *et al*. (2005) also observed redox-inactivation of Src kinase but in live cells, through the addition of H_2O_2 to primary HUVECs, HAECs, and E6 fibroblasts. This is in contrast to the cell-free assays used by Kemble *et al*. (2009), in which a redox-inactivation of Src was also observed. However Tang *et al*. reported that Src activity was not affected in cell free assays, clearly demonstrating a disconnect between the two systems.

In order to address the conflict between their results and the earlier studies supporting redox-activation of Src, Tang *et al*. propose an elegant compromise by outlining a scenario whereby both the localisation of the kinase, as well as the dose of H_2O_2 used, affect the outcome in terms of positive or negative regulation. The immunofluorescence data of Tang *et al*. appear to demonstrate that Src kinases residing in focal adhesion complexes or at the plasma membrane become inactivated after addition of H_2O_2, whereas those localised to the cytoplasm and compartments such as endosomes become activated. Tang *et al*. also comment on the importance of the dose of H_2O_2 used, they choose to use a relatively low dose (50-250 μM), describing how very high concentrations in the mM range, which cannot be claimed to be physiologically relevant, may eclipse the natural regulation of the kinase, producing highly artificial results. The addition of high doses of exogenous H_2O_2 is often used to demonstrate both the redox-activation and inactivation of Src but cannot accurately reproduce the temporally and spatially regulated cellular production of H_2O_2. Another alternative, the induction of ROS-producing enzymes would allow the concentration, proximity, duration and nature of the species

produced to more closely reflect that of the physiological situation, and is one method of introducing a much-needed cellular context into the debate on redox regulation of Src.

Irrespective of its consequence for Src kinase activity, the susceptibility of Src to redox regulation is a characteristic shared by other members of the Src family kinases (SFK). The first kinase determined to be redox regulated was the lymphocyte-specific tyrosine protein kinase p56lck (Lck) (Nakamura *et al.*, 1993). Nakamura and colleagues examined the tyrosine phosphorylation profile of T-cells after exposure to oxidative stress, in the form of the thiol-oxidising agent diamide, and discovered that Lck was phosphorylated at its autophosphorylation site Tyr394 after exposure to the oxidant. They also detected increased activity of Lck presumably as a consequence of this phosphorylation event, while other similar kinases such as p59fyn did not become activated.

More recently the SFK Lyn was demonstrated by Yoo *et al*. (2011) to be a 'redox sensor' in zebrafish neutrophils. In this elegant model of wound healing, neutrophilic Lyn undergoes oxidation at Cys466 upon exposure to extracellular H_2O_2 produced at the site of the wound, resulting in the autophosphorylation and activation of the kinase and selective stimulation of its downstream pathways. In this case Erk is activated whereas JNK and p38 remain un-stimulated. The redox activation of Lyn appears to be the dominant factor driving the directional migration of the neutrophils towards the wounded area. Although the paracrine signalling properties of H_2O_2 in wound healing have been well described (Niethammer *et al.*, 2009), Yoo *et al*. are the first to demonstrate a molecular connection between the redox signal and the neutrophil recruitment response.

The Src family are not the only kinases susceptible to redox-regulation. RTKs such as the insulin receptor (IR), epidermal growth factor receptor (EGFR), platelet-derived growth factor receptor (PDGFR) and c-Ret have all been reported to undergo direct oxidation (Nakashima *et al.*, 2002). In addition to this and as documented by Kemble *et al*. (2009) there is evidence to suggest that FGFR1 is negatively redox regulated while Lee *et al*. (2011) report that VEGFR undergoes oxidative activation.

Close investigation of the redox-regulation of proto-oncogenic RTK c-Ret by Kato *et al*.(2000) has revealed that oxidative activation of the kinase occurs *via* disulfide bond formation between cysteine residues on two different c-Ret molecules, resulting in dimerisation. The cysteine residue in question, Cys376, is necessary for the basal activity of the kinase, as well as its up-regulation in response to UV irradiation. As the authors point out, this cysteine is highly conserved in a number of receptor and non-RTKs such as Ros, c-Abl, Src, Fms, Fps, HIR, HER, and Lck, implying that a similar mechanism for oxidative regulation may operate with regard to all of these kinases. Interestingly, the corresponding residue in Src to c-Ret Cys376 is Cys498, which was not implicated in previously mentioned literature discussing Src redox regulation but was recently demonstrated by Rahman *et al*. (2010) to undergo S-nitrosylation upon exposure to NO leading to kinase activation. This development introduces the possibility that reactive nitrogen species (RNS) may also play a role in kinase regulation through cysteine modification.

In addition to Src, the range of redox-sensitive targets is broadening and diversifying to include a variety of kinases operating in a wide range of systems. Recent evidence has identified a redox element in the direct regulation of c-Abl

(Leonberg and Chai, 2007), Akt (Wani *et al.*, 2011), c-AMP-dependent protein kinase (Humphries *et al.*, 2005), Erk (Galli *et al.*, 2008), Ca(2+)/calmodulin-dependent protein kinase (Erickson *et al.*, 2008), cGMP–dependent protein kinase (PKG) Iα (Burgoyne *et al.*, 2007), ataxia–telangiectasia mutated (ATM) protein kinase (Guo *et al.*, 2010) and apoptosis signal-regulated kinase-1 (ASK-1) (Nadeau *et al.*, 2007). Additionally, evidence to support a role for direct redox regulation of several components of the MAPK signalling pathway (Greene *et al*.,2000 ; Galli *et al*., 2008), re-inforces the early work of Adler *et al*. (1999), who demonstrated the redox-dependent activation of JNK via the oxidative inactivation of its inhibitor GSH-S-transferase Pi.

This emerging body of literature adds to the ongoing shift in the redox-signalling paradigm by presenting evidence to support the hypothesis that redox signalling, particularly in the context of phosphorylation signal transduction, does not simply operate *via* the inhibition of phosphatases but also involves the direct regulation of redox-sensitive kinases.

One of the objectives of this chapter is to contribute to that shift in paradigm by providing evidence to support a role for the redox regulation of Src kinase in mediating the Nox-Ezrin communication which was elucidated in the previous chapter. This chapter will also clarify the nature of the relationship between FLT3 and Nox in the MOLM-13 AML cell and demonstrate the relevance of the FLT3-Nox-Src-Ezrin signalling pathway to the AML cell phenotype.

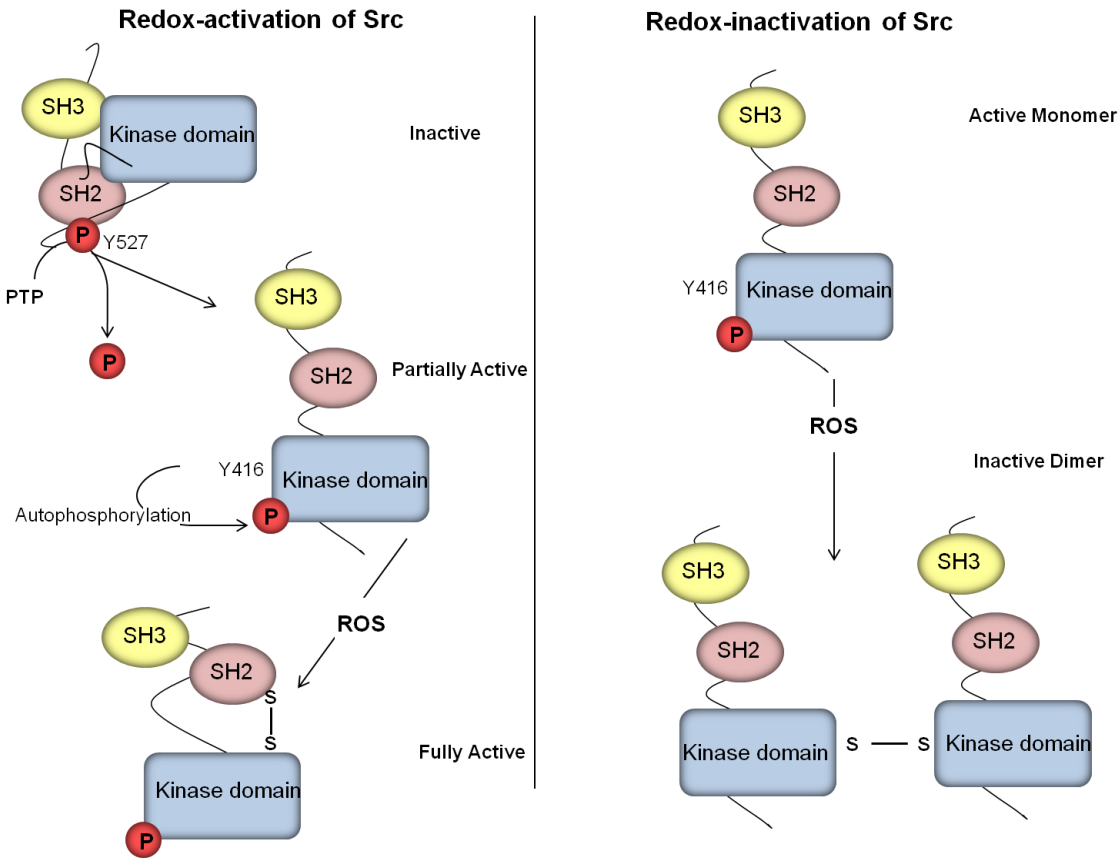


Figure 21. Models of Src kinase redox regulation

Contrasting models of the outcome of Src oxidation as proposed by Giannoni *et al*. (2005) (left) and Kemble *et al*. (2009) (right). The model of redox-activation of Src involves phases of Src activation, from the generally accepted inactive conformation due to inhibitory phosphorylation at C-terminal Y527, to the first phase of activation *via* relief of this inhibitory phosphate and autophosphorylation at Y416 of the catalytic domain. The final stage of activation requires oxidation of Cys245 of the SH2 domain and Cys487 of the catalytic domain resulting in intramolecular disulfide bond formation and an increase in kinase activity. Kemble *et al*. support the conflicting theory of redox inactivation of Src *via* oxidation of Cys277 on different Src molecules resulting in intermolecular disulfide bond formation, producing an inactive dimer.

Results

FLT3 signalling affects the redox state of MOLM-13 cells

The production of ROS downstream of FLT3 signalling has been reported by Sallmyr *et al*. (2008a) and Reddy *et al*. (2011), and recent work from our own laboratory (Woolley *et al.*, 2012) has shown that inhibition of FLT3-ITD by the staurosporine derivate PKC412 (Midostaurin) , which is currently in clinical trials for the treatment of AML (Kindler *et al.*, 2010), reduces the ROS levels of the FLT3-ITD containing MV4-11 cell line. A similar effect was observed in MOLM-13 cells (Figure 22A), corresponding to an increase in BIAM-labelled protein (Figure 22B) and a decrease in p-FLT3 (Figure 22C) with no significant decrease in cell viability at this concentration (Figure 22D). This suggests that PKC412 inhibits FLT3-ITD in the MOLM-13 cells and is affecting the redox state of the cell.

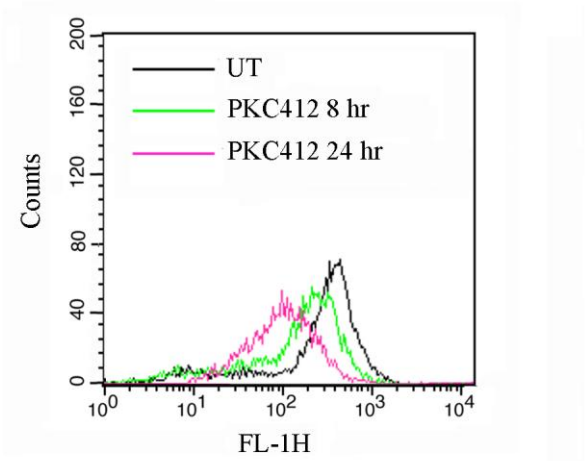
Inhibition of FLT3-ITD results in a decrease in p22phox protein levels in MOLM-13

Evidence in the literature strongly implicates FLT3 as being an upstream regulator of Nox with much of the data focusing on the oncogenic signalling by the constitutively active FLT3-ITD through STAT5 phosphorylation and NAPDH availability (Reddy *et al.*, 2011; Sallmyr *et al.*, 2008a). According to the findings of Reddy *et al*. (2011) FLT3-ITD inhibition *via* PKC412 does not reduce the mRNA levels of Nox components in MOLM-13 cells, however the authors did not examine the changes in the amount of Nox isoforms and regulatory subunits at the protein level. Treatment of MOLM-13 cells with PKC412 for up to 24 hours had

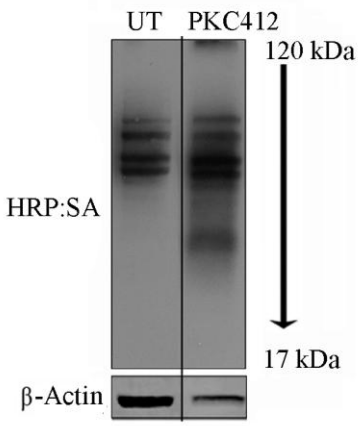
Figure 22. FLT3-driven redox signalling in MOLM-13 cells

A) Intracellular ROS levels measured by DCF fluorescence (FL1-H) in untreated MOLM-13 cells, overlaid with cells treated with 250 nM PKC412 for 8 hours and 24 hours. **B)** HRP-SA detection of BIAM-labelled (reduced) protein content of MOLM-13 cells treated with 250 nM PKC412 for 24 hours. **C)** Western blot analysis of the p-FLT3 levels of untreated MOLM-13 cells and cells treated with 250 nM PKC412 for 24 hours. Total FLT3 levels are shown as a loading control. **D)** Histogram represents the viability of MOLM-13 cells after 24 hour incubation with 250 nM PKC412 as determined by Trypan Blue staining. Samples were not found to be statistically significant. Statistical analysis was performed using Student's *t*-test to evaluate the difference between untreated and PKC412-treated samples. Significance was defined at the level of $P<0.05$.

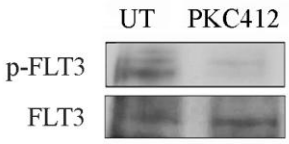
A


UT
PKC412 8 hr
PKC412 24 hr
Counts
FL-1H

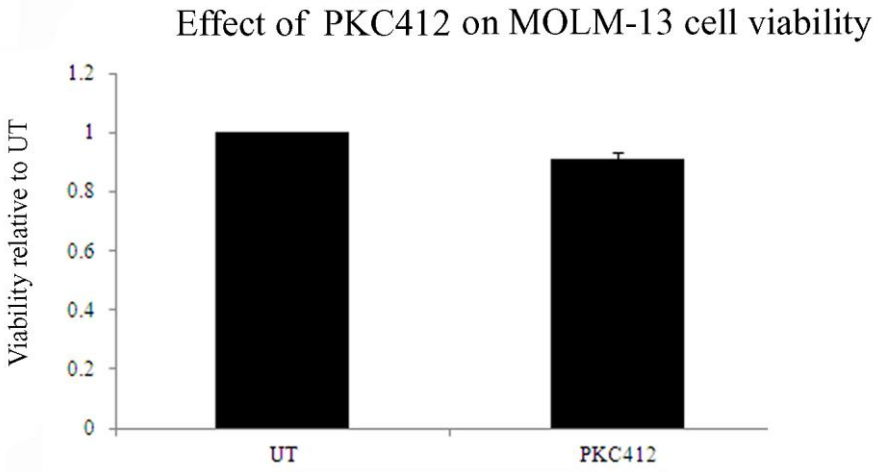
B


UT
PKC412
120 kDa
HRP:SA
17 kDa
β-Actin

C


UT
PKC412
p-FLT3
FLT3

D


Effect of PKC412 on MOLM-13 cell viability
Viability relative to UT
UT
PKC412

no effect on the protein levels of the majority of Nox proteins, did slightly reduce the levels of Nox 4 and p67phox, however it is the dramatic reduction in the levels of p22phox which is most striking (Figure 23). The decrease in p22phox protein is also observed by Woolley *et al*. (2012) in MV4-11 cells but similarly to Reddy *et al*., Woolley *et al*. noted that there was no change in p22phox mRNA levels. In fact, Woolley *et al*. went on to show that FLT3 affects the levels of p22phox through regulation of its ubiquitination and degradation.

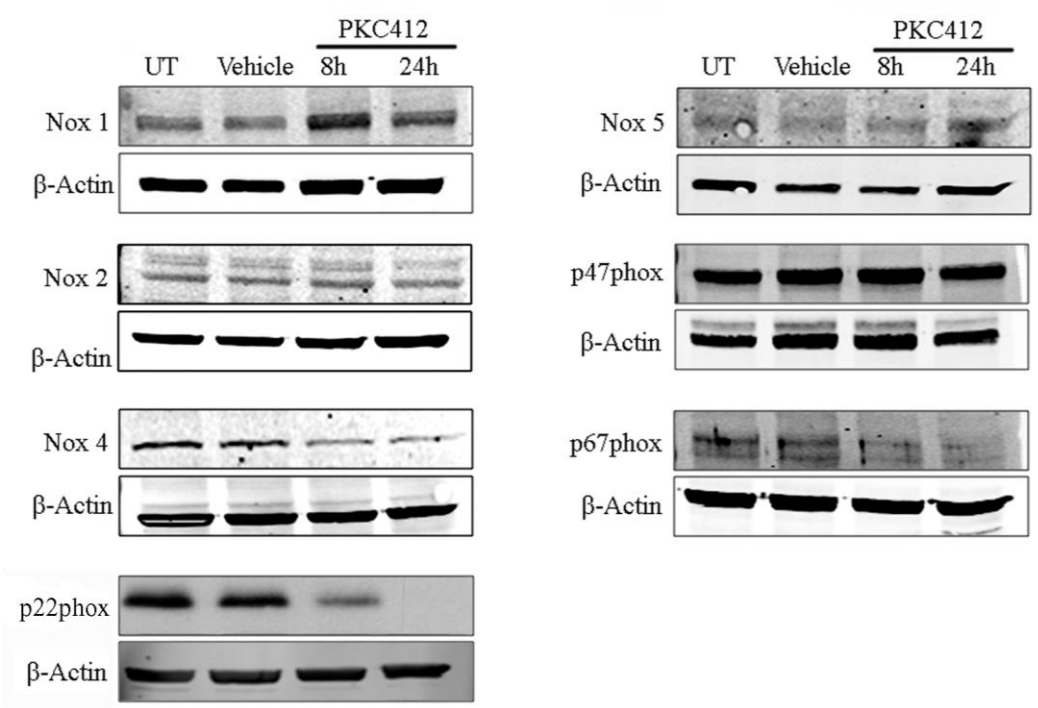


Figure 23. Effects of FLT3-ITD inhibitor PKC412 on Nox expression

Western blot analysis of Nox isoforms 1, 2, 4 and 5, as well as transmembrane protein p22phox, organiser subunit p47phox and activator subunit p67phox, in untreated MOLM-13 cells, cells treated with the DMSO vehicle only for 24 hours, or cells treated with 250 nM FLT3-ITD inhibitor PKC412 for 8 or 24 hours. β-Actin is shown as a loading control.

Redox effects of PKC412 are specifically due to its inhibition of FLT3-ITD

Although it has been shown in Figure 22C that PKC412 does reduce the amount of actively signalling p-FLT3 in MOLM-13 cells, the alterations in cellular redox state observed could be explained by off-target effects of the drug which are unrelated to its FLT3-ITD inhibition. For this reason, the HL60 cell line was employed to demonstrate that the redox effects of PKC412 are caused by inhibition of FLT3-ITD signalling. The HL60 cell line expresses only the wild type FLT3 receptor which becomes activated only upon stimulation by the FLT3 ligand (FL). As PKC412 has a higher affinity for the mutated version of the receptor, the HL60 cells are frequently used as negative control for the drug (Levis *et al.*, 2004; Seedhouse *et al.*, 2006; Woolley *et al.*, 2012). Indeed, in this case there was no effect on ROS or BIAM-labelled protein levels in the HL60 cells treated with 250 nM PKC412, nor was there any effect on the p22phox protein levels (Figure 24), a result also noted by Woolley *et al*. (2012). However, it must be noted that at higher concentrations of this drug, an inhibition of the wild type receptor is likely to occur.

Stimulation with the FLT3 ligand induces redox changes in HL60 cells

There are reported differences between the signalling pathways of the wild type FLT3 and the constitutively active mutant. This is attributed to the occasional prolonged retention of the mutant receptor in the ER, due to folding defects and impaired trafficking to the membrane (Choudhary *et al.*, 2009; Schmidt-Arras *et al.*, 2009), leading to a proximity to novel substrates and interacting partners that the wild type receptor is not exposed to in its location at the membrane. However, there is some overlap between the mutant and wild type FLT3 when both are localised to

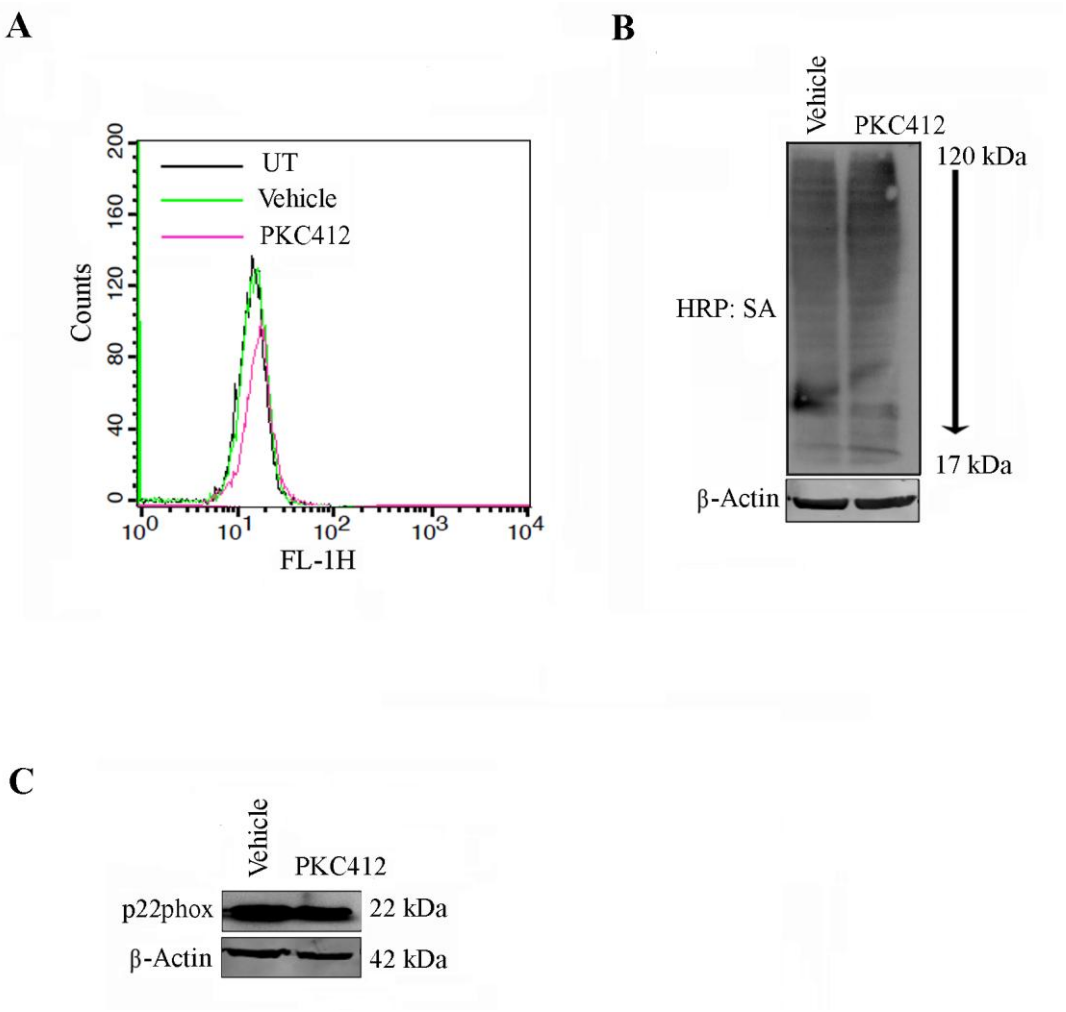


Figure 24. Effect of FLT3-ITD inhibitor PKC412 on the HL60 cell line

A) Intracellular ROS levels measured by DCF fluorescence (FL1-H) in untreated HL60 cells, overlaid with cells treated with 250 nM PKC412 for 24 hours. **B)** HRP-SA detection of BIAM-labelled (reduced) protein content of HL60 cells treated with the DMSO vehicle only and cells treated with 250 nM PKC412 for 24 hours. **C)** Western blot analyses of p22phox expression in HL60 cells treated with the DMSO vehicle only and in cells treated with 250 nM PKC412 for 24 hours. β-Actin is shown as a loading control.

the membrane, including stimulation of the Ras-MAPK and JAK-STAT pathways, PI3K, Src, and phospholipase C-gamma (PLCγ), so the spheres of influence of the two versions of the FLT3 receptor are clearly not mutually exclusive (Choudhary *et al.*, 2005; Gu *et al.*, 2011).

In order to determine if the FLT3-Nox-ROS sequence being investigated here is unique to the FLT3-ITD mutant, or is common to both the mutated and wild type forms, the FLT3 ligand (FL) was used to stimulate the wild type FLT3 receptor in HL60 cells and the redox readout of the cells was examined. Based on unpublished data from within our laboratory, which previously established the optimal dose for stimulation of the wild type HL60 cell receptor with the FL, 50 ng/ml of FL was used to stimulate the HL60 cells. Figure 25 shows that stimulation resulted in an increase in ROS levels corresponding to a decrease in BIAM-labelled protein and an increase in p-FLT3. Although the ROS burst induced by FLT3 ligand in HL60 cells appears modest when represented on the log scale of the FACS histogram, it is likely that as a physiologically relevant signalling event it is localised and concentrated in order to stimulate a specific target rather than triggering cell-wide oxidative stress. It appears that the FL-induced ROS burst is relative to the FLT3 status of the cell, as the MOLM-13 cells, heterozygous for the wild type receptor displayed less of an ROS increase and a smaller p-FLT3 induction (Figure 26).

Similarly, the MV4-11 cells which do not express the wild type receptor at all showed no change in ROS or p-FLT3 levels (Figure 26), thus acting as a negative control for the FLT3 ligand and demonstrating that the effects on the redox profile of the cells is related to ability of the ligand to stimulate the receptor and not due to off-target effects of the ligand itself.

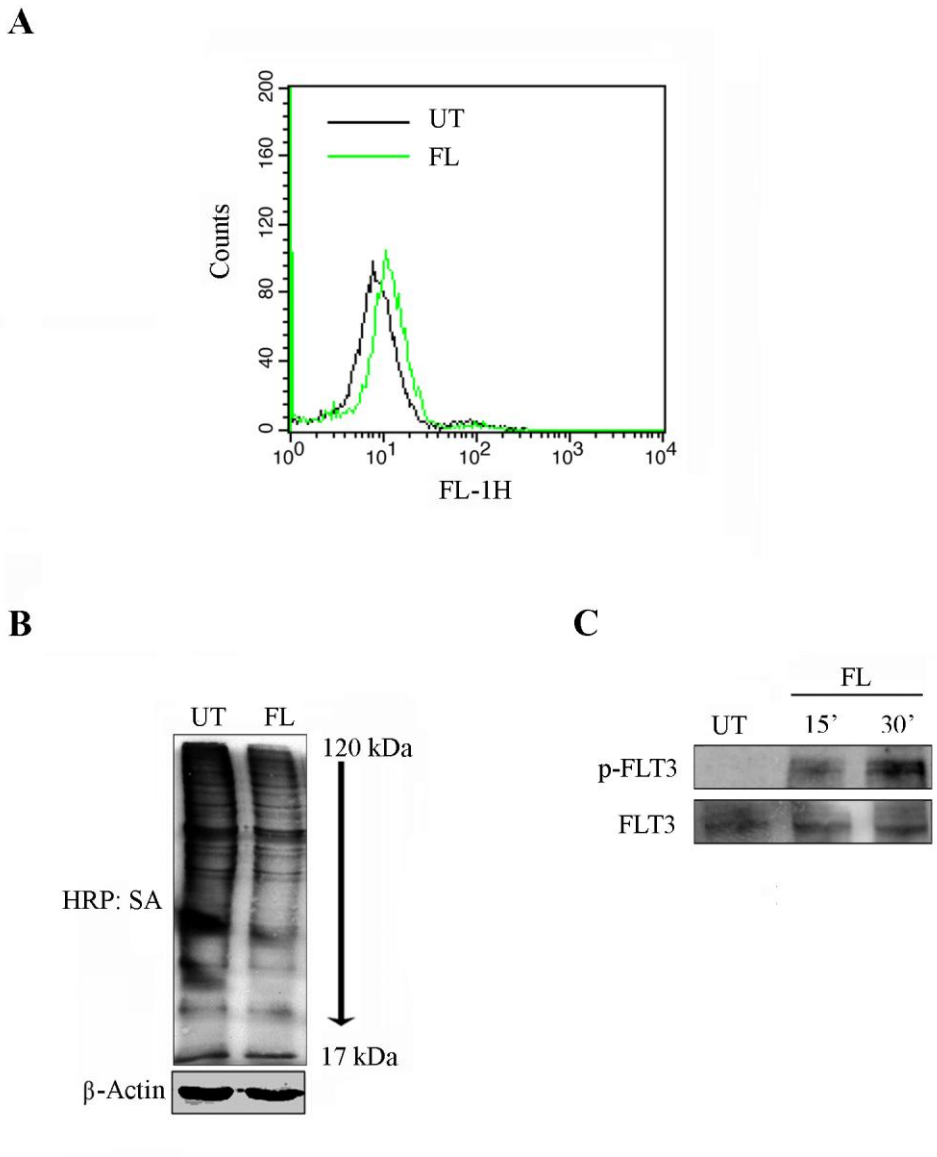


Figure 25. Effect of the FLT3 ligand (FL) on the HL60 cell line.

A) Intracellular ROS levels measured by DCF fluorescence (FL1-H) in untreated HL60 cells overlaid with cells stimulated with 50 ng/ml FL for 30 minutes. **B)** HRP-SA detection of BIAM-labelled (reduced) protein content of HL-60 cells stimulated with 50 ng/ml FL for 30 minutes. β-Actin is shown as a loading control. **C)** Western blot analysis of the p-FLT3 levels of untreated HL60 cells and cells stimulated with 50 ng/ml FL for 15 and 30 minutes. Total FLT3 levels are shown as a loading control.

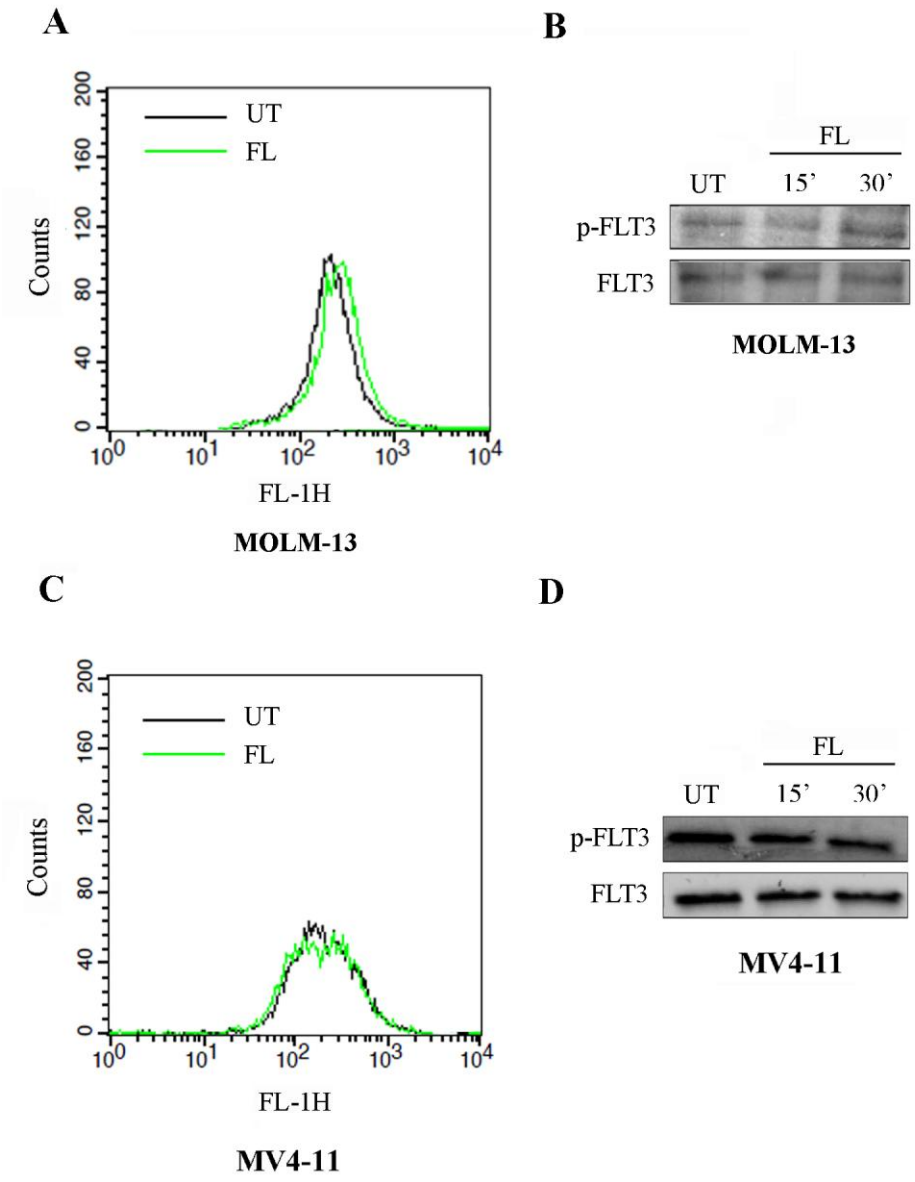


Figure 26. Effect of the FLT3 ligand (FL) on the MOLM-13 and MV4-11 cell lines. A) Intracellular ROS levels measured by DCF fluorescence (FL1-H) in untreated MOLM-13 cells overlaid with cells stimulated with 50 ng/ml FL for 30 minutes. **B)** Western blot analysis of the p-FLT3 levels of untreated MOLM-1 3 cells and cells stimulated with 50 ng/ml FL for 15 or 30 minutes. Total FLT3 levels are shown as a loading control. **C)** Intracellular ROS levels measured by DCF fluorescence (FL1-H) untreated MV4-11 cells overlaid with cells stimulated with 50 ng/ml FL for 30 minutes. **D)** Western blot analysis of the p-FLT3 levels of untreated MV4-11 cells and cells stimulated with 50 ng/ml FL for 15 or 30 minutes. Total FLT3 levels are shown as a loading control.

Stimulation of the wild type FLT3 receptor with the FLT3 ligand results in an increase in p22phox protein levels

Having observed that both FLT3-ITD and wild type activity are connected to the ROS levels of the AML cells, and that inhibition of the mutant receptor caused a decrease in p22phox levels in MOLM-13 cells, the next step was to determine if stimulation of the wild type receptor resulted in an increase in p22phox protein. Correlating well with the effects on the ROS levels, the ability of the ligand to increase p22phox levels appears to correspond to the FLT3 receptor status of the cell line in question and the ability to respond to the ligand. In this way HL60 cells showed the largest induction of p22phox, the same treatments in MOLM-13 cells induces a much smaller increase in p22phox levels, but the basal p22phox levels in MOLM-13 are higher than those in HL60 cells, and there was no effect on the p22phox levels of MV4-11 cells (Figure 27).

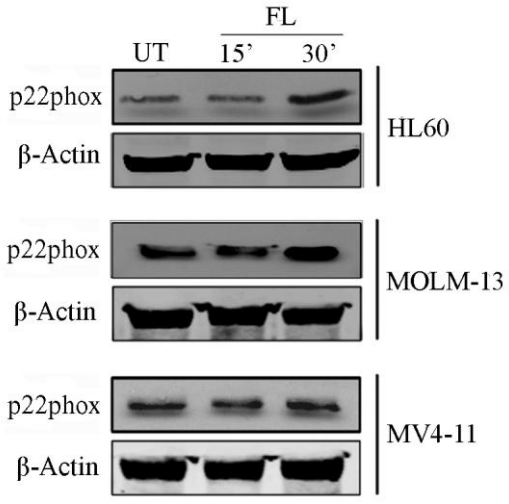


Figure 27. Effect of FLT3 ligand stimulation on the expression of p22phox in AML cell lines. Western blot analysis of the levels of p22phox protein expression in the untreated HL60, MOLM13 and MV4-11 cell lines, and cells stimulated with 50 ng/ml FL for 15 and 30 minutes. β-Actin is shown as a loading control.

FLT3 signals to Ezrin, a downstream target of Nox

To further probe the relationship between FLT3 and Nox, the ability of FLT3 to signal to Ezrin, the downstream target of Nox mediated p-Tyr signalling, was tested using both PKC412 and the FL. As FLT3 is a RTK, it is reasonable to assume that interfering with its activity; either positively or negatively, will affect the p-Tyr levels of the cell. This was demonstrated for MV4-11 and MOLM-13 cells treated with PKC412 (Figure 28A and B), and while the inhibitor again had no effect on the p-Tyr levels of HL60 cells (Figure 28C), the FL induced tyrosine phosphorylation (Figure 28D). In agreement with the general p-Tyr effects, tyrosine phosphorylation specifically of Ezrin was also affected by FLT3 signalling. PKC412 reduced the levels of p-Ezrin at the two tyrosine residues also regulated by Nox activity, Y146 and Y353, in both MOLM-13 (Figure 29A) and MV4-11 cells (Figure 29B). Again there was no effect of PKC412 on the p-Ezrin levels of HL60 cells (Figure 29C), but the FL did stimulate phosphorylation at both residues in this cell line (Figure 29D).

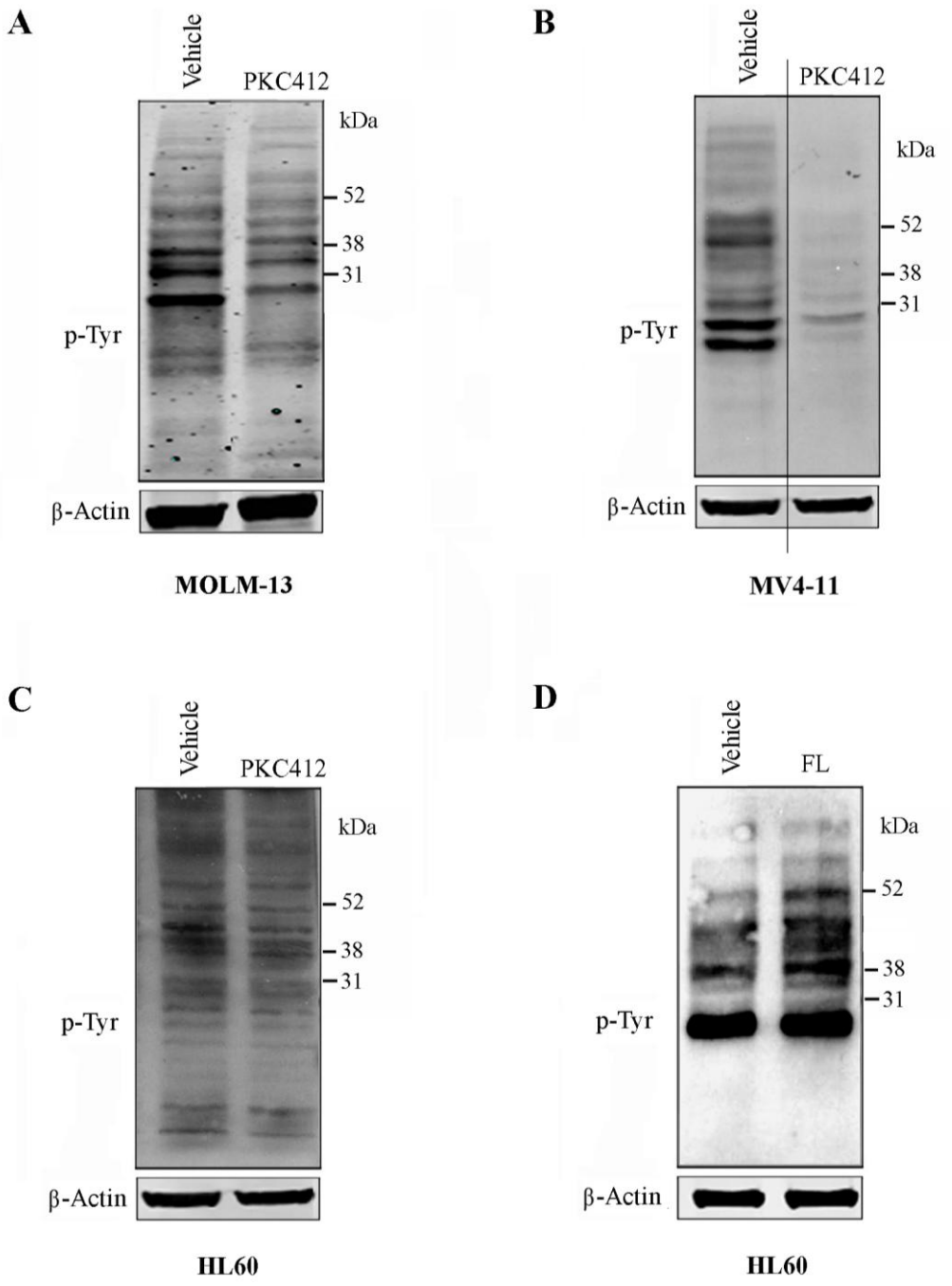


Figure 28. Effects of FLT3 signalling on the p-Tyr levels of AML cell lines. Western blot analyses of the p-Tyr profiles of **A)** MOLM-13 **B)** MV4-11 and **C)** HL60 cells treated with the DMSO vehicle only or with 250 nM PKC412 for 24 hours, and **D)** HL60 cells stimulated with 50 ng/ml FL for 15 or 30 minutes. β-Actin is shown as a loading control.

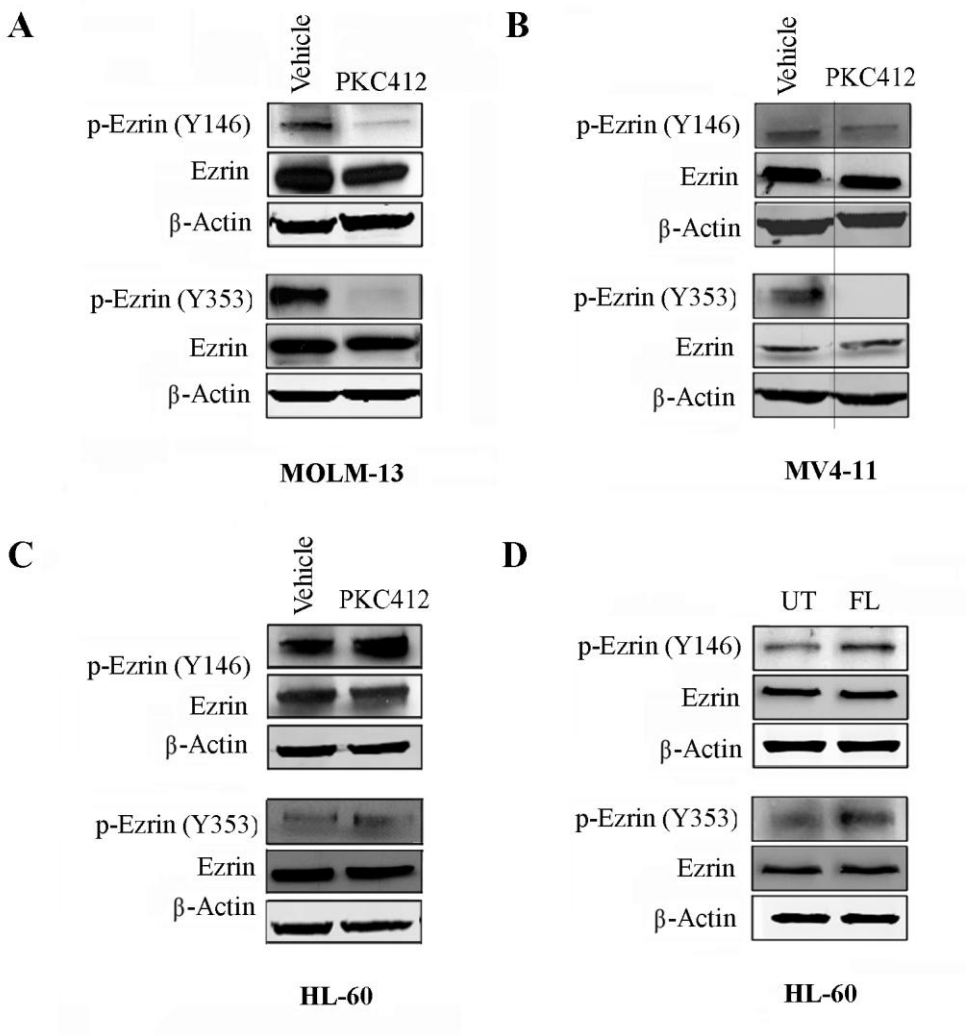


Figure 29. Effects of FLT3 signalling on Ezrin tyrosine phosphorylation.
Western blot analyses of p-Ezrin Y146 and Y353 in **A)** MOLM-13 **B)** MV4-11 and **C)** HL60 cells treated with the DMSO vehicle only or with 250 nM PKC412 for 24 hours, and **D)** HL60 cells stimulated with 50 ng/ml FL for 30 minutes. β-Actin is shown as a loading control.

Inhibition of Src results in a decrease in p-Ezrin Y353 and Y146

Taken together, these results indicate that FLT3 signalling in MOLM-13, MV4-11 and HL60 cells, drives the production of ROS by Nox, and influences the phosphorylation of Ezrin at tyrosines Y146 and Y353. If Ezrin tyrosine phosphorylation is dependent on ROS then this presents the possibility that the phosphorylation process is carried out by a redox-sensitive kinase. Early indications were that Ezrin was phosphorylated on Y146 and Y353 after stimulation of the EGF receptor (Bretscher, 1989, Krieg and Hunter, 1992), and more recent evidence has narrowed this down to indicate that Src kinase phosphorylates Ezrin on Y146 (Srivastava *et al.*, 2005; Wang *et al.*, 2003) and on another tyrosine residue Y477 (Heiska and Carpen, 2005; Mak *et al.*, 2012). Y146 is a conserved residue amongst the Ezrin-related proteins Radixin and Moesin as well as band 4.1, Talin and phosphatases PTPH1 and PTPMEG which all share homology of the N-terminal domain where this residue is located (Krieg and Hunter, 1992). Y353 however is unique to Ezrin and has been shown to be phosphorylated downstream of Syk kinase in B cell lines, though the same study also demonstrated that inhibition of Src kinase in these cells influenced phosphorylation at Y353 (Coffey *et al.*, 2009).

As Src is a kinase known to be redox regulated (Giannoni *et al.*, 2010), its documented involvement with Ezrin serves to further strengthen the premise that it may play a role in the FLT3-Nox-Ezrin pathway. The ability of Src to phosphorylate Ezrin at both Y146 and Y353 was confirmed in MOLM-13 cells using western blotting to examine the phosphorylation status of both residues after treatment with the SFK inhibitor PP2 (Figure 30).

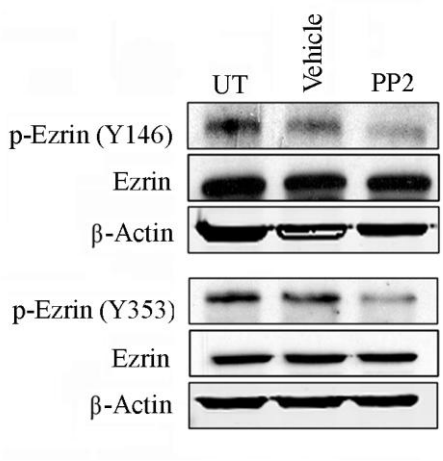


Figure 30. Effect of SFK inhibition on the tyrosine phosphorylation of Ezrin. Western blot analyses of p-Ezrin Y146 and Y353 in MOLM-13 cells treated with 20 μM of the SFK inhibitor PP2 for 24 hours. β-Actin is shown as a loading control.

Src activity is redox regulated

Next the possibility of redox regulation of Src downstream of Nox was examined. Initially, the effect of Nox inhibition, *via* DPI, on Src activity was investigated using western blotting. Src phosphorylation on Y416, reflecting active Src, was shown to be reduced upon treatment with DPI similarly to the reduction observed using the Src inhibitor PP2 (Figure 31A). Interestingly, active Src was shown to increase upon incubation of MOLM-13 cells with H_2O_2 (Figure 31A, lane 5), or of HL60 cells with FL (Figure 31B). Similar results were observed in MV4-11 cells (Figure 31C).

Src is reduced in response to inhibition of FLT3-ITD and Nox signalling

In order to confirm that these changes in p-Src Y416 correspond to changes in the redox state of Src, BIAM-labelling of MOLM-13 cell lysates followed by immunoprecipitation of Src and immunoblotting using HRP conjugated to streptavidin (HRP-SA) was carried out to determine the proportion of reduced Src (Figure 32) as in the procedure described by Giannoni *et al*. (2005). Compared to the untreated cells, an increase in reduced Src was observed upon treatment with either DPI or PKC412 (Figure 32A lanes 2 and 4), implying that the proportion of oxidised Src decreases after inhibition of ROS production either at the level of FLT3-induction of Nox or inhibition of Nox activity itself.

As expected, incubation with H_2O_2 (Figure 32A, lane 3) resulted in a decreased fraction of reduced Src, corresponding to an increase in oxidised Src. The reducing effect of DPI and PKC412 on Src also occurred in MV4-11 cells (Figure 32B), while PKC412 had no effect on the redox state of Src in HL60 cells (Figure 32C).

Comparison of the p-Src Y416 data with the results of the BIAM-labelling of Src, seems to align with the model of oxidative-activation of Src proposed by Giannoni *et al*. (2005) rather than the oxidative-inactivation of Src supported by Kemble *et al*. (2009). In this scenario, it appears that ROS production downstream of FLT3-ITD affect the activity of Src *via* alterations to its redox status.

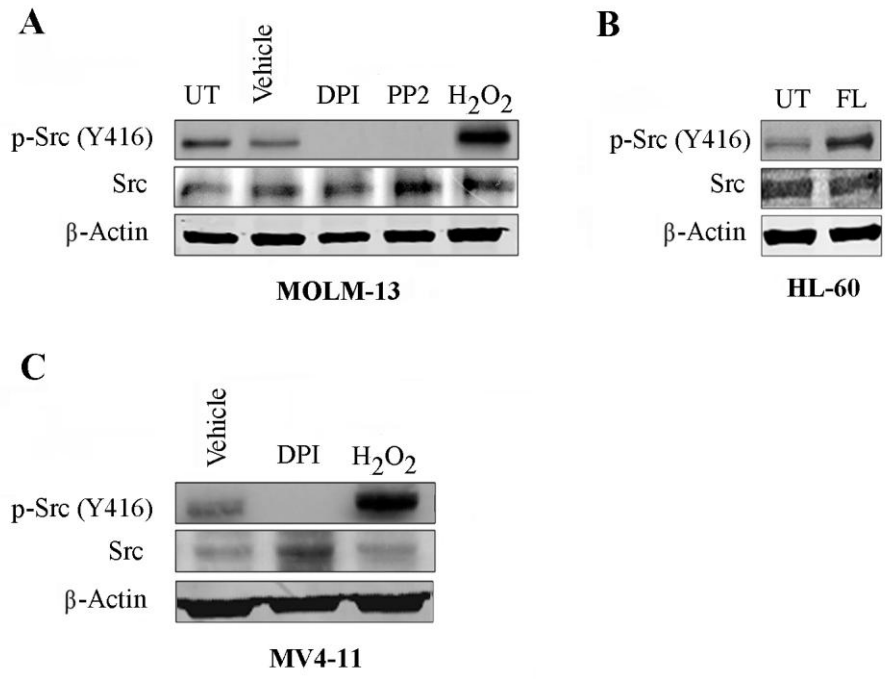


Figure 31. Effects of DPI, H_2O_2 and FLT3 ligand on Src activity.

Western blot analysis of p-Src Y416 in **A)** untreated MOLM-13 cells, cells treated with the DMSO vehicle only, 20 µM DPI for 24 hours, 20 µM Src inhibitor PP2 for 24 hours, or 100 µM H_2O_2 for 30 minutes, **B)** untreated HL60 cells and cells stimulated with 50 ng/ml FL for 30 minutes and **C)** MV4-11 cells treated with DMSO vehicle only or 20 µM DPI for 24 hours or 100 µM H_2O_2 for 30 minutes. β-Actin is shown as a loading control.

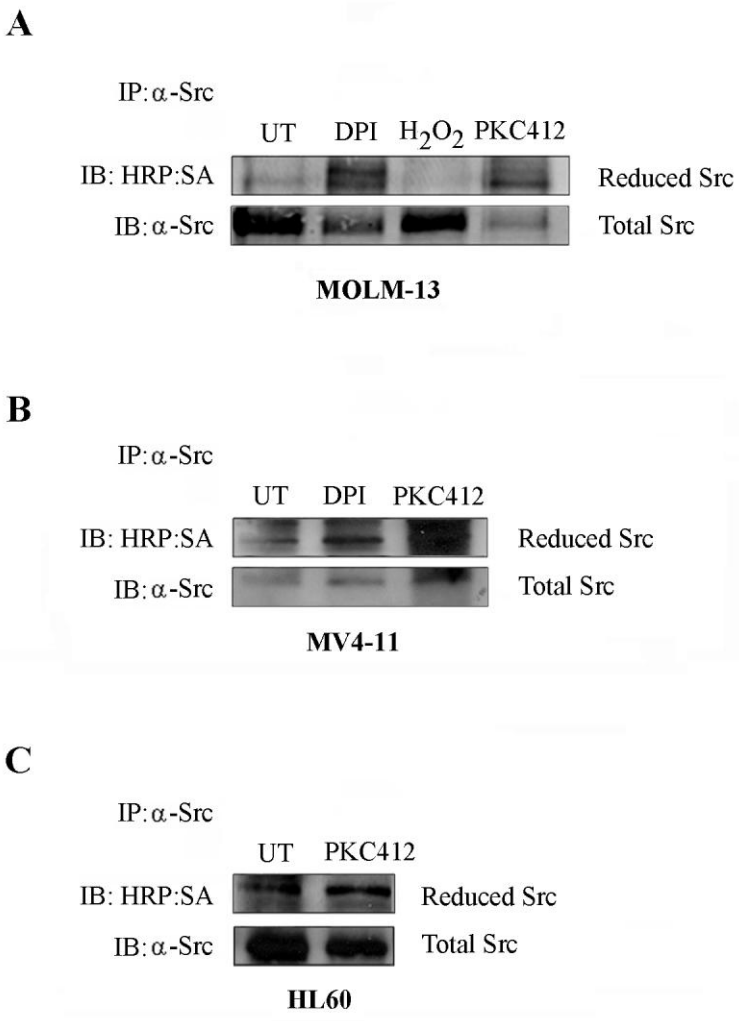


Figure 32. Redox regulation of Src in AML cells.

HRP-SA detection of BIAM-labelled (reduced) Src fraction of total Src immunoprecipitated from **A)** untreated MOLM-13 cells and cells treated with 20 µM DPI 24 hours, 100 µM H_2O_2 for 30 minutes or 250 nM PKC412 for 24 hours, **B)** untreated MV4-11 cells and cells treated with 20 µM DPI or 250 nM PKC412 for 24 hours, **C)** untreated HL60 cells and cells treated with 250 nM PKC412 for 24 hours.

Tyrosine phosphorylation downstream of Nox occurs through redox regulation of Src

As a redox-sensitive kinase, Src is in a position to translate the upstream ROS signal induced by FLT3 and generated by Nox, into downstream tyrosine phosphorylation of protein targets. To investigate the extent to which Src mediates the redox-driven tyrosine phosphorylation observed in MOLM-13 cells, cells were treated with either Src inhibitor PP2 alone or prior to H_2O_2 incubation and the p-Tyr levels of cells were then examined. Incubation with H_2O_2 induced an increase in p-Tyr levels in MOLM-13 (Figure 33A, lane 4) and in MV4-11 cells (Figure 33B). The Src inhibitor PP2 (Figure 33A, lane 5) prompted a decrease in p-Tyr to an extent similar to that of DPI (Figure 33A, lane 3). Furthermore, pre-incubation with PP2, prior to stimulation with H_2O_2, prevented the peroxide-induced increase in p-Tyr (Figure 33A, lane 6). This effect was also shown to apply specifically to Ezrin tyrosine phosphorylation, with both Y146 and Y353 showing increased phosphorylation in response to H_2O_2 and this increase being blocked upon pre-treatment with PP2 in MOLM-13 cells (Figure 33C). The susceptibility of Ezrin tyrosine phosphorylation to H_2O_2 was also observed in MV4-11 cells (Figure 33D). Altogether, this suggests an intermediary role for Src in translating the redox status of the cell into modifications at the protein level.

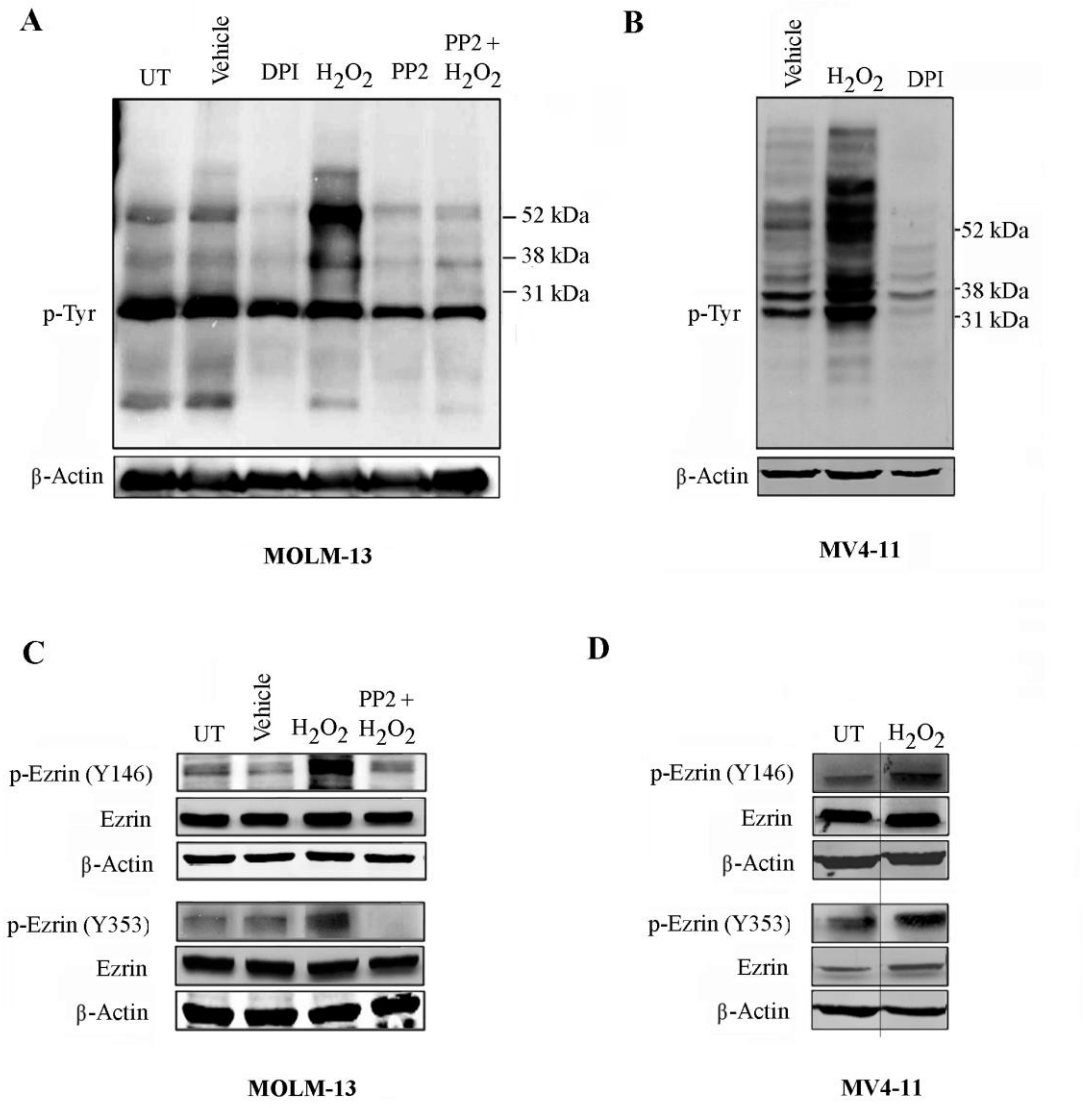


Figure 33. Effects of Src inhibition on Nox-driven tyrosine phosphorylation. Western blot analyses of **A)** p-Tyr levels in untreated MOLM-13 cells, cells treated with DMSO vehicle or 20 µM DPI for 24 hours, 100 µM H_2O_2 for 30 minutes, 20 µM PP2 for 24 hours, or pre-incubated with 20 µM PP2 for 24 hours prior to the introduction of 100 µM H_2O_2 for 30 minutes and **B)** p-Tyr levels in MV4-11 cells treated with DMSO vehicle for 24 hours, 100 µM H_2O_2 for 30 minutes or 20 µM DPI for 23 hours, **C)** p-Ezrin Y146 and Y353 in untreated MOLM-13 cells, cells treated with DMSO vehicle only or 100 µM H_2O_2 for 30 minutes, or pre-incubated with 20 µM PP2 for 24 hours prior to treatment with 100 µM H_2O_2 for 30 minutes, **D)** p-Ezrin Y146 and Y353 in MV4-11 cells treated with 100 µM H_2O_2 for 30 minutes. β-Actin is shown as a loading control.

siRNA-mediated knockdown of p22phox results in a decrease in p-Ezrin and p-Src

The effects of Nox inhibition *via* DPI on the downstream targets Src and subsequently Ezrin have been demonstrated. Given the mode of action of DPI and to eliminate the possibility that flavin-containing enzymes other than Nox may be responsible for these effects, MOLM-13 cells were transfected with siRNA targeting p22phox using the Amaxa Nucleofactor electroporation technology. The initial experiments using the programme recommended by Amaxa for MOLM-13 cell transfection had such a detrimental effect on cell viability that protein yields were too low to use for SDS-PAGE. As discussed in the previous chapter myeloid leukaemia cells have been widely classified as 'difficult to transfect' therefore some optimisation was required in order to find a programme which ensured transfection efficiency without compromising cell viability. As expected, very poor transfection efficiency was observed for the control 3486 bp maxGFP™ plasmid for all programmes tested, likely due to the size of the construct (Figure 34A), but upon transfection with the much smaller 21 bp siRNA targeting p22phox, an almost complete reduction in p22phox protein was observed for programme D023 (Figure 34B), with protein yield remaining substantial. Therefore this programme was used for the subsequent MOLM-13 siRNA experiments.

In agreement with the results observed using DPI, p22phox knockdown using siRNA in MOLM-13 cells reduced phosphorylation of Ezrin at both Y146 and Y353 and of Src at Y416 (Figure 35). This confirms that the effects previously observed using DPI may be attributable specifically to inhibition of Nox activity.

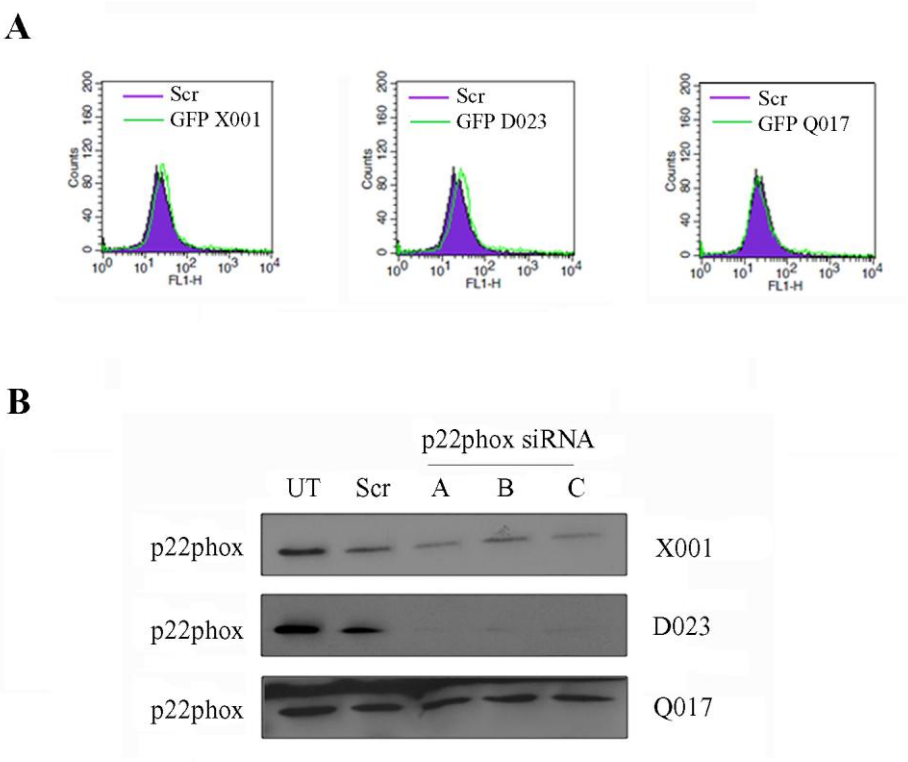


Figure 34. Optimisation of siRNA transfection of MOLM-13 cells.

A) Green fluorescent protein (GFP) fluorescence as measured on the FL1-H channel in untransfected MOLM-13 cells overlaid with cells transfected with 50 ng maxGFP™ plasmid, using three different Amaxa Nucleofactor electroporation programmes X001, D023 and Q017. **B)** Western blot analyses of p22phox protein levels from untransfected MOLM-13 cells, cells transfected with 50 ng scrambled siRNA control (Scr) or three different siRNAs targeting p22phox.

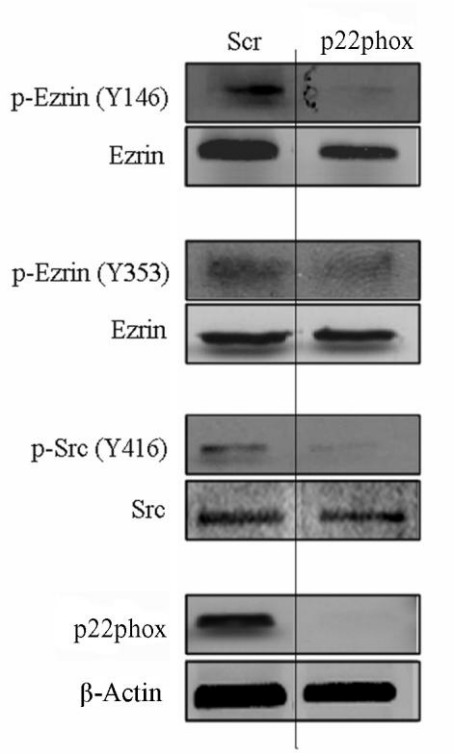


Figure 35. Effect of p22phox knockdown on downstream targets of Nox-driven ROS in MOLM-13 cells. Western blot analyses of p-Ezrin Y146, Y353, p-Src Y416 and p22phox protein levels from MOLM-13 cells transfected with scrambled siRNA control (Scr) or siRNA targeting p22phox. β-Actin is shown as a loading control.

siRNA knockdown of p22phox in HL60 cells demonstrates reliance of FLT3 signalling on p22phox

To clarify whether the increases in p-Ezrin and p-Src observed upon stimulation of HL60 cells with the FLT3 ligand are related to ROS levels, p22phox was knocked down using siRNA in HL60 cells and the cells were then stimulated with the FL. It was observed that levels of p-Ezrin Y353 and Y146 as well as p-Src 416 decreased upon p22phox knockdown (Figure 36) despite stimulation with the same concentration of FLT3 ligand (50ng/ml) for the same period of time which, in un-transfected cells, provoked the increases observed in Figures 29 and 31. This demonstrates that p22phox specifically mediates the FLT3 signal of which Ezrin and Src are downstream targets.

Inhibition of Nox, Src or FLT3 affects the localisation of Ezrin within MOLM-13 cells

FLT3 and Nox activity affects Ezrin tyrosine phosphorylation but the significance of this effect to the function of Ezrin is hard to predict based on the relative scarcity of literature regarding Ezrin tyrosine phosphorylation. Threonine phosphorylation of Ezrin, by comparison, has received the majority of attention because of its role in activation of the protein *via* relief of the auto-inhibitory conformation (Matsui, 1998; Simons *et al.*, 1998). Within the cell, activated Ezrin has been shown to localise to the cytoplasmic side of the plasma membrane (Turunen *et al.*, 1989) where it forms a dynamic link between F-actin and the plasma membrane proteins (Fehon *et al.*, 2010), and is significantly enriched in cell protrusions such as membrane ruffles and microvilli (Auvinen *et al.*, 2007; Pakkanen *et al.*, 1988). Immunofluorescence was carried out on MOLM-13 cells in order to

investigate whether the effect of FLT3, Nox or Src activity on Ezrin tyrosine phosphorylation also affects Ezrin localisation (Figure 37). In untreated cells, Ezrin staining was punctate with some localisation to the periphery of the cell.

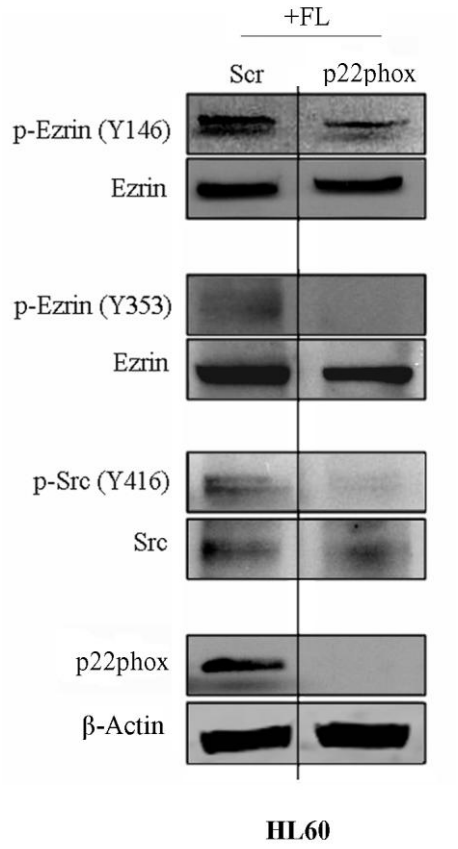
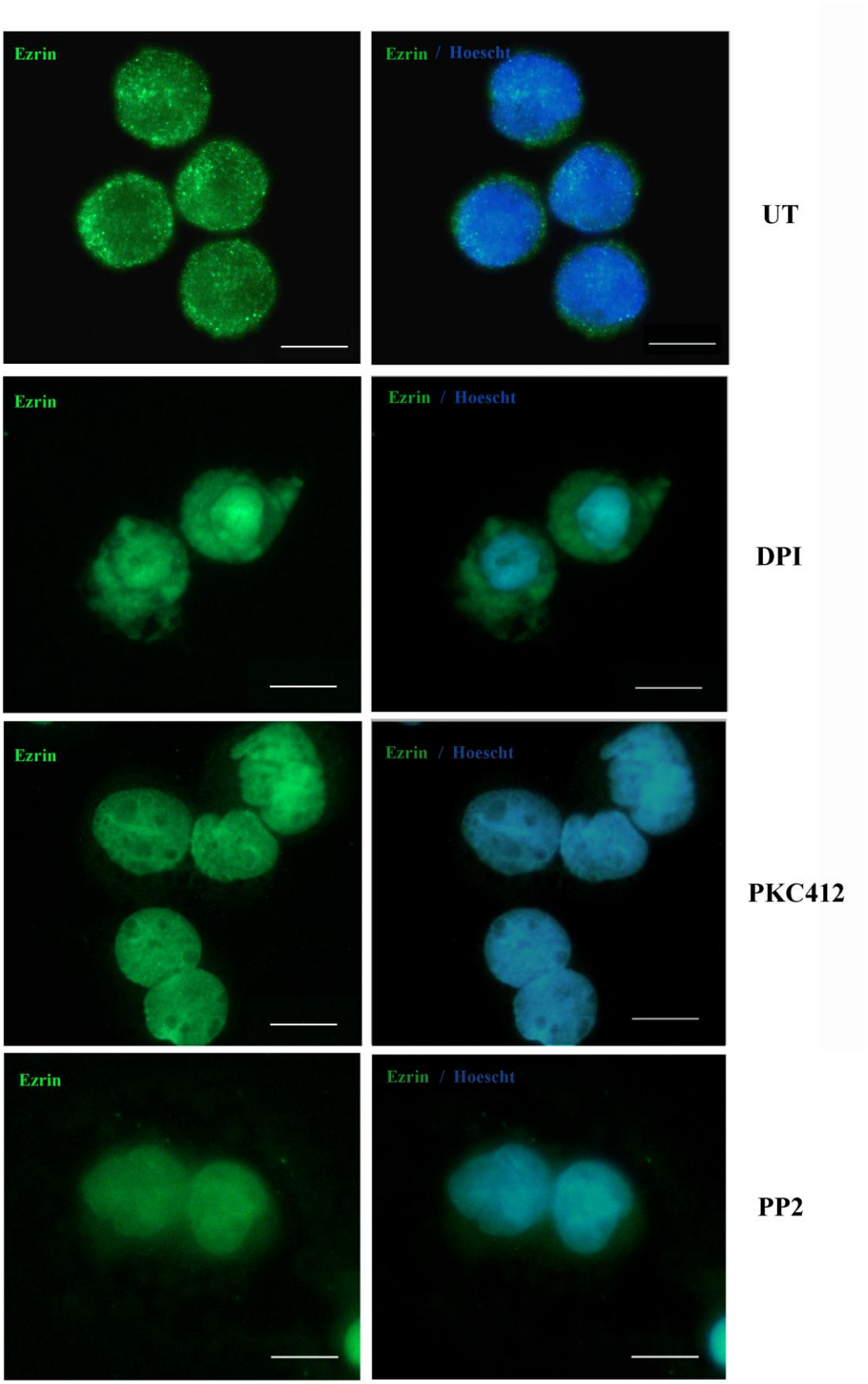


Figure 36. Effect of p22phox knockdown on the FLT3 ligand (FL) stimulation of HL60 cells. Western blot analyses of the levels of p-Ezrin Y146, Y353, p-Src Y416 and p22phox after FL stimulation (50 ng/ml for 30 minutes) of HL60 cells transfected with scrambled siRNA control (Scr) or siRNA targeting p22phox. β-Actin is shown as a loading control.

After 24 hour incubation with DPI, PKC412 or PP2, Ezrin can be seen to lose the punctate staining, move from the membrane to the cytosol, and accumulate in a peri-nuclear pattern, showing some co-localisation with the nuclear stain Hoescht. The same effect was observed for PKC412 in MV4-11 cells (Figure 38), while no change in Ezrin sub-cellular localisation was seen in HL60 cells treated with PKC412 (Figure 39). Nucleolar and nuclear localisation of Ezrin, as well as another ERM family member Moesin, have been previously observed (Barret *et al.*, 2000; Batchelor *et al.*, 2004; Melendez-Vasquez *et al.*, 2001) and Batchelor *et al*. have identified a nuclear localisation-sequence that is common to all three ERM proteins, but the consequences of this localisation are as yet undetermined.

Figure 37. Effects of inhibition of Nox, FLT3 or Src on Ezrin sub-cellular localisation in MOLM-13 cells. Immunofluorescence micrographs of Ezrin sub-cellular localisation (green) showing punctate staining at the periphery of untreated MOLM-13 cells, and cytoplasmic staining pattern with some co-localisation with the nuclear stain Hoescht (blue) in cells treated with 20 µM DPI, 250 nM PKC412, 20 µM PP2 for 24 hours. Ezrin/Hoescht denotes merged image. A representative micrograph is shown in each case. Scale bar represents 10 µm.


Ezrin
Ezrin / Hoescht
UT
Ezrin
Ezrin / Hoescht
DPI
Ezrin
Ezrin / Hoescht
PKC412
Ezrin
Ezrin / Hoescht
PP2

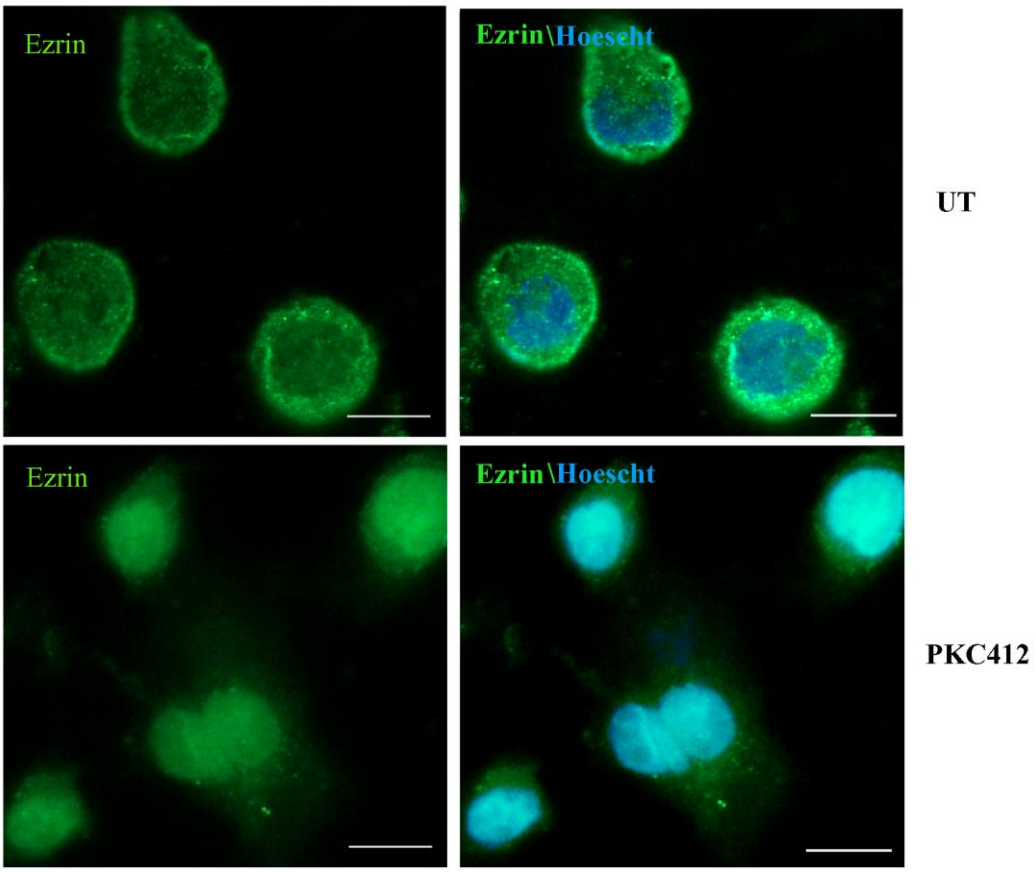


Figure 38. Effects of inhibition of FLT3-ITD on Ezrin sub-cellular localisation in MV4-11 cells. Immunofluorescence micrographs of Ezrin sub-cellular localisation (green) showing punctate staining at the periphery of untreated MV4-11 cells, and cytoplasmic staining pattern with some co-localisation with the nuclear stain Hoescht (blue) in cells treated with 250 nM PKC412, for 24 hours. Ezrin/Hoescht denotes merged image. A representative micrograph is shown in each case. Scale bar represents 10 µm.

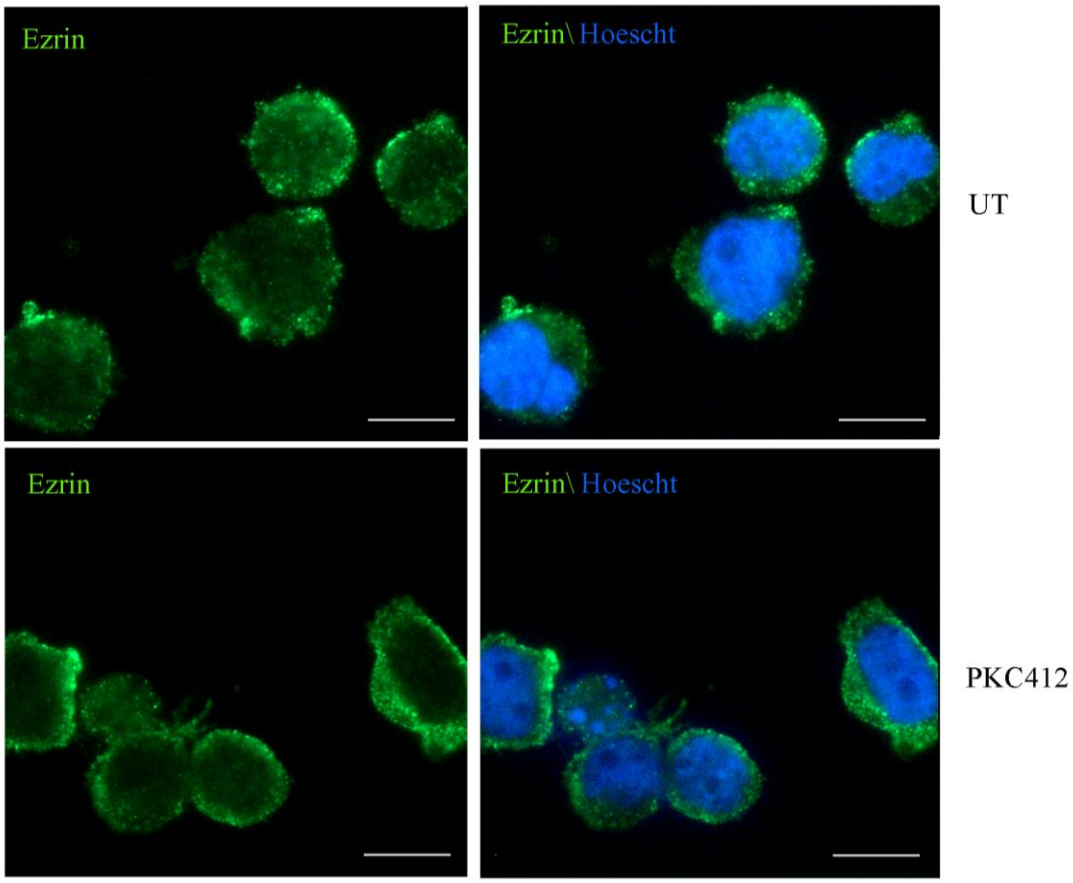


Figure 39. Effects of inhibition of FLT3-ITD on Ezrin sub-cellular localisation in HL60 cells. Immunofluorescence micrographs of Ezrin sub-cellular localisation (green) showing punctate staining at the periphery of untreated HL60 cells, and cytoplasmic staining pattern with some co-localisation with the nuclear stain Hoescht (blue) in cells treated with 250 nM PKC412, for 24 hours. Ezrin/Hoescht denotes merged image. A representative micrograph is shown in each case. Scale bar represents 10 µm.

Nox-driven changes in Ezrin localisation results in morphological changes in MOLM-13 cells

As a key regulator of the cytoskeleton, Ezrin has been shown to promote the formation of invasive and migratory features such as invadopodia, lammelipodia and ruffled edges (Brambilla and Fais, 2009; Martin *et al.*, 1997). The changes in Ezrin localisation due to FLT3 or Nox inhibition, seen in Figures 37 and 38, could therefore affect the ability of the cell to form these membrane protrusions. Scanning electron microscopy (SEM) was used to examine the morphology of MOLM-13 cells adhering to poly-l-lysine-coated coverslips, and showed that, in contrast to the spread, flattened appearance of untreated cells, cells treated with DPI, PKC412 or PP2 for 24 hours displayed a more bulbous retracted morphology (Figure 40). This is consistent with previous reports of changes in cell morphology coinciding with alterations in Ezrin sub-cellular localisation (Auvinen *et al.*, 2007; Bretscher, 1989; Krieg and Hunter, 1992). The untreated cells appear to be adhering to the poly-l-lysine at multiple points on the basal cell surface, while the cells treated with DPI, PKC412 or PP2 seem less connected. Viewing adhesion as a precursory step to the process of migration, this prompted the question of whether FLT3 or Nox inhibition, and the resulting effects on Ezrin and cell morphology, would affect the ability of MOLM-13 cells to migrate.

Inhibition of Nox or FLT3 results in a decreased ability of AML cells to migrate

As Ezrin expression has been associated with increased migration of tumour cells (Zhou *et al.*, 2010b), a reduction in its tyrosine phosphorylation, changes to its sub-cellular localisation and alterations to MOLM-13 cell morphology due to FLT3, Src or Nox inhibition could negatively influence the motility of MOLM-13 cells.

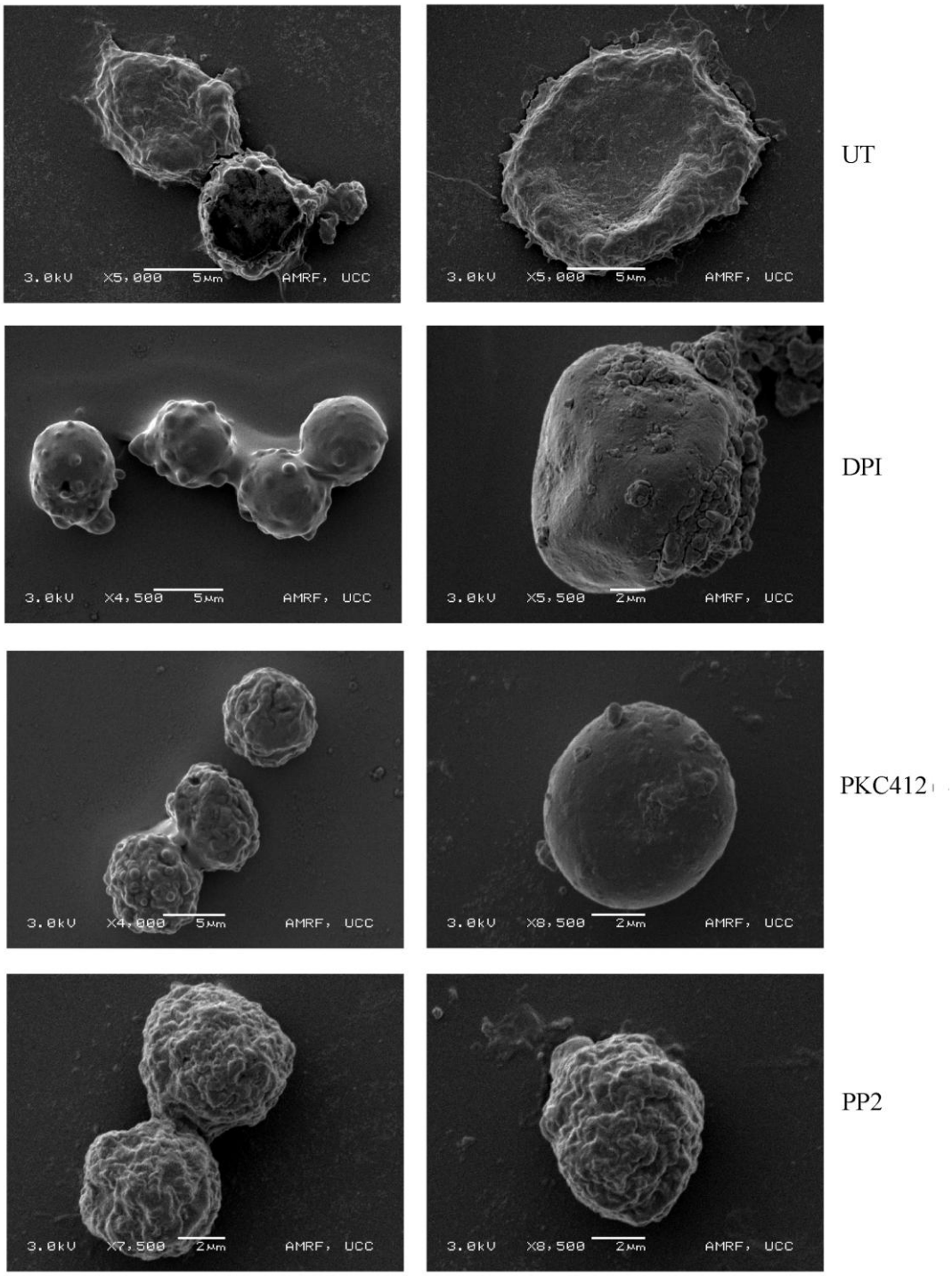


Figure 40. Effect of Nox or FLT3-ITD inhibition on MOLM-13 cell morphology. Scanning electron micrographs of untreated MOLM-13 cells compared to cells treated with 20 µM DPI, 250 nM PKC412 or 20 µM PP2 for 24 hours. Scale and accelerating voltages are indicated. A representative micrograph is shown in each case**.**

A chemotaxis assay was carried out to assess the ability of MOLM-13 cells to migrate across a transwell membrane. Compared to the untreated control, cells treated with DPI (Figure 41A), PKC412 (Figure 41B) or PP2 (Figure 41C) displayed a very significant and concentration-dependent decrease in migration, reflected by similar results in MV4-11 cells (Figure 42A). PKC412 had no effect on the migration of HL60 cells (Figure 42B). This demonstrated that the modulation of Ezrin tyrosine phosphorylation and sub-cellular localisation caused by FLT3 and Nox inhibition correlates with the effects of their inhibition on the motility of MOLM-13 cells and reflected the finding of Zhou *et al.* (2010) that Ezrin is a key mediator in the metastasis of another leukaemia cell line MOLT4.

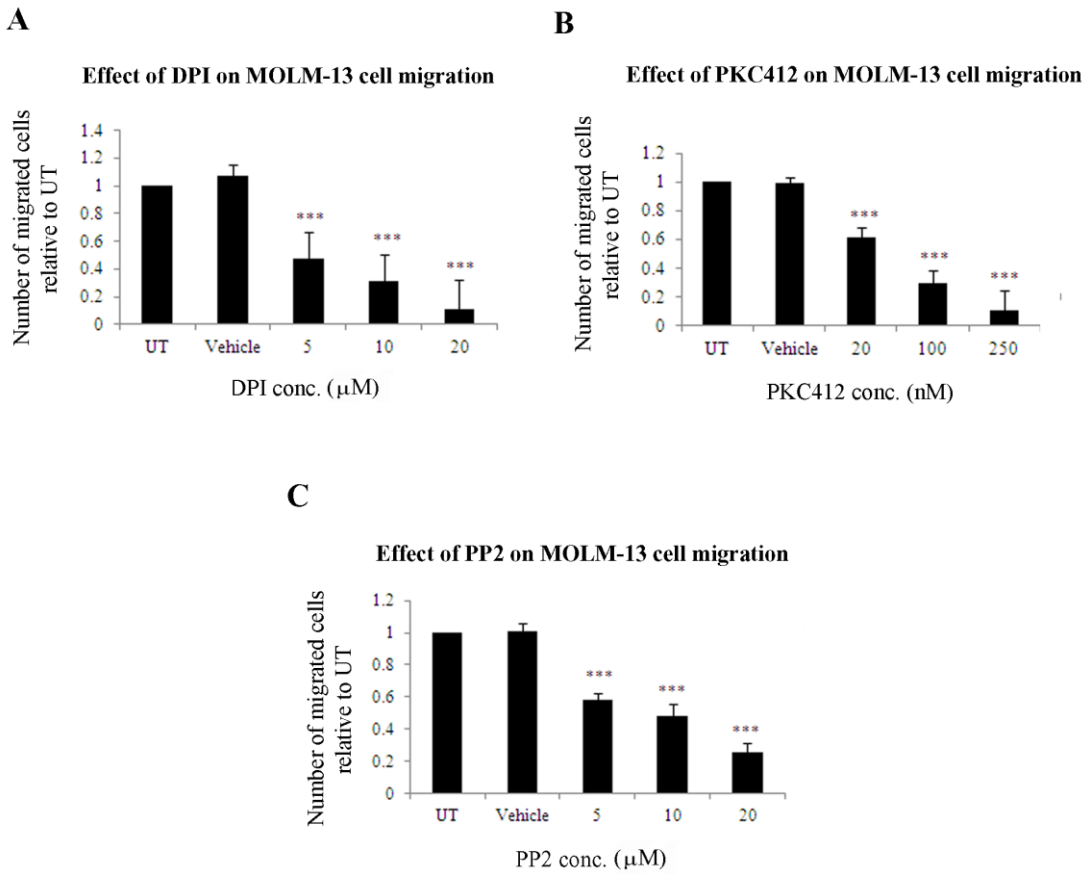


Figure 41. Effect of Nox, FLT3 or Src inhibition on the migration of MOLM-13 cells. Graphs depicting the migration, through a 5 μm polycarbonate membrane, of untreated MOLM-13 cells, cells treated with DMSO vehicle only and cells treated with increasing concentrations of DPI (A) PKC412 (B), or PP2 for 24 hours. Migration of untreated cells was used as a control (=1). Statistical analysis was performed using Student's *t*-test. *** denotes P<0.001.

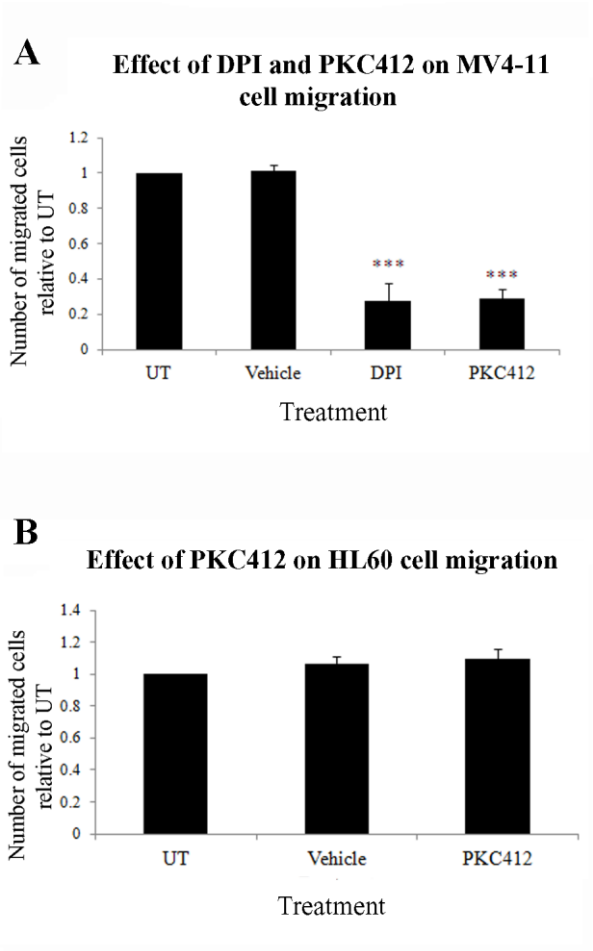


Figure 42. Effect of Nox or FLT3-ITD inhibition on the migration of MV4-11 and HL60 cells. Graph depicts the migration, through a 5 µm polycarbonate membrane, of **A)** untreated MV4-11 cells, cells treated with DMSO vehicle only and treated with 20 µM DPI or 250 nM PKC412 for 24 hours and **B)** untreated HL60 cells, cells treated with DMSO vehicle only and cells treated with 250 nM PKC412 for 24 hours. Migration of untreated cells was used as a control (=1). Statistical analysis was performed using Student's *t*-test. *** denotes P<0.001.

Discussion

Aberrant migration of leukaemic cells followed by extramedullary infiltration into secondary sites of bone marrow and organs are major complicating factors for AML (Fukuda *et al.*, 2005; Stefanidakis *et al.*, 2009). The role of FLT3 in regulating both the normal migration of haematopoietic progenitors, as well as the subversive migration of leukaemic cells has been demonstrated (Fukuda and Pelus, 2006). There is evidence to suggest that FLT3 signalling involves downstream activation of Nox and subsequent increase in ROS levels (Reddy *et al.*, 2011; Sallmyr *et al.*, 2008a) and it has also been established that ROS produced by Nox can promote and stabilise the cell protrusions that facilitate migration and invasion (Diaz *et al.*, 2009; Gianni *et al.*, 2011). With regard to the mechanism whereby Nox-derived ROS exert their effects on the cytoskeletal machinery of the cell, much data support a role for Src kinase in translating the upstream oxidant generation to the downstream protein modifications and the resulting phenotypic effects. Src has been shown to undergo oxidative activation upon integrin engagement (Chiarugi, 2008), which facilitates its interaction with cytoskeletal mediators leading to alterations in cell morphology associated with adhesion and invasion (Giannoni *et al.*, 2005).

Incorporation of a redox element into a signalling pathway appears to be fraught with difficulty, not least in terms of the perceived lack of specificity of oxidant targeting and the potentially detrimental effects such highly reactive molecules can cause to intracellular biomolecules such as DNA and lipids. Indeed the utilisation of ROS as signalling mediators in their own right has evolved to be tightly regulated spatially, temporally and in terms of substrate susceptibility. This regulation is facilitated by the discrete subcellular compartmentalisation of ROS

production (Chen *et al.*, 2009), the restricted availability of Nox activating and regulatory subunits (Gianni *et al.*, 2009;Terada, 2006) and the presence of cytosolic scavenging and neutralising enzymes such as Cu/Zn SODs, GSH peroxidase (Terada, 2006) and Prxs (Rhee and Woo, 2011; Rhee *et al.*, 2012) to prevent escape or accumulation of ROS to toxic levels. Substrate specificity is also regulated through co-localisation of ROS producing enzymes and the intended target of the oxidants produced, to distinct insulated intracellular compartments. The redox regulation of Src in the scenario presented in this chapter must involve proximity of the kinase to a p22phox-dependent Nox isoform as demonstrated by the p22phox knockdown experiments. As Nox 3 has been shown not to be expressed in these cells, Nox 1, 2 and possibly 4 are the incumbent isoforms.

The direct oxidation of Src supported by results presented in this chapter, does not exclude the possibility that concomitant oxidative-inactivation of a PTP which de-phosphorylates Ezrin is also occurring, and contributing to the changes in Ezrin tyrosine phosphorylation. Although on the whole there is very little literature surrounding de-phosphorylation of Ezrin, it is worth noting at this point an interesting paper from Forte *et al*. (2008) which demonstrates that the overexpression of dual specificity phosphatase of regenerating liver-3 (PRL-3), which is implicated in a range of metastatic tumours, causes the de-phosphorylation of Ezrin Y146 and Y353. Separately, it has been shown that PRL-3 is downstream of FLT3-ITD signalling (Zhou *et al.*, 2011) and is subject to redox regulation (Orsatti *et al.*, 2009), making it a highly promising candidate for a position in the FLT3-Nox-Ezrin pathway.

Similarly, the direct redox activation of Src does not prohibit the possibility that indirect redox activation of the kinase is also operating *via* oxidative-inactivation of a phosphatase, or indeed a kinase such as Csk, which inhibits Src activity. In fact, this study aims to provide evidence to complement rather than confront the established model of redox regulation of tyrosine phosphorylation, with the objective of broadening the current redox signalling paradigm to include direct redox regulation of kinases as a crucial component.

Ezrin has previously been shown to play a key role in the metastasis of leukaemic cells (Zhou *et al.*, 2010), as well as being associated with the migration and progression of a range of other cancers (Brambilla and Fais, 2009; Fais, 2004). Previously published data from Monni *et al*. (2008) has shown that Ezrin is phosphorylated downstream of another constitutively active FLT3 mutant, FLT3-D835Y. As neither MOLM-13 nor MV4-11 cells contain this mutation, the results of this and the previous chapter demonstrate a novel link between FLT3-ITD signalling and modulation of Ezrin tyrosine phosphorylation. Since the publication of this data (Corcoran and Cotter, 2013), further evidence has emerged linking the phosphorylation of Ezrin to oncogenic FLT3-ITD signalling. Habif *et al*. (2013) used 2D SDS-PAGE to identify Ezrin as a downstream target of FLT3-ITD-driven phosphorylation and mediator of proliferative signalling in AML cells.

Our data showed that FLT3-ITD or Nox inhibition affected Ezrin by causing a shift in its localisation from the plasma membrane to the cytoplasm and possibly the nucleus. This shift coincides with de-phosphorylation of Ezrin at two tyrosine sites Y146 and Y353, though it is possible that additional, at present unknown, mechanisms of FLT3-driven regulation of Ezrin are also contributing. The changes

in sub-cellular localisation of Ezrin are likely to affect the established function of Ezrin as a cytoskeletal regulatory protein. Specifically as an intermediary between F-actin and cell membrane proteins, its scaffolding function is inherently related to its location within the cell. The proximity of Ezrin to the cell membrane determines its ability to bind membrane-residing factors such as CD44 (Mori *et al.*, 2008), PtdIns(4,5)P_2 (Maniti *et al.*, 2012), ICAM-1 and 2 (Barreiro *et al.*, 2002) and EBP50 (LaLonde *et al.*, 2010) amongst others, and it is through these interactions that a link is formed between F-actin and the membrane leading to F-actin-rich membrane protrusions which facilitate cell motility (Arpin *et al.*, 2011; Saleh *et al.*, 2009). Although there is, to our knowledge, no evidence in the literature regarding the relevance of Ezrin tyrosine phosphorylation to its sub-cellular localisation, it is worth noting that inactive Ezrin has been repeatedly observed to be cytoplasmic rather than localising to the periphery of the cell and it is only upon activation that the protein shifts to the membrane (Bretscher *et al.*, 2002; Gary and Bretscher, 1995).

However, rather than viewing the translocation observed here as negative regulation of Ezrin, it is possible that Ezrin plays a role in both the cytoplasm and nucleus, perhaps as a signalling molecule. While it is accepted that threonine phosphorylation of Ezrin facilitates its activation (Ng *et al.*, 2001), less is known about the functional significance of Ezrin tyrosine phosphorylation. What data does exist seems to point towards a role for Ezrin tyrosine phosphorylation in signal transduction. Gautreau *et al*. (1999) have previously proposed that p-Ezrin Y353 operates as a survival signalling molecule through interactions with the PI3K/Akt pathway. Further evidence links phosphorylation on Ezrin Y146 to Src-dependent adhesion signalling promoting cell proliferation (Srivastava *et al.*, 2005) and

nominates another Src-phosphorylated residue Y477 as the effector of a malignant phenotype in Src-transformed cells (Heiska and Carpen, 2005; Heiska *et al.*, 2011), supported again by a recent report from Mak *et al*. (2012) proposing a role for phosphorylation of Y477 in invasion and migration.

The shuttling of cytoskeletal proteins to the nucleus is being increasingly acknowledged as a direct and mechanical mode of communication between the plasma membrane, the interface for receiving extracellular stimuli, and the nucleus, where those signals are integrated and translated into necessary adaptive changes for the cell (Aplin, 2003; Aplin and Juliano, 2001). Proteins such as actin, paxillin, zymixin and ZO-1 have been shown to localise to the nucleus and participate in mRNA transcription (Balda *et al.*, 2003; Chan *et al.*, 2007; Hofmann *et al.*, 2001; Woods *et al.*, 2002). Band 4.1 has been shown to facilitate splicing (Lallena *et al.*, 1998) as well as fulfilling its non-nuclear role in linking transmembrane proteins to the spectrin/actin cytoskeleton (Conboy, 1993) and both actin and band 4.1 play a role in maintaining the integrity of the nuclear matrix (Krauss *et al.*, 1997; Rando *et al.*, 2002).

Batchelor *et al.* (2004) also report the phenomenon of nuclear localisation of Ezrin, but in response to changes in cell density. They propose a structural role for Ezrin in the nucleus, similar to its role at the plasma membrane, and based on the affiliation that Ezrin has for actin, suggest that it could also facilitate transcription or export of mRNA from the nucleus as these are processes in which nuclear actin participates. The possible localisation of Ezrin to the nucleus in response to FLT3 or Nox inhibition could serve to communicate a signal of decreased FLT3 signalling at the cell membrane. This signal could trigger a response which, in its early stages,

manifests itself as a reduction in cell motility in order to conserve energy, but may later result in changes at the level of transcription of stress response genes as the cell attempts to adjust to and survive through the reduction in growth factor stimulation.

The effectiveness of the FLT3-ITD inhibitor PKC412, in impairing the migration of the AML cell line MOLM-13, highlights a potential mechanism whereby this inhibitor, currently in clinical trials for the treatment of AML, may prevent the spread of leukaemic blasts from the primary site of expansion to secondary extramedullary sites. The use of the HL60 cell line, which expresses only the wild type FLT3 receptor, as a negative control for PKC412 demonstrates that the observed effects of the drug are specific to FLT3-ITD signalling.

It is likely that FLT3 modulation of Ezrin tyrosine phosphorylation and sub-cellular localisation are not the only mechanisms whereby FLT3 regulates leukaemic cell migration and this crucial aspect of FLT3 signalling deserves further investigation to clearly elucidate all of the contributing effectors.

The realisation that ROS may directly oxidise kinases in a signalling context allows the reviewing of previously published data with a view to identifying additional redox-regulated kinases. Articles which reported the sensitivity of a kinase-driven signal transduction pathway to ROS can be revisited and, by removing the assumption that another factor mediates the connection between the oxidant and the kinase, the hypothesis of a redox-sensitive kinase can be examined. Pourmahram *et al*. (2008) provides an example of such an opportunity, as the authors detected a shift in sub-cellular localisation in PKCα in intrapulmonary arteries upon exposure to low concentrations of H_2O_2. Similarly, Kato (2000) and colleagues' discovery of

redox-sensitive cysteine residues in c-Ret which are conserved across a range of kinases should prompt investigation of the redox-sensitivity of those kinases.

Recently progress in the field of redox biology has been due to the development of methods for detection of redox-modifications, a subject which has been recently reviewed extensively in its own right (Butterfield and Dalle-Donne, 2012). In this study, BIAM-labelling of reduced cysteine residues was used to examine the redox state of Src, adapted from a protocol outlined by Bovin *et al*. (2010, 2008) and although efficient for this purpose, is by no means the only option for analysing the redox state of individual proteins. A novel approach from Haque *et al*. (2011) uses an antibody raised to detect oxidised forms of PTPs, allowing the analysis of the redox state of specific phosphatases.

Recent advances in the development of fluorescent and affinity-labelled probes for the high throughput detection and isolation of sulfenic acid modifications are described by Poole and Nelson (2008), and also recently covered by Paulsen and Carroll (2009). Concurrently, high throughput studies such as those conducted by Fomenko *et al*. (2007) and Weerapana *et al*. (2010) strive to quantify and characterise the reactive cysteine residues in native enzymes, with a view to predicting redox-relevant motifs. In addition to this, methodologies such as the carbonyl-based proteomics approach employed by Brioschi *et al*. (2012) are effective in identifying oxidative stress biomarkers which are invaluable from a prognostic and diagnostic perspective.

Redox regulation of signal transduction is a rapidly progressing field. The recent acceleration of research in this field has contributed to our understanding of the mechanisms whereby ROS exert their effects on target kinases and the

consequences of those effects both at the level of kinase activity and in terms of broader signalling and phenotypic implications. Data gleaned by analysing the physiological requirement for ROS production as a signalling device, can assist our understanding of the pathological situation which occurs when this system becomes deregulated. Implicating the redox regulation of kinases in the molecular basis of cancer and cardiovascular disease in particular, complements the established models of pathological oxidative stress but also provides new avenues and possibilities for targeted, antioxidant-based therapeutics**.**

In conclusion, we report a link between FLT3 signalling and Ezrin, mediated by Nox-derived ROS and the subsequent redox regulation of Src, which correlates with an effect of FLT3 and Nox activity on the morphology and migration of MOLM-13 cells. Similar effects observed in another FLT3-ITD expressing cell line MV4-11, suggests that this scenario may operate broadly in FLT3-ITD driven AML.

Chapter 5

Regulation of phosphatase expression and activity by FLT3-ITD in the MOLM-13 cell line

Abstract

Growth factor-driven tyrosine phosphorylation signalling cascades operate through the co-ordination of the activities of protein tyrosine kinases and protein tyrosine phosphatases. The negative regulation of potentially oncogenic tyrosine phosphorylation signalling by phosphatases has prompted the classification of several protein tyrosine phosphatases as tumour suppressors. Such phosphatases are frequently downregulated in tumours, at the level of transcription or through post-translational modifications leading to suppression in phosphatase activity. FLT3-ITD has been shown to promote tyrosine phosphorylation through the redox-activation of Src kinase but, as demonstrated in this section, also regulates a range of phosphatases to facilitate increased duration and intensity of the phosphorylation signal. Inhibition of FLT3-ITD using PKC412 resulted in changes at the level of phosphatase protein expression which reflected changes to the transcription of selected phosphatase genes. In addition to this, FLT3-ITD was shown to negatively regulate the tumour suppressor phosphatase SHP-1 at a post-translational level through increased ubiquitination and proteasomal degradation of SHP-1 protein.

Introduction

Efficient functioning of tyrosine phosphorylation as a signal transduction device requires co-operation and communication between the PTKs and the PTPs. The nature of the cellular functions dictated by tyrosine phosphorylation signalling, i.e. proliferation, cell cycle and survival, renders this signalling mechanism potentially oncogenic, should it become de-regulated. Indeed, it is estimated that up to 80% of all proto-oncogenes code for PTKs (Laczmanska and Sasiadek, 2011), making tight negative regulation of the phosphorylation cascade by PTPs especially crucial. It is understandable therefore, that many PTPs, such as Phosphatase and tensin homolog (PTEN), have been designated as tumour suppressors (Laczmanska and Sasiadek, 2011; Song *et al.*, 2012), and that the amount of genes which code for PTPs approximates the number which code for PTKs (Tonks, 2006) such is their responsibility to curb aberrant kinase activity.

The PTP superfamily, coded for by107 genes (Alonso *et al.*, 2004), includes the classical PTPs that are specific for tyrosine and also the dual specificity phosphatases (DSPs) which, due to a different active site structure, can de-phosphorylate serine and threonine as well as tyrosine residues and inositol phospholipids (Andersen *et al.*, 2004). A third subgroup within this superfamily is the pseudophosphatase PTPs which appear to be catalytically inactive although structurally resembling classical PTPs (Wishart and Dixon, 1998).

Although many PTPs play a role in negative regulation of potentially oncogenic signalling, it is worth noting that some can have a pro-oncogenic role by facilitating activation of pro-survival kinases through removal of an inhibitory phosphate or the inactivation of an inhibitory binding partner. An example of such a

PTP is SHP-2, which is known to become activated by EGFR and in turn activates the Ras -MAPK signalling pathway as well as SFKs (Matozaki *et al.*, 2009). There is some ambiguity surrounding the exact mechanism whereby SHP-2 activates these kinases, one model proposes that SHP-2 directly de-phosphorylates the p120 RasGAP binding site on Ras, thereby preventing the binding of the inhibitory molecule (Montagner *et al.*, 2005). Another possibility is that SHP-2 indirectly activates Ras-MAPK *via* the activation of SFK intermediates, in multi-step process which is thought to involve the dephosphorylation of a Csk-binding protein, preventing recruitment of Csk to the SFKs (Ren *et al.*, 2004; Zhang *et al.*, 2004). A further option proposed by Hanafusa *et al*. (2004), illustrates how SHP-2 may promote Ras-MAPK signalling through the inhibition, *via* dephosphorylation, of Sprouty, a negative regulator of Ras-MAPK.

In addition to its role in EGFR signal transduction, SHP-2 has also been implicated in the signalling pathways of Bcr-Abl, fibroblast-growth-factor receptor 3 (FGFR3), Ret and ERBB2, a member of the EGFR (Ostman *et al.*, 2006). SHP-2 is something of a node for the convergence of signals from a number of growth factor receptors and the relaying of those signals to a variety of substrates. So potent is its position as a signalling hub within the cell that autosomal dominant mutations in the SHP-2 gene *PTPN11*are thought to lead to 50% of cases of the complex Noonan syndrome which is associated with juvenile myelomonocytic leukaemia (JMML) (Tartaglia *et al.*, 2001). Incidence of *PTPN11*activating mutations are also found in ALL (Tartaglia *et al.*, 2004) and sporadic JMML patients (Tartaglia *et al.*, 2003), as well as AML, particularly of the M5 subgroup (Tartaglia *et al.*, 2005).

In addition to the activating mutations of SHP-2, the non-mutated form of the PTP is frequently found to be overexpressed and over-activated in FLT3-ITD containing leukaemic cells (Gu *et al.*, 2011; Xu *et al.*, 2005). SHP-2 appears to play an important role in normal haematopoiesis (Qu *et al.*, 2001; Nabinger and Chan, 2012) as well as leukemogenesis (Loh *et al.*, 2004) and is a crucial component of the wild type FLT3 signalling pathway. SHP-2 is known to interact with the wild type FLT3 receptor after FL stimulation and promote the downstream activation of MAPK (Zhang *et al.*, 1999; Muller *et al.*, 2008b).

The example of SHP-2 demonstrates how PTPs can both directly and indirectly facilitate pro-survival signalling downstream of growth factor stimulation. Specifically with regard to the AML situation, SHP-2 represents an important mechanism of FLT3-ITD-driven signal propagation *via* upregulation of a PTP which contributes positively to the signalling pathway.

PTPs, whether they function as positive or negative regulators of a growth factor signalling, are themselves subject to stringent regulation. The modes of regulation of PTP activity range from control of PTP gene transcription, to protein turnover *via* ubiquitination and degradation, and *via* post-translation modifications such as phosphorylation and oxidation, which render the enzyme temporarily, or sometimes permanently, inactive.

The mechanism of PTP oxidative regulation has been discussed in Chapter 4 as it provides a model for the oxidative regulation of other enzymes such as kinases, and appears to be co-ordinated with PTP phosphorylation (Chiarugi and Buricchi, 2007) to provide an efficient means of inactivating PTPs to facilitate oxidant-associated growth factor signalling. The functional relevance of PTP oxidation is

constantly expanding, as is the range of PTPs affected, hinting at a prevalence of growth factor-driven redox regulation of PTPs.

Indeed, oxidation of PTPs appears to be indispensible for the functioning of certain intracellular signalling pathways. Recent work by Choi *et al.*, (2011) shows how redox-mediated inactivation of SHP-1 participates in the M-CSF-induced proliferation of haematopoietic progenitors. They observed that the transient oxidation of SHP-1 affects the PI3K/Akt but not the MAPK survival pathway to stimulate BMM proliferation. This demonstrates how the specificity and integrity of the signal initiated by M-CSF binding its receptor c-Fms, and subsequently transmitted *via* ROS, can be maintained. Interestingly, Choi *et al*., also report that SHP-2 was not oxidised in their system, even upon exogenous addition of H_2O_2, despite its accepted status as redox-sensitive phosphatase in other systems (Meng *et al.*, 2002; Weibrecht *et al.*, 2007). Oxidation of PTPs in a signalling context requires the specificity of an enzyme-substrate reaction in order to maintain the integrity of the propagated signal. The sensitivity of individual PTPs to different oxidant species is one mechanism whereby this differential regulation is ensured.

Similarly, Juarez *et al.,* (2008) recently demonstrated that PTP1B is inhibited by H_2O_2 *in vivo*, but not by , the main type of ROS produced upon stimulation of the EGFR, which is itself negatively regulated by PTP1B. Although the role of endogenous antioxidants such as SODs are generally understood to be as safeguards against harmful increases in oxidants, the scenario described by Juarez *et al.*, depicts SOD as a positive regulator of EGFR signalling, facilitating increases in H_2O_2 levels, inactivation of PTP1B and propagation of the proliferative signal through the MAPK/Erk pathway downstream of EGFR.

The role of GF-mediated PTP oxidation in the physiology of normal cells has provided insights into how aberrant ROS production can compound stimulation of survival pathways by oncogenic RTK. The significance and complexity of PTP redox regulation in the context of oncogenic signalling was recently highlighted by Karisch *et al.* (2011). Here the authors used a global proteomic approach to assess the 'PTPome' or global cellular profile of PTPs, and then further modified this approach to quantify the 'PTP redoxome' or proportion of PTPs which are oxidised in normal and neoplastic cells. They observed an increase in PTP oxidation in tumour cells, with each tumour type having its own unique profile of oxidised PTPs.

The list of PTPs which are redox regulated in response to GF signalling continues to grow and amongst the most recent additions to this list, and of particular relevance to this study is the tumour suppressor DEP-1, which was shown by Godfrey *et al.* (2012) to be redox-inactivated in response to aberrant redox signalling driven by FLT3-ITD. The authors previously used shRNA-based screens to identify PTPs which negatively regulate FLT3-ITD signalling (Arora *et al.*, 2011) with the premise that constitutive oncogenic signalling from FLT3-ITD was likely to involve the negative regulation of inhibitory PTPs. The significance of this finding lies with the authors' observation that transformation of mouse haematopoietic progenitor cells by FLT3-ITD is so dependent on the redox regulation of DEP1, that blocking the ROS burst induced by FLT3-ITD was sufficient to halt transformation *in vivo* and in vitro. This effect was reversed upon knockdown of DEP1, both establishing the powerful tumour suppressive role of this phosphatase in leukaemia, as well as uncovering further details of the relatively obscure FLT3-ITD signalling pathway.

Much of the focus on the source of GF-stimulated ROS production centres on the Nox family of enzymes, however, the Lox were the subject of a recent study by Conrad *et al.* (2010). The authors reported on the oxidising mediators produced by 12/15-Lox which can act as second messengers by inactivating PTPs to amplify and prolonging PDGF-β receptor signalling. The signalling molecules in question were shown to be peroxidised arachadonic acid-derived lipids which induced oxidation of SHP-1, PTP-H1 and TC-PTP *in vitro*. This previously unrecognised class of oxidising mediators introduces another dimension to the already complex situation of PTP redox regulation, and they may also help to account for features of redox signalling which cannot be attributed to diffusible ROS.

While oxidation and phosphorylation allow the regulation of PTPs by effectively switching the enzyme on or off, modulation of PTP protein turnover rate is also an important aspect of PTP regulation. Ubiquitination is a post-translational modification which, through covalent labelling of proteins with ubiquitin moieties, directs their sub-cellular localisation and intracellular trafficking (Haglund and Dikic, 2005). The degree of ubiquitination determines the consequences of this labelling for the protein. Mono-ubiquitination, the reversible addition of single moiety to a single lysine residue, can signal that the protein is due to be endocytosed, targeted for endosomal sorting or nuclear export (Di Fiore *et al.*, 2003). The addition of chains of ubiquitin moieties either to a single lysine on the target protein, termed multiple monoubiquitination (Haglund *et al.*, 2003a), or to the lysine residues of target-bound ubiquitin itself, polyubiquitination (Pickart and Fushman, 2004), introduces further levels of complexity and tends to have more terminal consequences. Multiple monoubiquitination of activated RTKs leads to their

trafficking to the lysosome and degradation (Haglund *et al.*, 2003b), while the polyubiquitination, *via* ubiquitination of Ub^{Lys48} can label a range of targets for proteasomal degradation as established by Ciechanover, Hershko, and Rose (1998), and recognised by the 2004 Nobel Prize in Chemistry. Once degraded in the proteasome, the protein may be replaced by a newly synthesised version and the ubiquitin is recycled (Mani and Gelmann, 2005).

Physiologically, this process is crucial to eliminate damaged or misfolded proteins as well being necessary for the termination of endocytosed RTK signalling. Disruptions to the ubiquitination-proteasomal pathway resulting in increased degradation of proteins with a tumour-suppressive function, or retention and sustained activity of proto-oncogenic RTKs can contribute to oncogenesis (Ciechanover *et al.*, 1991; Rogers *et al.*, 1986) and is a feature in a range of tumour types including renal cell carcinoma (Clifford *et al.*, 2001), colorectal cancer (Sparks *et al.*, 1998), human papilloma virus(HPV)-driven cervical cancer (Scheffner *et al.*, 1993), BRCA1-dependent breast cancer (Starita and Parvin, 2003), glioblastoma (Schmidt *et al.*, 2003) and FLT3-ITD positive AML (Caligiuri *et al.*, 2007; Sargin *et al.*, 2007). Upregulation of PTP ubiquitination and degradation in particular, presents a possible mechanism whereby oncogenic RTKs can manipulate phosphorylation signalling cascades.

As well as post-translational modifications of the PTP proteins, PTPs, like many other proteins are regulated at the level of gene expression, through the requirements for binding of specific transcription factors, transcriptional activators, repressors and enhancers. Downregulation of the transcription of tumour suppressor PTPs, and PTPs which are presumed tumour suppressive due to their negative effect

on pro-oncogenic kinase signalling, is common in oncogenesis (Julien *et al.*, 2011; Song *et al.*, 2012). However, there is a scarcity of data regarding the specific expression profiles of PTPs in AML. A recent study from Arora *et al*. (2012) sought to address this by using RT-qPCR to analyse the mRNA levels of 92 PTPs in both patient samples and AML cell lines, including the MV4-11 cell line but not the MOLM-13 cell line. The authors' objective was to identify PTPs which were differentially expressed in FLT3-ITD AML compared to wild type AML and reported an up-regulation of several DSPs correlating with FLT3-ITD expression suggesting that oncogenic FLT3 signalling incorporates the functions of some PTPs. However this study did not identify any PTPs which showed decreased expression in FLT3-ITD samples compared to wild type FLT3 samples and concluded that in general very few differences in PTP mRNA expression could be observed between samples.

Although informative, the scope of the study was somewhat limited and it can be argued that comparison of a single FLT3-ITD cell line MV4-11 with three FLT3 wild type cell lines THP1, EOL1, RS4-11, may not be the most ideal model for establishing the relevance of FLT3-ITD signalling, as additional genetic lesions present in the individual cell lines are likely to be contributing to the PTP expression profiles. For the same reason any differences in PTP expression which might have been observed between the cell lines could not have been singularly attributed to FLT3-ITD. The use of 32D cells transfected with FLT3-ITD and wild type FLT3 provided the possibility of comparison to parental cells with the same genetic background. However, the changes in 32D PTP expression upon introduction of FLT3, disagreed with some of the data obtained from comparison of MV4-11 with

the wild type cell lines, and appeared to show that the wild type receptor was dictating the upregulation of the DSPs. In addition to this, the AML patient samples displayed discrepancies between the PTP expression levels as determined by RT-qPCR and those detected by Affymetrix.

In contrast, a study by Chen *et al*. (2005) showed that FLT3-ITD activity correlated to an increase in tyrosine phosphorylation which could not be explained by simply an increase in kinase activity but required a concomitant suppression of PTP activity, which the authors traced to a decrease SHP-1 mRNA expression, but it is possible that many other contributing PTPs are likely to be similarly affected.

These ambiguities in relation to FLT3 regulation of PTPs prompted the initiative of the next chapter, with the objective of identifying PTPs which are regulated by FLT3-ITD signalling in the MOLM-13 cell line, in order to further contribute to our model of the tyrosine signalling network which operates downstream of this receptor.

Results

Kinexus™ Phosphatase Expression Profile of MOLM-13 and MV-411 cells

To date, 107 genes coding for PTPs have been identified in the human genome (Alonso *et al.*, 2004) highlighting the importance of these molecules and the pathways that they regulate. Due to the role of phosphatases in negatively regulating proliferation and survival, cancer cells which successfully circumnavigate this innate regulation often display inactivating mutations, or methylation and silencing of regulatory phosphatase genes (Ostman *et al.*, 2006). The result of this is that cancer cell lines may only express functional proteins from a fraction of the total number of phosphatase genes which they contain. In examining the p-Tyr signalling mechanisms of FLT3 in the AML cell lines MOLM-13 and MV-411, the role of tyrosine phosphatases is important to consider and to do this it is necessary to first establish which phosphatases are expressed in these cell lines.

The Kinexus™ Phosphatase Screen 1.2 is a commercially available service which uses multi-immunoblotting to generate a phosphatase expression profile for a submitted lysate. The screen examined the expression of 30 tyrosine, serine/threonine and dual specificity phosphatases, in both cell lines and the results are represented as K_001 in Figures 43, 44, 45 and Table 2, 3 and 4.

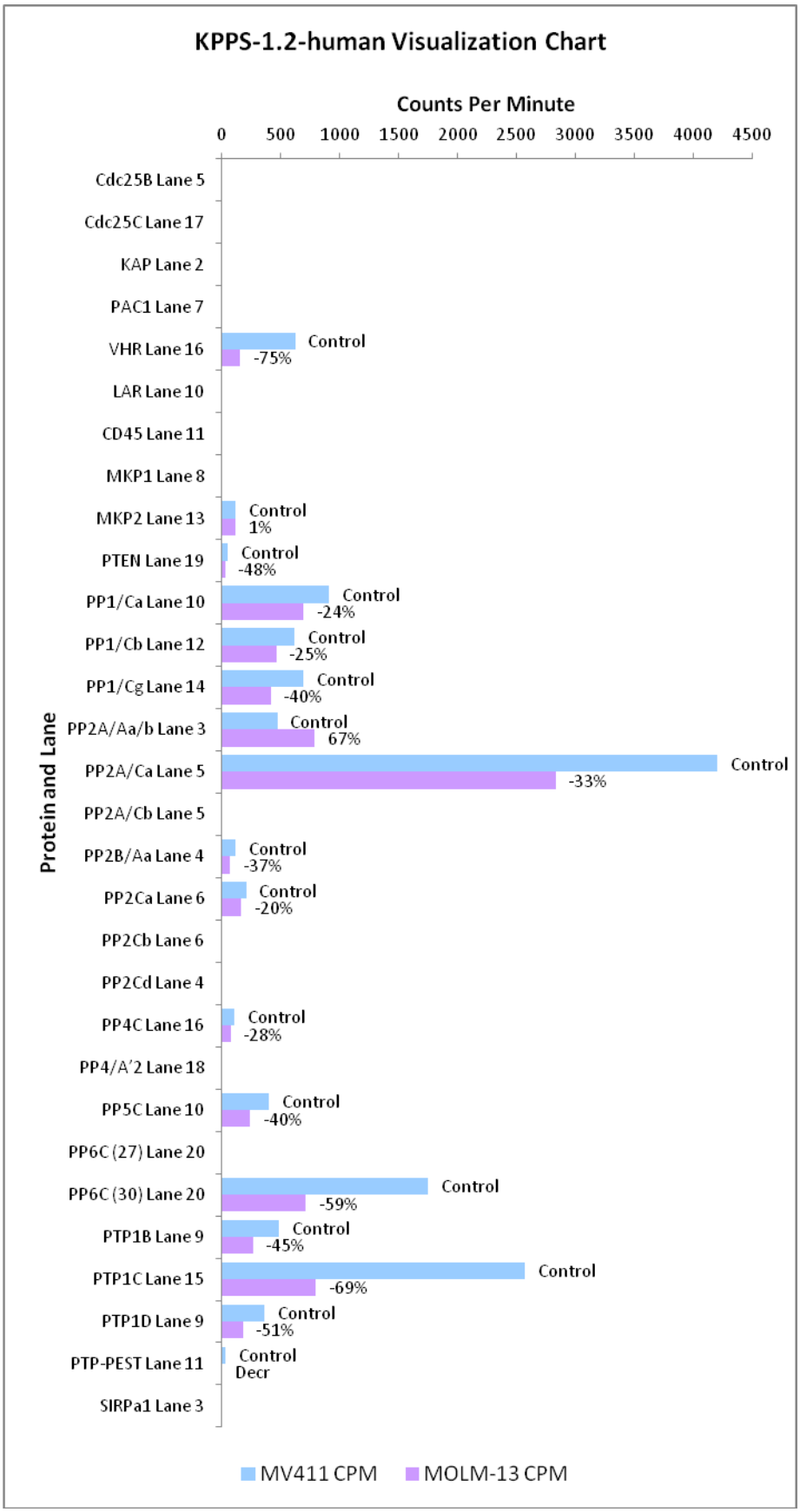
As expected, almost half of the phosphatases were not expressed at the protein level, including Cdc25B, Cdc25C and cyclin-dependent kinase associated phosphatase (KAP/CDK inhibitor 3), all of which regulate the cell cycle, the dual-specificity MAP-kinase protein phosphatase PAC1 and CD45. Both cell lines also had very low levels of PTEN. Down-regulation of PTEN is frequently observed in

cancer, both at the level of transcription, where the *PTEN* gene can become methylated or heavily regulated by transcription factors, competitive endogenous PTEN pseudogene RNA, and microRNAs, as well at the level of aberrant post-translational modifications to the PTEN protein such as phosphorylation, oxidation, ubiquitination and acetylation (Carracedo *et al.*, 2011).

In general, MV4-11 had higher levels of phosphatase expression than MOLM-13 but because of the possibility of regulation by post-translational modifications this may not reflect the differences of phosphatase activity within the cells.

Figure 43. Kinexus™ phosphatase expression screen K_001.

Histogram represents the results of the multi-immunoblotting carried out by Kinexus™ Phosphatase Expression Screen KPPS 1.2, to generate the phosphatase expression profiles of MV4-11 (blue), designated as control sample, and MOLM-13 (purple), designated as test sample. The identification and detection of each of 30 phosphatases (vertical axis) was based on immunoreactivity and apparent molecular mass. The corrected trace quantity of each band is expressed as counts per minute (CPM) (horizontal axis).


KPPS-1.2-human Visualization Chart
Counts Per Minute
0
500
1000
1500
2000
2500
3000
3500
4000
4500
Protein and Lane
Cdc25B Lane 5
Cdc25C Lane 17
KAP Lane 2
PAC1 Lane 7
VHR Lane 16
Control
-75%
LAR Lane 10
CD45 Lane 11
MKP1 Lane 8
MKP2 Lane 13
Control
1%
PTEN Lane 19
Control
-48%
PP1/Ca Lane 10
Control
-24%
PP1/Cb Lane 12
Control
-25%
PP1/Cg Lane 14
Control
-40%
PP2A/Aa/b Lane 3
Control
67%
PP2A/Ca Lane 5
Control
-33%
PP2A/Cb Lane 5
PP2B/Aa Lane 4
Control
-37%
PP2Ca Lane 6
Control
-20%
PP2Cb Lane 6
PP2Cd Lane 4
PP4C Lane 16
Control
-28%
PP4/A'2 Lane 18
PP5C Lane 10
Control
-40%
PP6C (27) Lane 20
PP6C (30) Lane 20
Control
-59%
PTP1B Lane 9
Control
-45%
PTP1C Lane 15
Control
-69%
PTP1D Lane 9
Control
-51%
PTP-PEST Lane 11
Control
Decr
SIRPa1 Lane 3
MV411 CPM
MOLM-13 CPM

KINETWORKS™ KPPS-1.2-HUMAN COMPARISON REPORT

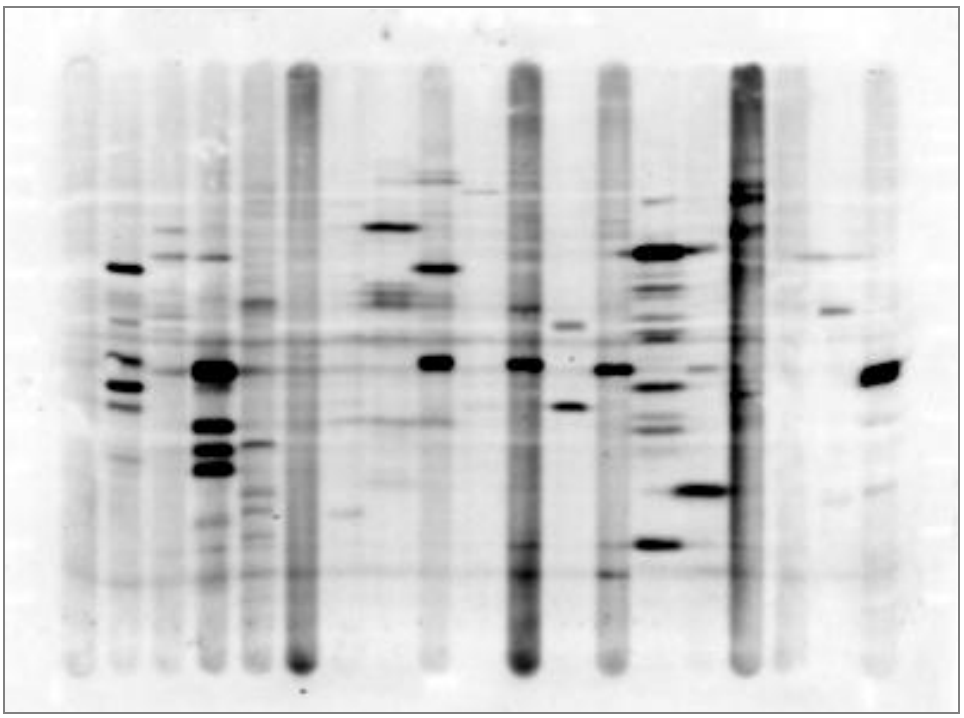
Corrected Data Comparison Of Corrected Trace Quantity (Counts per Minute) For the Following Samples			Kinexus ID Scan ID Sample Name	15213 65983 MV411	15214 65991 MOLM-13
FULL NAME OF PROTEIN	ABBREV	LANE	TYPE	C.P.M.	
Cell division cycle 25B phosphatase	Cdc25B	5	PSTYP		
Cell division cycle 25C phosphatase	Cdc25C	17	PSTYP		
Cyclin-dependent kinase associated phosphatase (CDK inhibitor 3, CIP2)	KAP	2	PSYP		
Dual specificity MAP kinase protein phosphatase	PAC1	7	PTYP		
Dual specificity protein phosphatase 3	VHR	16	PYP	622	154
LCA antigen-related (LAR) receptor tyrosine phosphatase	LAR	10	PYP		
Leukocyte common antigen CD45 receptor-tyrosine phosphatase (LCA, T200)	CD45	11	PYP		
MAP kinase phosphatase 1 (CL100, VH1)	MKP1	8	PTYP		
MAP kinase phosphatase 2 (VH2)	MKP2	13	PTYP	117	118
Phosphatidylinositol-3,4,5-trisphosphate 3-phosphatase deleted on chromosome 10	PTEN	19	PSTYP	50	26
Protein-serine phosphatase 1 - catalytic subunit - alpha isoform	PP1/Ca	10	PSTP	910	695
Protein-serine phosphatase 1 - catalytic subunit - beta isoform	PP1/Cb	12	PSTP	616	463
Protein-serine phosphatase 1 - catalytic subunit - gamma isoform	PP1/Cg	14	PSTP	693	413
Protein-serine phosphatase 2A - A regulatory subunit - alpha and beta isoforms	PP2A/Aa/b	3	PSTP	470	785
Protein-serine phosphatase 2A - catalytic subunit alpha isoform	PP2A/Ca	5	PSTP	4205	2830
Protein-serine phosphatase 2A - catalytic subunit beta isoform	PP2A/Cb	5	PSTP		
Protein-serine phosphatase 2B - catalytic subunit - alpha isoform	PP2B/Aa	4	PSTYP	115	72
Protein-serine phosphatase 2C - catalytic subunit - alpha isoform	PP2Ca	6	PSTP	205	163
Protein-serine phosphatase 2C - catalytic subunit - beta isoform	PP2Cb	6	PSTP		
Protein-serine phosphatase 2C - catalytic subunit - delta isoform	PP2Cd	4	PSTP		
Protein-serine phosphatase 4 - catalytic subunit (PPX/C)	PP4C	16	PSTP	104	75
Protein-serine phosphatase 4 - regulatory subunit (PPX/A'2)	PP4/A'2	18	PSTP		
Protein-serine phosphatase 5 - catalytic subunit (PPT)	PP5C	10	PSTP	400	240
Protein-serine phosphatase 6 - catalytic subunit (PPVC) (27)	PP6C	20	PSTP		
Protein-serine phosphatase 6 - catalytic subunit (PPVC) (30)	PP6C	20	PSTP	1749	713
Protein-tyrosine phosphatase 1B	PTP1B	9	PYP	485	265
Protein-tyrosine phosphatase 1C (SHP1, SHPTP1)	PTP1C	15	PYP	2571	799
Protein-tyrosine phosphatase 1D (SHP2, SHPTP2, Syp, PTP2C)	PTP1D	9	PYP	360	177
Protein-tyrosine phosphatase with PEST sequences (PTPG1, PTPN12)	PTP-PEST	11	PYP	32	
Signal regulatory protein substrate of PTP1D phosphatase (SHPS1)	SIRPa1	3	PYPsub		

Table 2: Kinexus™ phosphatase expression screen K_001, Comparison Report

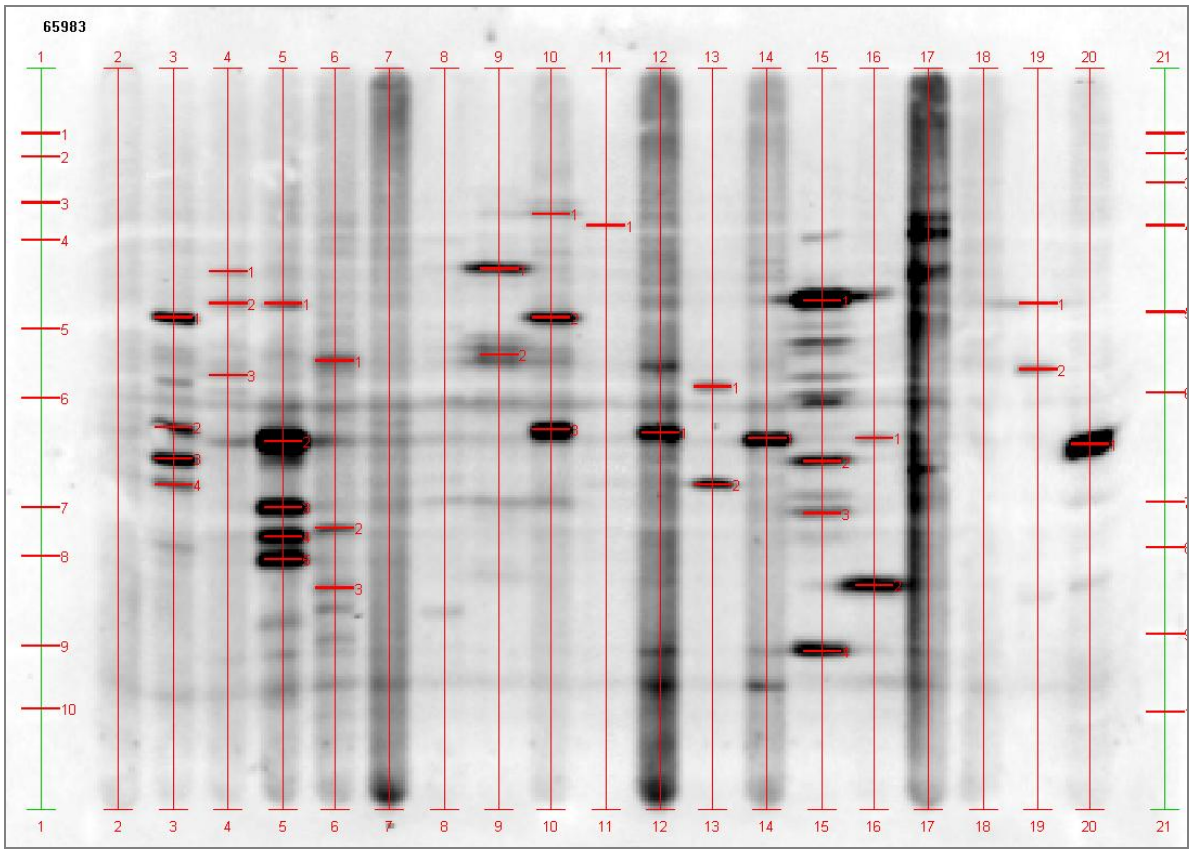
Comparison of the corrected trace quantity of each protein expressed as counts per minute (CPM) in the two samples MV4-11 and MOLM-13. The normalised trace quantity of each band is given. This adjustment is based on the difference in the total signal from the sum of all of the bands on individual immunoblots.

Figure 44. Kinexus™ phosphatase expression screen K_001, multi-immunoblot for MV4-11. Multi-immunoblot of MV4-11 sample with the detected bands **A)** unmarked and **B)** numbered according to lane and number of bands appearing per lane. Lanes 1 and 21 denote molecular weight markers used by Kinexus™. Band 1=201 kDa, Band 2= 156 kDa, Band 3= 106 kDa, Band 4=79 kDa, Band 5=48 kDa, Band 6= 37kDa.

A



B



KINEXUS

KINETWORKS™ PHOSPHATASE 1.2 SCREEN REPORT

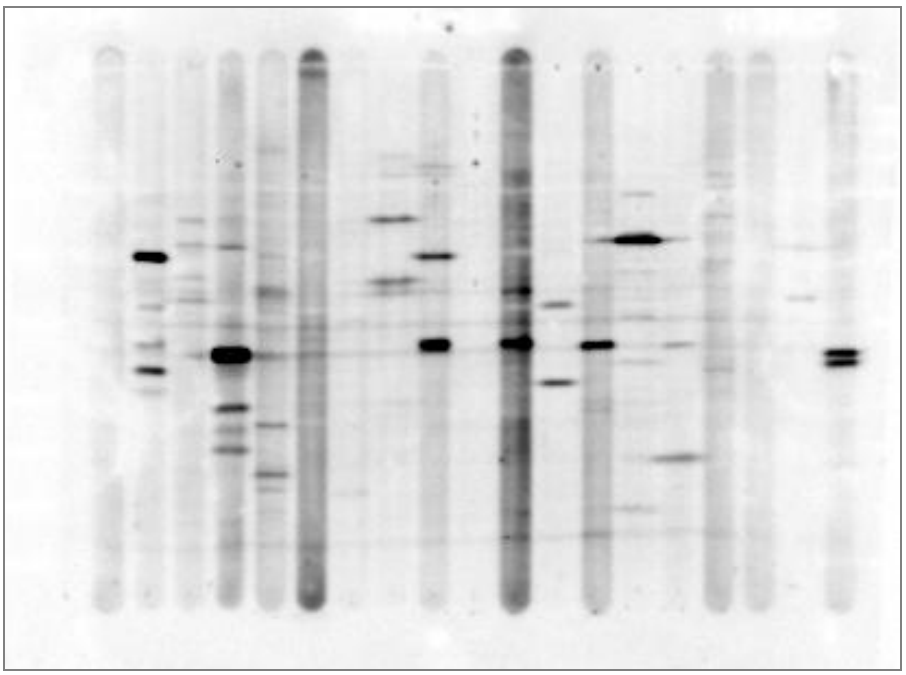
Sample MV411, Order 2431, Feb 22 2011

ScanID	GelType	Lane	Band	ProteinName	Abbrev	Type	~MW	Rel. Qty	Trace Qty	CPM
65983	KPPS-1.2	3	1	Protein-serine phosphatase 2A - A regulatory subunit - alpha and beta isoforms	PP2A/Aa/b	PSTP	51	22.7	2509	470
65983	KPPS-1.2	3	2	Unclassified	-	-	33	10.7	1181	221
65983	KPPS-1.2	3	3	Unclassified	-	-	29	25.5	2820	529
65983	KPPS-1.2	3	4	Unclassified	-	-	26	6.9	760	143
65983	KPPS-1.2	4	1	Unclassified	-	-	66	5.8	298	56
65983	KPPS-1.2	4	2	Protein-serine phosphatase 2B - catalytic subunit - alpha isoform	PP2B/Aa	PSTYP	55	12.0	616	115
65983	KPPS-1.2	4	3	Unclassified	-	-	41	6.7	343	64
65983	KPPS-1.2	5	1	Unclassified	-	-	55	1.8	679	127
65983	KPPS-1.2	5	2	Protein-serine phosphatase 2A - catalytic subunit alpha isoform	PP2A/Ca	PSTP	31	60.0	22424	4205
65983	KPPS-1.2	5	3	Unclassified	-	-	23	12.3	4611	865
65983	KPPS-1.2	5	4	Unclassified	-	-	20	6.1	2269	425
65983	KPPS-1.2	5	5	Unclassified	-	-	18	8.2	3077	577
65983	KPPS-1.2	6	1	Protein-serine phosphatase 2C - catalytic subunit - alpha isoform	PP2Ca	PSTP	43	16.7	1095	205
65983	KPPS-1.2	6	2	Unclassified	-	-	21	11.9	780	146
65983	KPPS-1.2	6	3	Unclassified	-	-	17	5.2	342	64
65983	KPPS-1.2	9	1	Protein-tyrosine phosphatase 1D (SHP2, SHPTP2, Syp, PTP2C)	PTP1D	PYP	65	23.0	1921	360
65983	KPPS-1.2	9	2	Protein-tyrosine phosphatase 1B	PTP1B	PYP	43	31.0	2589	485
65983	KPPS-1.2	10	1	Unclassified	-	-	91	4.8	583	109
65983	KPPS-1.2	10	2	Protein-serine phosphatase 5 - catalytic subunit (PPT)	PP5C	PSTP	49	17.7	2135	400
65983	KPPS-1.2	10	3	Protein-serine phosphatase 1 - catalytic subunit - alpha isoform	PP1/Ca	PSTP	32	40.2	4853	910
65983	KPPS-1.2	11	1	Protein-tyrosine phosphatase with PEST sequences (PTPG1, PTPN12)	PTP-PEST	PYP	84	6.5	169	32
65983	KPPS-1.2	12	1	Protein-serine phosphatase 1 - catalytic subunit - beta isoform	PP1/Cb	PSTP	32	20.8	3285	616
65983	KPPS-1.2	13	1	MAP kinase phosphatase 2 (VH2)	MKP2	PTYP	39	17.2	625	117
65983	KPPS-1.2	13	2	Unclassified	-	-	25	47.3	1716	322
65983	KPPS-1.2	14	1	Protein-serine phosphatase 1 - catalytic subunit - gamma isoform	PP1/Cg	PSTP	31	34.5	3696	693
65983	KPPS-1.2	15	1	Protein-tyrosine phosphatase 1C (SHP1, SHPTP1)	PTP1C	PYP	53	52.3	13711	2571
65983	KPPS-1.2	15	2	Unclassified	-	-	28	6.3	1659	311
65983	KPPS-1.2	15	3	Unclassified	-	-	22	3.7	961	180
65983	KPPS-1.2	15	4	Unclassified	-	-	13	10.4	2738	513
65983	KPPS-1.2	16	1	Protein-serine phosphatase 4 - catalytic subunit (PPX/C)	PP4C	PSTP	31	6.3	555	104
65983	KPPS-1.2	16	2	Dual specificity protein phosphatase 3	VHR	PYP	16	37.6	3319	622
65983	KPPS-1.2	19	1	Phosphatidylinositol-3,4,5-trisphosphate 3-phosphatase deleted on chromosome 10	PTEN	PSTYP	51	9.2	269	50
65983	KPPS-1.2	19	2	Unclassified	-	-	41	26.0	762	143
65983	KPPS-1.2	20	1	Protein-serine phosphatase 6 - catalytic subunit (PPVC) (30)	PP6C	PSTP	30	75.3	9327	1749

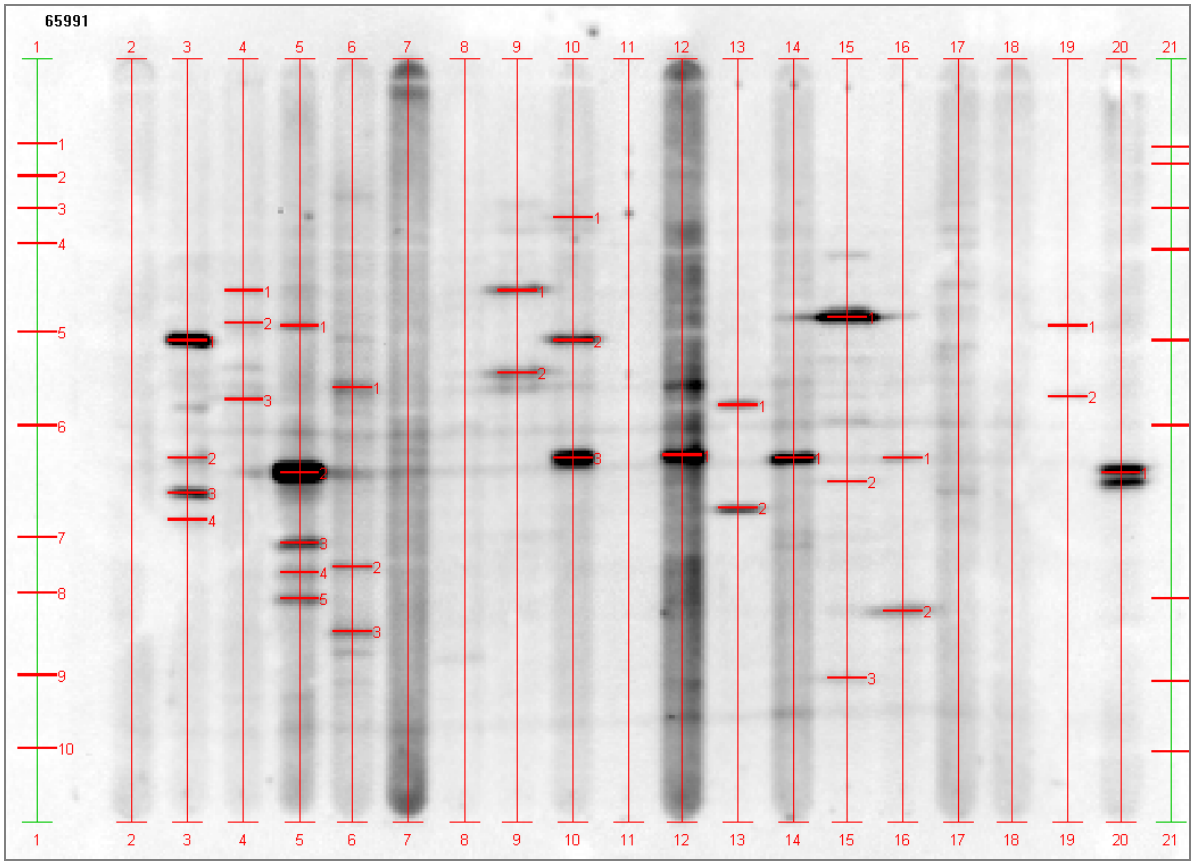
Table 3. Kinexus™ phosphatase expression screen K_001, sample report for MV4-11. Quantitative information regarding band intensities with reference to the immunoblot in Figure 44B, including the identities of all the target proteins identified as numbered bands, the estimated molecular mass for each numbered band, the relative quantity of the band expressed as a percentage of the total intensity of data in the lane in which the band appears, the trace quantity of each band taken to be the area under the band's intensity profile curve, the corrected trace quantity of each band expressed as counts per minute (cpm).

Figure 45. Kinexus™ phosphatase expression screen K_001, multi-immunoblot for MOLM-13. Multi-immunoblot of MOLM-13 sample with the detected bands **A)** unmarked and **B)** numbered according to lane and number of bands appearing per lane. Lanes 1 and 21 denote molecular weight markers used by Kinexus™. Band 1=201 kDa, Band 2= 156 kDa, Band 3= 106 kDa, Band 4=79 kDa, Band 5=48 kDa, Band 6= 37kDa.

A



B



KINEXUS

KINETWORKS™ PHOSPHATASE 1.2 SCREEN REPORT

Sample MOLM-13, Order 2431, Feb 22 2011

ScanID	GelType	Lane	Band	ProteinName	Abbrev	Type	~MW	Rel. Qty	Trace Qty	CPM
65991	KPPS-1.2	3	1	Protein-serine phosphatase 2A - A regulatory subunit - alpha and beta isoforms	PP2A/Aa/b	PSTP	47	53.5	4186	785
65991	KPPS-1.2	3	2	Unclassified	-	-	33	6.8	536	100
65991	KPPS-1.2	3	3	Unclassified	-	-	29	16.3	1278	240
65991	KPPS-1.2	3	4	Unclassified	-	-	26	2.6	207	39
65991	KPPS-1.2	4	1	Unclassified	-	-	62	6.9	214	40
65991	KPPS-1.2	4	2	Protein-serine phosphatase 2B - catalytic subunit - alpha isoform	PP2B/Aa	PSTYP	51	12.3	382	72
65991	KPPS-1.2	4	3	Unclassified	-	-	41	9.3	290	54
65991	KPPS-1.2	5	1	Unclassified	-	-	51	1.8	413	77
65991	KPPS-1.2	5	2	Protein-serine phosphatase 2A - catalytic subunit alpha isoform	PP2A/Ca	PSTP	32	67.4	15092	2830
65991	KPPS-1.2	5	3	Unclassified	-	-	24	4.8	1084	203
65991	KPPS-1.2	5	4	Unclassified	-	-	21	1.5	330	62
65991	KPPS-1.2	5	5	Unclassified	-	-	19	2.7	604	113
65991	KPPS-1.2	6	1	Protein-serine phosphatase 2C - catalytic subunit - alpha isoform	PP2Ca	PSTP	42	17.6	871	163
65991	KPPS-1.2	6	2	Unclassified	-	-	22	9.0	447	84
65991	KPPS-1.2	6	3	Unclassified	-	-	17	11.0	542	102
65991	KPPS-1.2	9	1	Protein-tyrosine phosphatase 1D (SHP2, SHPTP2, Syp, PTP2C)	PTP1D	PYP	62	24.6	942	177
65991	KPPS-1.2	9	2	Protein-tyrosine phosphatase 1B	PTP1B	PYP	44	36.9	1414	265
65991	KPPS-1.2	10	1	Unclassified	-	-	99	4.8	354	66
65991	KPPS-1.2	10	2	Protein-serine phosphatase 5 - catalytic subunit (PPT)	PP5C	PSTP	48	17.5	1279	240
65991	KPPS-1.2	10	3	Protein-serine phosphatase 1 - catalytic subunit - alpha isoform	PP1/Ca	PSTP	34	50.8	3705	695
65991	KPPS-1.2	12	1	Protein-serine phosphatase 1 - catalytic subunit - beta isoform	PP1/Cb	PSTP	34	22.1	2468	463
65991	KPPS-1.2	13	1	MAP kinase phosphatase 2 (VH2)	MKP2	PTYP	40	24.8	628	118
65991	KPPS-1.2	13	2	Unclassified	-	-	29	41.0	1042	195
65991	KPPS-1.2	14	1	Protein-serine phosphatase 1 - catalytic subunit - gamma isoform	PP1/Cg	PSTP	34	33.7	2202	413
65991	KPPS-1.2	15	1	Protein-tyrosine phosphatase 1C (SHP1, SHPTP1)	PTP1C	PYP	54	56.4	4261	799
65991	KPPS-1.2	15	2	Unclassified	-	-	32	2.6	200	37
65991	KPPS-1.2	15	3	Unclassified	-	-	17	4.5	339	64
65991	KPPS-1.2	16	1	Protein-serine phosphatase 4 - catalytic subunit (PPX/C)	PP4C	PSTP	34	13.3	402	75
65991	KPPS-1.2	16	2	Dual specificity protein phosphatase 3	VHR	PYP	21	27.1	821	154
65991	KPPS-1.2	19	1	Phosphatidylinositol-3,4,5-trisphosphate 3-phosphatase deleted on chromosome 10	PTEN	PSTYP	52	9.3	137	26
65991	KPPS-1.2	19	2	Unclassified	-	-	41	15.6	230	43
65991	KPPS-1.2	20	1	Protein-serine phosphatase 6 - catalytic subunit (PPVC) (30)	PP6C	PSTP	33	54.8	3801	713

Table 4. Kinexus™ phosphatase expression screen K_001, sample report for MOLM-13. Quantitative information regarding band intensities with reference to the immunoblot in Figure 45B, including the identities of all the target proteins identified as numbered bands, the estimated molecular mass for each numbered band, the relative quantity of the band expressed as a percentage of the total intensity of data in the lane in which the band appears, the trace quantity of each band taken to be the area under the band's intensity profile curve, the corrected trace quantity of each band expressed as counts per minute (cpm).

Effects of FLT3-ITD inhibition on phosphatase expression in MOLM-13 cells

To determine whether the expression of any of the phosphatases detected in MOLM-13 cells are subject to regulation by FLT3-ITD, a second phosphatase expression screen was carried out to compare the phosphatase profiles of untreated MOLM-13 cells compared to those treated with 250 nM PKC412 for 24 hours (K_002, Figure 46, 47, 48 and Table 5, 6 and 7). Inhibition of FLT3-ITD signalling resulted in alterations to most of the phosphatases detected and both increases and decreases in expression could be observed, suggesting that FLT3-ITD may negatively regulate the expression of some phosphatases and have a positive influence on others. Kinexus™ note that a change of >25% may be considered a real change.

Interestingly, many of the differences observed in phosphatase expression between MV4-11 cells and MOLM-13 cells, were reflected in the changes which occurred in MOLM-13 cells when treated with PKC412. As MV4-11 cells are homozygous for the FLT3-ITD mutation and MOLM-13 cells are heterozygous, there is likely to be decreased FLT3-ITD signalling in MOLM-13 cells, a situation analogous to the comparison of untreated MOLM-13 cells and those treated with PKC412. Many of the phosphatases displayed decreased expression upon FLT3-ITD inhibition, suggesting that there may be a common transcription factor under the control of FLT3-ITD. A decrease in phosphatase expression upon FLT3-ITD inhibition was not interpreted as being definitive evidence of a positive regulation, as it is possible that subsequent FLT3-driven post-translational modifications actually determine the activity of the enzyme. Upregulation of a range of proteins is likely to occur downstream of oncogenic FLT3 signalling, as FLT3-ITD is known to

influence several myeloid transcription factors such as PU.1 (Rosenbauer *et al.*, 2004)and C/EBPα (Radomska *et al.*, 2006) as well as STAT5 (Choudhary *et al.*, 2007) and FOXO (Takahashi, 2011). Not all of the upregulated proteins would necessarily contribute to the FLT3-ITD signalling pathway, it could be argued that thriving FLT3-ITD tumour cells are the ones in which upregulation of inhibitory phosphatases, occurring as a consequence of aberrant transcription factor activity, has been ameliorated to some extent by extensive negative regulation of the phosphatase proteins at the level of post-translational modifications. It is also possible that the expressed proteins are the non-functional products of mutated genes and neither represent an aid nor a threat to the FLT3-ITD signalling pathway, but again are simply by-products of increased transcription factor activity.

This profiling screened for only 30 phosphatases, of which 14 were not expressed in MOLM-13 cells. Of the 16 which were expressed, 9 were classified as serine/threonine phosphatases (PSTP), so the scope for examination of expression of classical tyrosine phosphatases (PYP) or dual specificity phosphatases (PSTYP or PTYP) became quite limited.

When deciding which phosphatases to progress with PTEN, SHP-2, PTP1B, VHR, MKP2, PP2B/Aa and SHP-1 were considered. The levels of PTEN appeared to be quite low in MOLM-13 cells as detected by the Kinexus**™** expression screen (Figure 47, Table 6) prompting concerns for the detection of this protein using conventional western blotting. It was recently reported by Godfrey *et al*. (2012) that PTEN is not oxidised downstream of FLT3-ITD in AML cells, reinforcing our evidence that in MOLM-13 cells PTEN appears to be regulated by FLT3 at the level of protein expression, though as this gene is frequently mutated in tumours it is

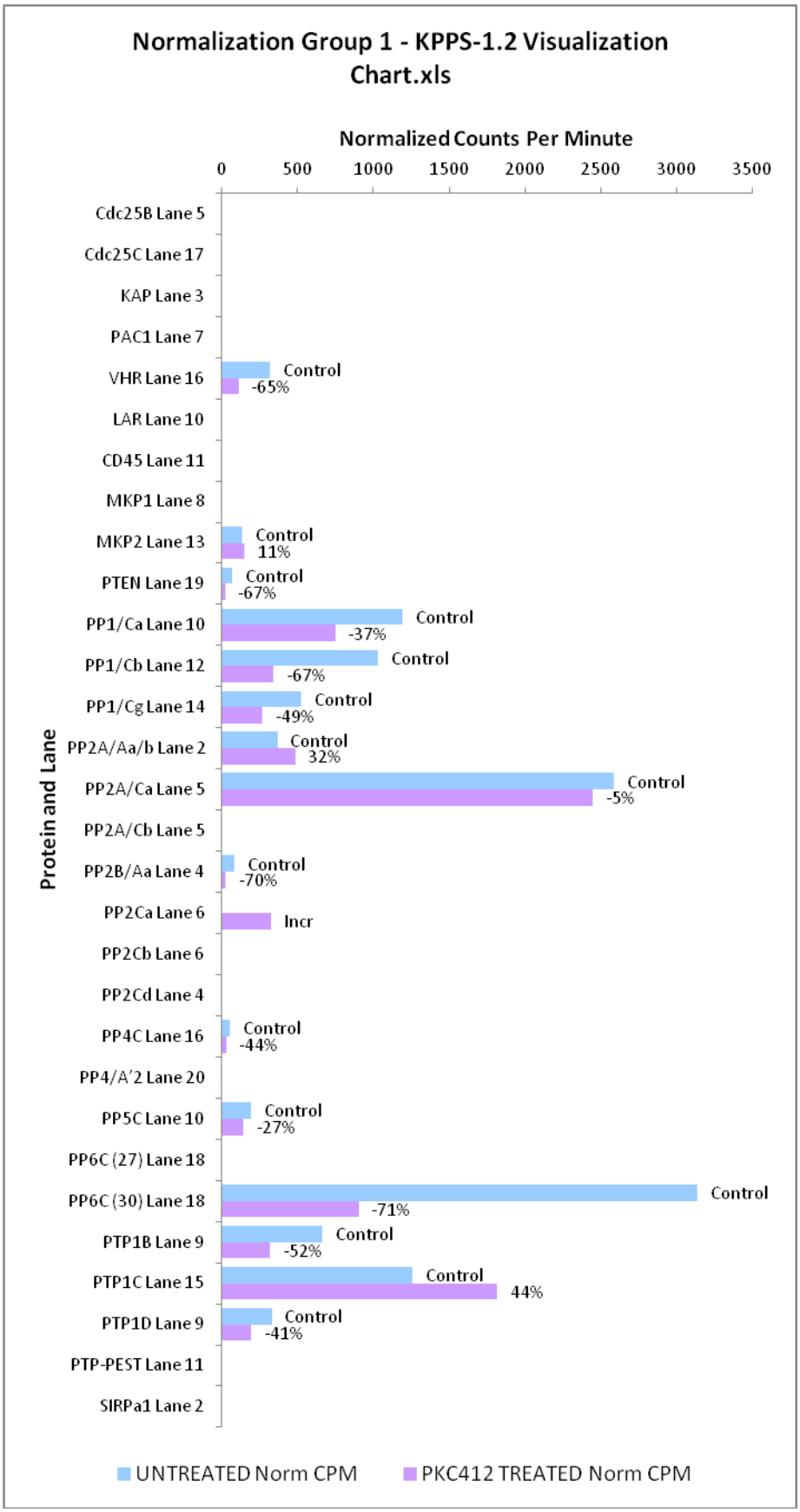
possible that the expression detected here may be of a dysfunctional mutant PTEN. As the mechanisms of regulation of PTEN expression are quite well elucidated, as is its role in leukemogenesis prevention (Zhang *et al.*, 2006; Yilmaz *et al.*, 2006), and it was decided that focusing on this phosphatase would not contribute the required element of novelty.

SHP-2 was also discounted from further study as its involvement in leukaemia and the FLT3-ITD signalling pathway in particular have been well documented recently (Nabinger and Chan, 2012; Muller *et al.*, 2008b). Of the remaining PTPs the two with the highest expression in untreated MOLM-13 cells as determined by the Kinexus™ screen, were chosen to ensure detection using conventional western blotting, PTP1B and SHP-1. These phosphatases were also selected because they represented opposing consequences of regulation downstream of FLT3-ITD. PTP1B expression decreased upon FLT3-ITD inhibition whereas the expression of SHP-1 increased.

It was also decided at this point to include two serine/threonine phosphatases for comparison. PP6C was selected due its high levels of expression in MOLM-13 cells, which decreased dramatically by 71% upon PKC412 treatment. PP2Cα was also an intriguing target as it appeared to be unexpressed in the untreated MOLM-13 cells yet its expression was induced upon FLT3-ITD inhibition.

Figure 46. Kinexus™ phosphatase expression screen K_002.

Histogram represents the results of the multi-immunoblotting carried out by Kinexus™ Phosphatase Expression Screen KPPS 1.2, to compare the phosphatase expression profiles of MOLM-13 cells which were untreated (blue), designated as control sample, and treated with 250 nM PKC412 for 24 hours (purple), designated as test sample. The identification and detection of each of 30 phosphatases (vertical axis) was based on immunoreactivity and apparent molecular mass. The corrected trace quantity of each band is expressed as counts per minute (CPM) (horizontal axis).


Normalization Group 1 - KPPS-1.2 Visualization Chart.xls
Normalized Counts Per Minute
0
500
1000
1500
2000
2500
3000
3500
Protein and Lane
Cdc25B Lane 5
Cdc25C Lane 17
KAP Lane 3
PAC1 Lane 7
VHR Lane 16
Control
-65%
LAR Lane 10
CD45 Lane 11
MKP1 Lane 8
MKP2 Lane 13
Control
11%
PTEN Lane 19
Control
-67%
PP1/Ca Lane 10
Control
-37%
PP1/Cb Lane 12
Control
-67%
PP1/Cg Lane 14
Control
-49%
PP2A/Aa/b Lane 2
Control
32%
PP2A/Ca Lane 5
Control
-5%
PP2A/Cb Lane 5
PP2B/Aa Lane 4
Control
-70%
PP2Ca Lane 6
Incr
PP2Cb Lane 6
PP2Cd Lane 4
PP4C Lane 16
Control
-44%
PP4/A'2 Lane 20
PP5C Lane 10
Control
-27%
PP6C (27) Lane 18
PP6C (30) Lane 18
Control
-71%
PTP1B Lane 9
Control
-52%
PTP1C Lane 15
Control
44%
PTP1D Lane 9
Control
-41%
PTP-PEST Lane 11
SIRPa1 Lane 2
UNTREATED Norm CPM
PKC412 TREATED Norm CPM

KINETWORKS™ KPPS-1.2-HUMAN COMPARISON REPORT

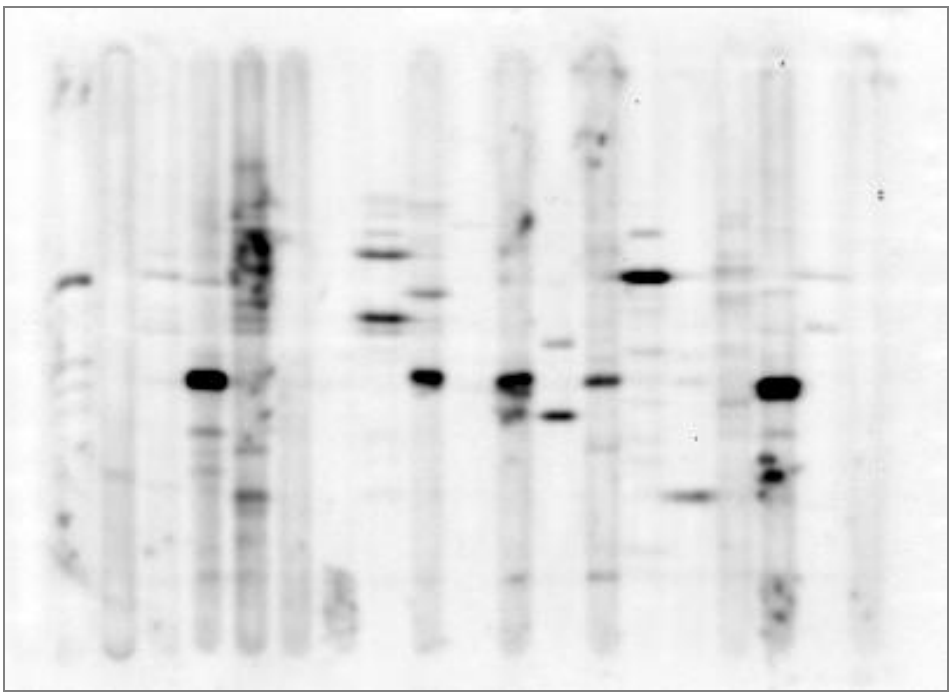
Normalized Data Comparison Of Normalized Counts per Minute For the Following Samples			Kinexus ID	16271	16272
			Scan ID	67535	67543
			Sample Name	UNTREATED	PKC412 TREATED
			Normalization	1	1
FULL NAME OF PROTEIN	ABBREV	LANE	TYPE	NORMALIZED C.P.M.	
Cell division cycle 25B phosphatase	Cdc25B	5	PSTYP		
Cell division cycle 25C phosphatase	Cdc25C	17	PSTYP		
Cyclin-dependent kinase associated phosphatase (CDK inhibitor 3, CIP2)	KAP	3	PSYP		
Dual specificity MAP kinase protein phosphatase	PAC1	7	PTYP		
Dual specificity protein phosphatase 3	VHR	16	PYP	316	110
LCA antigen-related (LAR) receptor tyrosine phosphatase	LAR	10	PYP		
Leukocyte common antigen CD45 receptor-tyrosine phosphatase (LCA, T200)	CD45	11	PYP		
MAP kinase phosphatase 1 (CL100, VH1)	MKP1	8	PTYP		
MAP kinase phosphatase 2 (VH2)	MKP2	13	PTYP	134	149
Phosphatidylinositol-3,4,5-trisphosphate 3-phosphatase deleted on chromosome 10	PTEN	19	PSTYP	67	22
Protein-serine phosphatase 1 - catalytic subunit - alpha isoform	PP1/Ca	10	PSTP	1191	749
Protein-serine phosphatase 1 - catalytic subunit - beta isoform	PP1/Cb	12	PSTP	1029	343
Protein-serine phosphatase 1 - catalytic subunit - gamma isoform	PP1/Cg	14	PSTP	525	266
Protein-serine phosphatase 2A - A regulatory subunit - alpha and beta isoforms	PP2A/Aa/b	2	PSTP	365	483
Protein-serine phosphatase 2A - catalytic subunit alpha isoform	PP2A/Ca	5	PSTP	2586	2444
Protein-serine phosphatase 2A - catalytic subunit beta isoform	PP2A/Cb	5	PSTP		
Protein-serine phosphatase 2B - catalytic subunit - alpha isoform	PP2B/Aa	4	PSTYP	83	25
Protein-serine phosphatase 2C - catalytic subunit - alpha isoform	PP2Ca	6	PSTP		321
Protein-serine phosphatase 2C - catalytic subunit - beta isoform	PP2Cb	6	PSTP		
Protein-serine phosphatase 2C - catalytic subunit - delta isoform	PP2Cd	4	PSTP		
Protein-serine phosphatase 4 - catalytic subunit (PPX/C)	PP4C	16	PSTP	54	30
Protein-serine phosphatase 4 - regulatory subunit (PPX/A'2)	PP4/A'2	20	PSTP		
Protein-serine phosphatase 5 - catalytic subunit (PPT)	PP5C	10	PSTP	194	142
Protein-serine phosphatase 6 - catalytic subunit (PPVC) (27)	PP6C	18	PSTP		
Protein-serine phosphatase 6 - catalytic subunit (PPVC) (30)	PP6C	18	PSTP	3136	904
Protein-tyrosine phosphatase 1B	PTP1B	9	PYP	665	320
Protein-tyrosine phosphatase 1C (SHP1, SHPTP1)	PTP1C	15	PYP	1258	1812
Protein-tyrosine phosphatase 1D (SHP2, SHPTP2, Syp, PTP2C)	PTP1D	9	PYP	328	195
Protein-tyrosine phosphatase with PEST sequences (PTPG1, PTPN12)	PTP-PEST	11	PYP		
Signal regulatory protein substrate of PTP1D phosphatase (SHPS1)	SIRPa1	2	PYPsub		

Table 5: Kinexus™ phosphatase expression screen K_002, Comparison Report

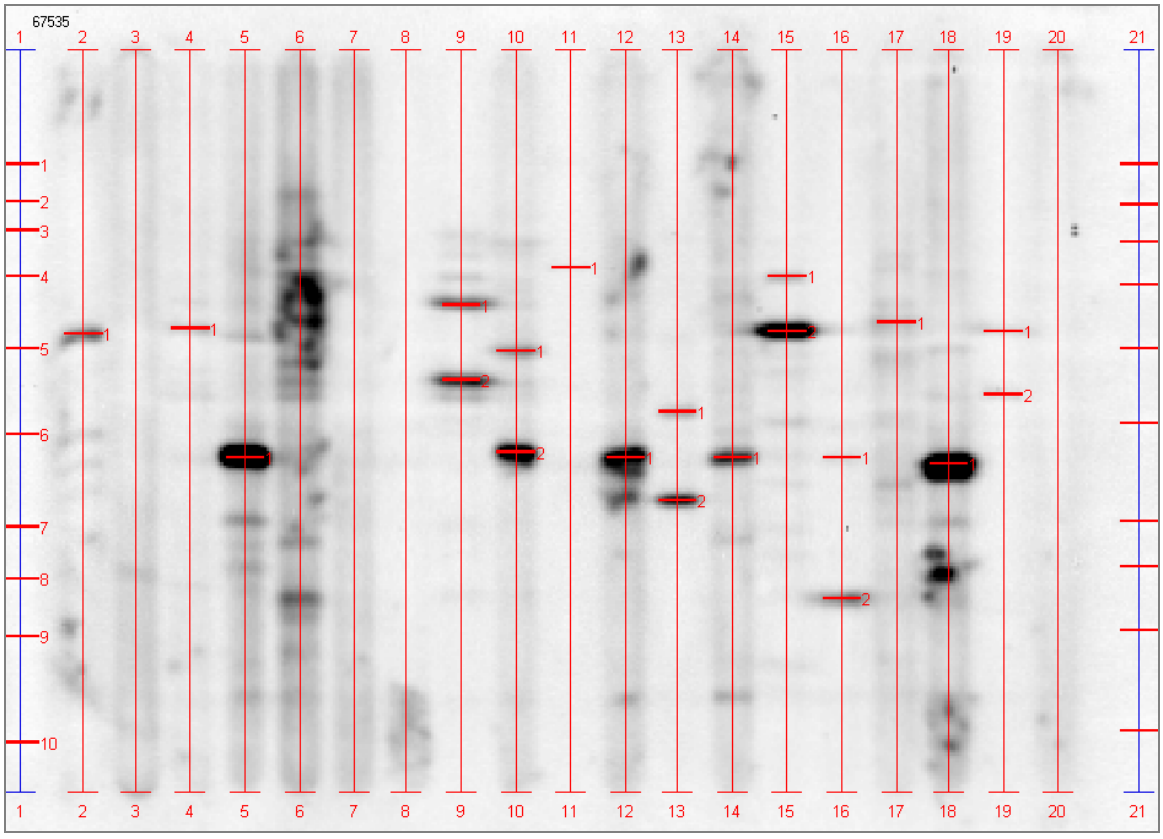
Comparison of the corrected trace quantity of each protein expressed as counts per minute (CPM) in the two samples of MOLM-13 cells untreated and treated with 250 nM PKC412 for 24 hours. The normalised trace quantity of each band is given. This adjustment is based on the difference in the total signal from the sum of all of the bands on individual immunoblots.

Figure 47. Kinexus phosphatase expression screen K_002, Multi-Immunoblot for untreated MOLM-13 sample. Multi-immunoblot of untreated MOLM-13 sample with the detected bands **A)** unmarked and **B)** numbered according to lane and number of bands appearing per lane. Lanes 1 and 21 denote molecular weight markers used by Kinexus™. Band 1=201 kDa, Band 2= 156 kDa, Band 3= 106 kDa, Band 4=79 kDa, Band 5=48 kDa, Band 6= 37kDa.

A



B



KINEXUS

KINETWORKS™ PHOSPHATASE 1.2 SCREEN REPORT

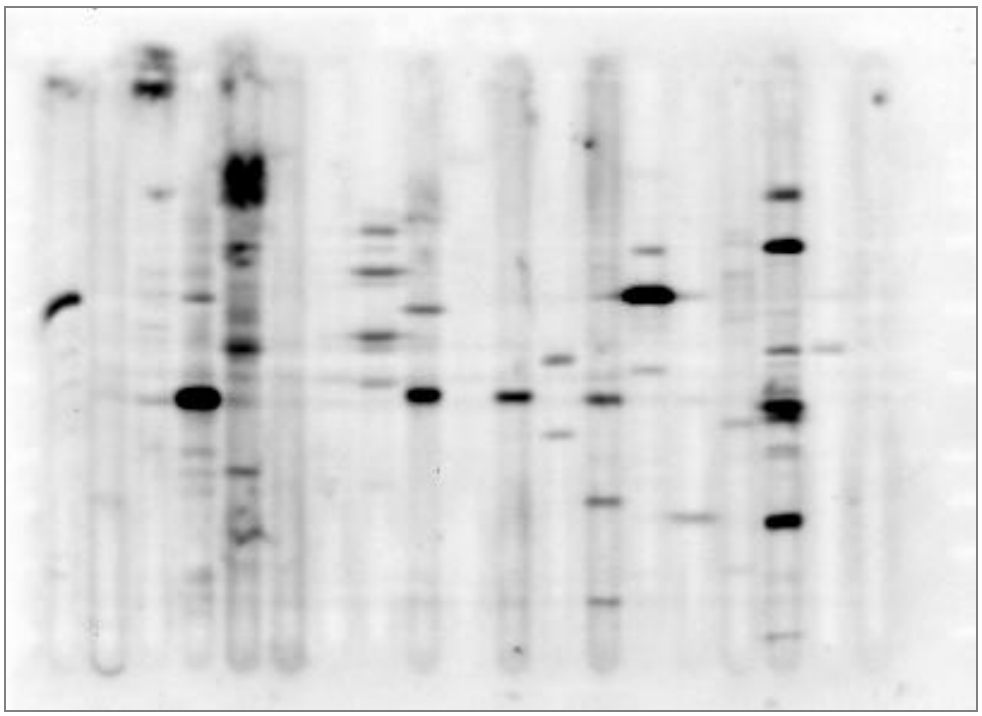
Sample UNTREATED, Order 2676, May 8 2012

ScanID	GelType	Lane	Band	ProteinName	Abbrev	Type	~MW	Rel. Qty	Trace Qty	CPM	Norm. CPM
67535	KPPS-1.2	2	1	Protein-serine phosphatase 2A - A regulatory subunit - alpha and beta isoforms	PP2A/Aa/b	PSTP	53	20.3	1505	282	365
67535	KPPS-1.2	4	1	Protein-serine phosphatase 2B - catalytic subunit - alpha isoform	PP2B/Aa	PSTYP	56	15.4	344	64	83
67535	KPPS-1.2	5	1	Protein-serine phosphatase 2A - catalytic subunit alpha isoform	PP2A/Ca	PSTP	33	54.8	10661	1999	2586
67535	KPPS-1.2	9	1	Protein-tyrosine phosphatase 1D (SHP2, SHPTP2, Syp, PTP2C)	PTP1D	PYP	66	24.2	1354	254	328
67535	KPPS-1.2	9	2	Protein-tyrosine phosphatase 1B	PTP1B	PYP	44	48.9	2742	514	665
67535	KPPS-1.2	10	1	Protein-serine phosphatase 5 - catalytic subunit (PPT)	PP5C	PSTP	48	10.1	801	150	194
67535	KPPS-1.2	10	2	Protein-serine phosphatase 1 - catalytic subunit - alpha isoform	PP1/Ca	PSTP	34	62.0	4911	921	1191
67535	KPPS-1.2	11	1	Unclassified	-	-	87	7.9	77	14	19
67535	KPPS-1.2	12	1	Protein-serine phosphatase 1 - catalytic subunit - beta isoform	PP1/Cb	PSTP	33	47.2	4241	795	1029
67535	KPPS-1.2	13	1	MAP kinase phosphatase 2 (VH2)	MKP2	PTYP	40	14.7	552	103	134
67535	KPPS-1.2	13	2	Unclassified	-	-	26	53.9	2030	381	492
67535	KPPS-1.2	14	1	Protein-serine phosphatase 1 - catalytic subunit - gamma isoform	PP1/Cg	PSTP	32	40.9	2162	405	525
67535	KPPS-1.2	15	1	Unclassified	-	-	83	5.8	427	80	103
67535	KPPS-1.2	15	2	Protein-tyrosine phosphatase 1C (SHP1, SHPTP1)	PTP1C	PYP	55	70.3	5184	972	1258
67535	KPPS-1.2	16	1	Protein-serine phosphatase 4 - catalytic subunit (PPX/C)	PP4C	PSTP	32	8.1	223	42	54
67535	KPPS-1.2	16	2	Dual specificity protein phosphatase 3	VHR	PYP	16	47.5	1303	244	316
67535	KPPS-1.2	17	1	Unclassified	-	-	59	10.5	497	93	121
67535	KPPS-1.2	18	1	Protein-serine phosphatase 6 - catalytic subunit (PPVC) (30)	PP6C	PSTP	31	56.3	12929	2424	3136
67535	KPPS-1.2	19	1	Phosphatidylinositol-3,4,5-trisphosphate 3-phosphatase deleted on chromosome 10	PTEN	PSTYP	55	18.6	277	52	67
67535	KPPS-1.2	19	2	Unclassified	-	-	42	21.1	314	59	76

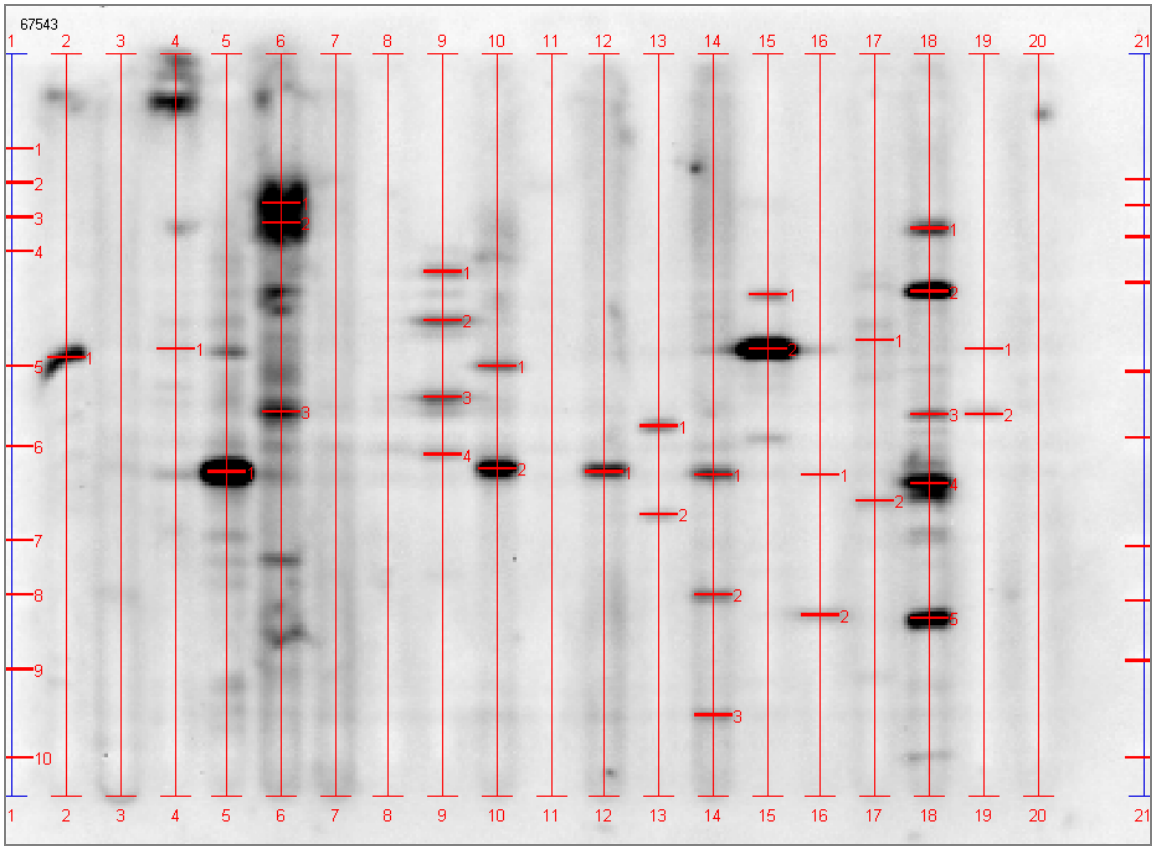
Table 6. Kinexus™ phosphatase expression screen K_002, Sample report for untreated MOLM-13. Quantitative information regarding band intensities with reference to the immunoblot in Figure 47B, including the identities of all the target proteins identified as numbered bands, the estimated molecular mass for each numbered band, the relative quantity of the band expressed as a percentage of the total intensity of data in the lane in which the band appears, the trace quantity of each band taken to be the area under the band's intensity profile curve, the corrected trace quantity of each band expressed as counts per minute (cpm).

Figure 48. Kinexus™ phosphatase expression screen K_002, Multi-Immunoblot for PKC412-treated MOLM-13 sample. Multi-immunoblot of PKC412-treated MOLM-13 sample with the detected bands **A)** unmarked and **B)** numbered according to lane and number of bands appearing per lane. Lanes 1 and 21 denote molecular weight markers used by Kinexus™. Band 1=201 kDa, Band 2= 156 kDa, Band 3= 106 kDa, Band 4=79 kDa, Band 5=48 kDa, Band 6= 37kDa.

A



B



KINEXUS

KINETWORKS™ PHOSPHATASE 1.2 SCREEN REPORT

Sample PKC412 TREATED, Order 2676, May 8 2012

ScanID	GelType	Lane	Band	ProteinName	Abbrev	Type	~MW	Rel. Qty	Trace Qty	CPM	Norm. CPM
67543	KPPS-1.2	2	1	Protein-serine phosphatase 2A - A regulatory subunit - alpha and beta isoforms	PP2A/Aa/b	PSTP	50	50.4	3158	592	483
67543	KPPS-1.2	4	1	Protein-serine phosphatase 2B - catalytic subunit - alpha isoform	PP2B/Aa	PSTYP	52	2.6	164	31	25
67543	KPPS-1.2	5	1	Protein-serine phosphatase 2A - catalytic subunit alpha isoform	PP2A/Ca	PSTP	33	68.4	15993	2999	2444
67543	KPPS-1.2	6	1	Unclassified	-	-	132	25.3	5684	1066	869
67543	KPPS-1.2	6	2	Unclassified	-	-	105	21.1	4730	887	723
67543	KPPS-1.2	6	3	Protein-serine phosphatase 2C - catalytic subunit - alpha isoform	PP2Ca	PSTP	42	9.4	2102	394	321
67543	KPPS-1.2	9	1	Unclassified	-	-	77	13.2	918	172	140
67543	KPPS-1.2	9	2	Protein-tyrosine phosphatase 1D (SHP2, SHPTP2, Syp, PTP2C)	PTP1D	PYP	61	18.3	1274	239	195
67543	KPPS-1.2	9	3	Protein-tyrosine phosphatase 1B	PTP1B	PYP	44	30.0	2091	392	320
67543	KPPS-1.2	9	4	Unclassified	-	-	36	11.0	766	144	117
67543	KPPS-1.2	10	1	Protein-serine phosphatase 5 - catalytic subunit (PPT)	PP5C	PSTP	49	9.0	931	175	142
67543	KPPS-1.2	10	2	Protein-serine phosphatase 1 - catalytic subunit - alpha isoform	PP1/Ca	PSTP	33	47.4	4903	919	749
67543	KPPS-1.2	12	1	Protein-serine phosphatase 1 - catalytic subunit - beta isoform	PP1/Cb	PSTP	33	42.6	2243	421	343
67543	KPPS-1.2	13	1	MAP kinase phosphatase 2 (VH2)	MKP2	PTYP	40	36.1	973	182	149
67543	KPPS-1.2	13	2	Unclassified	-	-	27	18.5	499	94	76
67543	KPPS-1.2	14	1	Protein-serine phosphatase 1 - catalytic subunit - gamma isoform	PP1/Cg	PSTP	32	25.0	1741	326	266
67543	KPPS-1.2	14	2	Unclassified	-	-	18	14.8	1032	193	158
67543	KPPS-1.2	14	3	Unclassified	-	-	11	9.0	627	118	96
67543	KPPS-1.2	15	1	Unclassified	-	-	71	4.5	664	125	102
67543	KPPS-1.2	15	2	Protein-tyrosine phosphatase 1C (SHP1, SHPTP1)	PTP1C	PYP	54	80.1	11861	2224	1812
67543	KPPS-1.2	16	1	Protein-serine phosphatase 4 - catalytic subunit (PPX/C)	PP4C	PSTP	32	8.7	199	37	30
67543	KPPS-1.2	16	2	Dual specificity protein phosphatase 3	VHR	PYP	17	31.4	717	134	110
67543	KPPS-1.2	17	1	Unclassified	-	-	57	7.9	196	37	30
67543	KPPS-1.2	17	2	Unclassified	-	-	29	18.8	467	87	71
67543	KPPS-1.2	18	1	Unclassified	-	-	112	7.8	1754	329	268
67543	KPPS-1.2	18	2	Unclassified	-	-	74	25.7	5792	1086	885
67543	KPPS-1.2	18	3	Unclassified	-	-	41	3.5	784	147	120
67543	KPPS-1.2	18	4	Protein-serine phosphatase 6 - catalytic subunit (PPVC) (30)	PP6C	PSTP	31	26.2	5913	1109	904
67543	KPPS-1.2	18	5	Unclassified	-	-	17	20.1	4541	851	694
67543	KPPS-1.2	19	1	Phosphatidylinositol-3,4,5-trisphosphate 3-phosphatase deleted on chromosome 10	PTEN	PSTYP	55	7.4	147	28	22
67543	KPPS-1.2	19	2	Unclassified	-	-	41	26.7	530	99	81

Table 7. Kinexus™ phosphatase expression screen K_002, Sample report for PKC412-treated MOLM-13. Quantitative information regarding band intensities with reference to the immunoblot in Figure 48B, including the identities of all the target proteins identified as numbered bands, the estimated molecular mass for each numbered band, the relative quantity of the band expressed as a percentage of the total intensity of data in the lane in which the band appears, the trace quantity of each band taken to be the area under the band's intensity profile curve, the corrected trace quantity of each band expressed as counts per minute (cpm).

Effect of FL stimulation on phosphatase expression in HL60 and MOLM-13 cells

While the use of PKC412 demonstrates a role for FLT3-ITD in regulating the expression of the selected phosphatases, it possible that this avenue of the FLT3-ITD signalling pathway overlaps with that of the wild type FLT3 receptor, as has been shown to be the case with regard to Ezrin and Src in previous chapters. To investigate this further, HL60 cells were treated with 50 ng/ml of the FL over a time period of 15 minutes to 24 hours and the expression of PP2Cα, PTP1B, PP6C and SHP-1 were examined by western blotting (Figure 49). Expression of PP2Cα was shown to increase upon PKC412 treatment but did not decrease upon FL stimulation of HL60 cells. PTP1B expression decreased in PKC412 treated cells and increased slightly after 30 minutes of FL stimulation of HL60 cells. PP6C levels decreased dramatically in PKC412 treated MOLM-13 cells but failed to increase in HL60 cells treated with the FL. Expression of SHP-1 increased in MOLM-13 cells upon FLT3-ITD inhibition but did not change in HL60 cells after stimulation with the FL. Therefore, with the exception of PTP1B, the expression of the phosphatases in HL60 cells treated with the FL did not reflect the opposite effects of PKC412 treatment in MOLM-13 cells.

Just as the levels of phosphatase expression in the MOLM-13 and MV4-11 cell lines differed, it is likely that the basal levels of phosphatase expression in HL60 cells are also different to those of MOLM-13 cells and may be a reason why stimulation of HL60 cells with the FL did not result in the changes in phosphatase expression which would be expected if the FLT3 wild type receptor was involved.

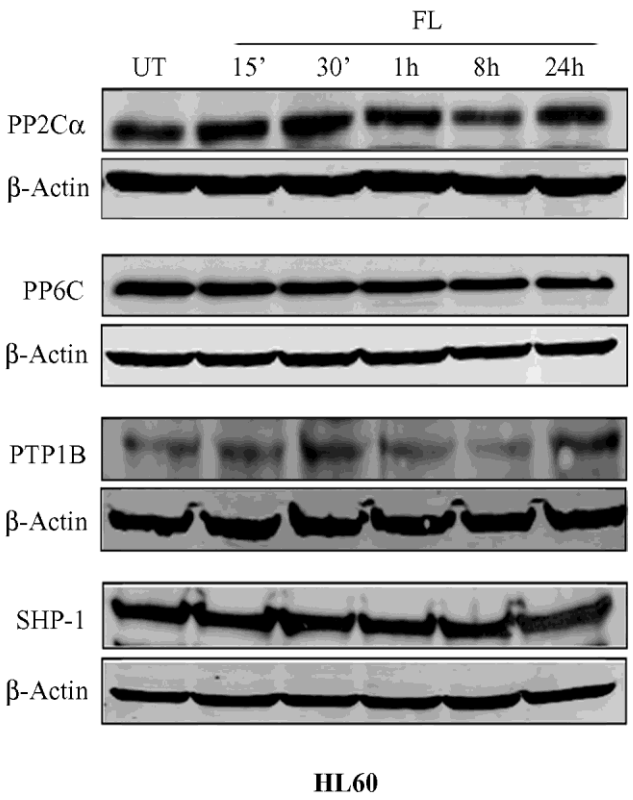


Figure 49. Effect of FLT3 ligand on the expression of phosphatases in HL60 cells. Western blot analyses of PP2Cα, PP6C, PTP1B and SHP-1 in HL60 cells stimulated with 50 ng/ml FL for 15 or 30 minutes or 1, 2, 8 or 24 hours. β-Actin is shown as a loading control.

Therefore, the effects of the FL stimulation on the expression of the selected phosphatases was investigated using the MOLM-13 cells, which are heterozygous for the FLT3 wild type receptor and have been demonstrated in Chapter 4 to respond to ligand stimulation, though understandably not to the same extent as the HL60 cells. However, the FL did not elicit a change in phosphatase expression in MOLM-13 cells (Figure 50), with the exception of PTP1B which, similarly to the result in HL60 cells, did undergo an increase in expression upon 30 minutes of FL stimulation. At this point it was concluded that the expression of PP2Cα, PP6C and SHP-1 are regulated by the FLT3-ITD signalling pathway in MOLM-13 cells, but not as a result of signalling from the wild type receptor. In contrast, expression of PTP1B appears to involve a pathway that is common to both.

Discrepancy in Kinexus™ _002 data

Upon investigating the effect of the FL stimulation on phosphatase expression in MOLM-13 cells, a discrepancy was observed between the levels of PP2Cα observed using conventional western blotting methods and those recorded by Kinexus™ phosphatase expression profiling in screen K_002. As mentioned previously PP2Cα was determined by K_002 to be expressed upon inhibition of FLT3-ITD but was not detected in the untreated MOLM-13 cells. However in Figure 50, expression of PP2Cα protein can clearly be observed in the untreated MOLM-13 cells. This prompted a re-assessment of the levels of PP2Cα expressed in untreated and PKC412-treated MOLM-13 cells. Western blotting revealed that in contrast to the data reported in K_002, PP2Cα expression decreased upon MOLM-13 cell treatment with PKC412 (Figure 51).

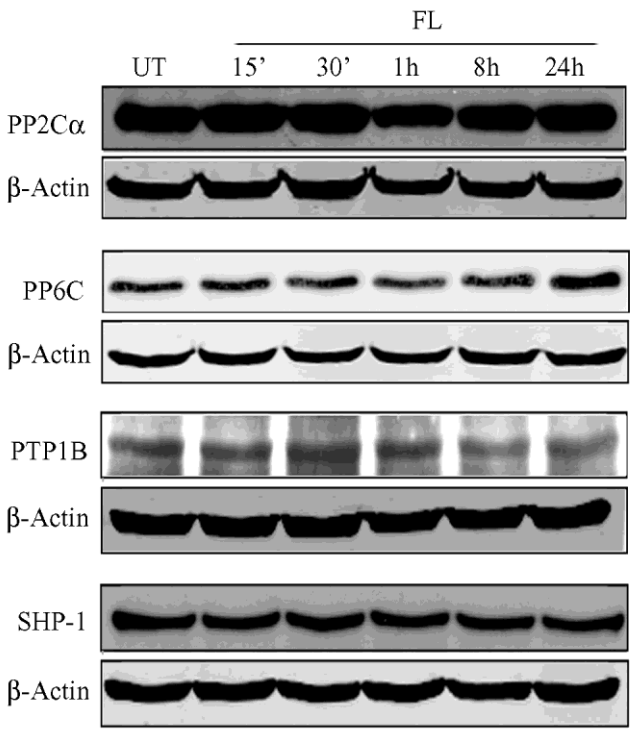


Figure 50. Effect of FLT3 ligand on the expression of phosphatases in MOLM-13 cells. Western blot analyses of PP2Cα, PP6C, PTP1B and SHP-1 in MOLM-13 cells stimulated with 50 ng/ml FL for 15 or 30 minutes or 1, 2, 8 or 24 hours. β-Actin is shown as a loading control.

Densitometric analyses confirmed that this decrease amounted to approximately 30% (Figure 51B). The reason for this anomaly cannot be fully determined; it is possible that the antibody used by Kinexus ™ to detect PP2Cα differed from our own, although this is unlikely to be the root of the problem as expression of PP2Cα can also be observed in both MOLM-13 and MV4-11 cells in K_001. Therefore it appears that there was a problem with this particular screen, perhaps some amount of PP2Cα degradation within the untreated sample.

Confirmation of Kinexus ™ data concerning PP6C, PTP1B and SHP-1

Whatever the reason for this inconsistency was, it caused some concern that the changes in expression reported in K_002 for other phosphatases may not reflect the actual effects of FLT3-ITD inhibition in MOLM-13 cells. Therefore western blotting was carried out to confirm the K_002 data for the selected phosphatases PP6C, PTP1B and SHP-1 (Figure 52). The trends observed in K_002 matched those observed in MOLM-13 cells using conventional western blotting, with both PP6C and PTP1B expression decreasing in PKC412 treated samples, and SHP-1 levels increasing.

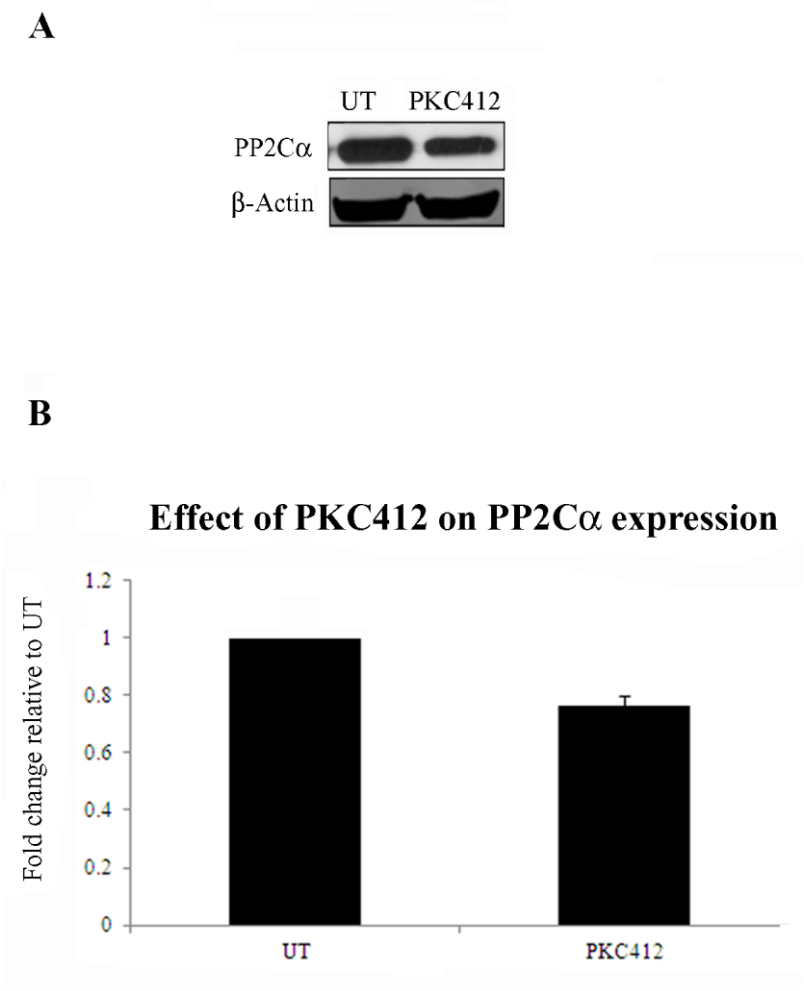


Figure 51: Confirmation of effect of PKC412 on PP2Cα expression in MOLM-13 cells. A) Western blot analysis of PP2Cα in untreated MOLM-13 cells and cells treated with 250 nM PKC412 for 24 hours. β-Actin is shown as a loading control. **B)** Histogram represents the densitometric analysis carried out on three individual biological replicates of MOLM-13 cells treated with 250 nM PKC412 for 24 hours.

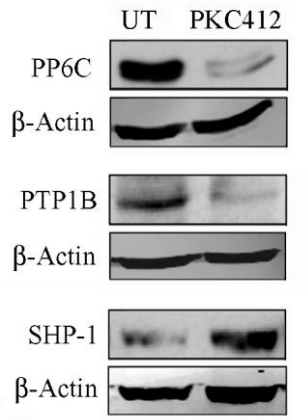


Figure 52. **Validation of K_002 data.**

Western blot analysis of PP6C, PTP1B and SHP-1 in untreated MOLM-13 cells and cells treated with 250 nM PKC412 for 24 hours. β-Actin is shown as a loading control.

FLT3-ITD regulates phosphatase expression at the level of transcription

Having determined that inhibition of FLT3-ITD signalling using PKC412 affects the protein levels of selected phosphatases, it was necessary to clarify whether this regulation was occurring at the level of gene expression, or was directly as a consequence of protein turnover. Quantitative reverse transcriptase polymerase chain reaction (RT-qPCR) was used to determine the whether the amount of mRNA being transcribed from each of the selected phosphatase genes was subject to change depending on FLT3-ITD activity. GAPDH was used as a housekeeping gene, despite being redox-sensitive (Butterfield *et al*., 2010), as no changes to its expression could be observed under the range of redox conditions used in previous western blotting experiments. Therefore it was concluded that GAPDH was stably expressed in our system, and was not sensitive to FLT3-ITD induced redox alterations.

The integrity of the isolated RNA was examined by separation of 500 ng of isolated RNA on a 0.8% Cyber Safe agarose gel. RNA was determined to be of good integrity if distinct, sharp bands for 28s and 18s rRNA were distinguishable, with no additional bands or smearing of the sample (Figure 53A). Amplification of the intended target transcripts, without amplification of secondary non-specific transcripts was confirmed by the appearance of single bands of the appropriate size after the amplification step (Figure 53B).

Quantification of the amplified transcripts revealed that transcription of PP2Cα was significantly decreased in MOLM-13 cells which had been treated with the FLT3-ITD inhibitor PKC412 for 24 hours (Figure 54), corresponding to the decrease in PP2Cα protein expression established in Figure 51. Similarly,

transcription of PP6C was also determined to be significantly decreased in PKC412-treated cells, which again correlated to the decrease in PP6C protein levels as detected by K_002 and confirmed in Figure 52. PTP1B mRNA was reduced in the PKC412-treated sample and although not a significant decrease, did correlate with the decrease in PTP1B protein observed in K_002 and confirmed in Figure 52.

The levels of SHP-1 mRNA also decreased upon PKC412 treatment. However, while the decrease in mRNA observed for the other phosphatases agreed with a decrease in protein in each case, SHP-1 had been shown to increase at the level of protein expression upon FLT3-ITD inhibition (K_002 and Figure 52), suggesting that additional regulation at a post-translational level was being applied which was affecting the rate of SHP-1 protein turnover.

SHP-1 is ubiquitinated downstream of FLT3-ITD

SHP-1 protein levels increased upon inhibition of FLT3-ITD yet its mRNA levels were observed to decrease, implying that although the amount of transcript being produced was positively regulated by FLT3-ITD, the resulting protein was being degraded at a fast rate. The net effect of this multi-layered regulation was lower levels of SHP-1 protein being present in untreated MOLM-13 cells than those in which FLT3-ITD is inhibited.

As SHP-1 is known to function in a tumour suppressive capacity (Wu *et al.*, 2003b), it is possible that upregulation of its transcription as a result of aberrant transcription factor activity, poses a threat to the FLT3-ITD signalling agenda. An increase in SHP-1 protein as a result of increased transcription could be effectively cancelled out by a high rate of SHP-1 degradation, so that the protein produced does not have the

chance to disrupt the oncogenic signals. As discussed in the introduction to this section, covalent addition of ubiquitin moieties is a mechanism of labelling proteins destined for degradation, and examination of the extent of ubiquitination of a particular protein can determine whether it is likely to be subject to proteasomal degradation.

Therefore, SHP-1 was immunoprecipitated from untreated and PKC412-treated MOLM-13 cells and the extent of its ubiquitination was determined using an anti-ubiquitin antibody. Cells were treated with lactacystin, an inhibitor of the proteasome, for duration of the PKC412 treatment, to prevent the degradation of the ubiquitinated SHP-1 and ensure its visualisation. Increased ubiquitination of SHP-1 was observed in the untreated MOLM-13 cells compared to those treated with PKC412 (Figure 55), confirming that although mRNA levels of SHP-1 decrease upon FLT3-ITD inhibition, the rate of SHP-1 turnover is higher when FLT3-ITD is active.

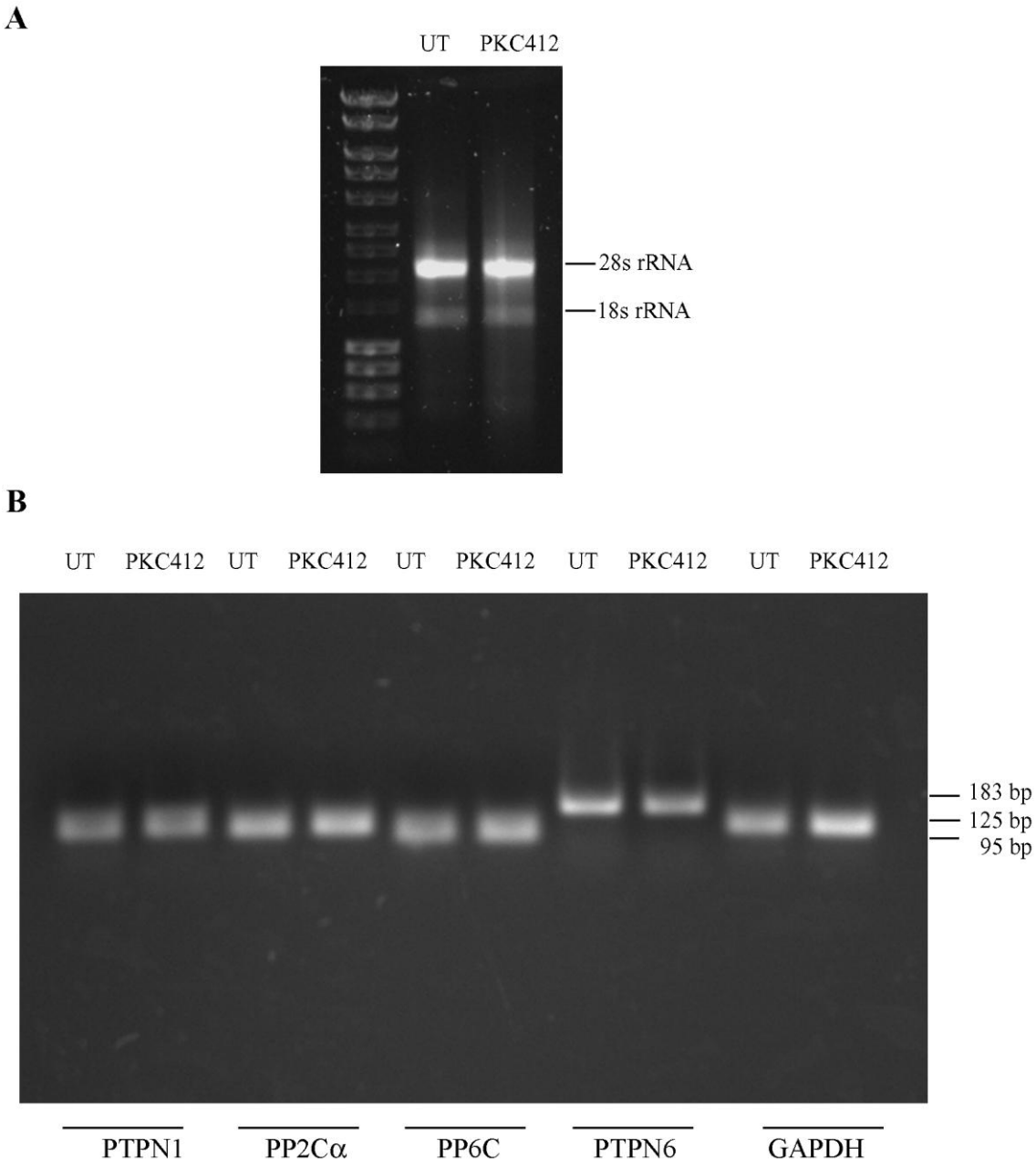


Figure 53: Integrity of RNA and RT-PCR amplification products

A) 500 ng of isolated RNA separated on 0.8% Cyber Safe agarose gel with 28s and 18s rRNA bands indicated. **B)** Amplification of the intended target transcripts, with product sizes indicated.

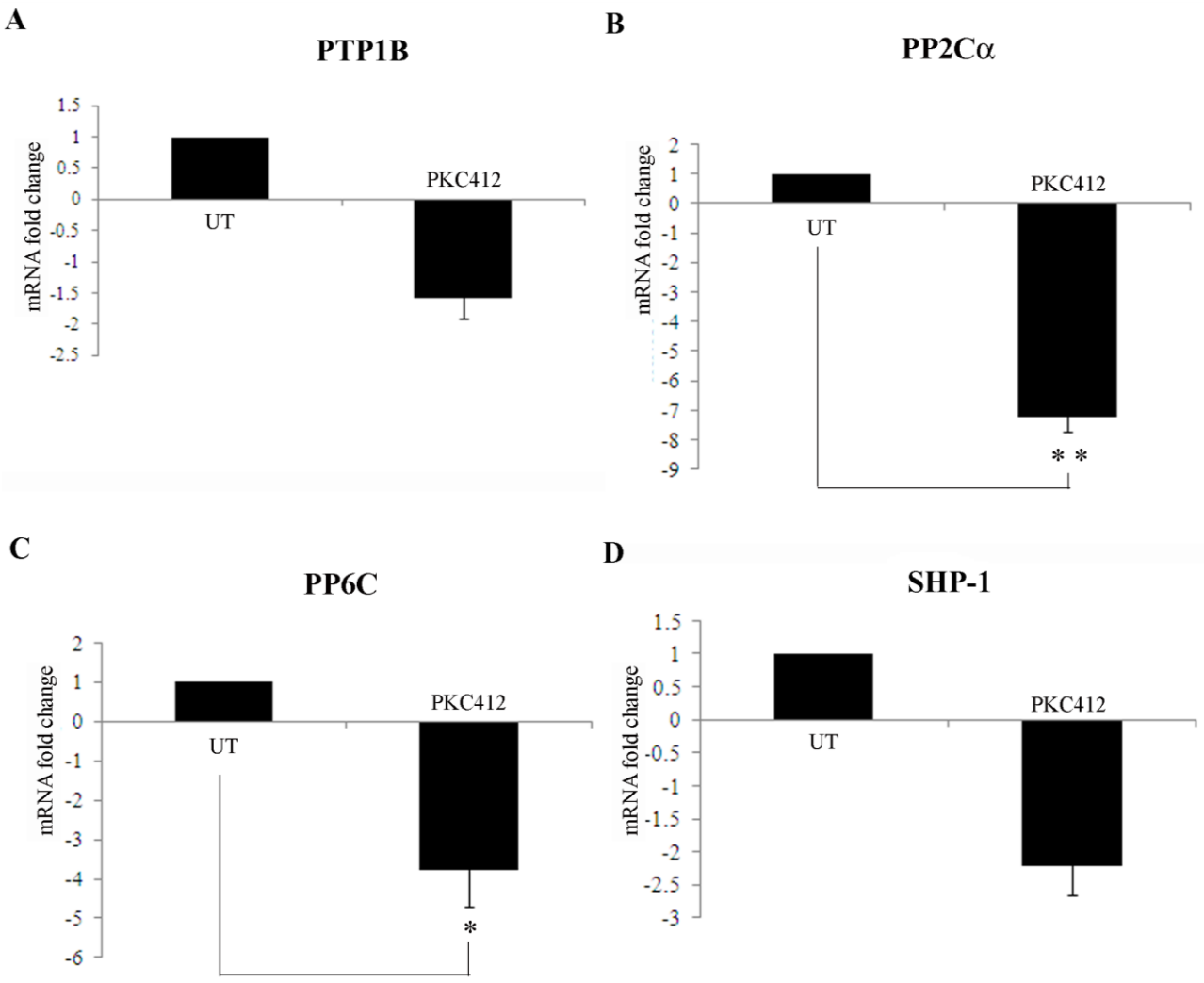


Figure 54. Effect of PKC412 on transcription of phosphatase mRNA in MOLM-13 cells. Histograms represent the mRNA fold change of **A)** PTP1B, **B)** PP2Cα, **C)** PP6C and **D)** SHP-1 as determined by qRT-PCR analysis. Results are expressed as fold change of each transcript relative to GAPDH. Statistical analysis was performed using Student's *t*-test to evaluate the difference between untreated and PKC412-treated samples. Significance was defined at the level of $P<0.05$.

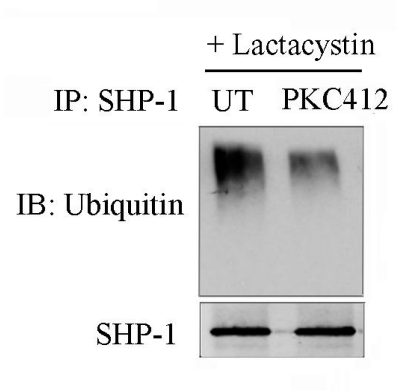


Figure 55. Effect of PKC412 on the ubiquitination of SHP-1 in MOLM-13 cells. Western blot analysis of SHP-1 immunoprecipitated from untreated MOLM-13 cells and cells treated with 250 nM PKC412 for 24 hours and immunoblotted using an anti-ubiquitin antibody. Both samples were treated with 5 μM Lactacystin for 24 hours to inhibit proteasomal degradation of ubiquitinated proteins. Total SHP-1 is shown as a loading control.

Oxidation state of phosphatases downstream of FLT3-ITD

The effect of FLT3-ITD on the transcription and ubiquitination of selected phosphatases shows that the oncogenic receptor dictates the regulation of phosphatases through several mechanisms. A recent study from Godfrey *et al*. (2012) highlighted the selective regulation of PTPs downstream of FLT3-ITD through oxidation and described how PTPs such as DEP-1 appear to be highly expressed in AML cells but are rendered enzymatically inactive through oxidation. With a view to further contributing to the data regarding PTP oxidation downstream of FLT3-ITD, it was decided to utilise a combination of BIAM-labelling of reduced proteins and the Kinexus^{TM} phosphatase expression screen to identify phosphatases which are oxidised in response to FLT3-ITD signalling. The experimental procedure involved the labelling of MOLM-13 cell lysates, untreated and PKC412-treated, with BIAM. The reduced phosphatases became labelled with biotin and were then depleted from the total lysate by incubation in spin columns containing streptavidin conjugated to sepharose beads. In theory, the biotin-depleted flow-through contains phosphatases which are not reduced, i.e. oxidised and by comparing the phosphatase profiles of the depleted untreated and depleted PKC412-treated samples it should be possible to identify phosphatases which are redox regulated as a result of FLT3-ITD activity.

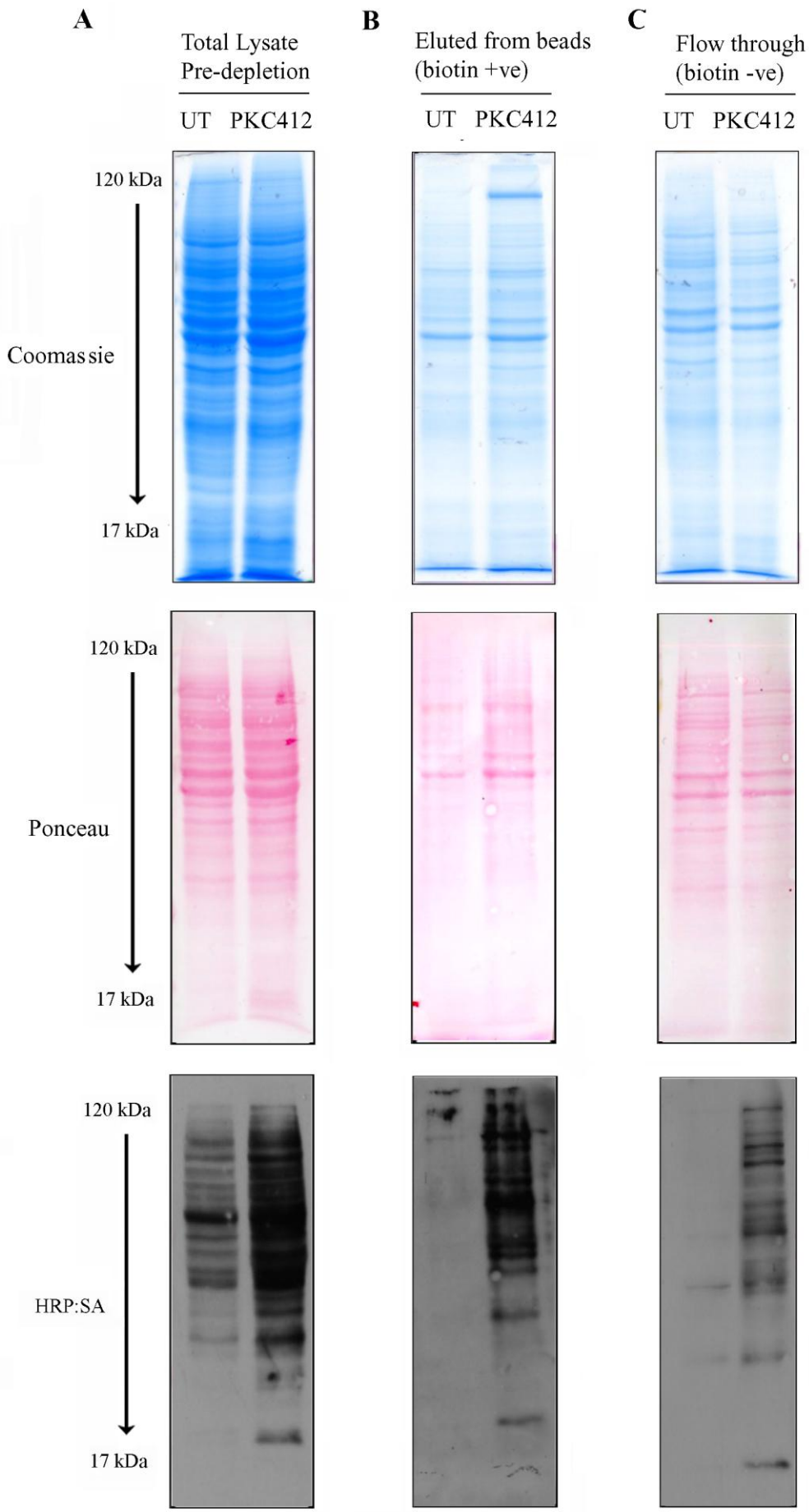
The method required some optimisation, as initial results showed that although there was higher BIAM-labelling in the PKC412 treated samples (Figure 56A, bottom panel) corresponding to a decrease in ROS, the flow-through which should be biotin-negative actually still contained a lot of biotin-labelled protein (Figure 56C, bottom panel). Compared to the flow-through, the fraction of protein

eluted from the streptavidin beads did show increased biotin labelling (Figure 56B, bottom panel), but the fact that so much biotin-labelled protein was escaping capture by the beads meant that there was little discernible difference in protein quantity between the untreated and PKC412-treated samples after depletion (Figure 56C, top panel), despite the increased biotin-labelling of the PKC412-treated sample suggesting that there should be quite an observable contrast.

An increase in the quantity of streptavidin-sepharose beads was shown to affect the amount of biotin-labelled protein which was being retained (Figure 57A), with three times the initial volume of beads finally depleting the flow-through substantially enough to result in a difference in protein yield between the depleted untreated and PKC412-treated samples (Figure 57B). The resulting depleted flow-through samples were used for Kinexus™ phosphatase expression screening K_003.

Figure 56. Preparatory analysis for K_003

Coomassie and Ponceau staining of total protein content and HRP-SA detection of BIAM-labelled (reduced) fraction of **A)** total lysates from untreated MOLM-13 cells and cells treated with 250 nM PKC412 for 24 hours, **B)** lysate eluted from streptavidin-sepharose beads, **C)** lysate flow-through after streptavidin-sepharose bead incubation.


A
Total Lysate
Pre-depletion
UT PKC412
B
Eluted from beads
(biotin +ve)
UT PKC412
C
Flow through
(biotin -ve)
UT PKC412
120 kDa
Coomassie
17 kDa
120 kDa
Ponceau
17 kDa
120 kDa
HRP:SA
17 kDa

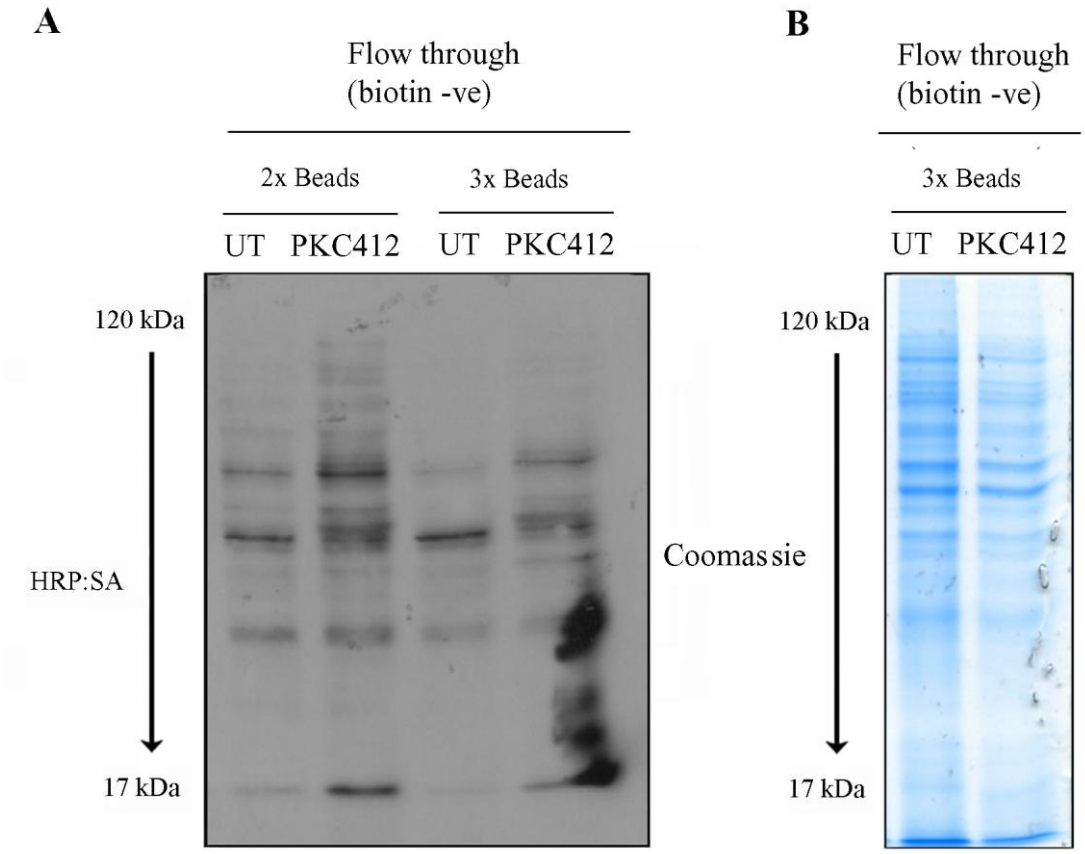


Figure 57. Optimisation of sample preparation for K_003.

A) HRP-SA detection of BIAM-labelled (reduced) fraction of lysate flow-through after incubation with increasing volumes of streptavidin-sepharose beads. **B)** Coomassie staining showing difference in protein content of untreated and PKC412-treated samples after depletion of BIAM-fraction using increased volume of streptavidin-sepharose beads.

The results of the Kinexus™ phosphatase profiling of the biotin-depleted untreated and PKC412-treated MOLM-13 samples (Figures 58, 59, 60 and Tables 8, 9 and 10) proved quite challenging to decipher. It was expected that some phosphatases would appear at decreased levels in the PKC412-treated sample compared to the untreated, representing phosphatases which are reduced in absence of FLT3-ITD signalling and oxidised in its presence. However, the differential expression of phosphatases in untreated and PKC412-treated samples made differences based on redox states hard to detect. Ideally, phosphatases would be observed to have similar expression levels in untreated and PKC412-treated samples, as determined by K_002, and then appear at a decreased level in the PKC412 sample after depletion of the reduced fraction. This would represent phosphatases which are oxidised downstream of FLT3-ITD, however this category failed to emerge in K_002, with no phosphatase showing equal levels in the untreated and PKC412-treated samples.

Another possibility which was anticipated was that phosphatases with increased levels of expression in PKC412-treated samples compared to untreated (determined by K_002), and decreased in PKC412-treated after biotin depletion (as determined by K_003), would represent a category of phosphatases which are negatively regulated by FLT3 at level of expression (i.e. PKC412 triggers an increase in expression) and at level of activity (PKC412 triggers an increase in the reduced, active fraction), however, this category was also not identified, probably due to the differences in expression masking any changes attributable to oxidation. The phosphatases were grouped and categorised according to their profiles in screens K_002 and K_003 and the results can be best summarised as follows;

Category 1)

Represents: Phosphatases which are regulated by FLT3-ITD at level of expression (transcription or translational) but not at level of oxidation.

Identified by: Differences in expression between untreated and PKC412-treated samples remain approximately the same despite depletion of Biotin-labelled/reduced fraction. These phosphatases do not undergo redox regulation but do incur changes at the level of protein expression.

Significance: FLT3-ITD regulates the activity of these phosphatases through their expression but not *via* redox modulation of their oxidation states.

Accounts for: SHP-1, PP1/Cα, PTEN

Category 2)

Represents: Phosphatases which appear to be positively regulated by FLT3-ITD at both the levels of expression and activity.

Identified by: Phosphatases are increased in untreated sample, as determined by K_002 and decreased in untreated samples after biotin-depletion, as determined by K_003.

Significance: FLT3-ITD positively regulates the protein expression of these phosphatases and also reduces their oxidation.

Accounts for: VHR, PP2A/Cα, PP5C, PP2Cα

Category 3)

Represents: Phosphatases which appear to be negatively regulated by FLT3-ITD at level of expression but positively regulated at level of activity.

Identified by: Phosphatases are increased in PKC412-treated samples compared to untreated samples at level of expression, as determined by K_002, and this increase is even more noticeable after biotin-depletion, suggesting that the untreated sample has been subject to greater depletion.

Significance: FLT3-ITD negatively regulates the expression of these phosphatases but does not affect their oxidation and may actually prevent it.

Accounts for: MKP2, PP2A/Aa/b

Category 4)

Represents: Phosphatases which appear positively regulated by FLT3 at level of expression and activity

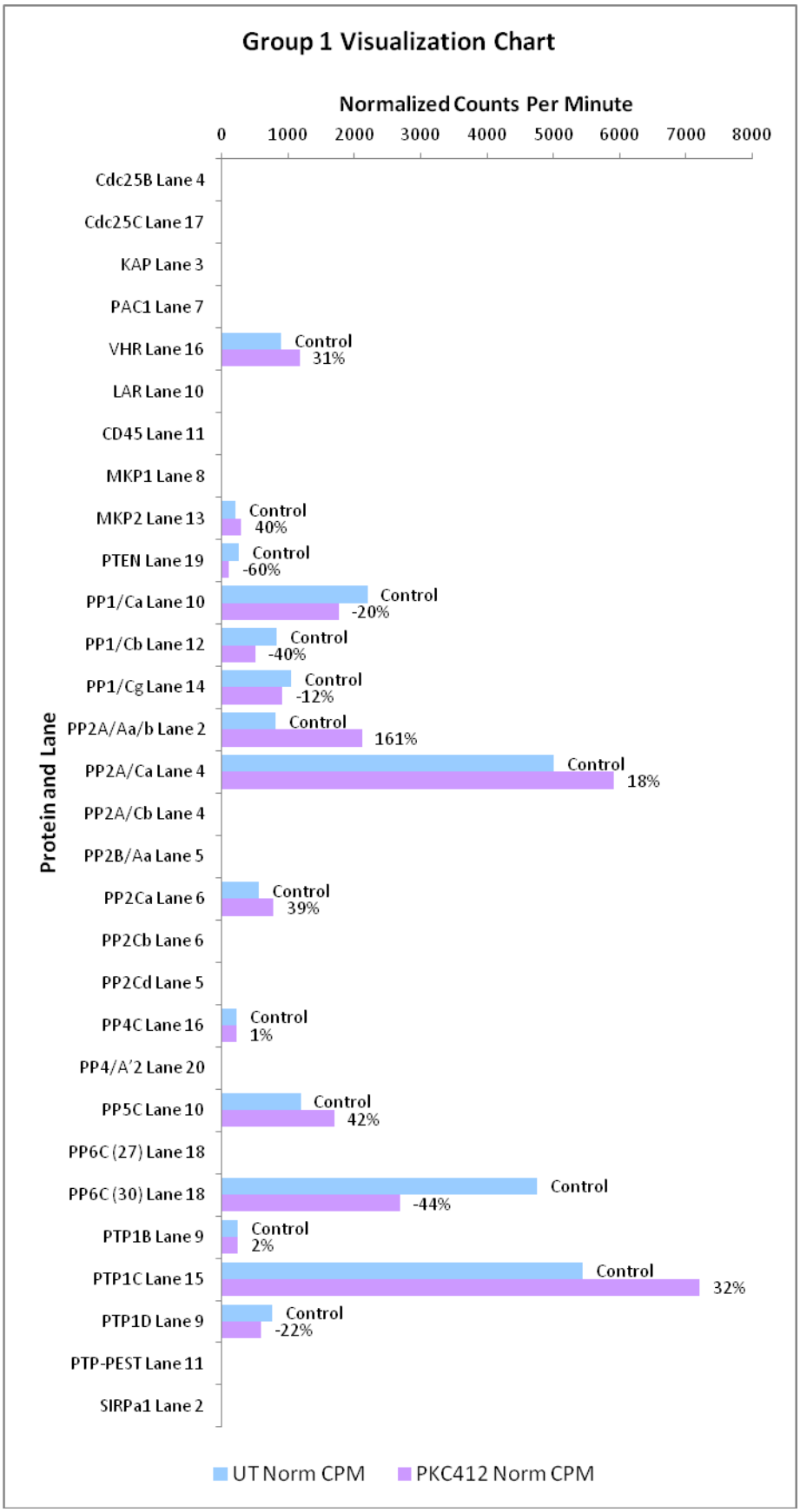
Identified by: Similarly to Category 2, phosphatases in this category show increased expression in untreated samples and are also increasingly present in untreated samples post biotin-depletion, but the difference between untreated and PKC412-treated is less noticeable after depletion, i.e. more protein has been removed from untreated sample during biotin-depletion than from the PKC412 treated sample.

Signifies: FLT3-ITD may positively regulate these phosphatases expression and also decrease their oxidation, though the latter effect may simply be due to induced changes in their sub-cellular localisation and removal from the vicinity of oxidant sources.

Accounts for: PP1/Cb, PP1/Cg , PP4C, PP6C, and PTP1B.

Figure 58: Kinexus™ phosphatase expression screen K_003.

Histogram represents the results of the multi-immunoblotting carried out by Kinexus™ Phosphatase Expression Screen KPPS 1.2, to compare the phosphatase expression profiles of BIAM-labelled and depleted MOLM-13 cells which were untreated (blue), designated as control sample, and treated with 250 nM PKC412 for 24 hours (purple), designated as test sample. The identification and detection of each of 30 phosphatases (vertical axis) was based on immunoreactivity and apparent molecular mass. The corrected trace quantity of each band is expressed as counts per minute (CPM) (horizontal axis).


Group 1 Visualization Chart
Normalized Counts Per Minute
0
1000
2000
3000
4000
5000
6000
7000
8000
Protein and Lane
Cdc25B Lane 4
Cdc25C Lane 17
KAP Lane 3
PAC1 Lane 7
VHR Lane 16
LAR Lane 10
CD45 Lane 11
MKP1 Lane 8
MKP2 Lane 13
PTEN Lane 19
PP1/Ca Lane 10
PP1/Cb Lane 12
PP1/Cg Lane 14
PP2A/Aa/b Lane 2
PP2A/Ca Lane 4
PP2A/Cb Lane 4
PP2B/Aa Lane 5
PP2Ca Lane 6
PP2Cb Lane 6
PP2Cd Lane 5
PP4C Lane 16
PP4/A'2 Lane 20
PP5C Lane 10
PP6C (27) Lane 18
PP6C (30) Lane 18
PTP1B Lane 9
PTP1C Lane 15
PTP1D Lane 9
PTP-PEST Lane 11
SIRPa1 Lane 2
Control
31%
Control
40%
Control
-60%
Control
-20%
Control
-40%
Control
-12%
Control
161%
Control
18%
Control
39%
Control
1%
Control
42%
Control
-44%
Control
2%
Control
32%
Control
-22%
UT Norm CPM
PKC412 Norm CPM

KINEXUS

KINETWORKS™ KPPS-1.2-HUMAN COMPARISON REPORT

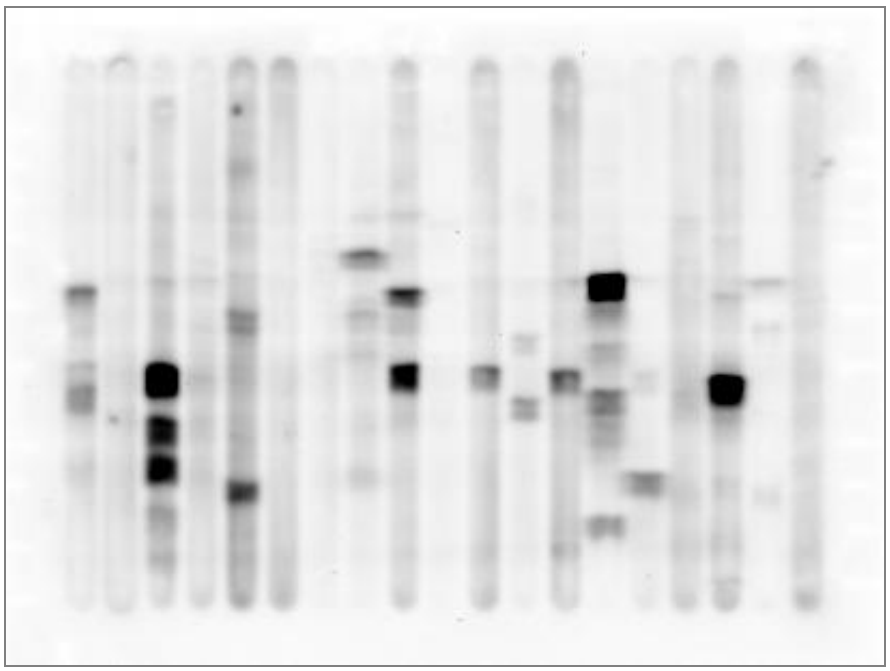
Normalized Data Comparison Of Normalized Counts per Minute For the Following Samples			Kinexus ID	16420	16421
			Scan ID	67623	67631
			Sample Name	UT	PKC412
			Normalization	1	1
FULL NAME OF PROTEIN	ABBREV	LANE	TYPE	)RMALIZED C.P	
Cell division cycle 25B phosphatase	Cdc25B	4	PSTYP		
Cell division cycle 25C phosphatase	Cdc25C	17	PSTYP		
Cyclin-dependent kinase associated phosphatase (CDK inhibitor 3, CIP2)	KAP	3	PSYP		
Dual specificity MAP kinase protein phosphatase	PAC1	7	PTYP		
Dual specificity protein phosphatase 3	VHR	16	PYP	895	1170
LCA antigen-related (LAR) receptor tyrosine phosphatase	LAR	10	PYP		
Leukocyte common antigen CD45 receptor-tyrosine phosphatase (LCA, T200)	CD45	11	PYP		
MAP kinase phosphatase 1 (CL100, VH1)	MKP1	8	PTYP		
MAP kinase phosphatase 2 (VH2)	MKP2	13	PTYP	205	286
Phosphatidylinositol-3,4,5-trisphosphate 3-phosphatase deleted on chromosome 10	PTEN	19	PSTYP	261	105
Protein-serine phosphatase 1 - catalytic subunit - alpha isoform	PP1/Ca	10	PSTP	2196	1760
Protein-serine phosphatase 1 - catalytic subunit - beta isoform	PP1/Cb	12	PSTP	827	499
Protein-serine phosphatase 1 - catalytic subunit - gamma isoform	PP1/Cg	14	PSTP	1045	915
Protein-serine phosphatase 2A - A regulatory subunit - alpha and beta isoforms	PP2A/Aa/b	2	PSTP	809	2111
Protein-serine phosphatase 2A - catalytic subunit alpha isoform	PP2A/Ca	4	PSTP	5009	5907
Protein-serine phosphatase 2A - catalytic subunit beta isoform	PP2A/Cb	4	PSTP		
Protein-serine phosphatase 2B - catalytic subunit - alpha isoform	PP2B/Aa	5	PSTYP		
Protein-serine phosphatase 2C - catalytic subunit - alpha isoform	PP2Ca	6	PSTP	563	782
Protein-serine phosphatase 2C - catalytic subunit - beta isoform	PP2Cb	6	PSTP		
Protein-serine phosphatase 2C - catalytic subunit - delta isoform	PP2Cd	5	PSTP		
Protein-serine phosphatase 4 - catalytic subunit (PPX/C)	PP4C	16	PSTP	217	220
Protein-serine phosphatase 4 - regulatory subunit (PPX/A'2)	PP4/A'2	20	PSTP		
Protein-serine phosphatase 5 - catalytic subunit (PPT)	PP5C	10	PSTP	1189	1691
Protein-serine phosphatase 6 - catalytic subunit (PPVC) (27)	PP6C	18	PSTP		
Protein-serine phosphatase 6 - catalytic subunit (PPVC) (30)	PP6C	18	PSTP	4758	2688
Protein-tyrosine phosphatase 1B	PTP1B	9	PYP	240	246
Protein-tyrosine phosphatase 1C (SHP1, SHPTP1)	PTP1C	15	PYP	5437	7204
Protein-tyrosine phosphatase 1D (SHP2, SHPTP2, Syp, PTP2C)	PTP1D	9	PYP	758	594
Protein-tyrosine phosphatase with PEST sequences (PTPG1, PTPN12)	PTP-PEST	11	PYP		
Signal regulatory protein substrate of PTP1D phosphatase (SHPS1)	SIRPa1	2	PYPsub		

Table 8: Kinexus™ phosphatase expression screen K_003, Comparison Report

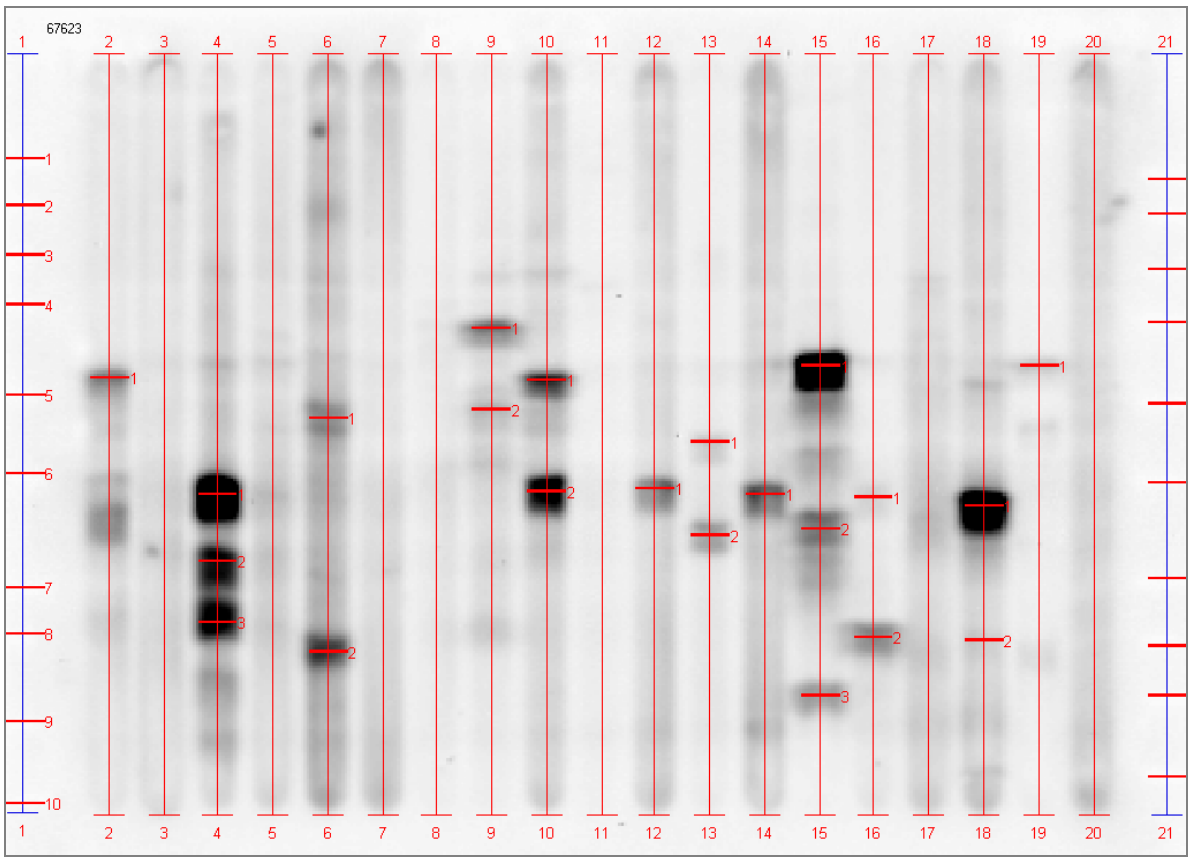
Comparison of the corrected trace quantity of each protein expressed as counts per minute (CPM) in the two samples of BIAM-labelled and depleted MOLM-13 cells untreated and treated with 250 nM PKC412 for 24 hours. The normalised trace quantity of each band is given. This adjustment is based on the difference in the total signal from the sum of all of the bands on individual immunoblots.

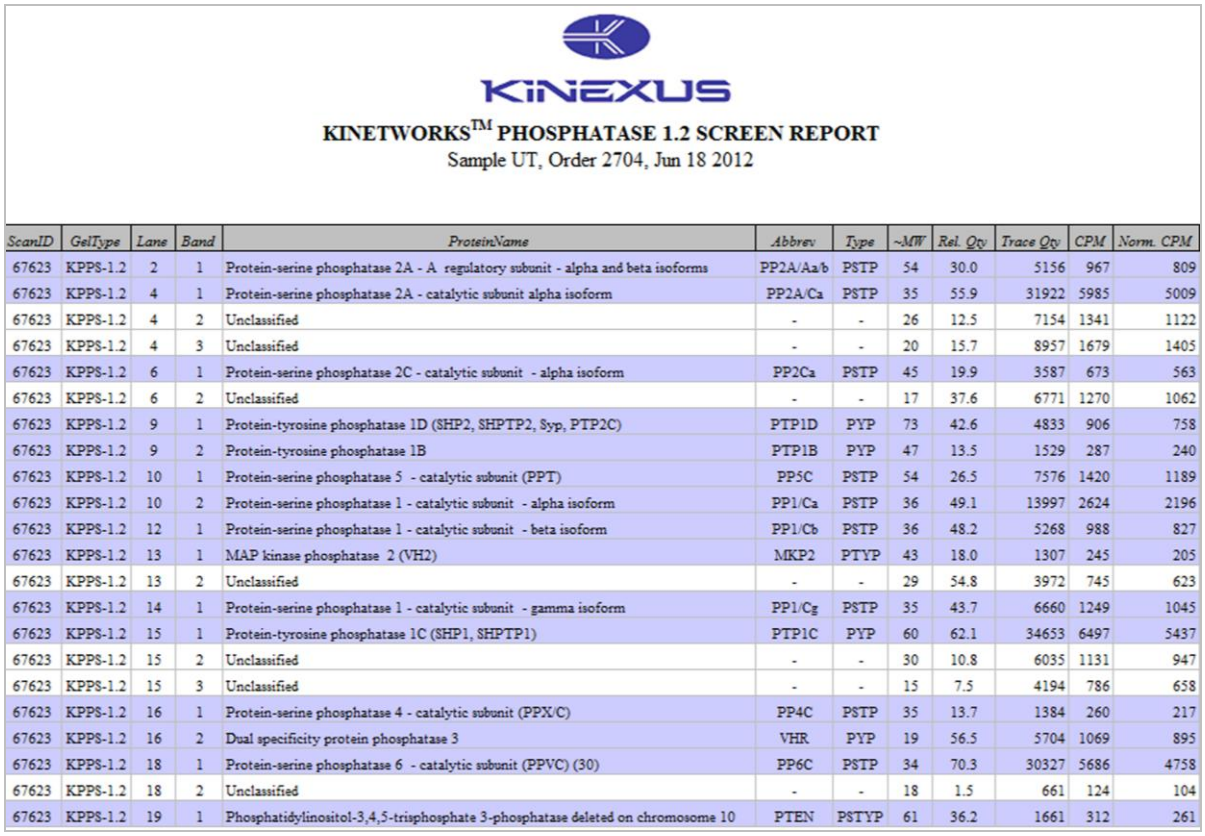
Figure 59. Kinexus™ phosphatase expression screen K_003, Multi-Immunoblot for BIAM-labelled and depleted untreated MOLM-13 sample. Multi-immunoblot of BIAM-labelled and depleted untreated MOLM-13 sample with the detected bands **A)** unmarked and **B)** numbered according to lane and number of bands appearing per lane. Lanes 1 and 21 denote molecular weight markers used by Kinexus™. Band 1=201 kDa, Band 2= 156 kDa, Band 3= 106 kDa, Band 4=79 kDa, Band 5=48 kDa, Band 6= 37kDa.

A



B





KINEXUS

KINETWORKS™ PHOSPHATASE 1.2 SCREEN REPORT

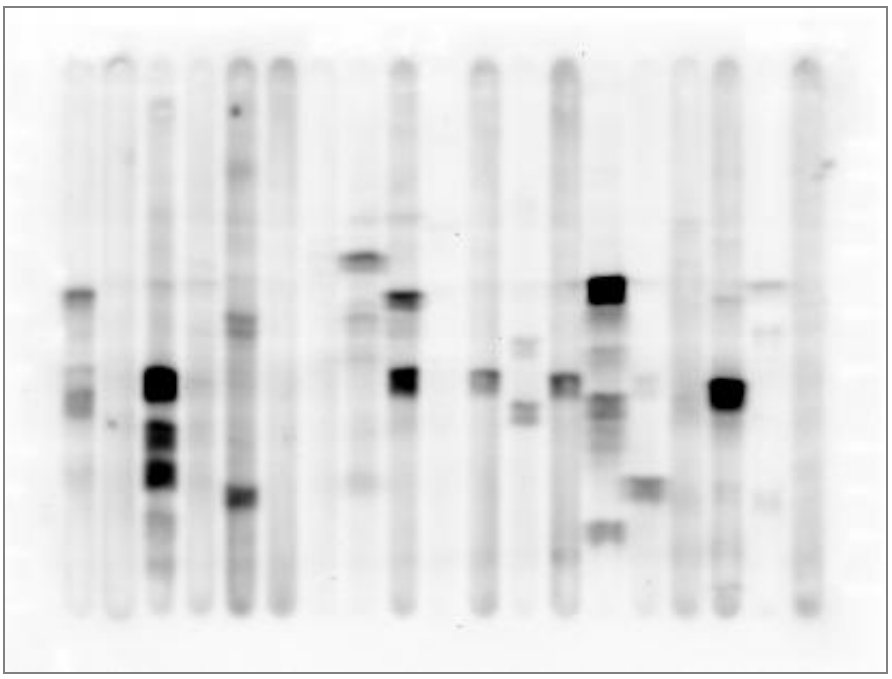
Sample UT, Order 2704, Jun 18 2012

ScanID	GelType	Lane	Band	ProteinName	Abbrev	Type	~MW	Rel. Qty	Trace Qty	CPM	Norm. CPM
67623	KPPS-1.2	2	1	Protein-serine phosphatase 2A - A regulatory subunit - alpha and beta isoforms	PP2A/Aa/b	PSTP	54	30.0	5156	967	809
67623	KPPS-1.2	4	1	Protein-serine phosphatase 2A - catalytic subunit alpha isoform	PP2A/Ca	PSTP	35	55.9	31922	5985	5009
67623	KPPS-1.2	4	2	Unclassified	-	-	26	12.5	7154	1341	1122
67623	KPPS-1.2	4	3	Unclassified	-	-	20	15.7	8957	1679	1405
67623	KPPS-1.2	6	1	Protein-serine phosphatase 2C - catalytic subunit - alpha isoform	PP2Ca	PSTP	45	19.9	3587	673	563
67623	KPPS-1.2	6	2	Unclassified	-	-	17	37.6	6771	1270	1062
67623	KPPS-1.2	9	1	Protein-tyrosine phosphatase 1D (SHP2, SHPTP2, Syp, PTP2C)	PTP1D	PYP	73	42.6	4833	906	758
67623	KPPS-1.2	9	2	Protein-tyrosine phosphatase 1B	PTP1B	PYP	47	13.5	1529	287	240
67623	KPPS-1.2	10	1	Protein-serine phosphatase 5 - catalytic subunit (PPT)	PP5C	PSTP	54	26.5	7576	1420	1189
67623	KPPS-1.2	10	2	Protein-serine phosphatase 1 - catalytic subunit - alpha isoform	PP1/Ca	PSTP	36	49.1	13997	2624	2196
67623	KPPS-1.2	12	1	Protein-serine phosphatase 1 - catalytic subunit - beta isoform	PP1/Cb	PSTP	36	48.2	5268	988	827
67623	KPPS-1.2	13	1	MAP kinase phosphatase 2 (VH2)	MKP2	PTYP	43	18.0	1307	245	205
67623	KPPS-1.2	13	2	Unclassified	-	-	29	54.8	3972	745	623
67623	KPPS-1.2	14	1	Protein-serine phosphatase 1 - catalytic subunit - gamma isoform	PP1/Cg	PSTP	35	43.7	6660	1249	1045
67623	KPPS-1.2	15	1	Protein-tyrosine phosphatase 1C (SHP1, SHPTP1)	PTP1C	PYP	60	62.1	34653	6497	5437
67623	KPPS-1.2	15	2	Unclassified	-	-	30	10.8	6035	1131	947
67623	KPPS-1.2	15	3	Unclassified	-	-	15	7.5	4194	786	658
67623	KPPS-1.2	16	1	Protein-serine phosphatase 4 - catalytic subunit (PPX/C)	PP4C	PSTP	35	13.7	1384	260	217
67623	KPPS-1.2	16	2	Dual specificity protein phosphatase 3	VHR	PYP	19	56.5	5704	1069	895
67623	KPPS-1.2	18	1	Protein-serine phosphatase 6 - catalytic subunit (PPVC) (30)	PP6C	PSTP	34	70.3	30327	5686	4758
67623	KPPS-1.2	18	2	Unclassified	-	-	18	1.5	661	124	104
67623	KPPS-1.2	19	1	Phosphatidylinositol-3,4,5-trisphosphate 3-phosphatase deleted on chromosome 10	PTEN	PSTYP	61	36.2	1661	312	261

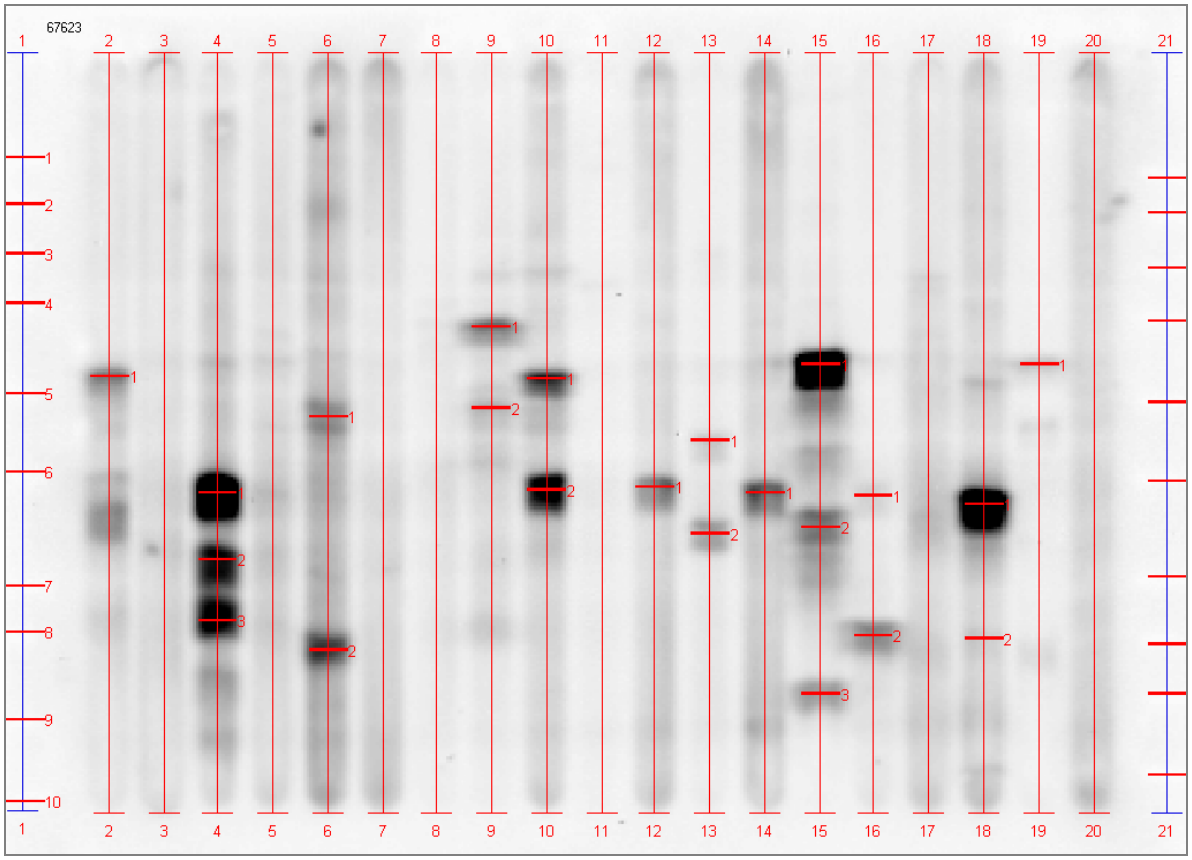
Table 9. Kinexus™ phosphatase expression screen K_003, Sample report for BIAM-labelled and depleted untreated MOLM-13. Quantitative information regarding band intensities with reference to the immunoblot in Figure 59B, including the identities of all the target proteins identified as numbered bands, the estimated molecular mass for each numbered band, the relative quantity of the band expressed as a percentage of the total intensity of data in the lane in which the band appears, the trace quantity of each band taken to be the area under the band's intensity profile curve, the corrected trace quantity of each band expressed as counts per minute (cpm).

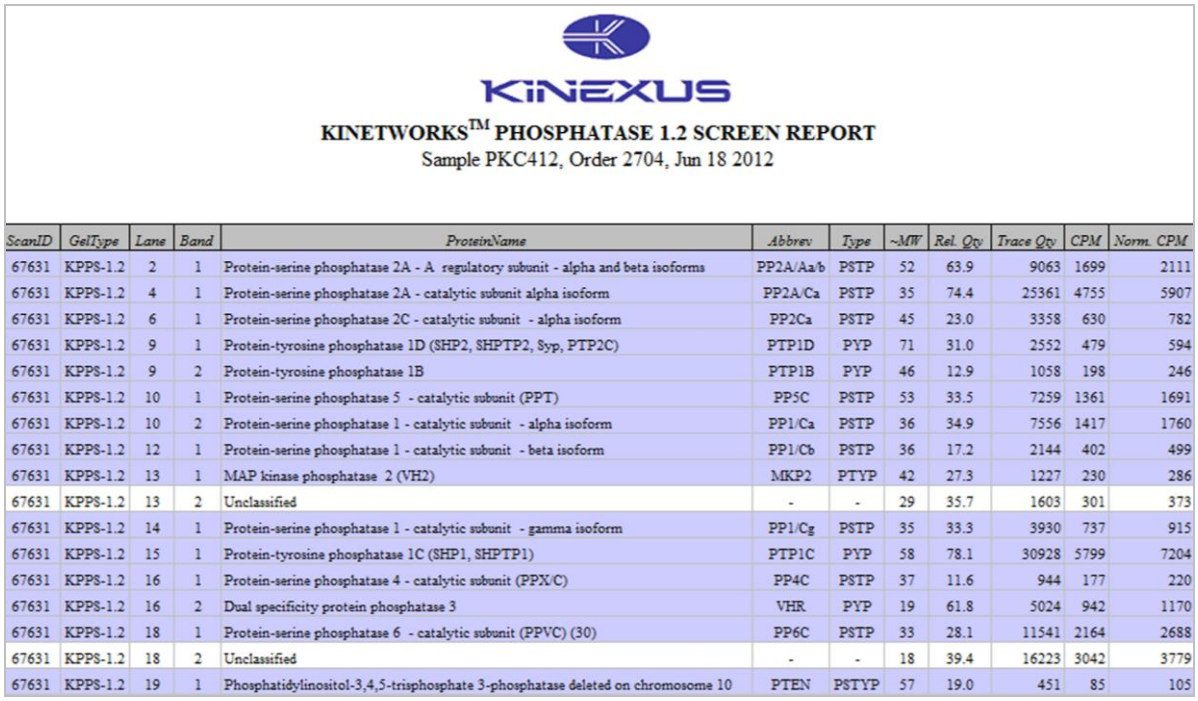
Figure 60. Kinexus™ phosphatase expression screen K_003, Multi-Immunoblot for BIAM-labelled and depletedPKC412-treated MOLM-13 sample. Multi-immunoblot of BIAM-labelled and depleted PKC412-treated MOLM-13 sample with the detected bands **A)** unmarked and **B)** numbered according to lane and number of bands appearing per lane. Lanes 1 and 21 denote molecular weight markers used by Kinexus™. Band 1=201 kDa, Band 2= 156 kDa, Band 3= 106 kDa, Band 4=79 kDa, Band 5=48 kDa, Band 6= 37kDa.

A



B





KINETWORKS™ PHOSPHATASE 1.2 SCREEN REPORT
Sample PKC412, Order 2704, Jun 18 2012

ScanID	GelType	Lane	Band	ProteinName	Abbrev	Type	~MW	Rel. Qty	Trace Qty	CPM	Norm. CPM
67631	KPPS-1.2	2	1	Protein-serine phosphatase 2A - A regulatory subunit - alpha and beta isoforms	PP2A/Aa/b	PSTP	52	63.9	9063	1699	2111
67631	KPPS-1.2	4	1	Protein-serine phosphatase 2A - catalytic subunit alpha isoform	PP2A/Ca	PSTP	35	74.4	25361	4755	5907
67631	KPPS-1.2	6	1	Protein-serine phosphatase 2C - catalytic subunit - alpha isoform	PP2Ca	PSTP	45	23.0	3358	630	782
67631	KPPS-1.2	9	1	Protein-tyrosine phosphatase 1D (SHP2, SHPTP2, Syp, PTP2C)	PTP1D	PYP	71	31.0	2552	479	594
67631	KPPS-1.2	9	2	Protein-tyrosine phosphatase 1B	PTP1B	PYP	46	12.9	1058	198	246
67631	KPPS-1.2	10	1	Protein-serine phosphatase 5 - catalytic subunit (PPT)	PP5C	PSTP	53	33.5	7259	1361	1691
67631	KPPS-1.2	10	2	Protein-serine phosphatase 1 - catalytic subunit - alpha isoform	PP1/Ca	PSTP	36	34.9	7556	1417	1760
67631	KPPS-1.2	12	1	Protein-serine phosphatase 1 - catalytic subunit - beta isoform	PP1/Cb	PSTP	36	17.2	2144	402	499
67631	KPPS-1.2	13	1	MAP kinase phosphatase 2 (VH2)	MKP2	PTYP	42	27.3	1227	230	286
67631	KPPS-1.2	13	2	Unclassified	-	-	29	35.7	1603	301	373
67631	KPPS-1.2	14	1	Protein-serine phosphatase 1 - catalytic subunit - gamma isoform	PP1/Cg	PSTP	35	33.3	3930	737	915
67631	KPPS-1.2	15	1	Protein-tyrosine phosphatase 1C (SHP1, SHPTP1)	PTP1C	PYP	58	78.1	30928	5799	7204
67631	KPPS-1.2	16	1	Protein-serine phosphatase 4 - catalytic subunit (PPX/C)	PP4C	PSTP	37	11.6	944	177	220
67631	KPPS-1.2	16	2	Dual specificity protein phosphatase 3	VHR	PYP	19	61.8	5024	942	1170
67631	KPPS-1.2	18	1	Protein-serine phosphatase 6 - catalytic subunit (PPVC) (30)	PP6C	PSTP	33	28.1	11541	2164	2688
67631	KPPS-1.2	18	2	Unclassified	-	-	18	39.4	16223	3042	3779
67631	KPPS-1.2	19	1	Phosphatidylinositol-3,4,5-trisphosphate 3-phosphatase deleted on chromosome 10	PTEN	PSTYP	57	19.0	451	85	105

Table 10. Kinexus™ phosphatase expression screen K_003, Sample report for BIAM-labelled and depleted PKC412-treated MOLM-13. Quantitative information regarding band intensities with reference to the immunoblot in Figure 60B, including the identities of all the target proteins identified as numbered bands, the estimated molecular mass for each numbered band, the relative quantity of the band expressed as a percentage of the total intensity of data in the lane in which the band appears, the trace quantity of each band taken to be the area under the band's intensity profile curve, the corrected trace quantity of each band expressed as counts per minute (cpm).

Discussion

The Kinexus™ phosphatase expression profiling allowed comparison of the expression of 30 PTPs, serine/threonine phosphatases and dual specificity phosphatases, under different experimental conditions. It was used by this study firstly to gain an insight into the range of phosphatases expressed by MOLM-13 cells. This provided the opportunity to identify phosphatases which are not being expressed by these cells, possibly due to mutation, deletion, gene silencing or downregulation at the level of translation. Phosphatases which negatively regulate pro-survival signalling are frequently found to be deleted, silenced or otherwise transcriptionally suppressed and downregulated in a range of tumours.

Perhaps the best example of this is the prototypical tumour suppressor PTEN. The *PTEN* gene is estimated to be the second most frequently mutated and deleted in human tumours after *TP53* (Yin and Shen, 2008) and, when it does remain un-affected through mutation, efficient transcription of *PTEN* is often prevented through microRNAs, competitive endogenous RNAs (the PTEN pseudogene), methylation and downregulation of it transcription factors (Carracedo *et al.*, 2011). Kinexus™ screen K_001 showed that PTEN is expressed at very low levels in both the MOLM-13 and MV4-11 AML cell lines compared to the other phosphatases. In contrast, Arora *et al*. (2012) reported that PTEN was amongst the most abundantly expressed phosphatases in both the AML cell lines, including MV4-11, and the AML patient samples which they examined , and Gauffin *et al*. (2009) noted that PTEN was overexpressed in the tissue microarrays that they conducted using samples taken from patients of paediatric ALL. However, the fact that PTEN was expressed to a greater extent in those studies is not a guarantee that the PTEN protein

is functional, nor does it preclude the likelihood of extensive post-translational modifications rendering the phosphatase inactive.

The second Kinexus™ screen, K_002, which compared the expression of phosphatases in the presence and absence of FLT3-ITD signalling, showed that PTEN levels decreased even further in PKC412-treated cells, suggesting that its protein expression is somehow linked to FLT3-ITD signalling. A role for PTEN in normal haematopoietic development and prevention of leukemogenesis has been repeatedly demonstrated (Peng *et al.*, 2010; Yilmaz *et al.*, 2006; Zhang *et al.*, 2006), and is known to negatively regulate a key component of the FLT3-ITD signal transduction necessary for myeloid cell transformation, the PI3K/Akt pathway (Brandts *et al.*, 2005). Peng *et al*. (2010) showed that PTEN expression is downregulated at the mRNA level by oncogenic Bcr-Abl in CML, and that restoration of the PTEN expression delays CML development, reduces the number of CML stem cells, and also slows progression of Bcr-Abl-driven B-ALL. Therefore, it is likely that in thriving leukaemic cell lines this phosphatase has been functionally suppressed to a large extent, either at a genetic level or through inhibitory post-translational modifications. Godfrey *et al*. (2012) concluded that PTEN is not oxidised downstream of FLT3-ITD in their AML model, but the phosphatase has been shown to undergo oxidative inactivation in association with growth factor signalling in other systems (Kwon *et al.*, 2004; Lee *et al.*, 2002) including T-ALL (Muller *et al.*, 2008a).

Similarly, in the third Kinexus™ phosphatase screen which used BIAM-labelling and depletion to examine the redox status of phosphatases in the context of FLT3-ITD signalling, the difference in the levels of PTEN between untreated and

PKC412-treated samples were almost identical to the differences observed in K_002, suggesting that the proportions of oxidised and reduced PTEN were the same regardless of FLT3-ITD signalling. It can be concluded that the apparent upregulation of PTEN observed upon FLT3-ITD activity, must be countered by alternative, non-redox, negative modulations of the proteins activity in order to remove any impedance to FLT3-ITD signalling. Of course the possibility that the PTEN being expressed and detected represents a non-functional gene product of mutated *PTEN* must also be taken into account.

The K_001 screen revealed that 14 of the phosphatases screened for were not detected in MOLM-13 cells. Of these, several are of interest from an oncogenic perspective. Cell division cycle 25B phosphatase (Cdc25B), cell division cycle 25C phosphatase (Cdc25C) and CDK inhibitor 3 (KAP/CIP2) are involved in the regulation of the cell cycle (Malumbres and Barbacid, 2009; Srivastava *et al.*, 2007; Xiao *et al.*, 2004). Dual specificity MAPK protein phosphatase (PAC-1) and MAPK phosphatase 1(VH1), are both inducible nuclear phosphatases (Owens and Keyse, 2007) and negative regulators of the MAPK pathway (Camps *et al.*, 2000). Interestingly, the *PAC-1* gene is a transcriptional target of p53, induced upon oxidative stress (Yin *et al.*, 2003) and leading to apoptosis through the negative regulation of its substrates Erk and p38 (Chu *et al.*, 1996). Although the MOLM-13 cells are reported to express wild type p53 (Kojima *et al.*, 2005) a downregulation of its activity could account for the lack of PAC-1 expression.

The leukocyte common antigen-related (LAR) receptor tyrosine phosphatase is a member of a subgroup of PTPs which contain an extracellular adhesion-molecule-like domain in addition to the classical PTP domain (Eswaran *et al.*, 2006).

Alternatively spliced isoforms of this phosphatase have been associated with breast carcinoma (Yang *et al.,* 1999) and it is possible that the antibodies used in the Kinexus™ screen do not detect these variants, accounting for the lack of detection of LAR.

Leukocyte common antigen CD45 receptor tyrosine phosphatase (CD45) is an antigen specific to haematopoietic cells and frequently used in cell sorting to identify leukocytes including AML cells of the myelomonocytic lineage (Saunders and Johnson, 2010). Godfrey *et al*. (2012) report that CD45 activity is slightly reduced in FLT3-ITD 32D cells. The absence of CD45 in our screen could again be due to the fact that two alternatively spliced variants of the protein are generated (Oberdoerffer *et al.,* 2008) and both may not be detectable using the Kinexus™ antibodies.

The relevance of several of the phosphatases identified is difficult to interpret as the data refers to specific isoforms of subunits which contribute to a phosphatase holoenzyme, for example protein serine phosphatase 2A catalytic subunit β isoform (PP2A/Cb), which does not appear to be expressed by either MOLM-13 or MV4-11. There is a scarcity of published data regarding such isoforms and so the significance of their lack of expression is not easily determined. Should the isoform represent a crucial component of the holoenzyme complex, for example a catalytic subunit, then it could be predicted that the enzyme may not function in its absence. Specifically with regard to PP2A/C, the β isoform is known to be the less abundant of two isoforms of the catalytic subunit (Sablina *et al.,* 2010) and the α isoform appears to be very highly expressed according to K_001 and K_002 . As both of the regulatory

subunits of PP2A, PP2A/Aa/b are present it may be that overall the PP2A holoenzyme is functional.

As the phosphatases which were not expressed in untreated MOLM-13 cells, remained un-expressed even after inhibition of FLT3-ITD signalling (K_002), it is likely that their suppression may not be linked to FLT3-ITD, and may be due to additional lesions. They may also represent gene deletion events which were originally connected to FLT3-ITD-driven transformation but are obviously irreversible, even upon relief of FLT3-ITD signalling.

The phosphatases which were selected for further study, PP2Cα, PTP1B, PP6C and SHP-1 showed changes in expression upon FLT3-ITD inhibition according to K_002. With the exception of PTP1B, the changes in expression were not reflected in counter-changes upon FL stimulation. This suggests that PP2Cα, PP6C and SHP-1 are subject to regulation by an aspect of FLT3-ITD pathway which deviates from that shared with the wild type receptor, while PTP1B, similarly to Ezrin and Src, is downstream of an effector or sequence of effectors common to both.

It was originally intended choose two phosphatases which increased in expression upon FLT3-ITD inhibition, PP2Cα and SHP-1, and two which underwent a reduction in expression when FLT3-ITD was inhibited, PP6C and PTP1B. However, PP2Cα was subsequently shown to be incorrectly recorded by the Kinexus™ K_002 screen, and was re-categorised as undergoing a decrease in expression in PKC412-treated samples. RT-PCR was used to establish whether the changes in phosphatase expression could be attributed to changes at the level of transcription, and this was concluded to be the case for the three phosphatases with

decreased expression in PKC412-treated samples, PP6C, PP2C α and PTP1B. As SHP-1 protein had been shown to increase in PKC412 samples, the decrease observed in its mRNA levels was seemingly contradictory until ubiquitination assays revealed that the upregulation of the transcription of SHP-1 in untreated MOLM-13 cells precedes extensive ubiquitination of the protein product, resulting in an increased rate of SHP-1 degradation downstream of FLT3-ITD.

To induce increased ubiquitination of SHP-1, FLT3-ITD is either regulating SHP-1 directly to render it more susceptible to ubiquitination, or is manipulating the ubiquitin ligase enzymes responsible for SHP-1 labelling and degradation. Simoneau *et al*. (2008) describe how phosphorylation of Ser 591on SHP-1 by cyclin dependent kinase 2 (CDK2) results in the proteasomal degradation of the phosphatase, removing its inhibitory effect on cell cycle progression. FLT3-ITD has been shown to downregulate a transcriptional repressor of CDK2, C/EBPα (Mizuki *et al.*, 2003) and in doing so may promote CDK2-mediated ubiquitination of SHP-1.

Alternatively, FLT3-ITD may regulate aspects of the ubiquitination machinery within the cell. Recent evidence from Habif *et al*. (2013) has shown that Ubiquilin 4, a ubiquitin-like protein which has been shown to both prevent and inhibit the degradation of targets proteins (Riley *et al.*, 2004), is subject to alterations in tyrosine phosphorylation downstream of FLT3-ITD, though it is unclear as to the consequences of this modification on the functioning of Ubiquilin 4. In the situation described by Woolley *et al*. (2012) FLT3-ITD controls the ubiquitination and degradation of p22phox *via* the inhibition of GSK3β, the kinase responsible for the phosphorylation of p22phox, which targets p22phox and many other proteins for degradation (Lee *et al.*, 2007; Leng *et al.*, 2010). If FLT3-ITD can indeed influence

the activity of enzymes involved in the ubiquitination pathway then it is likely that many more targets of FLT3-ITD-driven ubiquitination and proteasomal degradation will emerge.

SHP-1 has been designated as a putative tumour suppressor because of the negative impact it has on pro-survival, anti-apoptotic signalling pathways (Wu *et al.*, 2003a) and has been shown to de-phosphorylate FLT3 (Godfrey *et al.*, 2012). SHP-1 expression has been shown to be downregulated or completely abrogated in most leukaemia and lymphoma cell lines and tissues, as well as in oestrogen receptor (ER) negative breast cancer cell lines and some colorectal cancer cell lines (Wu *et al.*, 2003a). FLT3-ITD signalling has been reported to cause downregulation of SHP-1 activity through suppression of SHP-1 expression at both the mRNA and protein level (Chen *et al.*, 2005), though Arora *et al.* (2012) did not detect a difference in SHP-1 mRNA when comparing FLT3-ITD and wild type FLT3 cell lines. Our own data seem to point to an upregulation of SHP-1 at the level of transcription upon FLT3-ITD activity.

By utilising the combined resources of the SABiosciences Text Mining Application, a text-mining utility, an automated data extraction system and the UCSC Genome Browser, which contains reference sequence and working draft assemblies for a large collection of genomes, it was possible to determine the predicted transcription factor binding sites in the promoter of the gene which codes for SHP-1, *PTPN6*. Amongst the most relevant transcription factors predicted in this way were CREB, c-Myc, AP-1 and STAT5, all known to be stimulated by FLT3-ITD (Choudhary *et al.*, 2007; Gwin *et al.*, 2010; Rosen *et al.*, 2010) .

This study also proposes a downregulation of the activity of the protein itself through proteasomal degradation. Although SHP-1 is known to become oxidised downstream of growth factor signalling in other systems (Weibrecht *et al.*, 2007), by comparing its differential expression in K_002 and K_003 its redox state was determined to be independent of FLT3-ITD activity in this study.

PTP1B was shown to be downregulated at the level of protein expression in cells treated with PKC412. This decrease was further determined to be due to a decrease in *PTP1B* transcription upon PKC412 treatment. The SABiosciences Text Mining Application and the UCSC Genome Browser predicted binding sites in the promoter of the PTP1B gene, *PTPN1*, for CREB, the proto-oncogene which is activated downstream of FLT3-ITD and is also predicted to bind the *FLT3* gene promoter (Fukuda *et al.*, 2009; Shankar *et al.*, 2005); STAT5 and c-Myb, both of which are known effectors of FLT3-ITD (Gwin *et al.*, 2010; Obermann *et al.*, 2010).

Although this suggests that PTP1B expression is positively regulated by FLT3-ITD signalling, the reality may be that PTP1B activity is highly suppressed because of the threat it poses to the FLT3-ITD pathway. Evidence favours a role for PTP1B as a negative regulator of FLT3 through its de-phosphorylation (Godfrey *et al.*, 2012) and by preventing mis-localised FLT3-ITD signalling from the ER where PTP1B is resident (Bo *et al.*, 2005; Schmidt-Arras *et al.*, 2009). PTP1B is oxidised to varying degrees in tumour cell lines (Lou *et al.*, 2008) and is highly sensitive to H_2O_2 in particular (Groen *et al.*, 2005), yet despite this has been reported to be not oxidised downstream of FLT3-ITD (Godfrey *et al.*, 2012) which correlates with the data from K_003. Another option for negative regulation of PTP1B in this scenario

is through its serine phosphorylation by Akt (Ravichandran *et al.*, 2001), a constitutively active downstream effector of FLT3-ITD (Brandts *et al.*, 2005).

PP2Cα, also known as protein phosphatase 1A, is a serine threonine phosphatase which negatively regulates Smad1 and MAPK , and is also thought to be involved in TGF-β, CDK and pro-apoptotic p53 signalling, which has prompted the classification of PP2Cα as a tumour suppressor (Lammers *et al.*, 2007; Takekawa *et al.*, 1998). Re-evaluation of the expression of this phosphatase in MOLM-13 cells, after discrepancies were noted with regard to its detection in the Kinexus™ screens, confirmed that it is downregulated at the level of mRNA and protein upon FLT3-ITD inhibition. Similarly to the previously discussed phosphatases, the tumour suppressive nature of PP2Cα predicts that it would disrupt the FLT3-ITD oncogenic signalling, so it is likely to be inhibited at a post-translational level in order to contend with its upregulation at the mRNA level, which is probably due to the extensive induction of transcription factors downstream of FLT3-ITD.

The SABiosciences Text Mining Application and the UCSC Genome Browser predicted binding sites in the *PP2Cα* promoter for transcription factors such as CREB, c-Myc, an oncogene implicated in the FLT3-ITD pathway and downregulated upon FLT3-ITD inhibition (Radomska *et al.*, 2006) and STAT5 which is downstream of FLT3-ITD but not the wild type FLT3 receptor (Choudhary *et al.*, 2007).

K_003 suggests that PP2Cα is not oxidised downstream of FLT3-ITD and indeed there is no literature evidence to imply that it is redox regulated at all. It is more likely in this case that PP2Cα is subject to inhibitory phosphorylation, as has been demonstrated to occur (Kobayashi *et al.*, 1998).

PP6C is also a serine/threonine phosphatase which was shown in K_002 to be very highly expressed in untreated MOLM-13 cells, with this expression decreasing by 71% upon FLT3-ITD inhibition. Previously published data shows that PP6C is involved in synchronising the cell cycle with DNA repair and has been hypothesised to play a preventative role in the development of breast cancer (Douglas *et al.*, 2010; Zhong *et al.*, 2011). Data concerning the regulatory transcription factor binding sites in the *PP6C* gene was retrieved using SABiosciences Text Mining Application and the UCSC Genome Browser. The results predicted binding sites for a range of transcription enhancers and repressors including C/EBPα, a myeloid transcriptional regulator and FLT3-ITD-target (Mizuki *et al.*, 2003); CREB, and c-Myb, another proto-oncogenic transcription factor which contributes to the differentiation block driven by FLT3-ITD signalling (Zheng *et al.*, 2002).

The K_003 data appeared to show that PP6C was less oxidised in untreated cells, which could be explained by a shift in sub-cellular localisation from the cytoplasm, where there are abundant oxidant sources, to the nucleus, where there is less. If FLT3-ITD activity stimulated such a translocation, it could reflect the irradiation-induced shift in PP6C sub-cellular localisation observed by Douglas *et al.*(2010) and could represent an attempt to pre-empt any DNA damage which may occur due to the FLT3-ITD-induced ROS increase.

The procedure of BIAM-labelling and depletion of lysates combined with Kinexus™ phosphatase expression profiling was an ambitious enterprise, the results of which proved somewhat difficult to interpret. Inherent differences in the expression levels of phosphatases between untreated and treated samples appeared to

mask differences in redox status and perhaps this procedure would be better suited to the examination of redox regulation of proteins which are also not subject to changes at the level of protein expression. It did provide some information regarding phosphatases which appeared to be indifferent to the changes in ROS levels downstream of FLT3-ITD signalling.

In conclusion, FLT3-ITD regulation of phosphatase activity, both PTPs and DSPs, is complex and multi-layered. Interpretation of correlations between FLT3-ITD signalling and increases in phosphatase expression as being a novel indication of their contribution to the FLT3-ITD pathway is tempting but shallow. The upregulation of transcription factor activity downstream of FLT3-ITD inevitably results in the increase and decrease of a wide variety of proteins, and as the SHP-1 data demonstrates, FLT3-ITD may promote the expression of a phosphatase apparently at odds with its oncogenic agenda, but this does not guarantee that this phosphatase will be allowed to fulfil its function. Successful FLT3-ITD signalling incorporates the capacity to override such obstacles.

Chapter 6

General Discussion

At the time of writing, clinical trials are ongoing to determine the safety, tolerability, pharmacokinetics and pharmacodynamic activity of the TK inhibitor Midostaurin/PKC412 for use in patients suffering from both MDS and AML (Fischer *et al.*, 2010; Stone *et al.*, 2005). Midostaurin is one of the more recent incarnations of FLT3-ITD inhibitors which have undergone clinical examination. It follows on from Sorafenib (Nexavar®; Bayer Pharmaceuticals) and Sunitinib (Sutent®; Pfizer Inc.), two multi-targeting kinase inhibitors which were demonstrated to have especially potent activity against FLT3 (Al-Kali *et al.*, 2011; O'Farrell *et al.*, 2003) and have also been approved for use in solid tumours due to their concomitant anti-angiogenic properties (Kim *et al.*, 2009). Other targeted FLT3-ITD inhibitors currently in clinical trials for myeloproliferative disorders are Lestaurtinib/CEP-701 (Knapper *et al.*, 2006), which also targets the oncogenic JAK2/STAT5 signalling axis (Hexner *et al.*, 2008); Tandutinib/MLN518 which has been shown to be highly effective in inhibiting FLT3, PDGFRb, and Kit and is progressing to Phase II clinical trials (DeAngelo *et al.*, 2006; Shepard *et al.*, 2012); AC220, one of the first to completely inhibit FLT3 activity *ex vivo* at clinically relevant doses (Chao *et al.*, 2009; Zarrinkar *et al.*, 2009) and also currently in Phase II trials, and KW-2449, a multi-kinase inhibitor of FLT3, Abl, Abl-T315I, and Aurora kinase (Shiotsu *et al.*, 2009) also awaiting progression to Phase II (Pratz *et al.*, 2009).

The success of the Bcr-Abl inhibitor, Imatinib, in provoking a clinical response in patients with CML (Douglas Smith, 2011), and more recently in Philadelphia chromosome positive (Ph+) ALL (Maziarz, 2005), heightened expectations of targeted FLT3-ITD inhibitors which were anticipated to offer similar

success in the realm of AML. However, to date, FLT3-ITD inhibitors have proven somewhat less effective in a clinical setting than in pre-clinical studies (Pratz *et al.*, 2009), and have resulted in the rapid development of drug-resistant clonal cells associated with relapse (Wiernik, 2010).

The failure in translating the efficiency of FLT3-ITD inhibitors from pre-clinical cell culture studies to clinical responses in patients has been attributed, amongst other reasons, to the use of cell lines which are homozygous for the FLT3-ITD mutation, while most patients who are initially diagnosed with AML are heterozygous for the mutant allele and the wild type allele (Wiernik, 2010). Mori *et al*. (2009) showed that the presence of the FL-responsive wild type FLT3 receptor can interfere with the effectiveness of inhibitors in cells which express both the wild type and mutant forms of FLT3. Initially it was assumed that the reduced potency of targeted FLT3-ITD inhibitors against the wild type receptor would prevent suppression of normal haematopoietic progenitors in the bone marrow (Mori *et al.*, 2009), however it is now accepted that, to generate a clinically relevant response, the inhibitor must be demonstrated to be effective against the heterozygous leukaemic blasts. Another hypothesised reason for the lack of sustained FLT3-ITD inhibition in patients is pharmacokinetic failure. Target inhibition and cytotoxicity are confirmed in pre-clinical studies but, in patient trials, consideration of safety and tolerability becomes paramount and inhibition of FLT3-ITD signalling *in vivo* is not evaluated (Pratz *et al.*, 2009).

This highlights the importance of studies such as this one, which use clinically relevant AML models such as the MOLM-13 cell line which is heterozygous for the FLT3-ITD and wild type mutations. The effectiveness of the

FLT3-ITD inhibitor PKC412 was demonstrated across a range of signalling parameters and at the level of cell motility, yet this dose was shown to not significantly impact the viability of MOLM-13 cells. This allowed the signalling data to be attributed to the inhibition of FLT3-ITD only, without activation of apoptotic-related signalling pathways complicating the issue. To induce cytotoxicity in MOLM-13 cells, the duration of incubation must be increased beyond the point where FL-stimulation can compensate for the sustained inhibition of FLT3-ITD, but determining this point was beyond the scope of this study. By focusing on sub-lethal FLT3-ITD inhibition, it was possible to observe the effects on novel downstream targets of FLT3 signalling before apoptosis occurs. Identification of such novel FLT3-signalling effectors is vital in illuminating the relatively obscure FLT3 signal transduction pathway.

In his discussion of FLT3-ITD inhibitors, Wiernik (2010) predicts that in order to combat drug resistance and promote optimal application of these inhibitors, combinations of inhibitors as well as combinations of inhibitors and conventional chemotherapy will have to be considered. In fact many of the current clinical trials are demonstrating synergy between FLT3-ITD inhibitors and chemotherapeutic agents such as daunorubicin and cytarabine in the case of PKC412 (Stone *et al.*, 2012). However, Wiernik points to the exploitation of the cross-talk between FLT3-ITD and downstream pathways such as Ras/Raf/MEK/Erk, JAK/STAT and PI3K/Akt as promising equally effective synergistic effects and possibilities of overcoming the rapid resistance observed with FLT3-ITD inhibitors alone (Weisberg *et al.*, 2009; Wiernik, 2010).

To facilitate such multi-targeted therapeutic approaches, this study has provided evidence to support a role for Nox, Src kinase and Ezrin in the downstream signalling pathway of FLT3. The position of p22phox-dependent Nox in translating the growth factor signals originating at FLT3 into proteomic changes renders these enzymes potential targets in the treatment of FLT3-ITD-driven AML. Recently, Nox have become recognised as therapeutic targets in cardiovascular disease (Cave, 2009) and in neurodegenerative disorders (Gao *et al.*, 2012), two pathologies characterised by increased oxidative stress but seemingly untreatable using anti-oxidant-based approaches. Targeted suppression of Nox activity provides an alternate means of combating the redox-basis for these conditions, as it does for tumours in which Nox-derived ROS operate as oncogenic signalling mediators.

Several excellent reviews have recently discussed the potential for Nox-based therapeutics and highlighted the range of diseases which could benefit from such developments, but all have emphasised the lack of specificity of existing inhibitors which is hampering progression to clinically-relevant studies (Jaquet *et al.*, 2009; Krause *et al.*, 2012; Lambeth *et al.*, 2008). To date, there are no licensed Nox-based therapeutics but this is set to change. Currently a dual Nox 1 and 4 inhibitor GKT137831 (GenKyoTex) is completing Phase I clinical trials for the treatment of diabetic nephropathy, a complication of diabetes associated with increased Nox 4-mediated oxidative stress in the kidney (Sedeek *et al.*, 2010). Further progress in the development of similar isoform-specific small molecule inhibitors (Cifuentes-Pagano *et al.*, 2012; Jaquet *et al.*, 2009) may be able to provide the option, in the near future, of combining FLT3-ITD and Nox inhibition for effective intervention of the redox signalling pathway downstream of FLT3. In the meantime it is vital to use

studies such as this one to draw attention to the role of Nox enzymes in the pathology of AML.

The revelation of the redox-regulation of Src downstream of FLT3-ITD is another interesting outcome of this study, and introduces another possible avenue for therapeutic intervention. There are a multitude of Src kinase inhibitors in development to address the causative role of Src in solid tumours (Puls *et al.*, 2011) but its involvement in AML deserves further investigation. The role for Src in promoting the proliferation of AML blasts has already been established (Ozawa *et al.*, 2008), as has its position as a mediator of FLT3-ITD signalling (Leischner *et al.*, 2012; Robinson *et al.*, 2005) and TK inhibitors which target Src have already progressed through clinical trials for the treatment of CML (Schenone *et al.*, 2010). Insights into the oxidative activation of Src and the circumstances under which it occurs, such as those illustrated in this study, will allow the targeting of this aspect of oncogenic Src activation.

Furthermore, the indications are that Src is simply one of many redox-activated kinases, which function in physiological signal transduction but may also become deregulated under conditions of oxidative stress. The possibility of direct kinase activation through oxidation is a reality for a wide range of redox-mediated pathologies but requires much more examination if it is to become a therapeutically valuable target.

The identification of Ezrin as a downstream target of both Nox-derived ROS and FLT3, directed the focus of the study towards a much-neglected aspect of the pathology of leukaemia- the metastasis of leukaemic blasts. Metastasis is a phenomenon most often associated with solid tumours, despite the obvious ease at

which leukaemic cells may migrate throughout the body. Clinically, it is the overgrowth of bone marrow-resident leukaemic blasts which receive most attention, yet the aberrant migration and extramedullary infiltration of secondary sites such as distal marrow, gums, meninges, skin and lungs by circulating blasts remains a major complicating factor (Stefanidakis *et al.*, 2009; Voermans *et al.*, 2002). Such migration can manifest as myeloid sarcoma in up to 10% of AML cases (Krause, 1979; Wiernik and Serpick, 1970), and leukaemic cutis in 3% of cases (Agis *et al.*, 2002). When occurring as complications of AML, both conditions tend to present at the same time as the progression to systemic bone marrow leukaemia, and often at relapse stage suggesting that the opportunity to address this complication is in the early phases of the disease (Bakst *et al.*, 2011).

The ability of the leukaemic blasts to home to secondary sites appears provide a point of intervention, by disrupting the cellular adhesion molecules and chemokine signalling axes involved (Chen and Massagué, 2012; Voermans *et al.*, 2002) but interference with the cytoskeletal mechanics of the cancer cell motility is also worth considering. Ezrin has been touted as a potentially therapeutic target in the metastasis of solid tumours (Li *et al.*, 2008; Wu *et al.*, 2011), and small molecule inhibitors of Ezrin have already been screened and shown to be effective in combating invasive osteosarcoma by impairing Ezrin phosphorylation and actin-interactions (Bulut *et al.*, 2012). Studies such as ours and that of Zhou *et al*. (2010) show that the therapeutic applications of such inhibitors need not be limited to the metastases of solid tumours.

Finally, elucidation of the FLT3-ITD phosphorylation signal transduction pathway would not have been complete without consideration of the phosphatases

which are regulated by FLT3 signalling. This area was discovered to be complex and multi-faceted, and rich in potential for further study. It appears that FLT3-ITD is responsible for the increased transcription of a range of phosphatases whose anti-tumourigenic functions appear to be at odds with the FLT3-ITD signalling agenda. The identification of binding sites for FLT3-ITD-responsive oncogenic transcription factors in the promoter regions of these phosphatases provided an explanation for this upregulation, and prompts the question of how FLT3-ITD cells suppress the activity of these phosphatases once they have been produced. The situation of SHP-1 provides an example of how the upregulation of a tumour suppressive phosphatase at the level of transcription is ameliorated by subsequent post-translational modifications, such as ubiquitination and proteasomal degradation.

Again this area is potentially useful from a therapeutic point of view, if putative tumour suppressor proteins are upregulated as a consequence of FLT3-ITD signalling, then perhaps it would be possible to prevent the subsequent suppression of their activity and exploit their presence as anti-oncogenic agents.

In conclusion, the FLT3-ITD signal transduction pathway has been shown to invoke the production of ROS through the Nox family of enzymes, resulting in the redox-regulation of Src kinase and its downstream effector Ezrin. These findings demonstrate a molecular basis for leukaemic cell migration, offering opportunities for therapeutic intervention. In addition, FLT3-ITD has been shown to regulate the expression and post-translational modification of a number of anti-tumourigenic phosphatases, which also provides the opportunity of exploitation for therapeutic purposes.

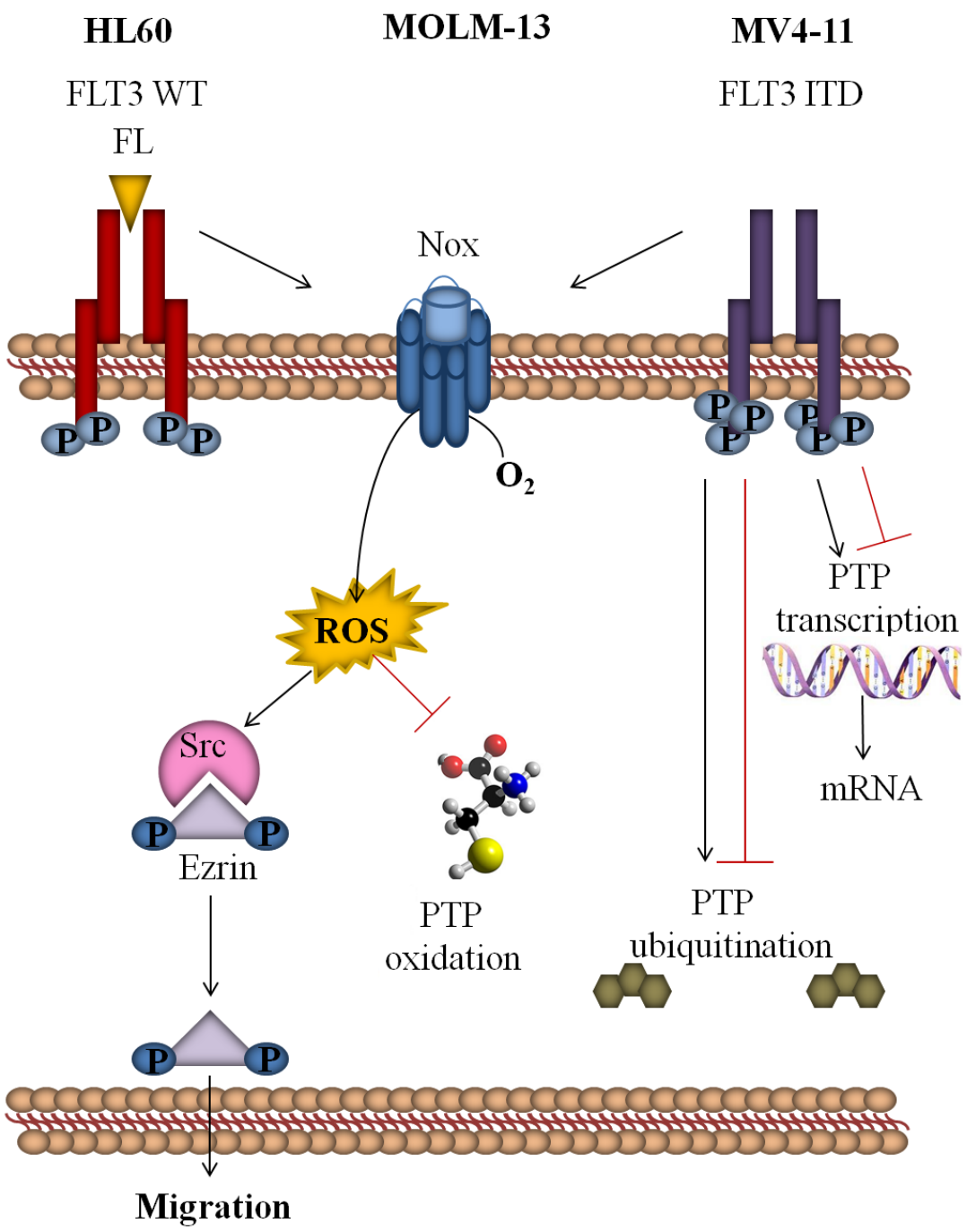


Figure 61. The downstream targets of FLT3 redox signalling in AML

Schematic illustrating the molecular basis of FLT3 signal transduction pathways operating in the AML cell, as elucidated by this study.

Bibliography

Abdelrahman M, Mazzon E, Bauer M, Bauer I, Delbosc S, Cristol J-P *et al.* (2005) Inhibitors of NADPH oxidase reduce the organ injury in hemorrhagic shock. *Shock* **23**:107-114

Abeloff MD. (2004) Clinical Oncology. *3rd edition*; St. Louis:2835–2839.

Adler V, Yin Z,Fuchs SY, Benezra M, Rosario L, Tew KD,Pincus MR, Sardana M, Henderson CJ, Wolf CR, Davis RJ, Ronai Z. (1999) Regulation of JNK signaling by GSTp. *EMBO J*;**18**:1321-1334

Aggerholm A, Guldberg P, Hokland M, Hokland P. (1999) Extensive intra- and interindividual heterogeneity of p15INK4B methylation in acute myeloid leukemia. *Cancer Res*;**59**:436-441

Agis H, Weltermann A, Fonatsch C, Haas O, Mitterbauer G, Mullauer L *et al.* (2002) A comparative study on demographic, hematological, and cytogenetic findings and prognosis in acute myeloid leukemia with and without leukemia cutis. *Ann Hematol*;**81**:90-95

Aitken RJ, Baker MA. (2004) Oxidative stress and male reproductive biology. *Reprod Fert Dev*;**16**:581-588

Akhand AA, Pu M, Senga T, Kato M, Suzuki H, Miyata T *et al.* (1999) Nitric oxide controls Src kinase activity through a sulfhydryl group modification-mediated Tyr-527-independent and Tyr-416-linked mechanism. *J Biol Chem*;**274**:25821-25826

Al-Kali A, Cortes J, Faderl S, Jones D, Abril C, Pierce S *et al.* (2011) Patterns of molecular response to and relapse after combination of sorafenib, idarubicin, and cytarabine in patients with FLT3 mutant acute myeloid leukemia. *Clin Lymphoma Myeloma Leuk*;**11**:361-366

Alonso A, Sasin J, Bottini N, Friedberg I, Friedberg I, Osterman A *et al.* (2004) Protein tyrosine phosphatases in the Human Genome. *Cell*;**117**:699-711

Ambasta RK, Griendling KK, Schmidt H, Busse R, Brandes RP. (2004) Direct interaction of the novel nox proteins with p22phox is required for the formation of a functionally active NADPH oxidase. *J Biol Chem*; **279**: 45935-45941.

Ameziane-El-Hassani R, Morand S, Boucher JL, Frapart YM, Apostolou D, Agnandji D *et al* .(2005) Dual oxidase-2 has an intrinsic Ca2+-dependent H2O2-generating activity. *J Biol Chem*;**280**:30046-30054

Andersen JN, Jansen PG, Echwald SM, Mortensen OH, Fukada T, Del Vecchio R *et al.* (2004) A genomic perspective on protein tyrosine phosphatases: gene structure, pseudogenes, and genetic disease linkage. *FASEB J*;**18**:8-30

Anensen N, Skavland J, Stapnes C, Ryningen A, Borresen-Dale AL, Gjertsen BT *et al.* (2006) Acute myelogenous leukemia in a patient with Li-Fraumeni syndrome treated with valproic acid, theophyllamine and all-trans retinoic acid: a case report. *Leukemia*;**20**:734-736

Aplin AE. (2003) Cell adhesion molecule regulation of nucleocytoplasmic trafficking. *FEBS Lett*;**534**:11-14

Aplin AE, Juliano RL. (2001) Regulation of nucleocytoplasmic trafficking by cell adhesion receptors and the cytoskeleton. *J Cell Biol*;**155**:187-191

Appelbaum FR, Baer MR, Carabasi MH, Coutre SE, Erba HP, Estey E *et al.* (2000) NCCN practice guidelines for acute myelogenous leukemia. *Oncology* **14**:53-61

Appenzeller-Herzog C, Riemer J, Zito E, Chin K-T, Ron D, Spiess M *et al* .(2010) Disulphide production by Ero1a-PDI relay is rapid and effectively regulated. *The EMBO journal*;**29**:3318-3329

Arnold RS, Shi J, Murad E, Whalen AM, Sun CQ, Polavarapu R *et al.* (2001) Hydrogen peroxide mediates the cell growth and transformation caused by the mitogenic oxidase Nox1. *Proc Natl Acad Sci U S A*;**98**:5550-5555

Arora D, Kothe S, van den Eijnden M, van Huijsduijnen R, Heidel F, Fischer T *et al.* (2012) Expression of protein-tyrosine phosphatases in Acute Myeloid Leukemia cells: FLT3 ITD sustains high levels of DUSP6 expression. *Cell Comm Signal*;**10**:19

Arora D, Stopp S, Bohmer SA, Schons J, Godfrey R, Masson K *et al.* (2011) Protein-tyrosine phosphatase DEP-1 controls receptor tyrosine kinase FLT3 signaling. *J Biol Chem*;**286**:10918-10929

Arpin M, Chirivino D, Naba A, Zwaenepoel I. (2011) Emerging role for ERM proteins in cell adhesion and migration. *Cell Adh Migr*;**5**:199-206

Arthur JR. (2000) The glutathione peroxidases. *Cell Mol Life Sci*;**57**:1825-1835

Austin H, Delzell E, Cole P. (1988) Benzene and leukemia. A review of the literature and a risk assessment. *Am J Epidemiol*;**127**:419-439

Auvinen E, Kivi N, Vaheri A. (2007) Regulation of ezrin localization by Rac1 and PIPK in human epithelial cells. *Exp Cell Res*;**313**:824-833

Bachmann M, Moroy T. (2005) The serine/threonine kinase Pim-1. *Int J Biochem Cell Biol*;**37**:726-730

Bakst RL, Tallman MS, Douer D, Yahalom J. (2011) How I treat extramedullary acute myeloid leukemia. *Blood*;**118**:3785-3793

Balda MS, Garrett MD, Matter K. (2003) The ZO-1-associated Y-box factor ZONAB regulates epithelial cell proliferation and cell density. *J Cell Biol*;**160**:423-432

Balgobind BV, Van Vlierberghe P, van den Ouweland AM, Beverloo HB, Terlouw-Kromosoeto JN, van Wering ER *et al.* (2008) Leukemia-associated NF1 inactivation in patients with pediatric T-ALL and AML lacking evidence for neurofibromatosis. *Blood*;**111**:4322-4328

Banfi B, Malgrange B, Knisz J, Steger K, Dubois-Dauphin M, Krause KH. (2004a) NOX3, a superoxide-generating NADPH oxidase of the inner ear. *J Biol Chem*;**279**:46065-46072

Banfi B, Molnar G, Maturana A, Steger K, Hegedus B, Demaurex N *et al.* (2001) A Ca(2+)-activated NADPH oxidase in testis, spleen, and lymph nodes. *J Biol Chem*;**276**:37594-37601

Banfi B, Tirone F, Durussel I, Knisz J, Moskwa P, Molnar GZ *et al.* (2004b) Mechanism of Ca2+ activation of the NADPH oxidase 5 (NOX5). *J Biol Chem*;**279**:18583-18591

Barreiro O, Yanez-Mo M, Serrador JM, Montoya MC, Vicente-Manzanares M, Tejedor R *et al.* (2002) Dynamic interaction of VCAM-1 and ICAM-1 with moesin and ezrin in a novel endothelial docking structure for adherent leukocytes. *J Cell Biol*;**157**:1233-1245

Barret C, Roy C, Montcourrier P, Mangeat P, Niggli V. (2000) Mutagenesis of the phosphatidylinositol 4,5-bisphosphate (PIP(2)) binding site in the NH(2)-terminal domain of ezrin correlates with its altered cellular distribution. *J Cell Biol*;**151**:1067-1080

Batchelor CL, Woodward AM, Crouch DH. (2004) Nuclear ERM (ezrin, radixin, moesin) proteins: regulation by cell density and nuclear import. *Exp Cell Res*;**296**:208-222

Battisti V, Maders LDK, Bagatini MD, Santos KF, Spanevello RM, Maldonado PA *et al* .(2008) Measurement of oxidative stress and antioxidant status in acute lymphoblastic leukemia patients. *Clin Biochem*;**41**:511-518

Bedard K, Krause K-H. (2007) The NOX family of ROS-generating NADPH oxidases : physiology and pathophysiology. *Physiol Rev*;**87**:245-313

Bennett JM, Catovsky D, Daniel M-T, Flandrin G, Galton DAG, Gralnick HR *et al.* (1976) Proposals for the classification of the acute leukaemias French-American-British (FAB) co-operative group. *British journal of haematology*;**33**:451-458

Berkelman T, Brubacher M, Chang H, Cross T, Strong W. (2000) Preventing horizontal streaks on 2D gels. *Bio-Rad Laboratories, Inc*

Berlett BS, Stadtman ER. (1997) Protein oxidation in aging, disease, and oxidative stress. *J Biol Chem*;**272**:20313-20316

Berryman M, Gary R, Bretscher A. (1995) Ezrin oligomers are major cytoskeletal components of placental microvilli: a proposal for their involvement in cortical morphogenesis. *J Cell Biol*;**131**:1231-1242

Bey EA, Xu B, Bhattacharjee A, Oldfield CM, Zhao X, Li Q *et al.* (2004) Protein kinase C delta is required for p47phox phosphorylation and translocation in activated human monocytes. *J Immunol*;**173**:5730-5738

Bienert GP, Moller AL, Kristiansen KA, Schulz A, Moller IM, Schjoerring JK *et al.* (2007) Specific aquaporins facilitate the diffusion of hydrogen peroxide across membranes. *J Biol Chem*;**282**:1183-1192

Bizzozero OJ, Jr., Johnson KG, Ciocco A. (1966) Radiation-related leukemia in Hiroshima and Nagasaki, 1946-1964. I. Distribution, incidence and appearance time. *N Engl J Med*;**274**:1095-1101

Bo A, Markova B, Choudhary C, Serve H, Bo F-d. (2005) Tyrosine phosphorylation regulates maturation of receptor tyrosine kinases. *Society*;**25**:3690-3703

Boivin B, Yang M, Tonks NK. (2010) Targeting the reversibly oxidized protein tyrosine phosphatase superfamily. *Sci Signal*;**3**:pl2

Boivin B, Zhang S, Arbiser JL, Zhang Z-Y, Tonks NK. (2008) A modified cysteinyl-labeling assay reveals reversible oxidation of protein tyrosine phosphatases in angiomyolipoma cells. *Proc Natl Acad Sci*;**105**:9959-9964

Bonnet D, Dick J. (1997) Human AML is organized as a hierarchy that originates from a primitive hematopoietic cell. *Nat Med*;**3**:730-737

Brambilla D, Fais S. (2009) The Janus-faced role of ezrin in "linking" cells to either normal or metastatic phenotype. *Int J Cancer*;**125**:2239-2245

Brandts CH, Sargin B, Rode M, Biermann C, Lindtner B, Schwable J *et al.* (2005) Constitutive activation of Akt by Flt3 internal tandem duplications is necessary for increased survival, proliferation, and myeloid transformation. *Cancer Res*;**65**:9643-9650

Bretscher A. (1989) Rapid phosphorylation and re-organization of Ezrin and Spectrin accompany morphological changes induced in A-431 cells by epidermal growth factor. *J Cell Biol*;**108**:921-930

Bretscher A, Edwards K, Fehon RG. (2002) ERM proteins and merlin: integrators at the cell cortex. *Nat Rev Mol Cell Biol*;**3**:586-599

Brioschi M, Polvani G, Fratto P, Parolari A, Agostoni P, Tremoli E *et al.* (2012) Redox proteomics identification of oxidatively modified myocardial proteins in human heart failure: implications for protein function. *PLoS ONE*;**7**:e35841

Brodsky SV, Zhang F, Nasjletti A, Goligorsky MS. (2004) Endothelium-derived microparticles impair endothelial function in vitro. *Am J Physiol Heart Circ Physiol*;**286**:1910-1915

Brown DI, Griendling KK. (2009) Nox proteins in signal transduction. *Free Radic Biol Med*;**47**:1239-1253

Bruserud O, Hovland R, Wergeland L, Huang TS, Gjertsen BT. (2003) Flt3-mediated signaling in human acute myelogenous leukemia (AML) blasts: a functional characterization of Flt3-ligand effects in AML cell populations with and without genetic Flt3 abnormalities. *Haematologica*;**88**:416-428

Bulut G, Hong SH, Chen K, Beauchamp EM, Rahim S, Kosturko GW *et al.* (2012) Small molecule inhibitors of ezrin inhibit the invasive phenotype of osteosarcoma cells. *Oncogene*;**31**:269-281

Burgoyne JR, Madhani M, Cuello F, Charles RL, Brennan JP, Schroder E *et al.* (2007) Cysteine redox sensor in PKGIa enables oxidant-induced activation. *Science*;**317**:1393-1397

Burnham C-AD, Shokoples SE, Tyrrell GJ. (2007) Rac1, RhoA, and Cdc42 participate in HeLa cell invasion by group B streptococcus. *FEMS Microbiol Lett*;**272**:8-14

Butterfield DA, Dalle-Donne I. (2012) Redox Proteomics. *Antioxid Redox Signal*

Butterfield DA., Hardas SS, Lange ML. (2010) Oxidatively modified glyceraldehyde-3-phosphate dehydrogenase (GAPDH) and Alzheimer's disease: many pathways to neurodegeneration. *J Alzheimers Dis*;**20**: 369-393.

Butturini A, Gale RP, Verlander PC, Adler-Brecher B, Gillio AP, Auerbach AD. (1994) Hematologic abnormalities in Fanconi anemia: an International Fanconi Anemia Registry study. *Blood*;**84**:1650-1655

Caligiuri MA, Briesewitz R, Yu J, Wang L, Wei M, Arnoczky KJ *et al.* (2007) Novel c-CBL and CBL-b ubiquitin ligase mutations in human acute myeloid leukemia. *Blood*;**110**:1022-1024

Calo V, Migliavacca M, Bazan V, Macaluso M, Buscemi M, Gebbia N *et al.* (2003) STAT proteins: from normal control of cellular events to tumorigenesis. *J Cell Physiol*;**197**:157-168

Camps M, Nichols A, Arkinstall S. (2000) Dual specificity phosphatases: a gene family for control of MAP kinase function. *FASEB J*;**14**:6-16

Carow CE, Levenstein M, Kaufmann SH, Chen J, Amin S, Rockwell P *et al.* (1996) Expression of the hematopoietic growth factor receptor FLT3 (STK-1/Flk2) in human leukemias. *Blood*;**87**:1089-1096

Carracedo A, Alimonti A, Pandolfi PP. (2011) PTEN level in tumor suppression: how much is too little? *Cancer Res*;**71**:629-633

Cave A. (2009) Selective targeting of NADPH oxidase for cardiovascular protection. *Curr Opin Pharmacol*;**9**:208-213

Chan CB, Liu X, Tang X, Fu H, Ye K. (2007) Akt phosphorylation of zyxin mediates its interaction with acinus-S and prevents acinus-triggered chromatin condensation. *Cell Death Diff*;**14**:1688-1699

Chantrain CF, Jijon P, De Raedt T, Vermylen C, Poirel HA, Legius E *et al.* (2007) Therapy-related acute myeloid leukemia in a child with Noonan syndrome and clonal duplication of the germline PTPN11 mutation. *Pediatr Blood Cancer*;**48**:101-104

Chao Q, Sprankle KG, Grotzfeld RM, Lai AG, Carter TA, Velasco AM *et al.* (2009) Identification of N-(5-tert-butyl-isoxazol-3-yl)-N'-{4-[7-(2-morpholin-4-yl-ethoxy)imidazo[2,1-b][1 ,3]benzothiazol-2-yl]phenyl}urea dihydrochloride (AC220), a uniquely potent, selective, and efficacious FMS-like tyrosine kinase-3 (FLT3) inhibitor. *J Med Chem*;**52**:7808-7816

Chatain N, Ziegler P, Fahrenkamp D, Jost E, Moriggl R, Schmitz-Van de Leur H *et al.* (2012) Src family kinases mediate cytoplasmic retention of activated STAT5 in BCR-ABL-positive cells. *Oncogene*;**27**:369

Chelikani P, Fita I, Loewen PC. (2004) Diversity of structures and properties among catalases. *Cell Mol Life Sci*;**61**:192-208

Chen J, Doctor RB, Mandel LJ. (1994) Cytoskeletal dissociation of ezrin during renal anoxia: role in microvillar injury. *Am J Physiol*;**267**:784-795

Chen K, Craige SE, Keaney JF. (2009) Downstream targets and intracellular compartmentalization in Nox signaling. *Antioxid Redox Signal*;**11**:2467-2480

Chen K, Kirber MT, Xiao H, Yang Y, Keaney JF. (2008a) Regulation of ROS signal transduction by NADPH oxidase 4 localization. *J Cell Biol*;**181**:1129-1139

Chen P, Levis M, Brown P, Kim KT, Allebach J, Small D. (2005) FLT3/ITD mutation signaling includes suppression of SHP-1. *J Biol Chem*;**280**:5361-5369

Chen Q, Massagué J. (2012) Molecular pathways: VCAM-1 as a potential therapeutic target in metastasis. *Clin Cancer Res*;**18**:5520-5525

Chen W, Shang WH, Adachi Y, Hirose K, Ferrari DM, Kamata T. (2008b) A possible biochemical link between NADPH oxidase (Nox) 1 redox-signalling and ERp72. *Biochem J*;**416**:55-63

Cheng G, Cao Z, Xu X, van Meir EG, Lambeth JD. (2001) Homologs of gp91phox: cloning and tissue expression of Nox3, Nox4, and Nox5. *Gene*;**269**:131-140

Chiarugi P. (2008) Minireview Src redox regulation : there is more than meets the eye. *Mol Cells*;**26**:329-337

Chiarugi P, Buricchi F. (2007) Protein tyrosine phosphorylation and reversible oxidation: two cross-talking posttranslation modifications. *Antioxid Redox Signal*;**9**:1-24

Chiarugi P, Cirri P. (2003) Redox regulation of protein tyrosine phosphatases during receptor tyrosine kinase signal transduction. *Trends Biochem Sci*;**28**:509-514

Choi HK, Kim TH, Jhon G-J, Lee SY. (2011) Reactive oxygen species regulate M-CSF-induced monocyte/macrophage proliferation through SHP1 oxidation. *Cell Signal*;**23**:1633-1639

Choi MH, Lee IK, Kim GW, Kim BU, Han YH, Yu DY *et al.* (2005) Regulation of PDGF signalling and vascular remodelling by peroxiredoxin II. *Nature*;**435**:347-353

Chou HC, Chen YW, Lee TR, Wu FS, Chan HT, Lyu PC *et al.* (2010) Proteomics study of oxidative stress and Src kinase inhibition in H9C2 cardiomyocytes: a cell model of heart ischemia-reperfusion injury and treatment. *Free Radic Biol Med*;**49**:96-108

Choudhary C, Brandts C, Schwable J, Tickenbrock L, Sargin Bl, Ueker A *et al.* (2007) Activation mechanisms of STAT5 by oncogenic Flt3-ITD. *Blood*;**110**:370-374

Choudhary C, Muller-Tidow C, Berdel WE, Serve H. (2005) Signal transduction of oncogenic Flt3. *Int J Hematol*;**82**:93-99

Choudhary C, Olsen JV, Brandts C, Cox J, Reddy PNG, Bohmer FD *et al.* (2009) Mislocalized activation of oncogenic RTKs switches downstream signaling outcomes. *Mol Cell*;**36**:326-339

Chowdhury AK, Watkins T, Parinandi NL, Saatian B, Kleinberg ME, Usatyuk PV *et al.* (2005) Src-mediated tyrosine phosphorylation of p47phox in hyperoxia-induced activation of NADPH oxidase and generation of reactive oxygen species in lung endothelial cells. *J Biol Chem*;**280**:20700-20711

Christiansen DH, Andersen MK, Pedersen-Bjergaard J. (2003) Methylation of p15INK4B is common, is associated with deletion of genes on chromosome arm 7q and predicts a poor prognosis in therapy-related myelodysplasia and acute myeloid leukemia. *Leukemia*;**17**:1813-1819

Christiansen DH, Andersen MK, Pedersen-Bjergaard J. (2001) Mutations with loss of heterozygosity of p53 are common in therapy-related myelodysplasia and acute myeloid leukemia after exposure to alkylating agents and significantly associated with deletion or loss of 5q, a complex karyotype, and a poor prognosis. *J Clin Oncol*;**19**:1405-1413

Chu Y, Solski PA, Khosravi-Far R, Der CJ, Kelly K. (1996) The mitogen-activated protein kinase phosphatases PAC1, MKP-1, and MKP-2 have unique substrate specificities and reduced activity in vivo toward the ERK2 sevenmaker mutation. *J Biol Chem*;**271**:6497-6501

Ciechanover A, DiGiuseppe JA, Bercovich B, Orian A, Richter JD, Schwartz AL *et al.* (1991) Degradation of nuclear oncoproteins by the ubiquitin system in vitro. *Proc Natl Acad Sci*;**88**:139-143

Cifuentes-Pagano E, Csanyi G, Pagano P. (2012) NADPH oxidase inhibitors: a decade of discovery from Nox2ds to HTS. *Cell Mol Life Sci*;**69**:2315-2325

Clayton AL, Hazzalin CA, Mahadevan LC. (2006) Enhanced histone acetylation and transcription: a dynamic perspective. *Mol Cell*;**23**:289-296

Clifford SC, Cockman ME, Smallwood AC, Mole DR, Woodward ER, Maxwell PH *et al.* (2001) Contrasting effects on HIF-1α regulation by disease-causing pVHL mutations correlate with patterns of tumourigenesis in von Hippel-Lindau disease. *Human Mol Genet*;**10**:1029-1038

Coffey GP, Rajapaksa R, Liu R, Sharpe O, Kuo C-C, Krauss SW *et al.* (2009) Engagement of CD81 induces ezrin tyrosine phosphorylation and its cellular redistribution with filamentous actin. *J Cell Sci*;**122**:3137-3144

Colavitti R, Finkel T. (2005) Reactive Oxygen Species as Mediators of Cellular Senescence. *IUBMB Life*;**57**:277-281

Conboy JG. (1993) Structure, function, and molecular genetics of erythroid membrane skeletal protein 4.1 in normal and abnormal red blood cells. *Sem Hematol*;**30**:58-73

Conrad M, Sandin A, Forster H, Seiler A, Frijhoff J, Dagnell M *et al.* (2010) 12/15-lipoxygenase-derived lipid peroxides control receptor tyrosine kinase signaling through oxidation of protein tyrosine phosphatases. *Proc Natl Acad Sci*;**107**:15774-15779

Cooke MS, Evans MD, Dizdaroglu M, Lunec J. (2003) Oxidative DNA damage: mechanisms, mutation, and disease. *FASEB J*;**17**:1195-1214

Corcoran A, Cotter TG. (2013) FLT3-driven redox-modulation of Ezrin regulates leukemic cell migration. *Free Radic Res*;**47**:20-34

Cordray P, Doyle K, Edes K, Moos PJ, Fitzpatrick FA. (2007) Oxidation of 2-Cys-peroxiredoxins by arachidonic acid peroxide metabolites of lipoxygenases and cyclooxygenase-2. *J Biol Chem*;**282**:32623-32629

Corn PG, Smith BD, Ruckdeschel ES, Douglas D, Baylin SB, Herman JG. (2000) E-cadherin expression is silenced by 5' CpG island methylation in acute leukemia. *Clin Cancer Res*;**6**:4243-4248

Crawley JB, Rawlinson L, Lali FV, Page TH, Saklatvala J, Foxwell BMJ. (1997) T Cell Proliferation in Response to Interleukins 2 and 7 Requires p38MAP Kinase Activation. *J Biol Chem*;**272**:15023-15027

Crepaldi T, Gautreau A, Comoglio PM, Louvard D, Arpin M. (1997) Ezrin is an effector of hepatocyte growth factor-mediated migration and morphogenesis in epithelial cells. *J Cell Biol*;**138**:423-434

Cross AR. (2000) p40(phox) Participates in the activation of NADPH oxidase by increasing the affinity of p47(phox) for flavocytochrome b(558). *Biochem J*;**349**:113-117

Cunnick JM, Dorsey JF, Standley T, Turkson J, Kraker AJ, Fry DW *et al.* (1998) Role of tyrosine kinase activity of epidermal growth factor receptor in the lysophosphatidic acid-stimulated mitogen-activated protein kinase pathway. *J Biol Chem*;**273**:14468-14475

Dalle-Donne I, Rossi R, Colombo G, Giustarini D & Milzani A. (2009) Protein S-glutathionylation: a regulatory device from bacteria to humans. *Trends Biochem Sci ;***34**: 85-96.

Dang L, Jin S, Su SM. (2010) IDH mutations in glioma and acute myeloid leukemia. *Trends Mol Med*;**16**:387-397

Dang PM, Stensballe A, Boussetta T, Raad H, Dewas C, Kroviarski Y *et al.* (2006) A specific p47phox -serine phosphorylated by convergent MAPKs mediates neutrophil NADPH oxidase priming at inflammatory sites. *J Clin Invest*;**116**:2033-2043

Davies MJ. (2005) The oxidative environment and protein damage. *Biochim Biophys Acta - Proteins and Proteomic;* **1703**: 93-109

De Deken X, Wang D, Many M-C, Costagliola S, Libert F, Vassart G *et al.* (2000) Cloning of two human thyroid cDNAs encoding new members of the NADPH oxidase family. *J Biol Chem*;**275**:23227-23233

DeAngelo DJ, Stone RM, Heaney ML, Nimer SD, Paquette RL, Klisovic RB *et al.* (2006) Phase 1 clinical results with tandutinib (MLN518), a novel FLT3 antagonist, in patients with acute myelogenous leukemia or high-risk myelodysplastic syndrome: safety, pharmacokinetics, and pharmacodynamics. *Blood*;**108**:3674-3681

Deem TL, Cook-Mills JM. (2004) Vascular cell adhesion molecule 1 (VCAM-1) activation of endothelial cell matrix metalloproteinases: role of reactive oxygen species. *Blood*;**104**:2385-2393

DeLeo FR, Burritt JB, Yu L, Jesaitis AJ, Dinauer MC, Nauseef WM. (2000) Processing and maturation of flavocytochrome b558 include incorporation of heme as a prerequisite for heterodimer assembly. *J Biol Chem*;**275**:13986-13993

Denu JM, Tanner KG. (1998) Specific and reversible inactivation of protein tyrosine phosphatases by hydrogen peroxide: evidence for a sulfenic acid intermediate and implications for redox regulation. *Biochemistry*;**37**:5633-5642

Di Fiore PP, Polo S, Hofmann K. (2003) When ubiquitin meets ubiquitin receptors: a signalling connection. *Nat Rev Mol Cell Biol*;**4**:491-497

Diaz BA, Shani G, Pass I, Anderson D, Quintavalle M, Courtneidge SA. (2009) Tks5-dependent, nox-mediated generation of reactive oxygen species is necessary for invadopodia formation. *Sci Signal*;**2**:ra53

Dohner K, Dohner H. (2008) Molecular characterization of acute myeloid leukemia. *Internal Medicine*;**93**:2-8

Dosil M, Wang S, Lemischka IR. (1993) Mitogenic signalling and substrate specificity of the Flk2/Flt3 receptor tyrosine kinase in fibroblasts and interleukin 3-dependent hematopoietic cells. *Mol Cell Biol*;**13**:6572-6585

Douglas P, Zhong J, Ye R, Moorhead GBG, Xu X, Lees-Miller SP. (2010) Protein Phosphatase 6 Interacts with the DNA-Dependent Protein Kinase Catalytic Subunit and Dephosphorylates γ-H2AX. *Mol Cell Biol*;**30**:1368-1381

Douglas Smith B. (2011) Imatinib for Chronic Myeloid Leukemia: The Impact of Its Effectiveness and Long-term Side Effects. *J Nat Cancer Inst*

Edens WA, Sharling L, Cheng G, Shapira R, Kinkade JM, Lee T *et al.* (2001) Tyrosine cross-linking of extracellular matrix is catalyzed by Duox, a multidomain oxidase/peroxidase with homology to the phagocyte oxidase subunit gp91phox. *J Cell Biol*;**154**:879-891

Erickson JR, Joiner ML, Guan X, Kutschke W, Yang J, Oddis CV *et al.* (2008) A dynamic pathway for calcium-independent activation of CaMKII by methionine oxidation. *Cell*;**133**:462-474

Esendagli G, Canpinar H, Lale Dogan A, Akkaya M, Kansu E, Guc D. (2009) Transfection of myeloid leukaemia cell lines is distinctively regulated by fibronectin substratum. *Cytotechnology*;**61**:45-53

Estey EH. (2001) Therapeutic options for acute myelogenous leukemia. *Cancer*;**92**:1059-1073

Eswaran J, Debreczeni JE, Longman E, Barr AJ, Knapp S. (2006) The crystal structure of human receptor protein tyrosine phosphatase kappa phosphatase domain 1. *Protein Sci*;**15**:1500-1505

Etoh T, Inoguchi T, Kakimoto M, Sonoda N, Kobayashi K, Kuroda J *et al.* (2003) Increased expression of NAD(P)H oxidase subunits, NOX4 and p22phox, in the kidney of streptozotocin-induced diabetic rats and its reversibity by interventive insulin treatment. *Diabetologia*;**46**:1428-1437

Evans DI, Steward JK. (1972) Down's syndrome and leukaemia. *Lancet*;**2**:1322

Fais S. (2004) A role for ezrin in a neglected metastatic tumor function. *Trends Mol Med*;**10**:249-250

Farquhar M, Bowen D. (2003) Oxidative Stress and the Myelodysplastic Syndromes. *Int J Hematol*;**77**:342-350

Fazioli F, Wong WT, Ullrich SJ, Sakaguchi K, Appella E, Di Fiore PP. (1993) The ezrin-like family of tyrosine kinase substrates: receptor-specific pattern of tyrosine phosphorylation and relationship to malignant transformation. *Oncogene*;**8**:1335-1345

Federici C, Brambilla D, Lozupone F, Matarrese P, Milito Ad, Lugini L *et al.* (2009) Pleiotropic function of ezrin in human metastatic melanomas. *Int J Cancer*;**124**: 2804–2812

Fehon RG, McClatchey AI, Bretscher A. (2010) Organizing the cell cortex: the role of ERM proteins. *Nat Rev Mol Cell Biol*;**11**:276-287

Ferraro D, Corso S, Fasano E, Panieri E, Santangelo R, Borrello S *et al.* (2006) Pro-metastatic signaling by c-Met through RAC-1 and reactive oxygen species (ROS). *Oncogene*;**25**:3689-3698

Fialkow PJ, Singer JW, Adamson JW, Vaidya K, Dow LW, Ochs J *et al.* (1981) Acute nonlymphocytic leukemia: heterogeneity of stem cell origin. *Blood*;**57**:1068-1073

Fischer T, Stone RM, Deangelo DJ, Galinsky I, Estey E, Lanza C *et al.* (2010) Phase IIB trial of oral Midostaurin (PKC412), the FMS-like tyrosine kinase 3 receptor (FLT3) and multi-targeted kinase inhibitor, in patients with acute myeloid leukemia and high-risk myelodysplastic syndrome with either wild-type or mutated FLT3. *J Clin Oncol*;**28**:4339-4345

Fomenko DE, Xing W, Adair BM, Thomas DJ, Gladyshev VN. (2007) High-throughput identification of catalytic redox-active cysteine residues. *Science*;**315**:387-389

Fontayne A, Dang PM-C, Gougerot-Pocidalo M-A, El Benna J. (2002) Phosphorylation of p47phox sites by PKC α, βII, δ, and ζ: effect on binding to p22phox and on NADPH oxidase activation. *Biochemistry*;**41**:7743-7750

Forte E, Orsatti L, Talamo F, Barbato G, De Francesco R, Tomei L. (2008) Ezrin is a specific and direct target of protein tyrosine phosphatase PRL-3. *Biochim Biophys Acta*;**1783**:334-344

Fukuda S, Broxmeyer HE, Pelus LM. (2005) Flt3 ligand and the Flt3 receptor regulate hematopoietic cell migration by modulating the SDF-1alpha(CXCL12)/CXCR4 axis. *Blood*;**105**:3117-3126

Fukuda S, Pelus LM. (2006) Internal tandem duplication of Flt3 modulates chemotaxis and survival of hematopoietic cells by SDF1alpha but negatively regulates marrow homing in vivo. *Exp Hematol*;**34**:1041-1051

Fukuda S, Singh P, Moh A, Abe M, Conway EM, Boswell HS *et al.* (2009) Survivin mediates aberrant hematopoietic progenitor cell proliferation and acute leukemia in mice induced by internal tandem duplication of Flt3. *Blood*;**114**:394-403

Galli S, Antico Arciuch VG, Poderoso C, Converso DP, Zhou Q, de Kier Joffé EB *et al.* (2008) Tumor cell phenotype is sustained by selective MAPK oxidation in mitochondria. *PLoS ONE*;**3**:e2379

Gao H-M, Zhou H, Hong J-S. (2012) NADPH oxidases: novel therapeutic targets for neurodegenerative diseases. *Trends Pharm Sci*;**33**:295-303

Gao Y, Dickerson JB, Guo F, Zheng J, Zheng Y. (2004) Rational design and characterization of a Rac GTPase-specific small molecule inhibitor. *Proc Natl Acad Sci*;**101**:7618-7623

Garfin DE. Cell structure, a practical approach. In: Davey J, Ward M, editors. Essential cell biology. Volume 1. Oxford, UK: Oxford University Publisher; 2003. p 197-268.

Gary R, Bretscher A. (1995) Ezrin self-association involves binding of an N-terminal domain to a normally masked C-terminal domain that includes the F-actin binding site. *Mol Biol Cell*;**6**:1061-1075

Gauffin F, Diffner E, Gustafsson B, Nordgren A, Wingren AG, Sander B *et al.* (2009) Expression of PTEN and SHP1, investigated from tissue microarrays in pediatric acute lymphoblastic, leukemia. *Pediatr Hematol Oncol*;**26**:48-56

Gautreau A, Poullet P, Louvard D, Arpin M. (1999) Ezrin, a plasma membrane-microfilament linker, signals cell survival through the phosphatidylinositol 3-kinase/Akt pathway. *Proc Natl Acad Sci*;**96**:7300-7305

Gianni D, Diaz B, Taulet N, Fowler B, Courtneidge SA, Bokoch GM. (2009) Novel p47(phox)-related organizers regulate localized NADPH oxidase 1 (Nox1) activity. *Sci Signal*;**2**:ra54

Gianni D, Taulet N, DerMardirossian C, Bokoch GM. (2011) cSrc-mediated phosphorylation of NoxA1 and Tks4 induces the reactive oxygen species (ROS)-dependent formation of functional invadopodia in human colon cancer cells. *Mol Biol Cell*;**21**:4287-4298

Gianni D, Taulet N, Zhang H, DerMardirossian C, Kister J, Martinez L *et al.* (2010) A Novel and Specific NADPH Oxidase-1 (Nox1) Small-molecule inhibitor blocks the formation of functional invadopodia in human colon cancer cells. *ACS Chem Biol*;**5**:981-993

Giannoni E, Buricchi F, Raugei G, Ramponi G, Chiarugi P. (2005) Intracellular reactive oxygen species activate Src tyrosine kinase during cell adhesion and anchorage-dependent Cell Growth *Mol Cell Biol*;**25**:6391-6403

Giannoni E, Taddei ML, Chiarugi P. (2010) Src redox regulation: again in the front line. *Free Radic Biol Med*;**49**:516-527

Gilbert C, Rollet-Labelle E, Naccache PH. (2002) Preservation of the pattern of tyrosine phosphorylation in human neutrophil lysates. II. A sequential lysis protocol for the analysis of tyrosine phosphorylation-dependent signalling. *J Immunol Methods*;**261**:85-101

Giles FJ, Stopeck AT, Silverman LR, Lancet JE, Cooper MA, Hannah AL *et al.* (2003) SU5416, a small molecule tyrosine kinase receptor inhibitor, has biologic activity in patients with refractory acute myeloid leukemia or myelodysplastic syndromes. *Blood*;**102**:795-801

Gill PS, Wilcox CS. (2006) NADPH oxidases in the kidney. *Antioxid Redox Signal*;**8**:1597-1607

Gilliland DG, Griffin JD. (2002) The roles of FLT3 in hematopoiesis and leukemia. *Blood*;**100**:1532-1542

Giustarini D, Milzani A, Aldini G, Carini M, Rossi R and Dalle-Donne I. (2005) S-nitrosation versus S-glutathionylation of protein sulfhydryl groups by S-nitrosoglutathione. *Antioxid Redox Signal* ;**7**: 930-939.

Godfrey R, Arora D, Bauer R, Stopp S, Muller JP, Heinrich T *et al.* (2012) Cell transformation by FLT3 ITD in acute myeloid leukemia involves oxidative inactivation of the tumor suppressor protein-tyrosine phosphatase DEP-1/ PTPRJ. *Blood*;**119**:4499-4511

Gorin Y, Ricono JM, Kim NH, Bhandari B, Choudhury GG, Abboud HE. (2003) Nox4 mediates angiotensin II-induced activation of Akt/protein kinase B in mesangial cells. *Am J Physiol Renal Physiol*;**285**:F219-229

Gorlach A, Brandes RP, Nguyen K, Amidi M, Dehghani F, Busse R. (2000) A gp91phox containing NADPH oxidase selectively expressed in endothelial cells is a major source of oxygen radical generation in the arterial wall. *Circ Res*;**87**:26-32

Greene EL, Houghton O, Collinsworth G, Garnovskaya MN, Nagai T, Sajjad T, Bheemanathini V, Grewal JS, Paul RV, Raymond JR. (2000) 5-HT(2A) receptors stimulate mitogen-activated protein kinase via H(2)O(2) generation in rat renal mesangial cells. *Am J Physiol Renal Physiol;* **278**: F650-658

Griendling KK, Minieri CA, Ollerenshaw JD, Alexander RW. (1994) Angiotensin II stimulates NADH and NADPH oxidase activity in cultured vascular smooth muscle cells. *Circ Res*;**74**:1141-1148

Griffin JD, Lowenberg B. (1986) Clonogenic cells in acute myeloblastic leukemia. *Blood*;**68**:1185-1195

Groen A, Lemeer S, van der Wijk T, Overvoorde J, Heck AJR, Ostman A *et al.* (2005) Differential oxidation of protein-tyrosine phosphatases. *J Biol Chem*;**280**:10298-10304

Gu T-l, Nardone J, Wang Y, Loriaux M, Villén J, Beausoleil S *et al.* (2011) Survey of activated FLT3 signaling in leukemia. *PLoS ONE*;**6**:e19169

Gunz FW, Veale AM. (1969) Leukemia in close relatives--accident or predisposition? *J Natl Cancer Inst*;**42**:517-524

Guo Z, Kozlov S, Lavin MF, Person MD, Paull TT. (2010) ATM activation by oxidative stress. *Science*;**330**:517-521

Guttmann RP, Ghoshal S. (2011) Thiol-protease oxidation in age-related neuropathology. *Free Radic Biol Med*;**51**:282-288

Gwin K, Frank E, Bossou A, Medina KL. (2010) Hoxa9 regulates Flt3 in lymphohematopoietic progenitors. *J Immunol*;**185**:6572-6583

G, Grasset MF, Kieffer-Jaquinod S, Kuhn L, Mouchiroud G, Gobert-Gosse S. (2013) Phosphoproteome analyses reveal specific implications of Hcls1, p21-Activated Kinase 1 and Ezrin in proliferation of a myeloid progenitor cell line downstream of wild-type and ITD mutant Fms-like Tyrosine kinase 3 receptors. *J Proteomics;*E-pub doi: 10.1016/j.jprot.2012.09.009

Haferlach C, Dicker F, Herholz H, Schnittger S, Kern W, Haferlach T. (2008) Mutations of the TP53 gene in acute myeloid leukemia are strongly associated with a complex aberrant karyotype. *Leukemia*;**22**:1539-1541

Haglund K, Di Fiore PP, Dikic I. (2003a) Distinct monoubiquitin signals in receptor endocytosis. *Trends Biochem Sci*;**28**:598-603

Haglund K, Dikic I. (2005) Ubiquitylation and cell signaling. *EMBO J*;**24**:3353-3359

Haglund K, Sigismund S, Polo S, Szymkiewicz I, Di Fiore PP, Dikic I. (2003b) Multiple monoubiquitination of RTKs is sufficient for their endocytosis and degradation. *Nat Cell Biol*;**5**:461-466

Hamanaka RB, Chandel NS. (2011)Warburg effect and redox balance. *Science*; **334**:1219-1220.

Hanafusa H, Torii S, Yasunaga T, Matsumoto K, Nishida E. (2004) Shp2, an SH2-containing protein-tyrosine phosphatase, positively regulates receptor tyrosine kinase signaling by dephosphorylating and inactivating the inhibitor Sprouty. *J Biol Chem*;**279**:22992-22995

Hanahan D, Weinberg RA. (2000) The hallmarks of cancer. *Cell*;**100**:57-70

Haque A, Andersen JN, Salmeen A, Barford D, Tonks NK. (2011) Conformation-Sensing Antibodies Stabilize the Oxidized Form of PTP1B and Inhibit Its Phosphatase Activity. *Cell*;**147**:185-198

Hart BA, Simons JM, Knaan-Shanzer S, Bakker NP, Labadie RP. (1990) Antiarthritic activity of the newly developed neutrophil oxidative burst antagonist apocynin. *Free Radic Biol Med*;**9**:127-131

Hayakawa F, Towatari M, Kiyoi H, Tanimoto M, Kitamura T, Saito H *et al.* (2000) Tandem-duplicated Flt3 constitutively activates STAT5 and MAP kinase and introduces autonomous cell growth in IL-3-dependent cell lines. *Oncogene*;**19**:624-631

Hayashi K, Yonemura S, Matsui T, Tsukita S. (1999) Immunofluorescence detection of ezrin/radixin/moesin (ERM) proteins with their carboxyl-terminal threonine phosphorylated in cultured cells and tissues. *J Cell Sci*;**112** 1149-1158

Heiska L, Carpen O. (2005) Src phosphorylates ezrin at tyrosine 477 and induces a phosphospecific association between ezrin and a kelch-repeat protein family member. *J Biol Chem*;**280**:10244-10252

Heiska L, Melikova M, Zhao F, Saotome I, McClatchey aI, Carpen O. (2011) Ezrin is key regulator of Src-induced malignant phenotype in three-dimensional environment. *Oncogene*:1-10

Henricks PA, Nijkamp FP. (2001) Reactive oxygen species as mediators in asthma. *Pulm Pharmacol Ther*;**14**:409-420

Heo J. (2011) Redox control of GTPases: from molecular mechanisms to functional significance in health and disease. *Antioxid Redox Signal*;**14**:689-724

Herman JG, Civin CI, Issa JP, Collector MI, Sharkis SJ, Baylin SB. (1997) Distinct patterns of inactivation of p15INK4B and p16INK4A characterize the major types of hematological malignancies. *Cancer Res*;**57**:837-841

Hershko A, Ciechanover A. (1998) The ubiquitin system. *Annu Rev Biochem*;**67**:425-479

Hess DT, Matsumoto A, Kim SO, Marshall HE, Stamler JS. (2005) Protein S-nitrosylation: purview and parameters. *Nat Rev Mol Cell Biol;* **6**: 150-166.

Heumuller S, Wind S, Barbosa-Sicard E, Schmidt HHHW, Busse R, Schroder K *et al.* (2008) Apocynin is not an inhibitor of vascular NADPH oxidases but an antioxidant. *Hypertension*;**51**:211-217

Hexner EO, Serdikoff C, Jan M, Swider CR, Robinson C, Yang S *et al.* (2008) Lestaurtinib (CEP701) is a JAK2 inhibitor that suppresses JAK2/STAT5 signaling and the proliferation of primary erythroid cells from patients with myeloproliferative disorders. *Blood*;**111**:5663-5671

Heymes C, Bendall JK, Ratajczak P, Cave AC, Samuel J-L, Hasenfuss G *et al.* (2003) Increased myocardial NADPH oxidase activity in human heart failure. *J Am Coll Cardiol*;**41**:2164-2171

Hicke L. (2001) Protein regulation by monoubiquitin. *Nat Rev Mol Cell Biol*;**2**:195-201

Hofmann W, Reichart B, Ewald a, Muller E, Schmitt I, Stauber RH *et al.* (2001) Cofactor requirements for nuclear export of Rev response element (RRE)- and constitutive transport element (CTE)-containing retroviral RNAs. An unexpected role for actin. *J Cell Biol*;**152**:895-910

Hole PS, Darley RL, Tonks A. (2012) Do reactive oxygen species play a role in myeloid leukemias? *Blood*;**117**:5816-5826

Hong H, Zeng J-S, Kreulen DL, Kaufman DI, Chen AF. (2006) Atorvastatin protects against cerebral infarction via inhibition of NADPH oxidase-derived superoxide in ischemic stroke. *Am J Physiol Heart Circ Physiol*;**291**:H2210-H2215

Hordijk PL. (2006) Regulation of NADPH oxidases. *Circ Res*;**98**:453-462

Hoshi T and Heinemann S. (2001) Regulation of cell function by methionine oxidation and reduction. *J Physiol;***531**: 1-11.

Hoyal CR, Gutierrez A, Young BM, Catz SD, Lin JH, Tsichlis PN *et al.* (2003) Modulation of p47PHOX activity by site-specific phosphorylation: Akt-dependent activation of the NADPH oxidase. *Proc Natl Acad Sci U S A*;**100**:5130-5135

Humphries KM, Deal MS, Taylor SS. (2005) Enhanced dephosphorylation of cAMP-dependent protein kinase by oxidation and thiol modification. *J Biol Chem*;**280**:2750-2758

Hunter T. (2009) Tyrosine phosphorylation: thirty years and counting. *Curr Opin Cell Biol*;**21**:140-146

Issa JP, Zehnbauer BA, Civin CI, Collector MI, Sharkis SJ, Davidson NE *et al.* (1996) The estrogen receptor CpG island is methylated in most hematopoietic neoplasms. *Cancer Res*;**56**:973-977

Issa JP, Zehnbauer BA, Kaufmann SH, Biel MA, Baylin SB. (1997) HIC1 hypermethylation is a late event in hematopoietic neoplasms. *Cancer Res*;**57**:1678-1681

Jackson SH, Devadas S, Kwon J, Pinto LA, Williams MS. (2004) T cells express a phagocyte-type NADPH oxidase that is activated after T cell receptor stimulation. *Nat Immunol*;**5**:818-827

Jaenisch R, Bird A. (2003) Epigenetic regulation of gene expression: how the genome integrates intrinsic and environmental signals. *Nat Genet*;**33** 245-254

Janssen-Heininger YM, Mossman BT, Heintz NH, Forman HJ, Kalyanaraman B, Finkel T, Stamler JS, Rhee SG, van der Vliet A. (2008) Redox-based regulation of signal transduction: principles, pitfalls, and promises. *Free Radic Biol Med*; **45**:1-17.

Jaquet V, Scapozza L, Clark RA, Krause KH, Lambeth JD.(2009) Small-molecule NOX inhibitors: ROS-generating NADPH oxidases as therapeutic targets. *Antioxid Redox Signal*;**11**:2535-2552

Jay DB, Papaharalambus CA, Seidel-Rogol B, Dikalova AE, Lassegue B, Griendling KK. (2008) Nox5 mediates PDGF-induced proliferation in human aortic smooth muscle cells. *Free Radic Biol Med*;**45**:329-335

Jemal A, Thomas A, Murray T, Thun M. (2002) Cancer statistics 2002. *CA Cancer J Clin*;**52**:23-47

Jiang L, He L, Fountoulakis M. (2004) Comparison of protein precipitation methods for sample preparation prior to proteomic analysis. *J Chromatog*;**1023**:317-320

Juarez JC, Manuia M, Burnett ME, Betancourt O, Boivin B, Shaw DE *et al.* (2008) Superoxide dismutase 1 (SOD1) is essential for H2O2-mediated oxidation and inactivation of phosphatases in growth factor signaling. *Proc Natl Acad Sci*;**105**:7147-7152

Julien SG, Dube N, Hardy S, Tremblay ML. (2011) Inside the human cancer tyrosine phosphatome. *Nat Rev Cancer*;**11**:35-49

Kanai F, Liu H, Field SJ, Akbary H, Matsuo T, Brown GE *et al.* (2001) The PX domains of p47phox and p40phox bind to lipid products of PI(3)K. *Nat Cell Biol*;**3**:675-678

Kantarjian H, O'Brien S, Cortes J, Wierda W, Faderl S, Garcia-Manero G *et al.* (2008) Therapeutic advances in leukemia and myelodysplastic syndrome over the past 40 years. *Cancer*;**113**:1933-1952

Karisch R, Fernandez M, Taylor P, Virtanen C, St-Germain Jonathan R, Jin Lily L *et al.* (2011) Global proteomic assessment of the classical protein-tyrosine phosphatome and "redoxome". *Cell*;**146**:826-840

Kato M, Iwashita T, Takeda K, Akhand AA, Liu W, Yoshihara M *et al.* (2000) Ultraviolet light induces redox reaction-mediated dimerization and superactivation of oncogenic Ret tyrosine kinases. *Mol Biol Cell*;**11**:93-101

Kawahara T, Ritsick D, Cheng G, Lambeth JD. (2005) Point mutations in the proline-rich region of p22phox are dominant inhibitors of Nox1- and Nox2-dependent reactive oxygen generation. *J Biol Chem*;**280**:31859-31869

Kawashima T, Bao YC, Nomura Y, Moon Y, Tonozuka Y, Minoshima Y *et al.* (2006) Rac1 and a GTPase-activating protein, MgcRacGAP, are required for nuclear translocation of STAT transcription factors. *J Cell Biol*;**175**:937-946

Kemble DJ, Sun G. (2009) Direct and specific inactivation of protein tyrosine kinases in the Src and FGFR families by reversible cysteine oxidation. *Proc Natl Acad Sci*;**106**:5070-5075

Kim A, Balis FM, Widemann BC. (2009) Sorafenib and Sunitinib. *The Oncologist*;**14**:800-805

Kim J-A, Neupane GP, Lee ES, Jeong B-S, Park BC, Thapa P. (2012) NADPH oxidase inhibitors: a patent review. *Exp OpinTherap Pat*;**21**:1147-1158

Kim S-Y, Lee J-G, Cho W-S, Cho K-H, Sakong J, Kim J-R *et al.* (2010) Role of NADPH oxidase-2 in lipopolysaccharide-induced matrix metalloproteinase expression and cell migration. *Immunol Cell Biol*;**88**:197-204

Kim YS, Morgan MJ, Choksi S, Liu ZG. (2007) TNF-induced activation of the Nox1 NADPH oxidase and its role in the induction of necrotic cell death. *Mol Cell*;**26**:675-687

Kindler T, Lipka DB, Fischer T. (2010) FLT3 as a therapeutic target in AML: still challenging after all these years. *Blood*;**116**:5089-5102

Kishore R, Qin G, Luedemann C, Bord E, Hanley A, Silver M *et al* .(2005) The cytoskeletal protein ezrin regulates EC proliferation and angiogenesis via TNF-alpha induced transcriptional repression of cyclin A. *J Clin Invest*;**115**

Knapper S, Burnett AK, Littlewood T, Kell WJ, Agrawal S, Chopra R *et al.* (2006) A phase 2 trial of the FLT3 inhibitor lestaurtinib (CEP701) as first-line treatment for older patients with acute myeloid leukemia not considered fit for intensive chemotherapy. *Blood*;**108**:3262-3270

Knaus UG, Heyworth PG, Evans T, Curnutte JT, Bokoch GM. (1991) Regulation of phagocyte oxygen radical production by the GTP-binding protein Rac 2. *Science*;**254**:1512-1515

Kobayashi T, Kusuda K, Ohnishi M, Wang H, Ikeda S, Hanada M *et al.* (1998) Isoform specific phosphorylation of protein phosphatase 2C expressed in COS7 cells. *FEBS Letters*;**430**:222-226

Kojima K, Konopleva M, Samudio IJ, Shikami M, Cabreira-Hansen M, McQueen T *et al.* (2005) MDM2 antagonists induce p53-dependent apoptosis in AML: implications for leukemia therapy. *Blood*;**106**:3150-3159

Kondo T, Takeuchi K, Doi Y, Yonemura S, Nagata S, Tsukita S. (1997) ERM (ezrin/radixin/moesin)-based molecular mechanism of microvillar breakdown at an early stage of apoptosis. *J Cell Biol*;**139**:749-758

Kosmider O, Gelsi-Boyer Vr, Cheok M, Grabar S, Della-Valle Vr, Picard Fo *et al.* (2009) TET2 mutation is an independent favorable prognostic factor in myelodysplastic syndromes (MDSs). *Blood*;**114**:3285-3291

Krause JR. (1979) Granulocytic sarcoma preceding acute leukemia: a report of six cases. *Cancer*;**44**:1017-1021

Krause KH, Lambeth D, Kronke M. (2012) NOX enzymes as drug targets. *Cell Mol Life Sci*;**69**:2279-2282

Krauss SW, Larabell CA, Lockett S, Gascard P, Penman S, Mohandas N *et al.* (1997) Structural protein 4.1 in the nucleus of human cells: dynamic rearrangements during cell division. *J Cell Biol*;**137**:275-289

Krieg J, Hunter T. (1992) Identification of the two major epidermal growth factor-induced tyrosine phosphorylation sites in the microvillar core protein ezrin. *J Biol Chem*;**267**:19258-19265

Kruger A, Gruning NM,Wamelink M M, Kerick M, Kirpy A, Parkhomchuk D, Bluemlein K, Schweiger MR, Soldatov A, Lehrach H, Jakobs C, Ralser M. (2011) The pentose phosphate pathway is a metabolic redox sensor and regulates transcription during the antioxidant response. *Antioxid Redox Signal*;**15**:311-324

Kuribayashi F, Nunoi H, Wakamatsu K, Tsunawaki S, Sato K, Ito T *et al.* (2002) The adaptor protein p40(phox) as a positive regulator of the superoxide-producing phagocyte oxidase. *Embo J*;**21**:6312-6320

Kwon J, Lee S-R, Yang K-S, Ahn Y, Kim YJ, Stadtman ER *et al.* (2004) Reversible oxidation and inactivation of the tumor suppressor PTEN in cells stimulated with peptide growth factors. *Proc Natl Acad Sci*;**101**:16419-16424

Kwong CH, Adams AG, Leto TL. (1995) Characterization of the effector-specifying domain of Rac involved in NADPH oxidase activation. *J Biol Chem*;**270**:19868-19872

Laczmanska I, Sasiadek MM. (2011) Tyrosine phosphatases as a superfamily of tumor suppressors in colorectal cancer. *Acta Biochim Pol*;**58**:467-470

Lallena MJ, Martinez C, Valcarcel J, Correas I. (1998) Functional association of nuclear protein 4.1 with pre-mRNA splicing factors. *J Cell Sci*;**111**:1963-1971

LaLonde DP, Garbett D, Bretscher A. (2010) A regulated complex of the scaffolding proteins PDZK1 and EBP50 with ezrin contribute to microvillar organization. *Mol Biol Cell*;**21**:1519-1529

Lambeth JD. (2004) NOX enzymes and the biology of reactive oxygen. *Nat Rev Immunol*;**4**:181-189

Lambeth JD, Krause KH, Clark RA. (2008) NOX enzymes as novel targets for drug development. *Semin Immunopathol*;**30**:339-363

Lammers T, Peschke P, Ehemann V, Debus J, Slobodin B, Lavi S *et al.* (2007) Role of PP2Calpha in cell growth, in radio- and chemosensitivity, and in tumorigenicity. *Molec Cancer*;**6**:65

Lanza F. (1998) Clinical manifestation of myeloperoxidase deficiency. *J Mol Med*;**76**:676-681

Lapouge K, Smith SJ, Walker PA, Gamblin SJ, Smerdon SJ, Rittinger K. (2000) Structure of the TPR domain of p67phox in complex with Rac GTP. *Mol Cell*;**6**:899-907

Laurent E, McCoy JW, 3rd, Macina RA, Liu W, Cheng G, Robine S *et al.* (2008) Nox1 is over-expressed in human colon cancers and correlates with activating mutations in K-Ras. *Int J Cancer*;**123**:100-107

Lee BC and Gladyshev VN. (2011) The biological significance of methionine sulfoxide stereochemistry. *Free Radic Biol Med*;**50**:221-227.

Lee JY, Yu SJ, Park YG, Kim J, Sohn J. (2007) Glycogen synthase kinase 3beta phosphorylates p21WAF1/CIP1 for proteasomal degradation after UV irradiation. *Mol Cell Biol*;**27**:3187-3198

Lee M, Choy WC, Abid MR. (2011) Direct sensing of endothelial oxidants by vascular endothelial growth factor receptor-2 and c-Src. *PLoS ONE*;**6**:e28454

Lee SR, Yang KS, Kwon J, Lee C, Jeong W, Rhee SG. (2002) Reversible inactivation of the tumor suppressor PTEN by H2O2. *J Biol Chem*;**277**:20336-20342

Lee YM, Kim BJ, Chun YS, So I, Choi H, Kim MS *et al.* (2006) NOX4 as an oxygen sensor to regulate TASK-1 activity. *Cell Signal*;**18**:499-507

Leischner H, Albers C, Grundler R, Razumovskaya E, Spiekermann K, Bohlander S *et al.* (2012) SRC is a signaling mediator in FLT3-ITD but not in FLT3-TKD positive AML. *Blood*;**119:**4026-4033

Leng S, Zhang W, Zheng Y, Liberman Z, Rhodes CJ, Eldar-Finkelman H *et al.* (2010) Glycogen synthase kinase 3β mediates high glucose-induced ubiquitination and proteasome degradation of insulin receptor substrate 1. *J Endocrinol*;**206**:171-181

Leonberg AK, Chai YC. (2007) The functional role of cysteine residues for c-Abl kinase activity. *Mol Cell Biochem*;**304**:207-212

Leslie NR, Lindsay Y, Ross SH, Downes CP. (2004) Redox regulation of phosphatase function. *Biochem Soc Transactions*;**32**:1018-1020

Levis M, Pham R, Smith BD, Small D. (2004) In vitro studies of a FLT3 inhibitor combined with chemotherapy: sequence of administration is important to achieve synergistic cytotoxic effects. *Blood*;**104**:1145-1150

Levis M, Small D. (2003) FLT3: ITDoes matter in leukemia. *Leukemia*;**17**:1738-1752

Li L, Cheung S-H, Evans EL, Shaw PE. (2010) Modulation of gene expression and tumor cell growth by redox modification of STAT3. *Cancer Res*;**70**:8222-8232

Li Q, Spencer NY, Oakley FD, Buettner GR, Engelhardt JF. (2009) Endosomal Nox2 facilitates redox-dependent induction of NF-kappaB by TNF-alpha. *Antioxid Redox Signal*;**11**:1249-1263

Li Q, Wu M, Wang H, Xu G, Zhu T, Zhang Y *et al.* (2008) Ezrin silencing by small hairpin RNA reverses metastatic behaviors of human breast cancer cells. *Cancer letters*;**261**:55-63

Lim WA, Pawson T. (2010) Phosphotyrosine signaling: evolving a new cellular communication system. *Cell*;**142**:661-667

Link AJ, LaBaer J. (2011) Trichloroacetic acid (TCA) precipitation of proteins. *Cold Spring Harb Protoc*;**1**:993-994

Little SE, Popov S, Jury A, Bax DA, Doey L, Al-Sarraj S *et al.* (2012) Receptor Tyrosine Kinase Genes Amplified in Glioblastoma Exhibit a Mutual Exclusivity in Variable Proportions Reflective of Individual Tumor Heterogeneity. *Cancer Res*;**72**:1614-1620

LLS. (2011a) The Leukemia and Lymphoma Society, Facts 2010 - 2011.**20**:96-100

LLS. (2011b) The Leukemia and Lymphoma Society, Leukemia facts and statistics.**20**:70-74

Locksley RM, Wilson CB, Klebanoff SJ. (1983) Increased respiratory burst in myeloperoxidase-deficient monocytes. *Blood*;**62**:902-909

Loh ML, Vattikuti S, Schubbert S, Reynolds MG, Carlson E, Lieuw KH *et al.* (2004) Mutations in PTPN11 implicate the SHP-2 phosphatase in leukemogenesis. *Blood*;**103**:2325-2331

Loria V, Dato I, Graziani F, Biasucci LM. (2008) Myeloperoxidase: A new biomarker of inflammation in ischemic heart disease and acute coronary syndromes. *Mediators Inflamm*;**20**

Lou Y-W, Chen Y-Y, Hsu S-F, Chen R-K, Lee C-L, Khoo K-H *et al.* (2008) Redox regulation of the protein tyrosine phosphatase PTP1B in cancer cells. *FEBS J*;**275**:69-88

Lu W, Hu Y, Chen G, Chen Z, Zhang H, Wang F *et al.* (2012) Novel role of NOX in supporting aerobic glycolysis in cancer cells with mitochondrial dysfunction and as a potential target for cancer therapy. *PLoS Biol*;**10**:e1001326

Lugini L, Lozupone F, Matarrese P, Funaro C, Luciani F, Malorni W *et al.* (2003) Potent phagocytic activity discriminates metastatic and primary human malignant melanomas: a key role of ezrin. *Lab Invest*;**83**:1555-1567

Luo S and Levine RL. (2009) Methionine in proteins defends against oxidative stress. *FASEB J*; **23**:464-472.

Lyle AN, Deshpande NN, Taniyama Y, Seidel-Rogol B, Pounkova L, Du P *et al.* (2009) Poldip2, a novel regulator of Nox4 and cytoskeletal integrity in vascular smooth muscle cells. *Circ Res*;**105**:249-259

Lyman SD. (1995) Biology of flt3 ligand and receptor. *Int J Hematol*;**62**:63-73

Lyman SD, James L, Zappone J, Sleath PR, Beckmann MP, Bird T. (1993) Characterization of the protein encoded by the flt3 (flk2) receptor-like tyrosine kinase gene. *Oncogene*;**8**:815-822

Mahadev K, Motoshima H, Wu X, Ruddy JM, Arnold RS, Cheng G *et al.* (2004) The NAD(P)H oxidase homolog Nox4 modulates insulin-stimulated generation of H2O2 and plays an integral role in insulin signal transduction. *Mol Cell Biol*;**24**:1844-1854

Mak H, Naba A, Varma S, Schick C, Day A, SenGupta SK *et al.* (2012) Ezrin phosphorylation on tyrosine 477 regulates invasion and metastasis of breast cancer cells. *BMC Cancer*;**12**:82

Maloney JA, Tsygankova OM, Yang L, Li Q, Szot A, Baysal K *et al.* (1999) Activation of ERK by Ca2+store depletion in rat liver epithelial cells. *Am J Physiol Cell Physiol*;**276**:C221-C230

Malumbres M, Barbacid M. (2009) Cell cycle, CDKs and cancer: a changing paradigm. *Nat Rev Cancer*;**9**:153-166

Mani A, Gelmann EP. (2005) The ubiquitin-proteasome pathway and its role in cancer. *J Clin Oncol*;**23**:4776-4789

Maniti O, Khalifat N, Goggia K, Dalonneau F, Guerin C, Blanchoin L *et al.* (2012) Binding of moesin and ezrin to membranes containing phosphatidylinositol (4,5) bisphosphate: A comparative study of the affinity constants and conformational changes. *Biochim Biophys Acta*;**1818**:2839-2849

Marit G, Cao Y, Froussard P, Ripoche J, Dupouy M, Elandaloussi A *et al.* (2000) Increased liposome-mediated gene transfer into haematopoietic cells grown in adhesion to stromal or fibroblast cell line monolayers. *Eur J Hematol*;**64**:22-31

Martin M, Roy C, Montcourrier P, Sahuquet a, Mangeat P. (1997) Three determinants in ezrin are responsible for cell extension activity. *Mol Biol Cell*;**8**:1543-1557

Martyn KD, Frederick LM, von Loehneysen K, Dinauer MC, Knaus UG. (2006) Functional analysis of Nox4 reveals unique characteristics compared to other NADPH oxidases. *Cell Signal*;**18**:69-82

Matozaki T, Murata Y, Saito Y, Okazawa H, Ohnishi H. (2009) Protein tyrosine phosphatase SHP-2: a proto-oncogene product that promotes Ras activation. *Cancer Sci*;**100**:1786-1793

Matsui T. (1998) Rho-kinase phosphorylates COOH-terminal threonines of Ezrin/Radixin/Moesin (ERM) Ppoteins and regulates their head-to-tail association. *J Cell Biol*;**140**:647-657

Matsuo Y, MacLeod RaF, Uphoff CC, Drexler HG, Nishizaki C, Katayama Y *et al.* (1997) Two acute monocytic leukemia (AML-M5a) cell lines (MOLM-13 and MOLM-14) with interclonal phenotypic heterogeneity showing MLL-AF9 fusion resulting from an occult chromosome insertion, ins(11;9)(q23;p22p23). *Leukemia*;**11**:1469-1477

Mayer BJ. (2008) Clues to the evolution of complex signaling machinery. *Proc Natl Acad Sci*;**105**:9453-9454

Mayer RJ, Davis RB, Schiffer CA, Berg DT, Powell BL, Schulman P *et al.* (1994) Intensive postremission chemotherapy in adults with acute myeloid leukemia. Cancer and Leukemia Group B. *N Engl J Med*;**331**:896-903

Maziarz RT. (2005) Ph+ ALL: another success for imatinib. *Blood*;**105**:3388-3389

McCord JM, Fridovich I. (1988) Superoxide dismutase: the first twenty years (1968-1988). *Free Radic Biol Med*;**5**:363-369

Méchin V, Damerval C, Zivy M. (2007) Total Protein Extraction with TCA-Acetone. *Methods Mol Biol*;**355**:1-8

Meier B, Cross AR, Hancock JT, Kaup FJ, Jones OT. (1991) Identification of a superoxide-generating NADPH oxidase system in human fibroblasts. *Biochem J*;**275 (Pt 1)**:241-245

Meischl C, Krijnen P, Sipkens J, Cillessen S, Muñoz I, Okroj M *et al.* (2006) Ischemia induces nuclear NOX2 expression in cardiomyocytes and subsequently activates apoptosis. *Apoptosis*;**11**:913-921

Melendez-Vasquez CV, Rios JC, Zanazzi G, Lambert S, Bretscher A, Salzer JL. (2001) Nodes of Ranvier form in association with Schwann cell processes. *Proc Natl Acad Sci*;**98**:1235-1240

Meng D, Lv DD, Fang J. (2008) Insulin-like growth factor-I induces reactive oxygen species production and cell migration through Nox4 and Rac1 in vascular smooth muscle cells. *Cardiovasc Res*;**80**:299-308

Meng TC, Fukada T, Tonks NK. (2002) Reversible oxidation and inactivation of protein tyrosine phosphatases in vivo. *Mol Cell*;**9**:387-399

Mimae T, Tsuta K, Kondo T, Nitta H, Grogan TM, Okada M *et al.* (2012) Protein expression and gene copy number changes of receptor tyrosine kinase in thymomas and thymic carcinomas. *Annals of Oncology*;**12**:3129-3137

Minetti M, Mallozzi C, Di Stasi AMM. (2002) Peroxynitrite activates kinases of the src family and upregulates tyrosine phosphorylation signaling. *Free Radic Biol Med*;**33**:744-754

Mitsushita J, Lambeth JD, Kamata T. (2004) The superoxide-generating oxidase Nox1 is functionally required for Ras oncogene transformation. *Cancer Res*;**64**:3580-3585

Mizuki M, Schwäble J, Steur C, Choudhary C, Agrawal S, Sargin B *et al.* (2003) Suppression of myeloid transcription factors and induction of STAT response genes by AML-specific Flt3 mutations. *Blood*;**101**:3164-3173

Monni R, Haddaoui L, Naba A, Gallais I, Arpin M, Mayeux P *et al.* (2008) Ezrin is a target for oncogenic Kit mutants in murine erythroleukemia. *Blood*;**111**:3163-3172

Montagner A, Yart A, Dance M, Perret B, Salles JP, Raynal P. (2005) A novel role for Gab1 and SHP2 in epidermal growth factor-induced Ras activation. *J Biol Chem*;**280**:5350-5360

Mori T, Kitano K, Terawaki S, Maesaki R, Fukami Y, Hakoshima T. (2008) Structural basis for CD44 recognition by ERM proteins. *J Biol Chem*;**283**:29602-29612

Mori Y, Kiyoi H, Ishikawa Y, Naoe T. (2009) FL-dependent wild-type FLT3 signals reduce the inhibitory effects of FLT3 inhibitors on wild-type and mutant FLT3 co-expressing cells. *Blood*;**114**:Abstract 2067.

Muller J, Sperl B, Reindl W, Kiessling A, Berg T.(2008a) Discovery of chromone-based inhibitors of the transcription factor STAT5. *Chembiochem*;**9**:723-727

Muller JP, Schonherr C, Markova B, Bauer R, Stocking C, Bohmer FD. (2008b) Role of SHP2 for FLT3-dependent proliferation and transformation in 32D cells. *Leukemia*;**22**:1945-1948

Mylonas C, Kouretas D. (1999) Lipid peroxidation and tissue damage. *In vivo*;**13**:295-309

Nabinger SC, Chan RJ. (2012) Shp2 function in hematopoietic stem cell biology and leukemogenesis. *Curr Opin Hematol*;**19**:273-279

Nadeau PJ, Charette SJ, Toledano MB, Landry J. (2007) Disulfide bond-mediated multimerization of Ask1 and its reduction by thioredoxin-1 regulate H2O2-induced c-Jun NH2-terminal kinase activation and apoptosis. *Mol Biol Cell*;**18**:3903-3913

Nakamura K, Hori T, Sato N, Sugie K, Kawakami T, Yodoi J. (1993) Redox regulation of a src family protein tyrosine kinase p56lck in T cells. *Oncogene*;**8**:3133-3139

Nakao M, Yokota S, Iwai T, Kaneko H, Horiike S, Kashima K *et al.* (1996) Internal tandem duplication of the flt3 gene found in acute myeloid leukemia. *Leukemia*;**10**:1911-1918

Nakashima I, Kato M, Akhand AA, Suzuki H, Takeda K, Hossain K *et al.* (2002) Redox-linked signal transduction pathways for protein tyrosine kinase activation. *Antioxid Redox Signal*;**4**:517-531

Nath KA, Norby SM. (2000) Reactive oxygen species and acute renal failure. *AM J Med*;**109**:665-678

Naughton R, Quiney C, Turner SD, Cotter TG. (2009) Bcr-Abl-mediated redox regulation of the PI3K/AKT pathway. *Leukemia* **23**:1432-1440

Ng T, Parsons M, Hughes WE, Monypenny J, Zicha D, Gautreau a *et al.* (2001) Ezrin is a downstream effector of trafficking PKC-integrin complexes involved in the control of cell motility. *EMBO J*;**20**:2723-2741

Nic M, Jirat J, Kosata B. IUPAC Compendium of Chemical Terminology. Oxford: Blackwell Scientific Publications; 2006.

Niethammer P, Grabher C, Look AT, Mitchison TJ. (2009) A tissue-scale gradient of hydrogen peroxide mediates rapid wound detection in zebrafish. *Nature*;**459**:996-999

Nolte F, Hofmann W-K. (2011) Molecular mechanisms involved in the progression of MDS. *Cell Stem Cell*;**8**:1-32

Nordberg J, Arner ES. (2001) Reactive oxygen species, antioxidants, and the mammalian thioredoxin system. *Free Radic Biol Med*;**31**:1287-1312

O'Donnell BV, Tew DG, Jones OT, England PJ. (1993) Studies on the inhibitory mechanism of iodonium compounds with special reference to neutrophil NADPH oxidase. *Biochem J*;**290** 41-49

O'Farrell PH. (1975) High resolution two-dimensional electrophoresis of proteins. *J Biol Chem*;**250**:4007-21.

O'Farrell AM, Foran JM, Fiedler W, Serve H, Paquette RL, Cooper MA *et al.* (2003) An innovative phase I clinical study demonstrates inhibition of FLT3 phosphorylation by SU11248 in acute myeloid leukemia patients. *Clin Cancer Res*;**9**:5465-5476

Oberdoerffer S, Moita LF, Neems D, Freitas RP, Hacohen N, Rao A. (2008) Regulation of CD45 alternative splicing by heterogeneous ribonucleoprotein, hnRNPLL. *Science*;**321**:686-691

Obermann EC, Arber C, Jotterand M, Tichelli A, Hirschmann P, Tzankov A. (2010) Expression of pSTAT5 predicts FLT3 internal tandem duplications in acute myeloid leukemia. *Ann Hematol*;**89**:663-669

Olsson I, Larsson K, Palmgren R, Bjellqvist B. (2002) Organic disulfides as a means to generate streak-free two-dimensional maps with narrow range basic immobilized pH gradient strips as first dimension. *Proteomics*;**2**:1630-1632

Orsatti L, Innocenti F, Lo Surdo P, Talamo F, Barbato G. (2009) Mass spectrometry study of PRL-3 phosphatase inactivation by disulfide bond formation and cysteine into glycine conversion. *Rapid Commun Mass Spectrom*;**23**:2733-2740

Ostman A, Frijhoff J, Sandin A, Bohmer FD. (2011) Regulation of protein tyrosine phosphatases by reversible oxidation. *J Biochem*;**150**:345-356

Ostman A, Hellberg C, Bohmer FD. (2006) Protein-tyrosine phosphatases and cancer. *Nat Rev Cancer*;**6**:307-320

Owens DM, Keyse SM. (2007) Differential regulation of MAP kinase signalling by dual-specificity protein phosphatases. *Oncogene*;**26**:3203-3213

Ozawa Y, Williams AH, Estes ML, Matsushita N, Boschelli F, Jove R *et al.* (2008) Src family kinases promote AML cell survival through activation of signal transducers and activators of transcription (STAT). *Leuk Res*;**32**:893-903

Pabst T, Mueller BU, Harakawa N, Schoch C, Haferlach T, Behre G *et al.* (2001) AML1-ETO downregulates the granulocytic differentiation factor C/EBPalpha in t(8;21) myeloid leukemia. *Nat Med*;**7**:444-451

Page P, Orchard M, Fioraso-Cartier L, Mottironi B; Patent: Pyrazolo pyridine derivatives as NADPH oxidase inhibitors. Switzerland, 2008.

Pai S-Y, Kim C, Williams DA. (2010) Rac GTPases in human diseases. *Dis Markers*;**29**:177-187

Pakkanen R, von Bonsdorff CH, Turunen O, Wahlstrom T, Vaheri A. (1988) Redistribution of Mr 75,000 plasma membrane protein, cytovillin, into newly formed microvilli in herpes simplex and Semliki Forest virus infected human embryonal fibroblasts. *Eur J Cell Biol*;**46**:435-443

Palmen MJHJ, Beukelman CJ, Mooij RGM, Pena AS, van Rees EP. (1995) Anti-inflammatory effect of apocynin, a plant-derived NADPH oxidase antagonist, in acute experimental colitis. *Nether J Med*;**47**:41-41

Papp E, Nardai G, Söti C, Csermely P. (2003) Molecular chaperones, stress proteins and redox homeostasis. *BioFactors*;**17**:249-257

Paquette RL, Landaw EM, Pierre RV, Kahan J, Lubbert M, Lazcano O *et al.* (1993) N-ras mutations are associated with poor prognosis and increased risk of leukemia in myelodysplastic syndrome. *Blood*;**82**:590-599

Parkos CA, Allen RA, Cochrane CG, Jesaitis AJ. (1987) Purified cytochrome b from human granulocyte plasma membrane is comprised of two polypeptides with relative molecular weights of 91,000 and 22,000. *J Clin Invest*;**80**:732-742

Pastore A, Piemonte F, Locatelli M, Lo Russo A, Gaeta LM, Tozzi G *et al.* (2001) Determination of blood total, reduced, and oxidized glutathione in pediatric subjects. *Clin Chem*;**47**:1467-1469

Paulsen CE, Carroll KS. (2009) Orchestrating redox signaling networks through regulatory cysteine switches. *ACS Chem Biol*;**5**:47-62

Peng C, Chen Y, Yang Z, Zhang H, Osterby L, Rosmarin AG *et al.* (2010) PTEN is a tumor suppressor in CML stem cells and BCR-ABL–induced leukemias in mice. *Blood*;**115**:626-635

Pfarr N, Korsch E, Kaspers S, Herbst A, Stach A, Zimmer C *et al.* (2006) Congenital hypothyroidism caused by new mutations in the thyroid oxidase 2 (THOX2) gene. *Clin Endocrinol (Oxf)*;**65**:810-815

Piccoli C, Ria R, Scrima R, Cela O, D'Aprile A, Boffoli D *et al.* (2005) Characterization of mitochondrial and extra-mitochondrial oxygen consuming reactions in human hematopoietic stem cells. Novel evidence of the occurrence of NAD(P)H oxidase activity. *J Biol Chem*;**280**:26467-26476

Pickart CM, Fushman D. (2004) Polyubiquitin chains: polymeric protein signals. *Curr Opin Chem Biol*;**8**:610-616

Piloto O, Wright M, Brown P, Kim KT, Levis M, Small D. (2007) Prolonged exposure to FLT3 inhibitors leads to resistance via activation of parallel signaling pathways. *Blood*;**109**:1643-1652

Pincus D, Letunic I, Bork P, Lim WA. (2008) Evolution of the phospho-tyrosine signaling machinery in premetazoan lineages. *Proc Natl Acad Sci*;**105**:9680-9684

Poole LB, Karplus PA, Claiborne A. (2004) Protein sulfenic acids in redox signaling. *Annu Rev Pharmacol Toxicol*;**44**:325-347

Poole LB, Nelson KJ. (2008) Discovering mechanisms of signaling-mediated cysteine oxidation. *Curr Opin Chem Biol*;**12**:18-24

Pourmahram GE, Snetkov VA, Shaifta Y, Drndarski S, Knock GA, Aaronson PI *et al.* (2008) Constriction of pulmonary artery by peroxide: role of Ca2+ release and PKC. *Free Radic Biol Med*;**45**:1468-1476

Pratz K, Levis M. (2008) Incorporating FLT3 inhibitors into acute myeloid leukemia treatment regimens. *Leuk Lymphoma*;**49**:852-863

Pratz KW, Cortes J, Roboz GJ, Rao N, Arowojolu O, Stine A *et al.* (2009) A pharmacodynamic study of the FLT3 inhibitor KW-2449 yields insight into the basis for clinical response. *Blood*;**113**:3938-3946

Prensner JR, Chinnaiyan AM. (2011) Metabolism unhinged: IDH mutations in cancer. *Nat Med*;**17**:291-293

Puls LN, Eadens M, Messersmith W. (2011) Current status of Src inhibitors in solid tumor malignancies. *The Oncologist*;**16**:566-578

Qu C-K, Nguyen S, Chen J, Feng G-S. (2001) Requirement of Shp-2 tyrosine phosphatase in lymphoid and hematopoietic cell development. *Blood*;**97**:911-914

Quentmeier H, Reinhardt J, Zaborski M, Drexler HG. (2003) FLT3 mutations in acute myeloid leukemia cell lines. *Leukemia* **17**:120-124

Rabilloud T. (2009) Solubilization of proteins in 2DE: an outline. *Methods Mol Biol*;**519**:19-30

Rabilloud T, Chevallet M. Proteome Research: Two-dimensional gel Electrophoresis and identification methods. Berlin: Springer; 2000.

Radomska HS, Bassères DS, Zheng R, Zhang P, Dayaram T, Yamamoto Y *et al.* (2006) Block of C/EBPα function by phosphorylation in acute myeloid leukemia with FLT3 activating mutations. *J Exp Med*;**203**:371-381

Rahman MA, Senga T, Ito S, Hyodo T, Hasegawa H, Hamaguchi M. (2010) S-nitrosylation at cysteine 498 of c-Src tyrosine kinase regulates nitric oxide-mediated cell invasion. *J Biol Chem*;**285**:3806-3814

Rando OJ, Zhao K, Janmey P, Crabtree GR. (2002) Phosphatidylinositol-dependent actin filament binding by the SWI/SNF-like BAF chromatin remodeling complex. *Proc Natl Acad Sci*;**99**:2824-2829

Ravichandran LV, Chen H, Li Y, Quon MJ. (2001) Phosphorylation of PTP1B at Ser(50) by Akt impairs its ability to dephosphorylate the insulin receptor. *Mol Endocrinol*;**15**:1768-1780

Ray PD, Huang B-W, Tsuji Y. (2012) Reactive oxygen species (ROS) homeostasis and redox regulation in cellular signaling. *Cellular Signalling*;**24**:981-990

Reddy MM, Fernandes MS, Salgia R, Levine RL, Griffin JD, Sattler M. (2011) NADPH oxidases regulate cell growth and migration in myeloid cells transformed by oncogenic tyrosine kinases. *Leukemia*;**25**:281-289

Reinehr R, Becker S, Eberle A, Grether-Beck S, Haussinger D. (2005) Involvement of NADPH oxidase isoforms and Src family kinases in CD95-dependent hepatocyte apoptosis. *J Biol Chem*;**280**:27179-27194

Reistad T, Mariussen E. (2005) A commercial mixture of the brominated flame retardant pentabrominated diphenyl ether (DE-71) induces respiratory burst in human neutrophil granulocytes in vitro. *Toxicol Sci*;**87**:57-65

Ren Y, Meng S, Mei L, Zhao ZJ, Jove R, Wu J. (2004) Roles of Gab1 and SHP2 in paxillin tyrosine dephosphorylation and Src activation in response to epidermal growth factor. *J Biol Chem*;**279**:8497-8505

Rey FE, Li X-C, Carretero OA, Garvin JL, Pagano PJ. (2002) Perivascular superoxide anion contributes to impairment of endothelium-dependent relaxation. *Circulation*;**106**:2497-2502

Rhee SG, Kang SW, Jeong W, Chang TS, Yang KS, Woo HA. (2005) Intracellular messenger function of hydrogen peroxide and its regulation by peroxiredoxins. *Curr Opin Cell Biol*;**17**:183-189

Rhee SG, Woo HA. (2011) Multiple functions of peroxiredoxins: peroxidases, sensors and regulators of the intracellular messenger H(2)O(2), and protein chaperones. *Antioxid Redox Signal*;**00**

Rhee SG, Woo HA, Kil IS, Bae SH. (2012) Peroxiredoxin functions as a peroxidase and a regulator and sensor of local peroxides. *J Biol Chem*;**287**:4403-4410

Richards SM, Clark EA. (2009) BCR-induced superoxide negatively regulates B-cell proliferation and T-cell-independent type 2 Ab responses. *Eur J Immunol*;**39**:3395-3403

Riley BE, Xu Y, Zoghbi HY, Orr HT. (2004) The effects of the polyglutamine repeat protein ataxin-1 on the UbL-UBA protein A1Up. *J Biol Chem*;**279**:42290-42301

Roberts TL, Idris A, Dunn JA, Kelly GM, Burnton CM, Hodgson S *et al.* (2009) HIN-200 proteins regulate caspase activation in response to foreign cytoplasmic DNA. *Science*;**323**:1057-1060

Robinson JM, Badwey JA. (1995) The NADPH oxidase complex of phagocytic leukocytes: a biochemical and cytochemical view. *Histochem Cell Biol*;**103**:163-180

Robinson LJ, Xue J, Corey SJ. (2005) Src family tyrosine kinases are activated by Flt3 and are involved in the proliferative effects of leukemia-associated Flt3 mutations. *Exp Hematol*;**33**:469-479

Roddie PH, Paterson T, Turner ML. (2000) Gene transfer to primary acute myeloid leukaemia blasts and myeloid leukaemia cell lines. *Cytokines Cell Mol Ther*;**6**:127-134

Rogers S, Wells R, Rechsteiner M. (1986) Amino acid sequences common to rapidly degraded proteins: the PEST hypothesis. *Science*;**234**:364-368

Rosen DB, Minden MD, Kornblau SM, Cohen A, Gayko U, Putta S *et al.* (2010) Functional characterization of FLT3 receptor signaling deregulation in acute myeloid leukemia by single cell network profiling (SCNP). *PLoS ONE*;**5**:e13543

Rosenbauer F, Wagner K, Kutok JL, Iwasaki H, Le Beau MM, Okuno Y *et al.* (2004) Acute myeloid leukemia induced by graded reduction of a lineage-specific transcription factor, PU.1. *Nat genet*;**36**:624-630

Roskoski Jr R. (2005) Src kinase regulation by phosphorylation and dephosphorylation. *Biochem Biophys Res Comm*;**331**:1-14

Sablina AA, Hector M, Colpaert N, Hahn WC. (2010) Identification of PP2A complexes and pathways involved in cell transformation. *Cancer Res*;**70**:10474-10484

Saleh HS, Merkel U, Geissler KJ, Sperka T, Sechi A, Breithaupt C *et al.* (2009) Properties of an ezrin mutant defective in F-actin binding. *J Mol Biol*;**385**:1015-1031

Sallmyr A, Fan J, Datta K, Kim K-T, Grosu D, Shapiro P *et al.* (2008a) Internal tandem duplication of FLT3 (FLT3/ITD) induces increased ROS production, DNA damage, and misrepair: implications for poor prognosis in AML. *Blood*;**111**:3173-3182

Sallmyr A, Fan J, Rassool FV. (2008b) Genomic instability in myeloid malignancies: increased reactive oxygen species (ROS), DNA double strand breaks (DSBs) and error-prone repair. *Cancer Lett*;**270**:1-9

Santos CX, Tanaka LY, Wosniak J, Laurindo FR. (2009) Mechanisms and implications of reactive oxygen species generation during the unfolded protein response: roles of endoplasmic reticulum oxidoreductases, mitochondrial electron transport, and NADPH oxidase. *Antioxid Redox Signal*;**11**:2409-2427

Sargin B, Choudhary C, Crosetto N, Schmidt MHH, Grundler R, Rensinghoff M *et al.* (2007) Flt3-dependent transformation by inactivating c-Cbl mutations in AML. *Blood*;**110**:1004-1012

Sattler M, Verma S, Shrikhande G, Byrne CH, Pride YB, Winkler T *et al.* (2000) The BCR/ABL tyrosine kinase induces production of reactive oxygen species in hematopoietic cells. *J Biol Chem*;**275**:24273-24278

Saunders AE, Johnson P. (2010) Modulation of immune cell signalling by the leukocyte common tyrosine phosphatase, CD45. *Cell Signal*;**22**:339-348

Schakowski F, Buttgereit P, Mazur M, Marten A, Schottker B, Gorschluter M *et al.* (2004) Novel non-viral method for transfection of primary leukemia cells and cell lines. *Genet Vacc Therapy*;**2**:1

Scheffner M, Huibregtse JM, Vierstra RD, Howley PM. (1993) The HPV-16 E6 and E6-AP complex functions as a ubiquitin-protein ligase in the ubiquitination of p53. *Cell*;**75**:495-505

Schenone S, Brullo C, Musumeci F, Botta M. (2010) Novel dual Src/Abl inhibitors for hematologic and solid malignancies. *Expert Opin Investig Drugs*;**19**:931-945

Schmidt-Arras D, Bo S-A, Koch S, Blei L, Cornils H, Bauer R *et al.* (2009) Anchoring of FLT3 in the endoplasmic reticulum alters signaling quality. *Methods*;**113**:3568-3576

Schmidt MHH, Furnari FB, Cavenee WK, Bögler O. (2003) Epidermal growth factor receptor signaling intensity determines intracellular protein interactions, ubiquitination, and internalization. *Proc Natl Acad Sci*;**100**:6505-6510

Schmitt CA, Fridman JS, Yang M, Baranov E, Hoffman RM, Lowe SW. (2002) Dissecting p53 tumor suppressor functions in vivo. *Cancer Cell*;**1**:289-298

Schroder K, Helmcke I, Palfi K, Krause KH, Busse R, Brandes RP. (2007) Nox1 mediates basic fibroblast growth factor-induced migration of vascular smooth muscle cells. *Arterioscler Thromb Vasc Biol*;**27**:1736-1743

Sedeek M, Callera G, Montezano A, Gutsol A, Heitz F, Szyndralewiez C *et al.* (2010) Critical role of Nox4-based NADPH oxidase in glucose-induced oxidative stress in the kidney: implications in type 2 diabetic nephropathy. *Am J Physiol Renal Physiol*;**299**:F1348-1358

Seedhouse CH, Hunter HM, Lloyd-Lewis B, Massip AM, Pallis M, Carter GI *et al.* (2006) DNA repair contributes to the drug-resistant phenotype of primary acute myeloid leukaemia cells with FLT3 internal tandem duplications and is reversed by the FLT3 inhibitor PKC412. *Leukemia*;**20**:2130-2136

Senga T, Miyazaki K, Machida K, Iwata H, Matsuda S, Nakashima I *et al.* (2000) Clustered cysteine residues in the kinase domain of v-Src: critical role for protein stability, cell transformation and sensitivity to herbimycin A. *Oncogene*;**19**:273-279

Serezani CH, Aronoff DM, Jancar S, Peters-Golden M. (2005) Leukotriene B4 mediates p47phox phosphorylation and membrane translocation in polyunsaturated fatty acid-stimulated neutrophils. *J Leukoc Biol*;**78**:976-984

Serrander L CL, Bedard K, Banfi B, Lardy B, Plastre O, Sienkiewicz A, Forro L, Schlegel W, Krause K-H. (2007) NOX4 activity is determined by mRNA levels and reveals a unique pattern of ROS generation. *Biochem J*;**406**:105-114.

Serrano F, Kolluri NS, Wientjes FB, Card JP, Klann E. (2003) NADPH oxidase immunoreactivity in the mouse brain. *Brain Res*;**988**:193-198

Shankar DB, Cheng JC, Kinjo K, Federman N, Moore TB, Gill A *et al.* (2005) The role of CREB as a proto-oncogene in hematopoiesis and in acute myeloid leukemia. *Cancer Cell*;**7**:351-362

Sheehan D. (2006) Detection of redox-based modification in two-dimensional electrophoresis proteomic separations. *Biochem Biophys Res Commun;* **349**:455-462.

Shelton MD, Chock PB, Mieyal JJ. (2005) Glutaredoxin: role in reversible protein S-glutathionylation and regulation of redox signal transduction and protein translocation. *Antioxid Redox Signal* ;**7**:348-366.

Shepard DR, Cooney MM, Elson P, Bukowski RM, Dreicer R, Rini BI *et al.* (2012) A phase II study of tandutinib (MLN518), a selective inhibitor of type III tyrosine receptor kinases, in patients with metastatic renal cell carcinoma. *Invest New Drugs*;**30**:364-367

Shiotsu Y, Kiyoi H, Ishikawa Y, Tanizaki R, Shimizu M, Umehara H *et al.* (2009) KW-2449, a novel multikinase inhibitor, suppresses the growth of leukemia cells with FLT3 mutations or T315I-mutated BCR/ABL translocation. *Blood*;**114**:1607-1617

Simon HU, Haj-Yehia A, Levi-Schaffer F. (2000) Role of reactive oxygen species (ROS) in apoptosis induction. *Apoptosis*;**5**:415-418

Simoneau M, Boulanger J, Coulombe G, Renaud MA, Duchesne C, Rivard N. (2008) Activation of Cdk2 stimulates proteasome-dependent truncation of

tyrosine phosphatase SHP-1 in human proliferating intestinal epithelial cells. *J Biol Chem*;**283**:25544-25556

Simons PC, Pietromonaco SF, Reczek D, Bretscher A, Elias L. (1998) C-terminal threonine phosphorylation activates ERM proteins to link the cell's cortical lipid bilayer to the cytoskeleton. *Biochem Biophys Res Commun*;**253**:561-565

Small D, Levenstein M, Kim E, Carow C, Amin S, Rockwell P *et al.* (1994) STK-1, the human homolog of Flk-2/Flt-3, is selectively expressed in CD34+ human bone marrow cells and is involved in the proliferation of early progenitor/stem cells. *Proc Natl Acad Sci U S A*;**91**:459-463

Smith BD, Levis M, Beran M, Giles F, Kantarjian H, Berg K *et al.* (2004) Single-agent CEP-701, a novel FLT3 inhibitor, shows biologic and clinical activity in patients with relapsed or refractory acute myeloid leukemia. *Blood*;**103**:3669-3676

Smith ME, Min J, Ganesh T, Diebold B, Kawahara T, Zhu Y *et al.* (2012) Ebselen and congeners inhibit NADPH oxidase 2-dependent superoxide generation by interrupting the binding of regulatory subunits. *Chem and Biol*;**19**:752-763

Song MS, Salmena L, Pandolfi PP. (2012) The functions and regulation of the PTEN tumour suppressor. *Nat Rev Mol Cell Biol*;**13**:283-296

Sparks AB, Morin PJ, Vogelstein B, Kinzler KW. (1998) Mutational analysis of the APC/β-Catenin/Tcf pathway in colorectal cancer. *Cancer Res*;**58**:1130-1134

Srivastava J, Elliott BE, Louvard D, Arpin M. (2005) Src-dependent Ezrin phosphorylation in adhesion- mediated signaling. *Mol Biol Cell*;**16**:1481-1490

Srivastava SK, Bansal P, Oguri T, Lazo JS, Singh SV. (2007) Cell division cycle 25B phosphatase is essential for benzo(a)pyrene-7,8-Diol-9,10-epoxide induced neoplastic transformation. *Cancer Res*;**67**:9150-9157

Stadtman ER, Moskovitz J and Levine RL. (2003) Oxidation of methionine residues of proteins: biological consequences. *Antioxid Redox Signal;* **5**: 577-582.

Stamler JS, Toone EJ, Lipton SA, Sucher NJ. (1997) (S)NO signals: translocation, regulation, and a consensus motif. *Neuron*;**18**: 691-696.

Starita LM, Parvin JD. (2003) The multiple nuclear functions of BRCA1: transcription, ubiquitination and DNA repair. *Curr Opin Cell Biol*;**15**:345-350

Stefanidakis M, Karjalainen K, Jaalouk DE, Gahmberg CG, O'Brien S, Pasqualini R *et al.* (2009) Role of leukemia cell invadosome in extramedullary infiltration. *Blood*;**114**:3008-3017

Stirewalt DL, Radich JP. (2003) The role of FLT3 in haematopoietic malignancies. *Nat Rev Cancer*;**3**:650-665

Stolk J, Hiltermann TJ, Dijkman JH, Verhoeven AJ. (1994) Characteristics of the inhibition of NADPH oxidase activation in neutrophils by apocynin, a methoxy-substituted catechol. *Am J Respir Cell Mol Biol*;**11**:95-102

Stone JR, Collins T. (2002) Rapid phosphorylation of heterogeneous nuclear ribonucleoprotein C1/C2 in response to physiologic levels of hydrogen peroxide in human endothelial cells. *J Biol Chem*;**277**:15621-15628

Stone JR, Maki JL, Collins T. (2003) Basal and hydrogen peroxide stimulated sites of phosphorylation in heterogeneous nuclear ribonucleoprotein C1/C2. *Biochemistry*;**42**:1301-1308

Stone RM, DeAngelo DJ, Klimek V, Galinsky I, Estey E, Nimer SD *et al.* (2005) Patients with acute myeloid leukemia and an activating mutation in FLT3 respond to a small-molecule FLT3 tyrosine kinase inhibitor, PKC412. *Blood*;**105**:54-60

Stone RM, Fischer T, Paquette R, Schiller G, Schiffer CA, Ehninger G *et al.* (2012) Phase IB study of the FLT3 kinase inhibitor midostaurin with chemotherapy in younger newly diagnosed adult patients with acute myeloid leukemia. *Leukemia*;**26**:2061-2068

Takahashi S. (2011) Downstream molecular pathways of FLT3 in the pathogenesis of acute myeloid leukemia: biology and therapeutic implications. *J Hematol Oncol*;**4**:13-13

Takahashi S. (2006) Inhibition of the MEK/MAPK signal transduction pathway strongly impairs the growth of Flt3-ITD cells. *Am J Hematol*;**81**:154-155

Takahashi S, Harigae H, Kaku M, Sasaki T, Licht JD. (2004) Flt3 mutation activates p21WAF1/CIP1 gene expression through the action of STAT5. *Biochem Biophys Res Commun*;**316**:85-92

Takekawa M, Maeda T, Saito H. (1998) Protein phosphatase 2C alpha inhibits the human stress-responsive p38 and JNK MAPK pathways. *EMBO J*;**17**:4744-4752

Tang D, Kang R, Zeh HJ, Lotze MT. (2011) High-mobility group box 1, oxidative stress, and disease. *Antioxid Redox Signal*;**14**:1315-1335

Tang H, Hao Q, Rutherford SA, Low B, Zhao ZJ. (2005) Inactivation of SRC family tyrosine kinases by reactive oxygen species in vivo. *J Biol Chem*;**280**:23918-23925

Tartaglia M, Martinelli S, Cazzaniga G, Cordeddu V, Iavarone I, Spinelli M *et al.* (2004) Genetic evidence for lineage-related and differentiation stage-related contribution of somatic PTPN11 mutations to leukemogenesis in childhood acute leukemia. *Blood*;**104**:307-313

Tartaglia M, Martinelli S, Iavarone I, Cazzaniga G, Spinelli M, Giarin E *et al.* (2005) Somatic PTPN11 mutations in childhood acute myeloid leukaemia. *Br J Haematol*;**129**:333-339

Tartaglia M, Mehler EL, Goldberg R, Zampino G, Brunner HG, Kremer H *et al.* (2001) Mutations in PTPN11, encoding the protein tyrosine phosphatase SHP-2, cause Noonan syndrome. *Nat Genet*;**29**:465-468

Tartaglia M, Niemeyer CM, Fragale A, Song X, Buechner J, Jung A *et al.* (2003) Somatic mutations in PTPN11 in juvenile myelomonocytic leukemia,

myelodysplastic syndromes and acute myeloid leukemia. *Nat Genet*;**34**:148-150

Tedesco S, Doyle H, Blasco J, Redmond G, Sheehan D. (2010) Oxidative stress and toxicity of gold nanoparticles in Mytilus edulis. *Aquat Toxicol*;**100**:178-186

Ten Freyhaus H, Huntgeburth M, Wingler K, Schnitker J, Baumer AT, Vantler M *et al.* (2006) Novel Nox inhibitor VAS2870 attenuates PDGF-dependent smooth muscle cell chemotaxis, but not proliferation. *Cardiovasc Res*;**71**:331-341

Terada LS. (2006) Specificity in reactive oxidant signaling: think globally, act locally. *J Cell Biol*;**174**:615-623

Thirman MJ, Gill HJ, Burnett RC, Mbangkollo D, McCabe NR, Kobayashi H *et al.* (1993) Rearrangement of the MLL gene in acute lymphoblastic and acute myeloid leukemias with 11q23 chromosomal translocations. *N Engl J Med*;**329**:909-914

Thomas DA, Faderl S, Cortes J, O'Brien S, Giles FJ, Kornblau SM *et al.* (2004) Treatment of Philadelphia chromosome-positive acute lymphocytic leukemia with hyper-CVAD and imatinib mesylate. *Blood*;**103**:4396-4407

Tonks NK. (2006) Protein tyrosine phosphatases: from genes, to function, to disease. *Nat Rev Mol Cell Biol*;**7**:833-846

Tothova Z, Kollipara R, Huntly BJ, Lee BH, Castrillon DH, Cullen DE *et al.* (2007) FoxOs are critical mediators of hematopoietic stem cell resistance to physiologic oxidative stress. *Cell*;**128**:325-339

Tsunawaki S, Kagara S, Yoshikawa K, Yoshida LS, Kuratsuji T, Namiki H. (1996) Involvement of p40phox in activation of phagocyte NADPH oxidase through association of its carboxyl-terminal, but not its amino-terminal, with p67phox. *J Exp Med*;**184**:893-902

Turunen O, Winqvist R, Pakkanen R, Grzeschik KH, Wahlstrom T, Vaheri A. (1989) Cytovillin, a microvillar Mr 75,000 protein. cDNA sequence, prokaryotic expression, and chromosomal localization. *J Bio Chem*;**264**:16727-16732

Uchida E, Mizuguchi H, Ishii-Watabe A, Hayakawa T. (2002) Comparison of the efficiency and safety of non-viral vector-mediated gene transfer into a wide range of human cells. *Biol Pharm Bulletin*;**25**:891-897

Ueno N, Takeya R, Miyano K, Kikuchi H, Sumimoto H. (2005) The NADPH oxidase Nox3 constitutively produces superoxide in a p22phox-dependent manner: its regulation by oxidase organizers and activators. *J Biol Chem*;**280**:23328-23339

Ueyama T, Geiszt M, Leto TL. (2006) Involvement of Rac1 in activation of multicomponent Nox1- and Nox3-based NADPH oxidases. *Mol Cell Biol*;**26**:2160-2174

Ugolev Y, Berdichevsky Y, Weinbaum C, Pick E. (2008) Dissociation of Rac1(GDP)-RhoGDI complexes by the cooperative action of anionic

liposomes containing phosphatidylinositol 3,4,5-trisphosphate, Rac guanine nucleotide exchange factor, and GTP. *J Biol Chem*;**283**:22257-22271

Ushio-Fukai M. (2006a) Localizing NADPH oxidase-derived ROS. *Sci Signal*;**2006**:re8

Ushio-Fukai M. (2006b) Redox signaling in angiogenesis: role of NADPH oxidase. *Cardiovasc Res*;**71**:226-235

Usui S, Oveson BC, Lee SY, Jo Y-J, Yoshida T, Miki A *et al.* (2009) NADPH oxidase plays a central role in cone cell death in retinitis pigmentosa. *J Neurochem*;**110**:1028-1037

Valencia A, Rajadurai A, Carle AB, Kochevar IE. (2006) 7-Dehydrocholesterol enhances ultraviolet A-induced oxidative stress in keratinocytes: Roles of NADPH oxidase, mitochondria, and lipid rafts. *Free Radic Biol Med*;**41**:1704-1718

Vardiman JW, Harris NL, Brunning RD. (2002) The World Health Organization (WHO) classification of the myeloid neoplasms. *Blood*;**100**:2292-2302

Vejrazka M, Micek R, Stipek S. (2005) Apocynin inhibits NADPH oxidase in phagocytes but stimulates ROS production in non-phagocytic cells. *Biochim Biophys Acta*;**1722**:143-147

Voermans C, Van Heese WPM, Jong ID, Gerritsen WR, Schoot CEVD. (2002) Migratory behavior of leukemic cells from acute myeloid leukemia patients. *Leukemia*:650-657

Von Löhneysen K, Noack D, Hayes P, Friedman JS, Knaus UG. (2012) Constitutive NADPH oxidase 4 activity resides in the composition of the B-loop and the penultimate C terminus. *J Biol Chem;* **287:** 8737-83745.

Wang Q, Pfeiffer GR, Gaarde Wa. (2003) Activation of SRC tyrosine kinases in response to ICAM-1 ligation in pulmonary microvascular endothelial cells. *J Biol Chem*;**278**:47731-47743

Wani R, Qian J, Yin L, Bechtold E, King SB, Poole LB *et al.* (2011) Isoform-specific regulation of Akt by PDGF-induced reactive oxygen species. *Proc Natl Acad Sci*

Ward PS, Patel J, Wise DR, Abdel-Wahab O, Bennett BD, Coller HA *et al.* (2010) The common feature of leukemia-associated IDH1 and IDH2 mutations is a neomorphic enzyme activity converting alpha-ketoglutarate to 2-hydroxyglutarate. *Cancer Cell*;**17**:225-234

Watt F, Molloy PL. (1988) Cytosine methylation prevents binding to DNA of a HeLa cell transcription factor required for optimal expression of the adenovirus major late promoter. *Genes Dev*;**2**:1136-1143

Weerapana E, Wang C, Simon GM, Richter F, Khare S, Dillon MB *et al.* (2010) Quantitative reactivity profiling predicts functional cysteines in proteomes. *Nature*;**468**:790-795

Weibrecht I, Bohmer SA, Dagnell M, Kappert K, Ostman A, Bohmer FD. (2007) Oxidation sensitivity of the catalytic cysteine of the protein-tyrosine phosphatases SHP-1 and SHP-2. *Free Radic Biol Med*;**43**:100-110

Weinberg F, Chandel NS. (2009) Reactive oxygen species-dependent signaling regulates cancer. *Cell Mol Life Sci*;**66**:3663-3673

Weisberg E, Barrett R, Liu Q, Stone R, Gray N, Griffin JD. (2009) FLT3 inhibition and mechanisms of drug resistance in mutant FLT3-positive AML. *Drug Resist Updat*;**12**:81-89

Weisberg E, Boulton C, Kelly LM, Manley P, Fabbro D, Meyer T *et al.* (2002) Inhibition of mutant FLT3 receptors in leukemia cells by the small molecule tyrosine kinase inhibitor PKC412. *Cancer Cell*;**1**:433-443

Wiernik P, Serpick A. (1970) Granulocytic Sarcoma (Chloroma). *Blood*;**35**:361-369

Wiernik PH. (2010) FLT3 inhibitors for the treatment of acute myeloid leukemia. *Clinical advances in hematology & oncology* **8**:429-436

Williams HC, Griendling KK. (2007) NADPH oxidase inhibitors: new antihypertensive agents? *J Cardiovasc Pharmacol*;**50**:9-16

Wishart MJ, Dixon JE. (1998) Gathering STYX: phosphatase-like form predicts functions for unique protein-interaction domains. *Trends Biochem Sci*;**23**:301-306

Wodnar-Filipowicz A. (2003) Flt3 ligand: role in control of hematopoietic and immune functions of the bone marrow. *Physiology*;**18**:247-251

Wood ZA, Poole LB, Karplus PA. (2003) Peroxiredoxin evolution and the regulation of hydrogen peroxide signaling. *Science*;**300**:650-653

Woods AJ, Roberts MS, Choudhary J, Barry ST, Mazaki Y, Sabe H *et al.* (2002) Paxillin associates with poly(A)-binding protein 1 at the dense endoplasmic reticulum and the leading edge of migrating cells. *J Bio Chem*;**277**:6428-6437

Woolley JF, Naughton R, Stanicka J, Gough DR, Bhatt L, Dickinson BC *et al.* (2012) H(2)O(2) production downstream of FLT3 is mediated by p22phox in the endoplasmic reticulum and is required for STAT5 signalling. *PLoS ONE*;**7**:e34050

Wu B, Li J, Huang D, Wang W, Chen Y, Liao Y *et al.* (2011) Baicalein mediates inhibition of migration and invasiveness of skin carcinoma through Ezrin in A431 cells. *BMC Cancer*;**11**:1-8

Wu C, Guan Q, Wang Y, Zhao ZJ, Zhou GW. (2003a) SHP-1 suppresses cancer cell growth by promoting degradation of JAK kinases. *J Cell Biochem*;**90**:1026-1037

Wu C, Sun M, Liu L, Zhou GW. (2003b) The function of the protein tyrosine phosphatase SHP-1 in cancer. *Gene*;**306**:1-12

Wu RF, Xu YC, Ma Z, Nwariaku FE, Sarosi GA, Jr., Terada LS. (2005) Subcellular targeting of oxidants during endothelial cell migration. *J Cell Biol*;**171**:893-904

Wu W-S. (2006) The signaling mechanism of ROS in tumor progression. *Cancer Metastasis Rev*;**25**:695-705

Xi G, Shen X, Maile LA, Wai C, Gollahon K, Clemmons DR. (2011) Hyperglycemia enhances IGF-I stimulated Src activation via increasing

Nox4-derived reactive oxygen species in a PKC-gamma-dependent manner in vascular smooth muscle cells. *Diabetes*;**61**:104-113

Xiao D, Johnson CS, Trump DL, Singh SV. (2004) Proteasome-mediated degradation of cell division cycle 25C and cyclin-dependent kinase 1 in phenethyl isothiocyanate-induced G2-M-phase cell cycle arrest in PC-3 human prostate cancer cells. *Mol Cancer Ther*;**3**:567-575

Xiao Q, Luo Z, Pepe AE, Margariti A, Zeng L, Xu Q. (2009) Embryonic stem cell differentiation into smooth muscle cells is mediated by Nox4-produced H2O2. *Am J Physiol Cell Physiol*;**296**:C711-723

Ximenes VF, Kanegae MPP, Rissato SR, Galhiane MS. (2007) The oxidation of apocynin catalyzed by myeloperoxidase: Proposal for NADPH oxidase inhibition. *Arch Biochem Biophys*;**457**:134-141

Xu R, Yu Y, Zheng S, Zhao X, Dong Q, He Z *et al.* (2005) Overexpression of Shp2 tyrosine phosphatase is implicated in leukemogenesis in adult human leukemia. *Blood*;**106**:3142-3149

Yang S, Sharrocks A. Interplay of the SUMO and MAP Kinase Pathways In: Berger SL, Nakanishi O, Haendler B, editors. The Histone Code and Beyond. Volume 57: Springer; 2006.

Yang T, Zhang JS, Massa SM, Han X, Longo FM. (1999) Leukocyte common antigen–related tyrosine phosphatase receptor: Increased expression and neuronal-type splicing in breast cancer cells and tissue. *Mol Carcinog*;**25**:139-149

Yen KE, Bittinger MA, Su SM, Fantin VR. (2010) Cancer-associated IDH mutations: biomarker and therapeutic opportunities. *Oncogene*;**29**:6409-6417

Yilmaz OH, Valdez R, Theisen BK, Guo W, Ferguson DO, Wu H *et al.* (2006) Pten dependence distinguishes haematopoietic stem cells from leukaemia-initiating cells. *Nature*;**441**:475-482

Yin Y, Liu YX, Jin YJ, Hall EJ, Barrett JC. (2003) PAC1 phosphatase is a transcription target of p53 in signalling apoptosis and growth suppression. *Nature*;**422**:527-531

Yin Y, Shen WH. (2008) PTEN: a new guardian of the genome. *Oncogene*;**27**:5443-5453

Yoo SK, Starnes TW, Deng Q, Huttenlocher A. (2011) Lyn is a redox sensor that mediates leukocyte wound attraction in vivo. *Nature*;**480**:109-112

Yu JH, Lim JW, Kim KH, Morio T, Kim H. (2005) NADPH oxidase and apoptosis in cerulein-stimulated pancreatic acinar AR42J cells. *Free Radic Biol Med*;**39**:590-602

Yuzhalin AE, Kutikhin AG. (2012) Inherited variations in the SOD and GPX gene families and cancer risk. *Free Radic Res*;**46**:581-599

Zarrinkar PP, Gunawardane RN, Cramer MD, Gardner MF, Brigham D, Belli B *et al.* (2009) AC220 is a uniquely potent and selective inhibitor of FLT3 for the treatment of acute myeloid leukemia (AML). *Blood*;**114**:2984-2992

Zhang J, Grindley JC, Yin T, Jayasinghe S, He XC, Ross JT *et al.* (2006) PTEN maintains haematopoietic stem cells and acts in lineage choice and leukaemia prevention. *Nature*;**441**:518-522

Zhang S, Mantel C, Broxmeyer HE. (1999) Flt3 signaling involves tyrosyl-phosphorylation of SHP-2 and SHIP and their association with Grb2 and Shc in Baf3/Flt3 cells. *J Leukoc Biol*;**65**:372-380

Zhang SQ, Yang W, Kontaridis MI, Bivona TG, Wen G, Araki T *et al.* (2004) Shp2 regulates SRC family kinase activity and Ras/Erk activation by controlling Csk recruitment. *Mol Cell*;**13**:341-355

Zhao S, Lin Y, Xu W, Jiang W, Zha Z, Wang P *et al.* (2009) Glioma-derived mutations in IDH1 dominantly inhibit IDH1 catalytic activity and induce HIF-1 alpha. *Science*;**324**:261-265

Zhao X, Carnevale Ka, Cathcart MK. (2003) Human monocytes use Rac1, not Rac2, in the NADPH oxidase complex. *J Biol Chem*;**278**:40788-40792

Zheng R, Friedman AD, Small D. (2002) Targeted inhibition of FLT3 overcomes the block to myeloid differentiation in 32Dcl3 cells caused by expression of FLT3/ITD mutations. *Blood*;**100**:4154-4161

Zheng R, Small D. (2005) Mutant FLT3 signaling contributes to a block in myeloid differentiation. *Leuk Lymphoma*;**46**:1679-1687

Zhong J, Liao J, Liu X, Wang P, Liu J, Hou W *et al.* (2011) Protein phosphatase PP6 is required for homology-directed repair of DNA double-strand breaks. *Cell Cycle*;**10**:1411-1419

Zhou B, Leng J, Hu M, Zhang L, Wang Z, Liu D *et al.* (2010a) Ezrin is a key molecule in the metastasis of MOLT4 cells induced by CCL25/CCR9. *Leukemia*;**34**:769-776

Zhou J, Bi C, Chng WJ, Cheong LL, Liu SC, Mahara S *et al.* (2011) PRL-3, a metastasis associated tyrosine phosphatase, is involved in FLT3-ITD signaling and implicated in anti-AML therapy. *PLoS ONE*;**6**:e19798

Zhu P, Tan MJ, Huang R-L, Tan CK, Chong HC, Pal M *et al.* (2011) Angiopoietin-like 4 protein elevates the prosurvival intracellular O2(-):H2O2 ratio and confers anoikis resistance to tumors. *Cancer cell*;**19**:401-415

Zito E, Melo EP, Yang Y, Wahlander A, Neubert Ta, Ron D. (2010) Oxidative protein folding by an endoplasmic reticulum-Localized peroxiredoxin. *Mol Cell*;**40**:787-797

Appendix 1

FLT3-driven redox-modulation of Ezrin regulates leukemic cell migration. Corcoran A, Cotter TG.(2013) *Free Radic Res*; Jan;47(1):20-34.

Appendix 2

Redox Regulated Growth Factor Survival Signalling. Woolley, J., Corcoran, A., Groeger, G., Landry, W., Cotter, T.G. (2013) *Antioxid Redox Signal*; in press.

Appendix 3

Redox Regulation of Kinases. Corcoran, A., Cotter, T.G. (2013) *FEBS J;* under review.